

Stem Cell-based Adipose Tissue Engineering

Dissertation zur Erlangung des Doktorgrades
der Naturwissenschaften (Dr. rer. nat.)
der Fakultät Chemie/Pharmazie
der Universität Regensburg



vorgelegt von
Markus Neubauer
aus Rosenheim
im November 2004

Diese Doktorarbeit entstand in der Zeit von Mai 2000 bis November 2004 am Lehrstuhl für Pharmazeutische Technologie an der Universität Regensburg.

Die Arbeit wurde von Prof. Dr. Achim Göpferich angeleitet.

Promotionsgesuch eingereicht am: 12. November 2004

Datum der mündlichen Prüfung: 21. Dezember 2004

Die Arbeit wurde angeleitet von: Prof. Dr. Göpferich

Prüfungsausschuss:	Vorsitzender:	Prof. Dr. Heilmann
	Erstgutachter:	Prof. Dr. Göpferich
	Zweitgutachter:	Prof. Dr. Franz
	Drittprüfer:	Prof. Dr. Buschauer

Meinen Eltern,
meiner Schwester Marita
und meiner Frau Uschi
gewidmet in Liebe und Dankbarkeit

“Life without fat is possible but not that much fun.”

Philipp E. Scherer

(at the Keystone conference “Molecular control of adipogenesis and obesity”, 2004)

Table of Contents

Chapter 1	Introduction – Strategies for Adipose Tissue Engineering.....	7
Chapter 2	Goals of the Thesis.....	51
Chapter 3	Modulators of the Adipogenesis of Mesenchymal Stem Cells.....	55
Chapter 4	Basic Fibroblast Growth Factor Enhances PPAR γ Ligand-induced Adipogenesis of Mesenchymal Stem Cells.....	79
Chapter 5	A Study on the Mechanisms of the Effect of bFGF on the Adipogenesis of MSCs under Clonal Conditions.....	97
Chapter 6	Stem Cell Seeding and Proliferation on Scaffolds with Different Pore Sizes.....	121
Chapter 7	Adipose Tissue Engineering Based on Mesenchymal Stem Cells and Fibroblast Growth Factor <i>in vitro</i>	143
Chapter 8	Adsorption, Desorption, and Covalent Binding of bFGF to Derivatives of PEG-PLA Polymers.....	165
Chapter 9	Instant Surface Modification of 3-D Polymeric Scaffolds Allows for the Tethering of bFGF and Generation of Vascularized Constructs.....	187
Chapter 10	Summary and Conclusion.....	207
Appendices	List of Abbreviations.....	215
	Curriculum vitae.....	219
	List of Publications.....	221
	Acknowledgements.....	227

Chapter 1

Strategies for Adipose Tissue Engineering

Markus Neubauer,¹ M.S., Claudia Fischbach,² Ph.D., Barbara Weiser,¹ M.S., Achim Goepferich,¹ Ph.D., Torsten Blunk,¹ Ph.D.

¹ Department of Pharmaceutical Technology, University of Regensburg,
Universitaetsstrasse 31, D-93040 Regensburg, Germany

² Engineering Sciences Lab, Harvard University, 40 Oxford St., Cambridge, MA 02138, USA

to be submitted in parts as review entitled “Adipose Tissue Engineering” to Tissue Eng.

Abstract

In reconstructive and plastic surgery, there exists an overwhelming demand for adipose tissue surrogates to replace fat tissue following tumor resections, complex trauma and congenital abnormalities as well as to augment tissues for cosmetic purposes. However, the optimal approach to adipose tissue replacement and reconstruction still remains elusive after decades of research. The fast growing field of tissue engineering may provide alternative strategies that improve upon the conventional surgical options. In this review, we highlight recent approaches based on tissue engineering techniques including *de novo* genesis of adipose tissue and cell-based therapies. A brief overview of basic processes involved in the differentiation of adipocytes and in the development of adipose tissue is followed by a summary of the applicable tissue engineering strategies, cell sources, and materials.

Introduction

A plethora of research approaches have been applied the engineering of bone, cartilage, liver, skin, and other tissues since the beginning of the 1990s. Soft tissue engineering, however, still remains a neglected discipline although there is an outstanding and continuously increasing demand for adipose tissue surrogates. The American Society of Plastic Surgeons (ASPS) reported that more than 68,000 breast reconstructions were performed and more than 39,000 burn cases were treated in the U.S. in 2003 [1]. In general, adipose tissue substitutes are required in reconstructive and plastic surgery, for instance, for tissue reconstruction following a mastectomy and other tumor resections, posttraumatic defect reconstruction (especially burns), treatment of congenital abnormalities and augmentation of breast, cheek and chin as well as facial rejuvenation in regard to wrinkles (reviewed in [2,3]).

Beyond interest in the field of surgery, adipose tissue is also intrinsic to the basic science study of several diseases, such as hypertension, dyslipidemias, cardiovascular problems, type 2 diabetes mellitus, and obesity [4]. Traditionally, fat tissue has been viewed as filling and a cushion material and as the “oil can” of the body, that is, as storage center for triacylglycerols [5]. More recently, however, adipose tissue has been recognized as an important secretory and endocrine organ [6-8]. Adipocytes secrete factors such as leptin, angiotensinogen, tumor necrosis factor α (TNF α), interleukin-6, adipsin, and adiponectin [9]. In this capacity, fat is involved in the regulation of energy balance, insulin sensitivity, immunological responses, and vascular diseases [10].

In the following chapters, current surgical techniques in fat reconstruction will be presented first, followed by a brief overview of the characteristics of adipose tissue and insights into adipogenic differentiation processes. Thereafter, tissue engineering will be introduced as an alternative to surgical techniques. Then recently published approaches towards adipose tissue engineering, including *de novo* adipogenesis and cell-based strategies, will be summarized and discussed. Herein, the three major components of tissue engineering, cells, cell carriers, and growth factors, will be described in detail. The important role of neovascularization is discussed in the following section. Subsequently, the role of engineered adipose tissue constructs in basic research will be illustrated and, finally, the authors provide a perspective on adipose tissue engineering, including an estimation of the current state of the art and of the critical issues to be investigated or optimized in the future.

Surgical techniques for the substitution of adipose tissue

In plastic and reconstructive surgery, fat grafts are utilized as filling material for the reconstruction of soft tissue defects [11-13]. A source of excess adipose tissue is available from almost every individual, that is, donor tissue availability is not the limiting factor. For these reasons, autologous fat grafts would appear to be optimal for the restoration of soft tissue volume and contour defects by the “replacement of like with like” [2,14]. However, autologous adipose tissue remains minimally effective due to insufficient neovascularization. In the long term, this leads to necrosis and apoptosis in free fat grafts and resultant tissue resorption over time [15]. The unpredictable shrinkage of the fat graft requires repeated surgery and a hardly calculable hypercorrection, respectively. In some cases, autografting causes donor site morbidity, accompanied by scar formation [2,14,16].

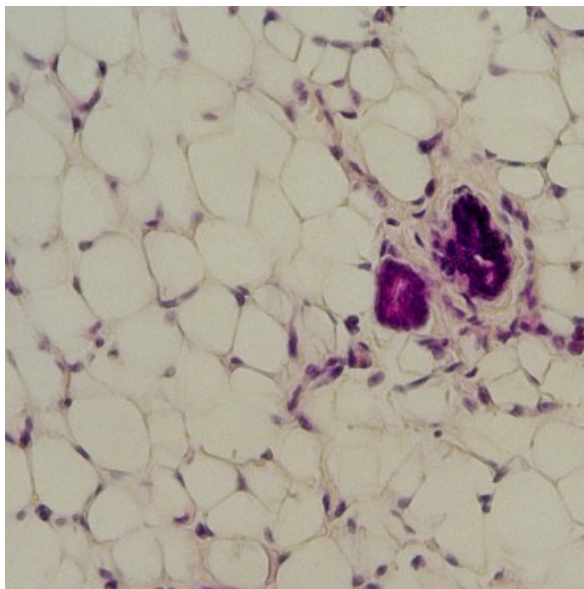
Another standard approach involves the injection of single cell suspensions of mature adipocytes following various aspiration techniques. Again, this method does not appear suitable, because exposure of the fragile adipocytes to the mechanical forces during liposuction traumatizes about 90% of the adipocytes [3,16].

Alternative approaches to soft tissue replacement traditionally include alloplastic and allogeneic products, such as Teflon, silicon implants and bovine collagen. More recent options utilize autologous injectable collagen as dermal allograft scaffolds [3,14]. Each of these methods is accompanied by certain drawbacks, including foreign body reactions, allergic reactions, infection transmission, and ultimately, a failure to integrate into the recipient site and tendencies towards migration [14].

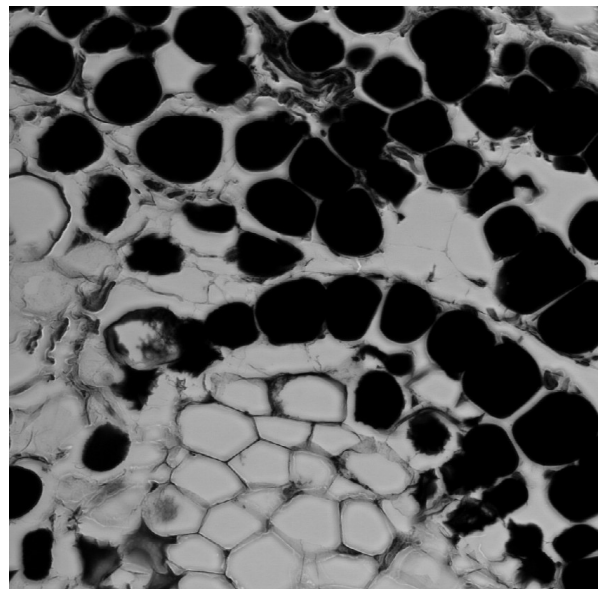
Thus, although numerous techniques and materials have been developed and have undergone practical tests, an optimum strategy for the regeneration and replacement of adipose tissue still remains elusive. For this reason, tissue engineering may represent a promising alternative to replace and regenerate fat.

What are the characteristics of adipose tissue?

In order to generate adipose tissue by means of tissue engineering, one should be aware of the composition of this type of tissue. Fat is composed of blood cells, endothelial cells, pericytes, fibroblasts, adipose precursor cells, and adipocytes [17]. The latter constitute about one third to two thirds of the total cell number within native adipose tissue [17]. Fat is subdivided into brown adipose tissue (BAT) and white adipose tissue (WAT). Brown fat cells are morphologically and functionally distinct from white adipocytes. BAT functions primarily to dissipate energy in the form of heat [18]. Phenotypically, brown fat cells are rich in mitochondria and accumulate lipids in multiple small droplets [19].



native adipose tissue
(H&E staining)



native adipose tissue
(OsO₄ staining)

Fig. 1 Mature adipose tissue dissected from the upper part of the femur of rats were stained with H&E and OsO₄. Dissolution of lipid inclusions with organic solvents during dehydration in the paraffin embedding procedure led to blank spaces within the cells. In the H&E stain, cell nuclei were stained violet. OsO₄ crosslinked intracellular lipids which then appear black.

The tissue commonly recognized as “the fat” and the distinctly larger proportion of the body fat consists of WAT. Mature adipocytes of WAT occur as cells with one large lipid droplet and very little cytoplasm with the nucleus located at edge of the cell [20]. This morphology is described as the signet ring form and the cell may be termed a univacuolar adipocyte. Typically, mature adipose tissue consists of adipocytes with a hexagonal shape; each adipocyte is in direct contact with neighboring cells with capillaries interspersed throughout (Fig. 1). During adipogenesis, the differentiation of precursor cells into adipocytes, or in times

of energy expenditure, adipocytes adopt a multivacuolar phenotype containing several discrete lipid droplets (Fig. 2).

Fat is distributed throughout the body and its large depots are located in epididymal, parametrial and perirenal regions [21]. Adipose tissue from different sites of the body undergo a physiological specialization with regard to lipid composition, responses to diet, lipolytic activity, and the secretion of various factors [21].

As a metabolically active and secretory tissue, adipose tissue is highly vascularized [11,22]. The neogenesis of adipose tissue in the embryonic stage is closely associated with the development of a vascular network [17]. Postnatal fat growth still occurs, either by hypertrophy of established adipocytes, i.e. the increase of the adipocyte size, or by hyperplasia, i.e. the increase of the number of adipocytes [23]. Reduction in fat mass is associated with a decrease in fat cell size; whether or not the reversion of mature adipocytes to immature phenotypes plays a role in this respect is still unclear [23].

Adipogenesis – the differentiation of precursor cells into adipocytes

The exact origin of the adipocyte is still poorly understood. Likely, the earliest stage in adipocyte differentiation are pluripotent stem cells which give rise to mesenchymal precursor cells (reviewed in [24]) (Fig. 2). These multipotent precursor cells have the capacity to undergo differentiation at least towards the chondrogenic, osteogenic, and adipogenic lineages. Commitment of precursor cells to the adipogenic lineage leads to preadipocytes, which terminally differentiate into mature adipocyte upon environmental stimulation. Most of the knowledge of the molecular mechanisms of adipogenesis *in vitro* has been obtained in studies with preadipocytic cell lines such as 3T3-L1, 3T3-F442A, and Ob1771 [25]. In summary, more than 300 proteins are supposed to be involved in the structural and functional morphogenesis during adipocyte differentiation [9]. Some of the most prominent factors belong to different families of transcription factors, which will be briefly introduced in the next section.

Transcription factors. Peroxisome proliferator-activated receptors (PPARs) are members of the superfamily of nuclear hormone receptors (reviewed in [26]). Three known members of the PPAR family exist: PPAR α , PPAR δ , and PPAR γ , and two isoforms of PPAR γ are known: PPAR γ 1 and PPAR γ 2. The latter is abundantly and specifically expressed in adipocytes. PPAR γ and its obligate heterodimeric partner, retinoid X receptor α (RXR α), are key regulators of adipocytic gene expression in lipid metabolism. The ectopic expression of

PPAR γ under adipogenic conditions in multiple non-progenitor cell lines results in adipocyte differentiation [27].

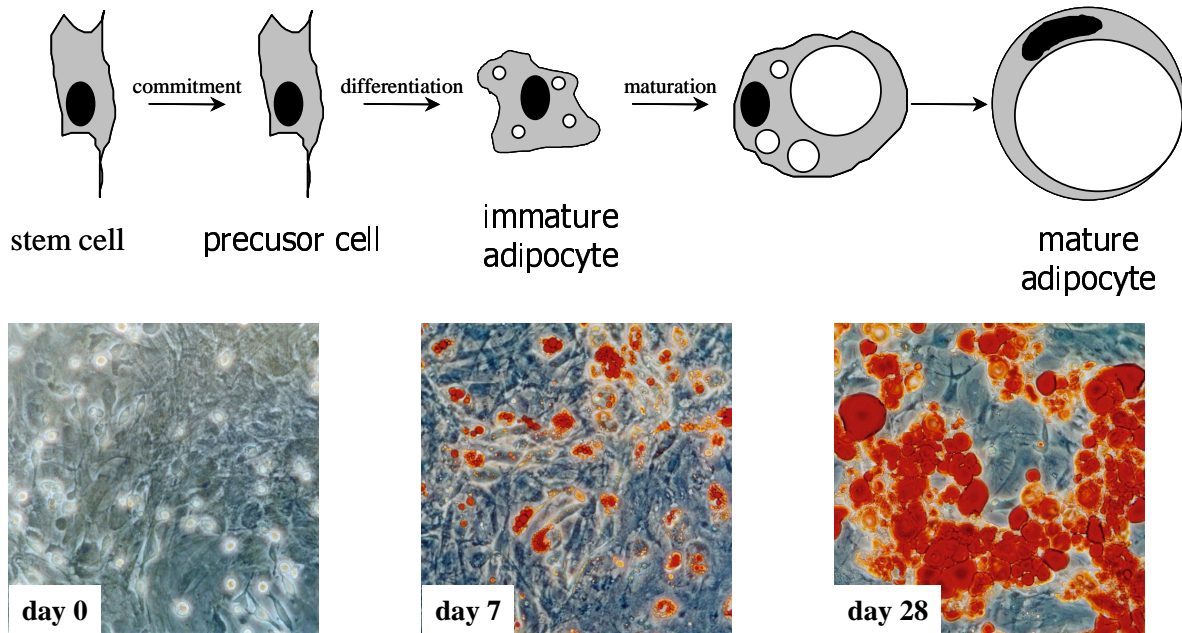


Fig.2 Differentiation of adipocytes. Fat cells are commonly thought to derive from stem cells. The pictures show rat mesenchymal stem cells (MSCs) in the undifferentiated state (day 0), in an immature state seven days after induction with a hormonal cocktail (as described in Chapter 3 and 4), and four weeks after induction exhibiting an advanced maturation. Some of the adipocytes shown are fully differentiated, containing one large lipid droplet per cell. Lipid inclusions were stained red using the lipophilic dye Oil Red O.

The CCAAT/enhancer-binding proteins (C/EBPs) belong to the family of leucine zipper transcription factors with three important members: C/EBP α , C/EBP β , and C/EBP δ (reviewed in [28,29]). C/EBPs can form homodimers and heterodimers with each other. Their distribution is not limited to adipose tissue. However, they play a crucial role in adipogenesis; the ectopic expression of C/EBP α and C/EBP β provokes adipogenesis in fibroblasts [30,31]. Sterol regulatory element binding proteins (SREBPs) represent another group of transcription factors known to modulate gene transcription for proteins involved in lipid metabolism (reviewed in [32]). Again, this family has three important members: SREBP-1a, SREBP-1c, and SREBP-2. In adipose tissue, SREBP-1c is mainly expressed. All three members activate similar gene expression, however, with different efficiencies. Fatty acid biosynthesis is mainly driven by SREBP-1a and SREBP-1c; cholesterol metabolism is affected by SREBP-2. The important role of SREBP1 is suggested by the fact that adipogenic differentiation of fibroblasts is enhanced by overexpressing SREBP-1 after viral transfection [33].

Transcriptional cascade. In the course of time, linear and parallel transcriptional cascades emerge, mediating adipocyte differentiation; the gene expression of several mediators are downregulated or upregulated (reviewed in[34]). After reaching confluency, preadipocytes express the lipoprotein lipase (LPL) via an unknown mechanism [35]. In addition, initial events include the repression or inactivation of inhibitory proteins expressed by undifferentiated preadipocytes. A prominent example of an inhibitory protein represents preadipocyte factor 1 (Pref-1) [36]. Immediately after the exposure of preadipocytes to inducing agents, the transient expression of C/EBP β and C/EBP δ is activated, which (in turn) mediates the expression of C/EBP α and PPAR γ [37,38]. Thereafter, C/EBP α and PPAR γ each stimulate the expression of the other in a positive feedback loop [39]. At this stage, multiple genes characterizing the adipogenic phenotype are *de novo* or increasingly expressed in cells displaying massive lipid accumulation [19]. The products of these genes include glycerophosphate dehydrogenase (GPDH), fatty acid synthase (FAS), glucose transporter 4 (Glut 4), the insulin receptor, the adipocyte-specific fatty acid binding protein (aP2), and many more. SREBP-1c is upregulated early and can synergize with the PPAR-C/EBP pathway by inducing gene expression of PPAR γ [40] and production of endogenous PPAR γ ligand [41].

Adipogenic inducers. A wide variety of low-molecular weight drugs and hormones are commonly used to induce the adipogenesis of preadipocytes and stem cells. Insulin in pharmacological doses has been shown to increase the number of differentiated adipocytes and the amount of accumulated lipids, likely by cross-activation of the insulin-like growth factor (IGF) receptor [19]. Glucocorticoids, usually administered in the form of dexamethasone, bind to the nuclear hormone glucocorticoid receptor (GR), whereas the transcriptional targets remain unclear [19]. Ensured mechanisms of glucocorticoid action are the induction of C/EBP δ [38] and the reduction of pref-1 expression [42]. High intracellular cAMP levels, caused by the phosphodiesterase inhibitor 3-isobutyl-1-methylxanthine (IBMX), strongly exert adipogenesis by a not completely understood mechanism. IBMX has been shown to produce an increase in C/EBP β [43] and a reduced suppression of the C/EBP α promoter by decreasing levels of the Sp1 transcription factor [44]. Thiazolidinediones, certain prostaglandines, and indomethacin have been proven to strongly induce adipogenesis as ligands of PPAR γ [45,46]. Furthermore, growth hormone (GH), thyroid hormone, retinoic acid, and other hormones have been described to affect adipocyte differentiation [19]. The most preferred and robust induction regimen in basic research consists of a glucocorticoid, IBMX, and insulin (sometimes combined with indomethacin).

This part of the review does not claim comprehensiveness. A plethora of additional molecules is involved in the complex process of adipogenesis, which is excellently described in detail in other reviews [5,9,47-55].

Tissue Engineering as alternative to surgical techniques

In general, four major strategies have been adopted for the generation of artificial tissues: (1) the use of isolated cells or cell substitutes, (2) the implantation of matrices, (3) the use of cells placed on or within matrices, and (4) the administration of tissue-inducing substances [56,57]. Recently, promising new therapy strategies based on tissue engineering techniques have been developed to generate fat surrogates. On the one hand, cell-based therapy approaches emerged, and on the other hand, tissue-inducing substances were administered in order to induce *de novo* adipogenesis.

Cell-based strategies

Cell-based adipose tissue engineering approaches aim at the generation of cell-scaffold constructs that result in mature fat tissue *in vitro* and *in vivo*, respectively. The basic strategy of these approaches is quite similar (Fig. 3): (a) cells are isolated from the desired donor site of a species, (b) undifferentiated cells are propagated *ex vivo* until the required cell number is obtained, (c) cells are seeded onto and/or into a cell carrier, and (d) subsequently cultivated and differentiated *in vitro* or implanted. Most of these approaches are based on the three critical components in tissue engineering: cells, scaffolds, and growth factors [58]. In the following parts, the use of these critical components in publications concerning adipose tissue engineering will be elucidated in detail and potential alternatives will be discussed. Table 1 summarizes the cell types that have been used as well as the growth factors and inducing regimens applied in adipose tissue engineering approaches.

Cells and growth factors

In tissue engineering in general, potential cell sources include autologous cells from the patient, allogeneic cells from a human donor, and xenogeneic cells from a different species [56]. Autologous cells seem to be most preferable due to the exclusion of immune rejections and legal problems [59]. However, there are a couple of issues to be considered: First, a relevant cell type has to be identified that is applicable for the specific purpose [60]. Second, a process of cell isolation has to be existent providing facile isolation of an appropriate cell number combined with a low degree of donor-site morbidity [61]. Third, cells must allow for

ex vivo culture and have a capacity for extensive expansion in order to obtain an appropriate cell number to replace a specific defect [61].

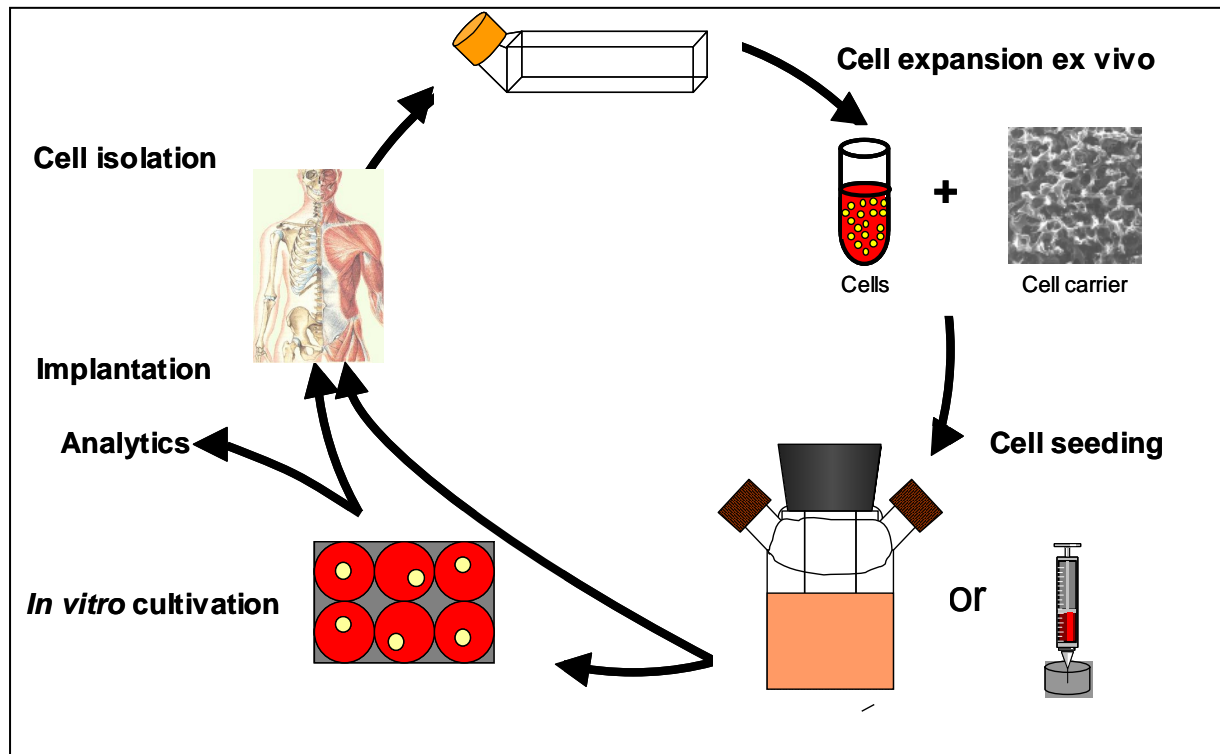


Fig. 3 Strategies of cell-based adipose tissue engineering approaches. Cells are isolated from the body, expanded *ex vivo* and seeded onto cell carriers by various methods. Cell-polymer constructs can be cultivated *in vitro* and subsequently implanted or can be directly implanted.

Cell types and the influence of growth factors on proliferation and differentiation. Potential candidates for the cellular component in adipose tissue engineering can be found among cells of the adipogenic differentiation lineage [62]. Stages in adipocyte differentiation include pluripotent or totipotent stem cells, mesenchymal precursor cells, preadipocytes, immature, and finally mature adipocytes (Fig. 2) [24]. To date, mature adipocytes, preadipocytes, preadipocytic cell lines, and mesenchymal stem cells have been used as cell sources in adipose tissue engineering approaches (Table 1) [63-78].

Mature adipocytes have certain drawbacks for the use in tissue engineering in regard to their fragility [3], their buoyancy rendering *ex vivo* cell culture more difficult [3], and their extremely low proliferation potential [79]. Yuksel et al. implanted diced, mature adipose tissue mixed with PLGA/PEG microspheres containing IGF-1, insulin, and basic fibroblast growth factor (bFGF). The added growth factors resulted in an increase in fat graft survival [80]. In another approach, mature adipocytes were placed in a collagen gel to develop a skin

model. The aim was to investigate the influence of adipocytes on the behavior of co-cultured keratinocytes and dermal fibroblasts [72].

Preadipocytes can be isolated from many fat depots within the body by minimally invasive liposuction or by enzymatic digestion of adipose tissue [3]. A potential up-scaling technique for cell washing and dissociation of liposuctioned tissue has already been presented [14]. A shortage of autologous donor tissue is, in the case of adipose tissue, very unlikely in most individuals. Preadipocytes are described to possess the capacity for expansion. Innumerable publications exist identifying extracellular and intracellular signals that modulate preadipocyte growth and differentiation. It is impossible to give a comprehensive overview, but a selection of important and widely used growth factors, hormones, and drugs is presented here. A wide variety of growth factors such as IGF-1, IGF-2, platelet-derived growth factor (PDGF), transforming growth factor β_1 (TGF β_1), acidic fibroblast growth factor (aFGF), and basic fibroblast growth factor (bFGF) have been found to provoke stimulatory effects on preadipocyte proliferation [81,82]. Principally, differentiation of preadipocytes can be induced by the supplementation of hormones and substrates to the growth medium. Glucocorticoids (corticosterone, cortisol, dexamethason, hydrocortisone), phosphodiesterase inhibitors (3-isobutyl-1-methylxanthin (IBMX), forskolin), peroxisome proliferator-activated receptor γ (PPAR γ) ligands (thiazolidinediones, 15-Deoxy-Delta(12,14), prostaglandin J2), indomethacin, fibrates (clofibrate, bezafibrate, fenofibrate), insulin, and triiodothyronine have been used to induce adipogenesis of preadipocytes [83-88]. Again, growth factors have been found to modulate preadipocyte differentiation. Basic FGF, EGF, PDGF, TGF β , and TNF α have been reported to diminish or suppress adipogenesis of preadipocytes [89-92]; in contrast, IGF-1 enhances adipogenic conversion [93].

Several issues have to be considered in regard to aforementioned data. Most data were assessed by the use of preadipocytes from various species from different sites or by the use of preadipocytic cell lines. Preadipocytes from different species may respond to signals differently, that is, it is difficult to transfer information from species to species. For instance, rat adipocyte precursor cells undergo differentiation after exposure to insulin, transferrin, and triiodothyronine, whereas rabbit preadipocytes do not respond to these inducers [83]. The use of preadipocytic cell lines such as 3T3-L1 or 3T3-F442A reveals at least two drawbacks. Their aneuploid status may influence their propensity to undergo adipogenesis. Furthermore, the use of cell lines does not allow for the assessment of depot-specific differences in cell behavior [19]. It has repeatedly been shown that variations in the number, growth and differentiation of preadipocytes derived from different sites of the body exist [21,85,94-97].

As yet, preadipocytes from different sites (epididymal, mammary, subcutaneous, omentum) isolated from humans, rats, and sheep have been used for adipose tissue engineering (Table 1). These studies were conducted in order to test of new materials and optimize cell carriers and culture conditions for preadipocyte-based tissue engineering, on the one hand [65,69,70,76,77], and the generation of adipose tissue *in vitro* or *in vivo* providing a quality comparable to native fat, on the other hand [63,64,66-68,71,73,75,78]. The growth factors bFGF and EGF were administered to stimulate preadipocyte proliferation [65,66,69,71,77]. The compositions of inducing regimens range from a widely used hormonal cocktail (glucocorticoid, IBMX, insulin \pm indomethacin) to thiazolidinediones and triiodothyronine-containing mixtures.

Cell Type	Donor Site	Species	Adipogenic Inducers	Growth Factor	Model	Ref.
MSC	bone marrow	rat	D, IBMX, IM, I	bFGF	<i>in vitro</i>	Ch.7
PA	epididymal	rat	-	-	<i>in vitro</i> / <i>in vivo</i>	[63]
PA	epididymal	rat	-	-	<i>in vivo</i>	[67]
PA	epididymal	rat	I, T3	-	<i>in vivo</i>	[64]
PA	subcutaneous	human	-	EGF	<i>in vivo</i>	[65]
PA	subcutaneous	human	D, I	bFGF	<i>in vitro</i> / <i>in vivo</i>	[77]
PA	subcutaneous	human	D, I	bFGF	<i>in vivo</i>	[69]
PA	mammary	human	C, Tro	-	<i>in vitro</i>	[68]
PA	n.d.	human	HC, IBMX, I	-	<i>in vitro</i>	[76]
PA	mammary	human	HC, I, T3, CT	-	<i>in vitro</i>	[75]
PA	mammary	human	D, I, T3	bFGF	<i>in vivo</i>	[71]
PA	omentum	sheep	-	FGF	<i>in vivo</i>	[66]
3T3-L1	-	mouse	CS, IBMX, IM, I	-	<i>in vitro</i>	[70]
3T3-L1	-	mouse	CS, IBMX, IM, I	-	<i>in vitro</i> / <i>in vivo</i>	[78]
3T3-F442A	-	mouse	-	-	<i>in vivo</i>	[73]
Adipocyte	abdominal	rat	-	-	<i>in vitro</i>	[72]
Adipocyte	inguinal	rat	-	IGF-1, I, bFGF	<i>in vivo</i>	[80]

Table 1 Cell types and sources, inducing regimens, and growth factors used in cell-based adipose tissue engineering approaches. All cell types are primary cells except of 3T3-L1 and 3T3-F442A which are preadipocytic cell lines (Abbreviations: C: Cortisol, CS: corticosterone, CT: cholera toxin, D: dexamethasone, HC: hydrocortisone, I: insulin, IBMX: 3-isobutyl-1-methylxanthine, IM: indomethacin, MSC: mesenchymal stem cell; PA: preadipocyte, T3: triiodothyronine, Tro: troglitazone).

Stem cells represent another potential cell source for adipose tissue engineering. The National Institutes of Health suggests a definition of stem cell: “A stem cell is a cell from the embryo, fetus, or adult that has, under certain conditions, the ability to reproduce itself for long periods or, in the case of adult stem cells, throughout the life of the organism. It also can give rise to specialized cells that make up the tissues and organs of the body.”[98]. Examples of such stem cells include the totipotent zygote, embryonic stem cells (ESs), hematopoietic stem cells (HSCs) and mesenchymal stem cells (MSCs) and further stem cells derived from distinct adult somatic tissues [99]. A wide variety of somatic stem cells were discovered in and isolated from adult tissues, for instance, from bone marrow [100-102], brain [103], muscle [104], fat [105], blood [106], liver [107], and skin [108]. This review is restricted to stem cells isolated from bone marrow, where stem cells are prevalent in adults, and to stem cells isolated from adipose tissue, where stem cells can be easily isolated.

Mesenchymal stem cells - the definition of an MSC still remains a challenge due to the fact that neither the origin of MSCs is clearly evidenced nor are specific phenotype markers known to select MSCs from the heterogeneous population derived from bone marrow [109]. For these reasons, the nomenclature is not definite and thus, various synonyms like bone marrow stromal (stem) cells, bone marrow progenitor cells, multipotent adult progenitor cells, bone marrow stromal fibroblasts, bone marrow mesenchymal progenitor cells and many more are commonly used. Bone marrow-derived MSCs show adherent, clonogenic, non-phagocytic and fibroblastic habits and possess the capability of multipotent differentiation. These cells were originally called fibroblastic colony-forming cells or colony-forming units-fibroblastic (CFU-F) [110,111]. Apart from that, MSCs can be defined, as well as other stem cells, as cells with a high capacity of self-renewal and a potential to differentiate into a variety of cell types [112].

Bone marrow samples can easily be obtained following a simple bone marrow aspiration [112]. Bone marrow is composed of at least three cellular systems: hematopoietic, endothelial and stromal. In adult bone marrow, macrophages, adipocytes, osteogenic cells, hematopoietic cells, cells originating from blood vessels and “reticular” cells coexist and partially cooperate [113]. The simplest way to isolate MSCs is through their adherence to plastic without further purification and was reported as early as 1974 by Friedenstein et al [114]. In order to isolate the “pure” MSC, bone marrow can be preliminarily purified by gradient centrifugation techniques to remove cells with different densities like hematopoietic cells. Subsequently, cells can be sorted by fluorescence-activated cell sorting (FACS) or magnetic cell sorting (MACS) via detection of positively or negatively expressed surface antigens using

fluorescence-labeled and magnetic-labeled antibodies, respectively. The most abundantly used negative antigens are the hematopoietic markers CD34 and CD45 for this purpose, whereas MSCs have been reported to be positive for Stro-1, CD29, CD44, CD90, CD105, CD106 and many more [102,112,113]. Stro-1 is supposed to represent the nearest approximation to identify the “pure” MSC, though a few hematopoietic cells weakly express Stro-1 [109,115]. Apart from that, subpopulations can also be separated by FACS utilizing the size and granularity of the cells as criteria [116]. However, as yet, no definite marker has been found to identify and isolate the “pure” MSC.

Adipose-tissue derived stem cells, also called processed lipoaspirate cells (PLA cells), are isolated by collagenase digestion following liposuction [117,118]. Most of the surface proteins expressed by MSCs have been demonstrated to also be expressed by PLA cells, with the exception of Stro-1 [117].

MSCs possess a high expansion potential, that is, *ex vivo* expansion is possible over 15 passages and about 40 population doublings resulting in a billion-fold expansion [119]. Stimulation of the proliferation of MSCs, their life span and the retention of the differentiation potential during the expansion has been shown to be strongly influenced by growth factors. Different laboratories have proved the expression of growth factor receptors (bFGF-R, EGF-R, PDGF-R, TGF β_{1+2} -R) on the surface of MSCs [102,120]. Basically, the minimum conditions for the initial growth of MSCs under serum-free conditions requires participation of at least four growth factors: PDGF, bFGF, TGF- β and EGF [121]. bFGF has repeatedly been reported to strongly stimulate the proliferation of MSCs [122-127]. Furthermore, EGF, IGF-1, and PDGF-BB increase the growth of MSCs [128-131], whereas TGF β_1 is controversially discussed [131,132]. The retention of the differentiation potential of cells after extensive expansion is another capacity of bFGF.[125,133]

The expansion of PLA cells has been demonstrated over 15 passages including more than 20 population doublings [118].

Aging of MSCs is associated with a decrease in the maximal life span and accelerated senescence of MSC [134]. An extension of the life span of MSCs can be achieved by supplementation of growth factors such as bFGF [125,133]. The origin of senescence is attributed to the lack of telomerase activity in MSCs [135]. Telomerase-transduced cells exhibit reduced senescence, extended life span and additionally, retention of the differentiation potential [136,137].

PLA cells exhibited only weak senescence, virtually undetectable after one passage and, after 15 passages, less than 15% of cells exhibited the senescence marker β -galactosidase [118].

In regard to the differentiation potential, Owen proposed a system of marrow stromal stem cells in 1988 and found CFU-F to give rise to at least fibroblastic, reticular, adipocytic and osteogenic lineages [101]. Recently, MSCs were shown to differentiate into a wide variety of mesenchymal tissues like those mentioned above and, additionally, into cartilage, muscle, tendon, and marrow stroma [138]. Until recently, ESs and adult stem cells were strictly distinguished because ESs have been shown to be pluripotent and adult stem cells are supposed to be multipotent. Pluripotent stem cells have the ability to give rise to types of cells that develop from any of the three germ layers (mesoderm, endoderm, and ectoderm) from which all the cells of the body arise [98]. Cells capable of differentiating into lineages of one germ layer are called multipotent. Adult stem cells were supposed to be multipotent, but recent results indicate a pluripotency [109,139,140]. Adult stem cells derived from different adult tissues were shown to transdifferentiate into lineages of germ layers unrelated to their origin, a phenomenon called plasticity [98]. MSCs gave rise to cells outside the limb-bud mesoderm, including endothelium, neuroectoderm and endoderm [141].

PLA cells also have the capacity of multipotent differentiation towards the adipogenic, chondrogenic, myogenic, and osteogenic lineages [118].

Adipogenic differentiation is commonly induced by exposure of MSCs and PLA cells to a hormonal cocktail consisting of dexamethasone, IBMX, indomethacin, and insulin in various combinations and concentrations [102,118,142-144] or to thiazolidinediones [145-147] as single inducers or in combination with the hormonal cocktail or parts of it (Chapter 3,4).

As explained for preadipocytes, donor diversity and age-related diversity of PLA cells and MSCs exist as shown in [147,148].

MSCs derived from rats have been used in our laboratory. Seeding and cultivation of MSCs onto PLGA scaffolds over four weeks leads to generation of cell-polymer constructs exhibiting characteristics of adipose tissue. Partially unilocular adipocytes embedded in structures considered to be extracellular matrix yielded a high adipocytic enzyme activity and clear gene expression of GLUT4 and PPAR γ 2.

Pluripotent embryonic stem cells (ESs) have to be mentioned at this point as a future possibility. Among stem cells, the fertilized oocyte and blastomeres of 2-, 4- and 8-cell-stage embryos are totipotent, whereas cells of the inner cell mass of blastocysts, embryonic ectoderm and primordial germ cells are only pluripotent [149], because they do not form placenta [150]. Murine embryonic stem cell lines were established in the early 1980s [151], human ESs later in 1998.[152] ESs and embryonal germ cells have been isolated from the inner cell mass of blastocysts and from primordial germ cells, respectively. Mouse ESs can be

virtually infinitely propagated in the presence of leukaemia inhibitory factor (LIF), whereby human ESs require culture on mouse embryonic feeder (MEF) cell layers with basic fibroblast growth factor (bFGF) and Matrigel or on laminin in MEF-conditioned medium [153]. Differentiation experiments were performed towards a wide variety of cell types of all three primary germ layers like skeletal muscle cells, vascular smooth muscle cells, cardiomyocytes, neural cells, and adipocytes [154]. Growth factors and especially retinoic acid were found to play crucial roles in the differentiation processes of ESs [154,155]. ESs have been shown to give rise to adipocytes following the administration of retinoic acid for a precise period of time [156,157]. Due to their virtually unlimited proliferation and differentiation potential, ESs seem to be the most attractive candidate for the tissue engineering applications. However, ethical concerns will restrict the use of these cells in the field of tissue engineering and transplantation for the time being [158].

Scaffolds

In principle, the scaffold material is supposed to provide a template for the three-dimensional shape of the desired tissue and to provide initial, transient stability [60]. The newly developed tissue, that is, the cells and secreted extracellular matrix, is responsible for the long-term maintenance. In this context, the scaffold should be recognized as an artificial extracellular matrix allowing for cell attachment, migration, proliferation, differentiation, and maintenance of a mature tissue [159]. Furthermore, the optimum scaffold material matches the properties of the tissue at the implantation site [160]. In general, there are several requirements in the design and fabrication of scaffolds for tissue engineering [159-162]:

1. biocompatibility of the bulk and the degradation products
2. appropriate mechanical properties for the new tissue and the surrounding tissue
3. high surface area for specific and numerous cell interactions
4. high porosity to allow cellular and capillary ingrowth and nutrient supply
5. high interconnectivity of the pores to provide a uniform cell distribution and sufficient supply of cells located at inner parts of the scaffolds with oxygen and nutrients
6. appropriate surface structure and chemistry for an improved control of the cellular behaviour
7. biodegradability (if desired) at a controlled rate in concert with tissue formation

A wide variety of synthetic (polyglycolic acid (PGA), lactide/glycolide copolymers (PLGA), polytetrafluoroethylene), partially synthetic (HYAFF[®] 11, a benzyl ester of hyaluronic acid)

and natural materials (alginate, collagen, fibrin glue, matrigel) have been used in adipose tissue engineering approaches (Table 2). Cell carriers have been employed as sponges, fiber meshes and hydrogels (Fig. 4) .

The synthetic polymers polylactic acid (PLA) and PGA as well as the copolymer PLGA are widely used, have a long history as an FDA-approved suture material, are reasonably biocompatible and have a tunable degradation rate that can be tailored from weeks to years [161,162]. However, these polymers possess the following drawbacks. The release of acidic degradation products may affect cell function by acidification of the microenvironment and can lead to acylation of peptides and proteins [163]. Furthermore, these polymers exhibit a high stiffness which may be disadvantageous for soft tissue engineering purposes [161]. The lack of chemical reactive groups renders a surface modification of scaffolds made from these materials more difficult and requires complex reactions in order to introduce additional functional groups, such as carboxylic groups, peroxides, and thiols [164-166]. Nevertheless, adipose tissue engineering approaches using PLGA scaffolds seem promising in regard to *in vitro* (Chapter 7) and *in vivo* [63,67] tissue formation (Table 1). First, preadipocytes attached to PLGA scaffolds with a range of pore size from 135 to 633 μm generated by a salt leaching technique [63]. Preadipocytes differentiated into adipocytes *in vivo* without any inducing additives and the size of newly developed adipocytes almost reached that of native adipocytes. Second, MSCs were seeded onto PLGA sponges with pore size from 100 to 300 μm obtained by a solid lipid template technique (Chapter 7). MSCs partially differentiated into mature adipocytes and formed a tissue-like structure by secreting ECM-like compounds within four weeks. Synthetic, strongly hydrophobic polytetrafluoroethylene fiber meshes proved useful to seed preadipocytes, but required a prior coating with proteins, preferably with fibronectin, to enable cell adhesion [76]. Seeded on these meshes, preadipocytes underwent adipogenesis following administration of a hormonal adipogenic cocktail (Table 1).

Semisynthetic benzylesters of hyaluronic acid (HYAFF[®]11) appear to be suitable for fat engineering *in vitro* and *in vivo* (Table 2) [65,68]. Hyaluronic acid (HA) is one of a group of glycosaminoglycans (GAGs) that are important components of the extracellular matrix [167]. Sponges with a pore size ranging from 50 to 400 μm and non-woven fibers with an interfiber distance between 100 and 300 μm were applied. *In vitro*, HYAFF[®]11 sponges with different esterification grades all allowed preadipocyte attachment and led to sporadically distributed, immature adipocytes exhibiting very low activity of adipocytic marker enzyme [68]. *In vivo*,

HYAFF[®] 11 sponges were shown to be superior to collagen sponges and non-woven HYAFF fiber carriers and exhibited mature adipocytes after two months [65].

Scaffold Material	Type Fabrication technique	Pore size [μm]	Modification	Ref.
PLGA (75:25)	sponge solid lipid templating	100-300	-	Ch. 7
PLGA (75:25)	sponge particulate (NaCl) leaching	135-633	-	[63]
polytetrafluoroethylene	fiber mesh n.d.	52	collagen, albumin, FN coating	[76]
fibrin glue	hydrogel mixing of cells and gel	-	-	[64]
collagen	hydrogel mixing of cells and gel	-	-	[75]
collagen	sponge directional solidification	50	-	[65]
HYAFF [®] 11	sponge phase inversion	50-340	-	
HYAFF [®] 11, nonwoven	fiber mesh n.d.	100-300	-	
collagen	sponge directional solidification	40	-	[77]
alginate	hydrogel	-	RGD	[66]
PLGA (75:25)	sponge particulate (NaCl) leaching	135-633	-	[67]
HYAFF [®] 11, different esterification grade	sponge n.d.	200, 400	FN coating	[68]
collagen	sponge directional solidification	65 \pm 7, 98 \pm 15	-	[69]
collagen	sponge freeze-drying, crosslinking	60-100	microspheres with bFGF	[71]
PGA	fiber mesh n.d.	n.d.	-	[70]
PGA	fiber mesh n.d.	n.d.	-	[78]
matrigel	hydrogel mixing of cells and gel	-	-	[73]
collagen	hydrogel mixing of cells and gel	-	-	[72]

Table 2 Scaffold materials and types used in cell-based adipose tissue engineering approaches. Furthermore, pore size and fiber distances, respectively, are summarized. (Abbreviation: FN: fibronectin)

Among the wide variety of potential natural scaffold materials, fibrin glue, alginate, collagen, and Matrigel were employed in fat engineering (Table 2). For sure, natural materials such as GAGs and collagen may well reflect the structure and functional properties of native ECM and have a low toxicity and chronic inflammatory response [167]. Administration of these materials as injectable gels (e.g. alginates) would allow for minimally-invasive surgery. However, disadvantages of all natural materials such as batch-to-batch variations, poor mechanical performances, and difficult structure manipulation due their complex chemical structure have to be mentioned in regard to their use in tissue engineering [159,162].

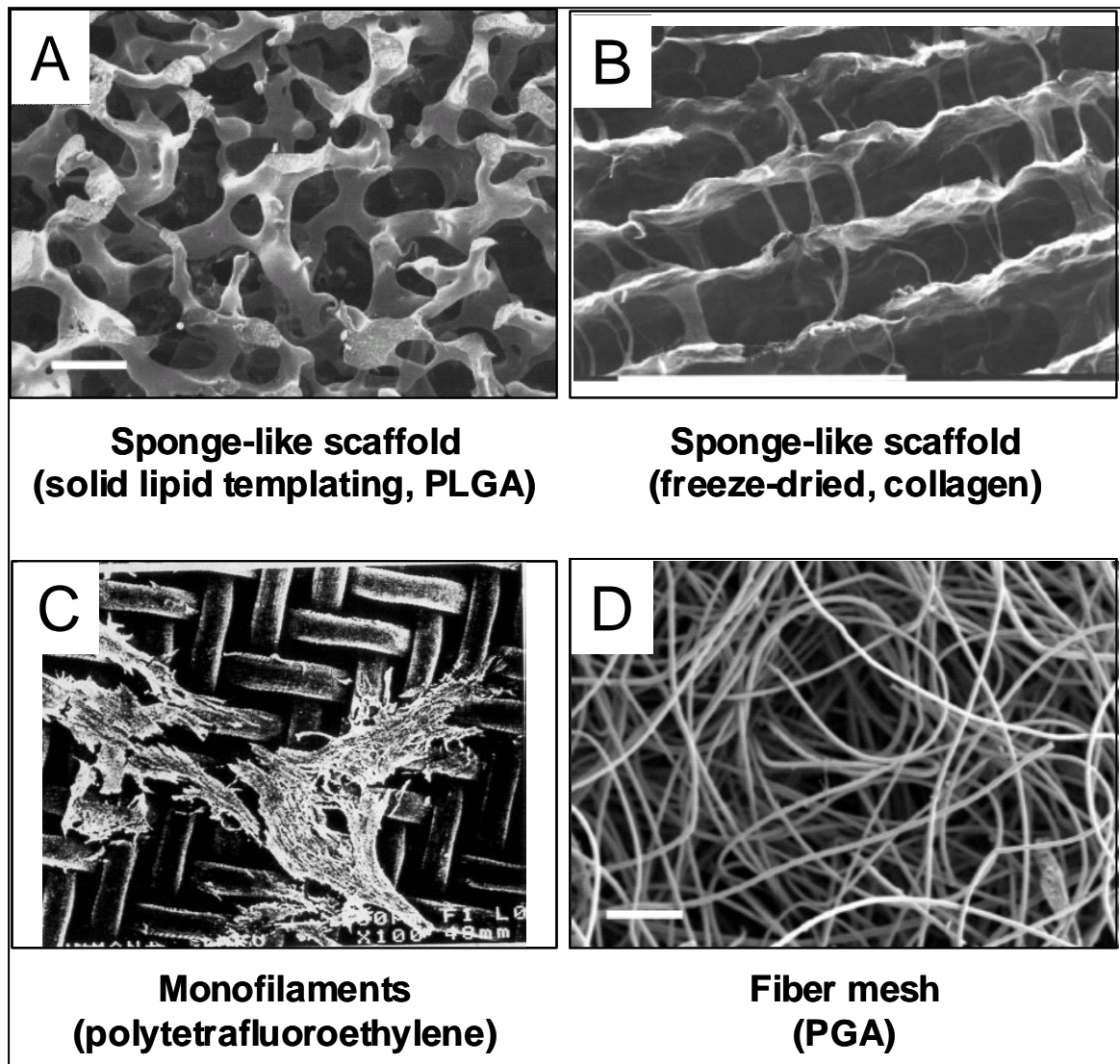


Fig. 4 Microstructure of different scaffold types. (A) Sponge-like structure obtained by a lipid solid templating technique (scale bar: 200 μm) (Chapter 7), (B) sponge-like structure obtained by freeze-drying and a directional solidification technique (scale bar: 100 μm) [77], (C) monofilament structure (scale bar: 60 μm) [76], (D), fiber mesh (scale bar: 200 μm) [70,78]. In picture C, preadipocytes are attached to the biomaterial. All other scaffolds are shown without cells.

Fibrin glue can be produced from the patient's own blood and, thus, it can be recognized as a potentially autologous scaffold material [168]. Enzymatic polymerization of fibrinogen in the presence of thrombin forms hydrogels with a degradation rate, which can be regulated by the addition of aprotinin, a proteinase inhibitor. For adipose tissue engineering, preadipocytes were suspended in fibrin glue and implanted into a fibrous capsule, which was provoked by a prior implantation of silicon tubes into muscle tissue [64]. This technique yielded nearly normal adipose tissue within the fibrous capsule stable over one year. However, the relevance of this method for the application in the field of reconstructive and plastic surgery is questionable.

Alginates are widely used in the field of drug delivery and tissue engineering because they are cheap, biocompatible, non-toxic, and gelation can be simply triggered with divalent cations, such as Ca^{2+} or Mg^{2+} [168]. Nevertheless, pure alginates are not suitable for tissue engineering purposes, because their high hydrophilicity suppresses protein adsorption, which strongly reduces their ability to interact with cells. For this reason, alginates have been modified with lectins [169] and RGD-containing adhesion peptides [66]. Halberstadt et al. subcutaneously injected preadipocyte-seeded alginate gels and alginate gels with a covalently bound RGD-containing peptide into sheep [66]. Preadipocytes attached and proliferated in the RGD-modified gels and, after three months, well-defined adipose tissue was recovered at the implantation site. However, it remains unclear whether the new adipose tissue was derived from the implanted preadipocytes or from attracted endogenous preadipocytes or other precursor cells.

Collagen represents the most abundant component of native ECM [167]. Therefore, collagen matches some of the optimum scaffold material, because specific amino acid sequences are recognized by cells and degraded by cell-produced enzymes (collagenases). Disadvantages include the poor mechanical strength, potential immunogenicity, and the high price [168]. At least 13 types of collagen are known [170] exhibiting different properties. Mizuno et al. reported that only one type of collagen, type I, was able to support osteogenesis of MSCs *in vivo*, whereas collagen types II, III, and V did not possess this property [171]. For adipose tissue engineering, collagen hydrogels and sponges have been employed *in vitro* and *in vivo* [65,69,72,75,77]. Mammary epithelial cells and adipocytes were mixed with a collagen solution and co-cultured in a 3-D collagen gel *in vitro* [75]. After three weeks, clusters of adipocytes and tubular structures of epithelial cells were noticed. Beyond the use of preadipocytes, a mature adipocyte culture in collagen gels was performed, aimed at the reconstruction of a skin model to assess effects of fat cells on keratinocytes and dermal

fibroblast in co-culture *in vitro* [72]. Collagen sponges fabricated by a directional solidification method and subsequent freeze-drying were intensively investigated by von Heimburg et al. [65,69,77] Effects of different pore sizes of 40, 50, 65, and 98 μm on cell penetration and tissue formation were assessed *in vitro* and *in vivo*. An enlargement of the pore size tends to be advantageous in regard to cellular penetration, distribution, and differentiation. This fact is not surprising in consideration of the size of mature adipocytes, which can exceed 100 μm . Adipose tissue was only seen proximal to the scaffold surface surrounded by slightly calcified tissue. Von Heimburg stated that the HYAFF[®]11 sponges appear superior to collagen scaffolds with regard to cellularity. However, the pore size of collagen sponges (50 μm) was distinctly smaller as compared to that of the HYAFF[®]11 sponges (50-340 μm) in this study [65].

De novo adipogenesis in vivo

Since adipocyte precursor cells are present in adipose tissue, the fat cell number in most of the depots can increase, for instance, following a high-carbohydrate or a high-fat diet [172]. The idea of *de novo* adipogenesis is to utilize this mechanism, that is, to mobilize endogenous cells. Thus, *de novo* approaches function without the use of exogenous cells and cell carriers such as scaffolds; adipose tissue development is induced by the delivery of specific growth factor(s) and other inducing agents and the subsequent migration, proliferation, and differentiation of endogenous cells. First reported in 1998, *de novo* adipose tissue formation and neovascularization was provoked by the injection of a mixture of Matrigel and bFGF into mice [173]. It was additionally reported that platelet-derived growth factor (PDGF) is as potent as bFGF, whereas insulin, insulin-like growth factor-1 (IGF-1), and growth hormone (GH) were less potent in regard to the induction of *de novo* adipogenesis [173]. An improvement of this method was achieved by the controlled release of bFGF from gelatin microspheres mixed with Matrigel [174,175]. Co-implantation of Matrigel and bFGF-incorporated microspheres revealed a higher percentage of adipose mass and increased angiogenesis in the explant than Matrigel mixed with free bFGF. Alternatively, *de novo* generation of adipose tissue was achieved by long-term, local delivery of IGF-1 and insulin from PLGA/PEG microspheres in rats [176]. Delivery of insulin or IGF-1 exclusively also resulted in an increased *de novo* adipogenesis which was, however, inferior to the provoked adipogenesis by the simultaneous delivery of insulin and IGF-1. Masuda et al. combined the growth factors from the abovementioned systems and delivered growth factors by a co-release of bFGF, insulin, and IGF-1 from photocured, styrenated gelatin microspheres [177]. A rapid

delivery of the angiogenic factor bFGF and a prolonged release of insulin and IGF-1 resulted in a highly vascularized, mature adipose tissue.

Mechanistic studies were performed by Toriyama et al. investigating the time course of *de novo* adipogenesis induced by bFGF-containing Matrigel [178]. Three biological main events turned out to be involved in this process: neovascularization, the spontaneous migration of endogenous fibroblast-like preadipocytes or stem cells, and the subsequent differentiation of attracted cells into adipocytes. In detail, within a few days, a multiple cell layer, consisting of fibroblast-like cells and endothelial/epithelial cells, was formed on both sides of implanted Matrigel. Thereafter, the cells proximal to the Matrigel underwent a change in cell shape and constitution of cell organelles, accompanied by an invasion of phagocytes. Phagocytic degradation of the Matrigel seemed to stimulate the maturation of all cells. Subsequently, invaded cells started to accumulate lipid droplets provided that these cells were in contact with newly formed capillaries. After five weeks [173], full maturation of adipocytes was achieved and could be maintained over at least 15 weeks [174].

The abovementioned mechanistic observations suggest the existence of a close relationship between the formation of blood vessels and adipogenesis. Indeed, it is well known that the earliest adipogenic event is associated with the organization of a vascular network [17,19,22]. However, there is no evidence of whether adipogenesis can induce angiogenesis, vice versa, or both [19].

Vascularization of adipose tissue

Adipose tissue is a highly vascularized tissue; each adipocyte is attached to at least one capillary [2]. Vascularization is a pivotal requirement not only for adipose tissue engineering. Cells at a distance of more than 200 μm from a blood supply tend to be metabolically inactive or necrotic [162]. For instance, transplanted fat flaps undergo necrosis and resorption due to insufficient neovascularization [2]. The importance of blood vessel formation for the development of adipose tissue is indicated by the aforementioned fact that angiogenesis precedes adipogenesis in the embryonic stage. Several findings also suggest a close relationship and cross-talk of (pre-)adipocytes and vascular cells in adult organisms. One study impressively demonstrates the reciprocal regulation of adipogenesis and angiogenesis in an *in vivo* model [179]. Dominant negative expression of PPAR γ in preadipocytes led not only to the failure of adipogenic differentiation, but also reduced angiogenesis. Reciprocally, antibody blocking of the vascular endothelial-derived growth factor (VEGF) receptor-2 reduces angiogenesis and, surprisingly, additionally inhibited the adipogenesis of

preadipocytes. In a further study, ob/ob mice, leptin knock-out obese mice, have been treated with various angiogenesis inhibitors, such as angiostatin, endostatin, and TNP-470. This therapy caused decreased endothelial cell proliferation and increases apoptosis in the adipose tissue and led to a loss of adipose tissue mass that is similar to that resulting from leptin replacement [180]. Furthermore, the adipocyte-secreted hormone leptin modulated vascular permeability and stimulated angiogenesis in synergy with bFGF and VEGF [181]. Adipose tissue-derived endothelial cells could promote the proliferation [182] and differentiation [183,184] of preadipocytes.

All of these facts underline the significance of a blood vessel supply to growing adipose tissue in regard to the differentiation of precursor cells and long-term maintenance of the tissue.

In the presented adipose tissue engineering approaches, blood vessel ingrowth into cell-polymer constructs have been reported in several cell-based approaches. Vascular support of implanted preadipocyte-loaded constructs has been observed using sponges made from collagen [69,77], HYAFF[®]11 [65], PLGA [67], and PGA fibers [78] as well as hydrogels made from fibrin glue [64]. However, a long-term study by Patrick et al. clearly demonstrated the elusiveness of long-term maintenance of an engineered adipose tissue and elucidates a major challenge for future approaches [67]. Preliminary results from Dolderer et al. promise the generation of vascularized adipose tissue by an alternative tissue engineering approach [185]. This group places large polycarbonate chambers around vascular pedicles and adds fat flaps. After 12 weeks, the chamber is reported to be filled with new, vascularized, and transferable adipose tissue. Alternatively, co-cultures of endothelial cells and preadipocytes in a fibrin matrix could enable the early formation of a blood vessel network *in vivo* [186]. However, this study used an egg model with a chorioallantoic membrane and adipogenesis was neither induced nor investigated.

The structure of scaffolds may play a crucial role in regard to vascularization. Pore size and interconnectivity have to be optimal for the ingrowth of fibrovascular tissue. In general, a pore size of 5 μm is supposed to be sufficient for neovascularization, however, 500 μm are required for a rapid vascularization and for the survival of transplanted cells [162].

Remarkably, all of the aforementioned approaches towards *de novo* adipogenesis result in highly vascularized adipose tissue and long-term maintenance over at least 15 weeks has been reported [174]. Probably, the *de novo* adipogenesis approaches represent the currently most promising way to obtain optimally vascularized fat tissue. This strategy reflects the prenatal mechanism of neogenesis of adipose tissue *in vivo*.

Engineered adipose tissue in basic research

As yet, basic research on adipose tissue differentiation and function has been performed using especially preadipocytic cell lines such as 3T3-L1 and 3T3-F442A in conventional 2-D cell culture systems. These systems provide standardized conditions and are, thus, certainly indispensable tools to gain deep insights into the molecular control of adipogenesis and to facilitate the discovery of molecules secreted by adipocytes. But it is worth mentioning that these systems have at least two major drawbacks. The aneuploid status of the cells may modulate their differentiation capacity and they are cultivated out of their normal 3-D context with an altered extracellular matrix [19].

Primary cells such as preadipocytes and mesenchymal stem cells may circumvent the first of the mentioned drawbacks. However, standardized cell populations and cell culture techniques are necessary basic requirements. Donor-to-donor and age-related diversities of isolated cells as well as impurities of an isolated cell population are described difficulties [109,147,148]. A mixture of cell types such as macrophages, fibroblasts, endothelial cells, and hematopoietic cells are still present following cell isolation. As explained in the above “Cells” section, the use of preadipocytes is associated with the fact that cells from different body sites exhibit different behaviors. In addition, the procurement of “pure” MSCs still remain elusive though extensive efforts approach to develop an appropriate isolation technique.

In vivo, cells are embedded in a 3-D matrix. However, cells are conventionally cultured in a 2-D monolayer *in vitro* for most basic research purposes. Recent findings suggest that cells differentially behave in 2-D and 3-D cell culture [78,188-190]. Monolayer cultures have been repeatedly shown to yield a different cell phenotype and, for instance, differential expression profiles of extracellular matrix components, surface molecules, and differentiation markers as compared to cells in 3-D culture. In detail, a cross-modulation of β 1-integrin and EGF-receptor signalling has been shown in a tumor cell line in 3-D cell culture, whereas in a 2-D monolayer culture, the cross-modulation did not occur [187]. Another example of the differential cell behavior has been proven in 3-D thermoreversible gels as compared to 2-D culture of osteogenesis of MSCs [188]. Important differentiation markers such as osteopontin, osteocalcin, and alkaline phosphatase are upregulated, whereas an adipogenic marker, LPL, was downregulated in 3-D culture as compared to the 2-D assay. BMP-2 exerts differential effects on gene expression of VEGF, osteopontin, and collagen I during osteogenic differentiation of MSCs in a 2-D monolayer culture onto PLGA films and in a 3-D culture using PLGA scaffolds [189]. In a recent adipose tissue engineering approach, 3T3-L1 cells seeded onto PGA fibers yielded an increased secretion of leptin and laminin as compared to

the 2-D culture [78]. Furthermore, utilizing this model, it is possible to generate adipose tissue *in vitro* that resembles mature fat *in vivo*.

Beyond these facts, cultivation of advanced differentiated and mature adipocytes requires special techniques of 2-D cell culture due to their rounded shape and their buoyancy. In 3-D cell culture, the adipocytes are embedded and detained in a solid matrix and are thus capable of developing their natural shape. In this context, it is worth mentioning that the cell shape, cytoskeletal components [25,190] and ECM structure and composition [25,191-194] have recently been found to strongly influence adipocyte differentiation and function.

In conclusion, the generation of adipose tissue by utilizing tissue engineering techniques will not only be useful to supply tissues for reconstructive and plastic surgery, but will also be helpful to provide 3-D cell culture models that simulate *in vivo* conditions to study differentiation events, secretory processes, cell-cell interactions, and cell-matrix interactions.

Conclusion and Perspective

Three cell types have been tested in adipose tissue engineering approaches so far: mature adipocytes, preadipocytes, and mesenchymal stem cells. Studies based on preadipocytes provide the most extensive and detailed information and can be considered as the most advanced strategy in cell-based adipose tissue engineering. Engineered fat that phenotypically resembles native fat has been achieved *in vivo* [63,78] and, in one case using the preadipocytic cell line 3T3-L1, also *in vitro* [78]. Most of the studies, both *in vitro* and *in vivo*, are restricted to a phenotypical characterization by means of histology and reflection of lipid accumulation of the generated tissues, whereas proofs of functionality, that is for instance the capability to secrete adipocyte-specific hormones or the responsiveness to lipolytic drugs, and evidence of the expression of adipocyte-specific genes on the mRNA and protein level so far are rare. Stem cells, especially MSCs, represent an attractive alternative for adipose tissue engineering. As yet, MSCs have been applied in the fields of bone [196-201], cartilage [202-205], and tendon [206] engineering. The *in vitro* study on adipose tissue engineering performed in our laboratory provides promising results for future research (Chapter 7). An overview of representative examples of engineered adipose tissue constructs using different cell types and strategies is shown in Figure 5.

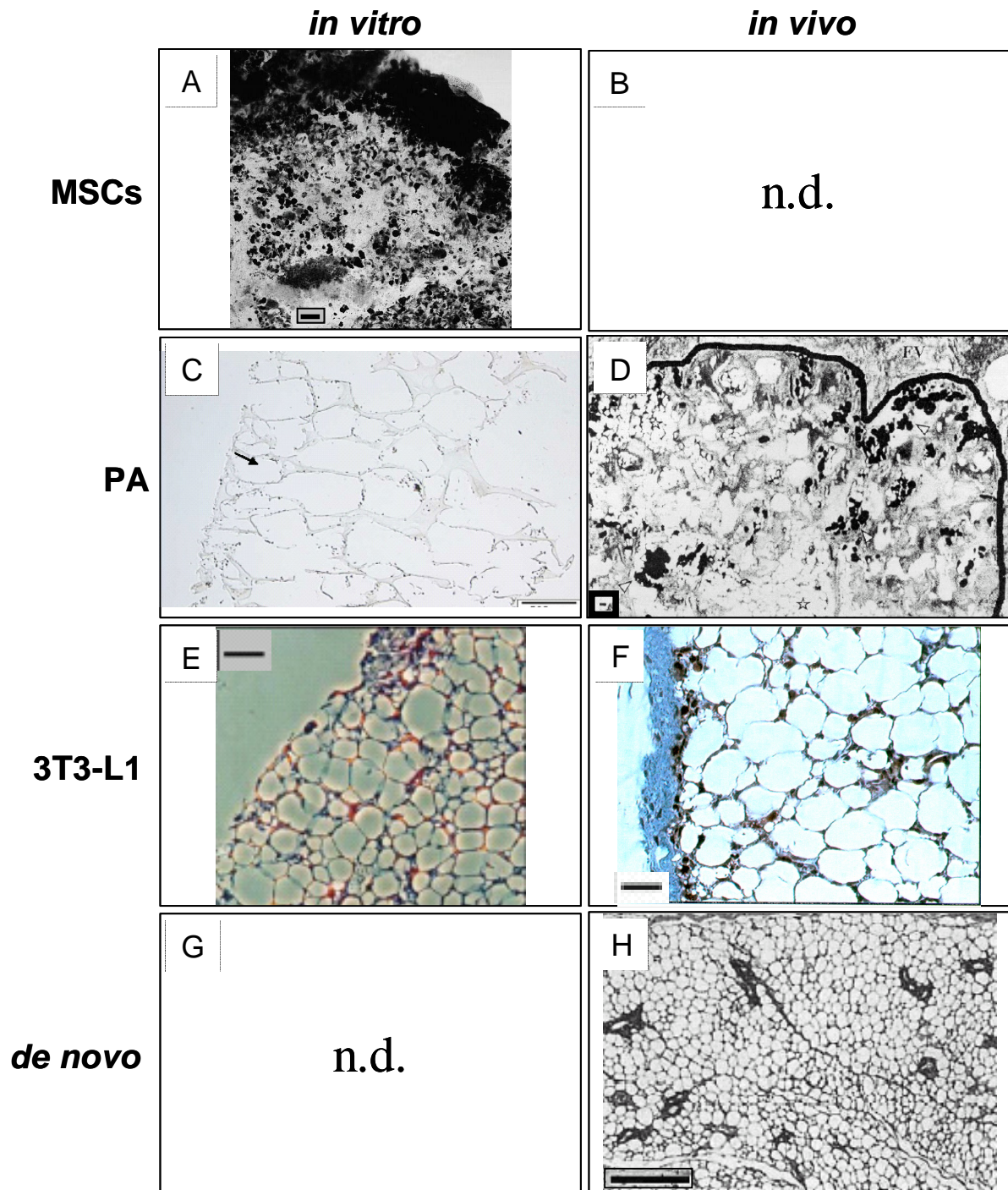


Fig. 5 Overview of *in vitro* and *in vivo* engineered adipose tissue constructs using MSCs, primary preadipocytes, and the preadipocytic cell line 3T3-L1 as cell sources (A-F). Furthermore, adipose tissue obtained by a *de novo* adipogenesis approach is shown (H). Sections were stained with H&E (E-H) or OsO₄ (A-D). Scale bars represent 100 μ m (A), 500 μ m (C), 50 μ m (D,E), 30 μ m (F), and 200 μ m (H). Pictures originate from [Chapter 7] (A), [68] (C), [67] (D), [78] (E,F), [175] (H).

Many biomaterials tested appear to be promising for the use in adipose tissue engineering *in vitro* and *in vivo*. So far, the focus has been on traditional materials such as PLGA, collagen, hyaluronic acid, alginate, and fibrin. Potential progress in this respect is based on the surface modification of these or alternative materials. The modification, for example, may aim at the enhancement of cell adhesion by the application of adhesion peptides such as the RGD motif. Principally, RGD peptides can be adsorbed or covalently bound to substrates, as already shown in one study on adipose tissue engineering by Halberstadt et al. [66]. Furthermore, adipocyte precursor cell adhesion, proliferation, and differentiation can strongly be influenced by components of the ECM which play a pivotal role in the adipocyte development [191-194]. Materials comprising such components or parts of them may improve adipose tissue development. Angiogenesis turns out to be a key process in fat development *in vivo*. Many attempts in fat engineering achieve a considerable degree of vascularized tissue. The delivery of angiogenic factors such as VEGF, bFGF, and PDGF with controlled release devices may be a useful tool to induce or enhance angiogenesis. Tabatas group demonstrated the superiority of controlled released bFGF as compared to the administration of the free growth factor in the *de novo* genesis of vascularized adipose tissue [174,175] and in the *in vivo* formation of fat tissue following implantation of preadipocytes [71]. Recently developed vascularization models will be helpful for the further elucidation of angiogenesis and its affecting factors in adipose tissue [207,208].

In conclusion, a variety of promising approaches have emerged in adipose tissue engineering with the goal of generating fat surrogates for reconstructive and plastic surgery as well as for use in basic research. Up to now, approaches for *de novo* adipogenesis appear to be most promising in regard to the degree of vascularization and long-term maintenance of engineered fat. For cell-based therapies, preadipocytes and stem cells in combination with various materials are useful for gaining knowledge on cell-biomaterial interactions, appropriate materials and culture conditions, and many more parameters. It is difficult to compare the results that have been presented, because different cells, materials, scaffold types and sizes, pore sizes, seeding techniques, cell numbers, and inducing regimens have been employed (Table 1 and 2). Cell-based engineered surrogates have to be optimized in regard to long-term maintenance and optimum vascularization in order to provide a superior substitute to the current surgical gold-standard, the autologous fat graft.

References

- [1] American Society of Plastic Surgeons. (2003) Statistics of the American Society of Plastic Surgeons. <http://www.plasticsurgery.org>.
- [2] Patrick CWJ. 'Adipose tissue engineering: the future of breast and soft tissue reconstruction following tumor resection'. *Semin Surg Oncol* (2000); **19**: 302-311.
- [3] Patrick CW, Jr. 'Tissue engineering strategies for adipose tissue repair'. *Anat Rec* (2001); **263**: 361-366.
- [4] Hotamisligil GS. 'Molecular mechanisms of insulin resistance and the role of the adipocyte'. *Int J Obes Relat Metab Disord* (2000); **24**: S23-S27.
- [5] Morrison RF, Farmer SR. 'Hormonal signaling and transcriptional control of adipocyte differentiation'. *J Nutr* (2000); **130**: 3116S-3121S.
- [6] Trayhurn P, Beattie JH. 'Physiological role of adipose tissue: white adipose tissue as an endocrine and secretory organ'. *Proc Nutr Soc* (2001); **60**: 329-339.
- [7] Flier JS. 'The adipocyte: storage depot or node on the energy information superhighway?'. *Cell* (1995); **80**: 15-18.
- [8] Mora S, Pessin JE. 'An adipocentric view of signaling and intracellular trafficking'. *Diabetes Metab Res Rev* (2002); **18**: 345-356.
- [9] Morrison RF, Farmer SR. 'Insights into the transcriptional control of adipocyte differentiation'. *J Cell Biochem* (1999); **Suppl 32/33**: 59-67.
- [10] Kim S, Moustaid-Moussa N. 'Secretory, endocrine and autocrine/paracrine function of the adipocyte'. *J Nutr* (2000); **130**: 3110S-3115S.
- [11] Smahel J. 'Adipose tissue in plastic surgery'. *Ann Plast Surg* (1986); **16**: 444-453.
- [12] Billings E Jr, May JW, Jr. 'Historical review and present status of free fat graft autotransplantation in plastic and reconstructive surgery'. *Plast Reconstr Surg* (1989); **83**: 368-381.
- [13] Ellenbogen R. 'Fat transfer: current use in practice'. *Clin Plast Surg* (2000); **27**: 545-556.
- [14] Katz AJ, Lull R, Hedrick MH, Futrell JW. 'Emerging approaches to the tissue engineering of fat'. *Clin Plast Surg* (1999); **26**: 587-603.
- [15] Nishimura T, Hashimoto H, Nakanishi I, Furukawa M. 'Microvascular angiogenesis and apoptosis in the survival of free fat grafts'. *Laryngoscope* (2000); **110**: 1333-1338.
- [16] Patrick CW, Jr., Chauvin PB, Robb G.L. 'Tissue engineered adipose tissue'. In: Patrick CW, Jr., Mikos AG, McIntire L.V., editors. *Frontiers in tissue engineering*. Oxford: Elsevier Science, 1998. p. 369-382.

- [17] Ailhaud G, Grimaldi P, Negrel R. 'Cellular and molecular aspects of adipose tissue development'. *Annu Rev Nutr* (1992); **12**: 207-233.
- [18] Lowell BB, Flier JS. 'Brown adipose tissue, beta 3-adrenergic receptors, and obesity'. *Annual Review of Medicine* (1997); **48**: 307-316.
- [19] Rosen ED, Spiegelman BM. 'Molecular Regulation of Adipogenesis'. *Annu Rev Cell Dev Biol* (2000); **16**: 145-171.
- [20] Kühnel, W. 'Binde- und Stützgewebe'. In: Kühnel, W. *Taschenatlas der Zytologie, Histologie und mikroskopischen Anatomie*. Stuttgart, New York: Thieme, 1999. p.96-153.
- [21] Pond CM. 'Physiological specialisation of adipose tissue'. *Prog Lipid Res* (1999); **38**: 225-248.
- [22] Crandall DL, Hausman GJ, Kral JG. 'A review of the microcirculation of adipose tissue: anatomic, metabolic, and angiogenic perspectives'. *Microcirculation* (1997); **4**: 211-232.
- [23] Lau DCW. 'Adipose tissue growth and differentiation: view from the chair'. *Int J Obes Relat Metab Disord* (2000); **24**: S20-S22.
- [24] Gregoire FM, Smas CM, Sul HS. 'Understanding adipocyte differentiation'. *Physiol Rev* (1998); **78**: 783-809.
- [25] Smas CM, Sul HS. 'Control of adipocyte differentiation'. *Biochem J* (1995); **309**: 697-710.
- [26] Brun RP, Spiegelman BM. 'PPAR γ and the molecular control of adipogenesis'. *J Endocrinol* (1997); **155**: 217-218.
- [27] Tontonoz P, Hu E, Spiegelman BM. 'Stimulation of adipogenesis in fibroblasts by PPAR γ 2, a lipid-activated transcription factor'. *Cell* (1994); **79**: 1147-1156.
- [28] Lane MD, Tang QQ, Jiang MS. 'Role of the CCAAT enhancer binding proteins (C/EBPs) in adipocyte differentiation'. *Biochem Biophys Res Commun* (1999); **266**: 677-683.
- [29] Darlington GJ, Ross SE, MacDougald OA. 'The Role of C/EBP Genes in Adipocyte Differentiation'. *J Biol Chem* (1998); **273**: 30057-30060.
- [30] Lin FT, Lane MD. 'CCAAT/enhancer binding protein α is sufficient to initiate the 3T3-L1 adipocyte differentiation program'. *Proc Natl Acad Sci USA* (1994); **91**: 8757-8761.
- [31] Wu Z, Xie Y, Bucher NL, Farmer SR. 'Conditional ectopic expression of C/EBP β in NIH-3T3 cells induces PPAR γ and stimulates adipogenesis'. *Genes Dev* (1995); **9**: 2350-2363.
- [32] Brown MS, Goldstein JL. 'The SREBP pathway: regulation of cholesterol metabolism by proteolysis of a membrane-bound transcription factor'. *Cell* (1997); **89**: 331-340.

- [33] Kim JB, Spiegelman BM. 'ADD1/SREBP1 promotes adipocyte differentiation and gene expression linked to fatty acid metabolism'. *Genes Dev* (1996); **10**: 1096-1107.
- [34] Brun RP, Kim JB, Hu E, Altiook S, Spiegelman BM. 'Adipocyte differentiation: a transcriptional regulatory cascade'. *Curr Opin Cell Biol* (1996); **8**: 826-832.
- [35] Amri EZ, Dani C, Doglio A, Etienne J, Grimaldi P, Ailhaud G. 'Adipose cell differentiation: evidence for a two-step process in the polyamine-dependent Ob1754 clonal line'. *Biochem J* (1986); **238**: 115-122.
- [36] Smas CM, Kachinskas D, Liu CM, Xie X, Dircks LK, Sul HS. 'Transcriptional control of the pref-1 gene in 3T3-L1 adipocyte differentiation. Sequence requirement for differentiation-dependent suppression'. *J Biol Chem* (1998); **273**: 31751-31758.
- [37] Lin F, MacDougald OA, Diehl AM, Lane MD. 'A 30-kDa alternative translation product of the CCAAT/enhancer binding protein α message: Transcriptional activator lacking antimitotic activity'. *Proc Natl Acad Sci USA* (1993); **90**: 9606-9610.
- [38] Wu Z, Bucher NL, Farmer SR. 'Induction of peroxisome proliferator-activated receptor γ during the conversion of 3T3 fibroblasts into adipocytes is mediated by C/EBP β , C/EBP δ , and glucocorticoids'. *Mol Cell Biol* (1996); **16**: 4128-4136.
- [39] Wu Z, Rosen ED, Brun R, Hauser S, Adelmant G, Troy AE, McKeon C, Darlington GJ, Spiegelman BM. 'Cross-regulation of C/EBP α and PPAR γ controls the transcriptional pathway of adipogenesis and insulin sensitivity'. *Mol Cell* (1999); **3**: 151-158.
- [40] Fajas L, Schoonjans K, Gelman L, Kim JB, Najib J, Martin G, Fruchart JC, Briggs M, Spiegelman BM, Auwerx et a. 'Regulation of peroxisome proliferator-activated receptor γ expression by adipocyte differentiation and determination factor 1/sterol regulatory element binding protein 1: Implications for adipocyte differentiation and metabolism'. *Mol Cell Biol* (1999); **19**: 5495-5503.
- [41] Kim JB, Wright HM, Wright M, Spiegelman BM. 'ADD1/SREBP1 activates PPAR γ through the production of endogenous ligand'. *Proc Natl Acad Sci USA* (1998); **95**: 4333-4337.
- [42] Smas CM, Chen L, Zhao L, Latasa MJ, Sul HS. 'Transcriptional repression of pref-1 by glucocorticoids promotes 3T3-L1 adipocyte differentiation'. *J Biol Chem* (1999); **274**: 12632-12641.
- [43] Cao Z, Umek RM, McKnight SL. 'Regulated expression of three C/EBP isoforms during adipose conversion of 3T3-L1 cells'. *Genes Dev* (1991); **5**: 1538-1552.
- [44] Tang QQ, Jiang MS, Lane MD. 'Repressive effect of Sp1 on the C/EBP α gene promoter: role in adipocyte differentiation'. *Mol Cell Biol* (1999); **19**: 4855-4865.

- [45] Kliewer SA, Willson TM. 'The nuclear receptor PPAR γ - bigger than fat'. *Curr Opin Genet Dev* (1998); **8**: 576-581.
- [46] Lehmann JM, Lenhard JM, Oliver BB, Ringold GM, Kliewer SA. 'Peroxisome Proliferator-activated receptors α and γ are activated by indomethacin and other non-steroidal anti-inflammatory drugs'. *J Biol Chem* (1997); **272**: 3406-3410.
- [47] Rangwala SM, Lazar MA. 'Transcriptional control of adipogenesis'. *Annu Rev Nutr* (2000); **20**: 535-559.
- [48] MacDougald OA, Lane MD. 'Transcriptional regulation of gene expression during adipocyte differentiation'. *Annu Rev Biochem* (1995); **64**: 345-373.
- [49] Loftus TM, Lane MD. 'Modulating the transcriptional control of adipogenesis'. *Curr Opin Genet Dev* (1997); **7**: 603-608.
- [50] Cornelius P, MacDougald OA, Lane MD. 'Regulation of adipocyte development'. *Annu Rev Nutr* (1994); **14**: 99-129.
- [51] Tong Q, Hotamisligil GS. 'Molecular mechanisms of adipocyte differentiation'. *Rev Endocr Metabol Disord* (2001); **2**: 349-355.
- [52] Mandrup S, Lane MD. 'Regulating Adipogenesis'. *J Biol Chem* (1997); **272**: 5367-5370.
- [53] Ailhaud G. 'Molecular mechanisms of adipocyte differentiation'. *J Endocrinol* (1997); **155**: 201-202.
- [54] Auwerx J, Martin G, Guerre-Millo M, Staels B. 'Transcription, adipocyte differentiation, and obesity'. *J Mol Med* (1996); **74**: 347-352.
- [55] Gregoire FM. 'Adipocyte differentiation: from fibroblast to endocrine cell'. *Exp Biol Med* (2001); **226**: 997-1002.
- [56] Griffith LG, Naughton G. 'Tissue Engineering - current challenges and expanding opportunities'. *Science* (2002); **295**: 1009-1014.
- [57] Langer R, Vacanti JP. 'Tissue engineering'. *Science* (1993); **260**: 920-926.
- [58] Tabata Y. 'Recent progress in tissue engineering'. *Drug Discov Today* (2001); **6**: 483-487.
- [59] Curtis A, Riehle M. 'Tissue engineering: the biophysical background'. *Phys Med Biol* (2001); **46**: R47-R65.
- [60] Bonassar LJ, Vacanti CA. 'Tissue engineering: the first decade and beyond'. *J Cell Biochem* (1998); **Suppl. 30/31**: 297-303.
- [61] Heath CA. 'Cells for tissue engineering'. *Trends Biotechnol* (2000); **18**: 17-19.
- [62] Beahm EK, Walton RL, Patrick CW, Jr. 'Progress in adipose tissue construct development'. *Clin Plast Surg* (2003); **30**: 547-58.

- [63] Patrick CW, Jr., Chauvin PB, Hobley J, Reece GP. 'Preadipocyte seeded PLGA scaffolds for adipose tissue engineering'. *Tissue Eng* (2001); **5**: 139-151.
- [64] Schoeller T, Lille S, Wechselberger G, Otto A, Mowlawi A, Piza-Katzer H. 'Histomorphologic and volumetric analysis of implanted autologous preadipocyte cultures suspended in fibrin glue: a potential new source for tissue augmentation'. *Aesthetic Plast Surg* (2001); **25**: 57-63.
- [65] von Heimburg D, Zachariah S, Low A, Pallua N. 'Influence of different biodegradable carriers on the *in vivo* behavior of human adipose precursor cells'. *Plast Reconstr Surg* (2001); **108**: 411-420.
- [66] Halberstadt C, Austin C, Rowley J, Culberson C, Loeb sack A, Wyatt S, Coleman S, Blacksten L, Burg K, Mooney et a. 'A hydrogel material for plastic and reconstructive applications injected into the subcutaneous space of a sheep'. *Tissue Eng* (2002); **8**: 309-319.
- [67] Patrick CW, Jr., Zheng B, Johnston C, Reece GP. 'Long-term implantation of preadipocyte-seeded PLGA scaffolds'. *Tissue Eng* (2002); **8**: 283-293.
- [68] Halbleib M, Skurk T, de Luca C, von Heimburg D, Hauner H. 'Tissue engineering of white adipose tissue using hyaluronic acid-based scaffolds. I: *in vitro* differentiation of human adipocyte precursor cells on scaffolds'. *Biomaterials* (2003); **24**: 3125-3132.
- [69] von Heimburg D, Kuberka M, Rendchen R, Hemmrich K, Rau G, Pallua N. 'Preadipocyte-loaded collagen scaffolds with enlarged pore size for improved soft tissue engineering'. *Int J Artif Organs* (2003); **26**: 1064-1076.
- [70] Fischbach C, Seufert J, Staiger H, Hacker M, Neubauer M, Goepferich A, Blunk T. 'Three-dimensional *in vitro* model of adipogenesis: Comparison of culture conditions'. *Tissue Eng* (2004); **10**: 215-229.
- [71] Kimura Y, Ozeki M, Inamoto T, Tabata Y. 'Adipose tissue engineering based on human preadipocytes combined with gelatin microspheres containing basic fibroblast growth factor'. *Biomaterials* (2003); **24**: 2513-2521.
- [72] Sugihara H, Toda S, Yonemitsu N, Watanabe K. 'Effects of fat cells on keratinocytes and fibroblasts in a reconstructed rat skin model using collagen gel matrix culture'. *Br J Dermatol* (2001); **144**: 244-253.
- [73] Kawaguchi N, Toriyama K, Nicodemou-Lena E, Inou K, Torii S, Kitagawa Y. 'Reconstituted basement membrane potentiates *in vivo* adipogenesis of 3T3-F442A cells'. *Cytotechnology* (1999); **31**: 215-220.
- [74] Yuksel E, Weinfeld AB, Cleek R, Wamsley S, Jensen J, Boutros S, Waugh JM, Shenaq SM, Spira M. 'Increased free fat-graft survival with the long-term, local delivery of insulin,

insulin-like growth factor-I, and basic fibroblast growth factor by PLGA/PEG microspheres'. *Plast Reconstr Surg* (2000); **105**: 1712-1720.

[75] Huss FR, Kratz G. 'Mammary epithelial cell and adipocyte co-culture in a 3-D matrix: the first step towards tissue-engineered human breast tissue'. *Cells Tissues Organs* (2001); **169**: 361-367.

[76] Kral JG, Crandall DL. 'Development of a human adipocyte synthetic polymer scaffold'. *Plast Reconstr Surg* (1999); **104**: 1732-1738.

[77] von Heimburg D, Zachariah S, Kuhling H, Heschel I, Schoof H, Hafemann B, Pallua N. 'Human preadipocytes seeded on freeze-dried collagen scaffolds investigated *in vitro* and *in vivo*'. *Biomaterials* (2001); **22**: 429-438.

[78] Fischbach C, Spruss T, Weiser B, Neubauer M, Becker C, Hacker M, Gopferich A, Blunk T. 'Generation of mature fat pads *in vitro* and *in vivo* utilizing 3-D long-term culture of 3T3-L1 preadipocytes'. *Exp Cell Res* (2004); **300**: 54-64.

[79] Sugihara H, Yonemitsu N, Toda S, Miyabara S, Funatsumaru S, Matsumoto T. 'Unilocular fat cells in three-dimensional collagen gel matrix culture'. *J Lipid Res* (1988); **29**: 691-697.

[74] Yuksel E, Weinfeld AB, Cleek R, Wamsley S, Jensen J, Boutros S, Waugh JM, Shenaq SM, Spira M. 'Increased free fat-graft survival with the long-term, local delivery of insulin, insulin-like growth factor-I, and basic fibroblast growth factor by PLGA/PEG microspheres'. *Plast Reconstr Surg* (2000); **105**: 1712-1720.

[81] Butterwith SC, Goddard C. 'Regulation of DNA synthesis in chicken adipocyte precursor cells by insulin-like growth factors, platelet-derived growth factor and transforming growth factor- β '. *J Endocrinol* (1991); **131**: 203-209.

[82] Butterwith SC, Peddie CD, Goddard C. 'Regulation of adipocyte precursor DNA synthesis by acidic and basic fibroblast growth factors: Interaction with heparin and other growth factors'. *J Endocrinol* (1993); **137**: 369-374.

[83] Reyne Y, Nougues J, Dolor JP. 'Differentiation of rabbit adipocyte precursor cells in a serum-free medium'. *In Vitro Cell Dev Biol* (1989); **25**: 747-752.

[84] Wiederer O, Loffler G. 'Hormonal regulation of the differentiation of rat adipocyte precursor cells in primary culture'. *J Lipid Res* (1987); **28**: 649-658.

[85] Adams M, Montague CT, Prins JB, Holder JC, Smith SA, Sanders L, Digby JE, Sewter CP, Lazar MA, Chatterjee VK, O'Rahilly S. 'Activators of peroxisome proliferator-activated receptor γ have depot-specific effects on human preadipocyte differentiation'. *J Clin Invest* (1997); **100**: 3149-3153.

- [86] Gharbi-Chihi J, Teboul M, Bismuth J, Bonne J, Torresani J. 'Increase of adipose differentiation by hypolipidemic fibrate drugs in Ob 17 preadipocytes: requirement for thyroid hormones'. *Biochim Biophys Acta* (1993); **1177**: 8-14.
- [87] Smyth MJ, Wharton W. 'Multiparameter flow cytometric analysis of the effects of indomethacin on adipocyte differentiation in A31T6 cells'. *Cell Prolif* (1993); **26**: 103-114.
- [88] Shenaq SM, Yuksel E. 'New research in breast reconstruction: adipose tissue engineering'. *Clin Plast Surg* (2002); **29**: 111-125.
- [89] Hauner H, Roehrig K, Petruschke T. 'Effects of epidermal growth factor (EGF), platelet-derived growth factor (PDGF) and fibroblast growth factor (FGF) on human adipocyte development and function'. *Eur J Clin Invest* (1995); **25**: 90-96.
- [90] Roncari DA, Le Blanc PE. 'Inhibition of rat perirenal preadipocyte differentiation'. *Biochem Cell Biol* (1990); **68**: 238-242.
- [91] Petruschke T, Hauner H. 'Tumor necrosis factor- α prevents the differentiation of human adipocyte precursor cells and causes delipidation of newly developed fat cells'. *J Clin Endocrinol Metab* (1993); **76**: 742-747.
- [92] Petruschke T, Rohrig K, Hauner H. 'Transforming growth factor β (TGF- β) inhibits the differentiation of human adipocyte precursor cells in primary culture'. *Int J Obes Relat Metab Disord* (1994); **18**: 532-536.
- [93] Schmidt W, Poll-Jordan G, Loffler G. 'Adipose conversion of 3T3-L1 cells in a serum-free culture system depends on epidermal growth factor, insulin-like growth factor I, corticosterone, and cyclic AMP'. *J Biol Chem* (1990); **265**: 15489-15495.
- [94] Cousin B, Casteilla L, Dani C, Muzzin P, Revelli JP, Penicaud L. 'Adipose tissues from various anatomical sites are characterized by different patterns of gene expression and regulation'. *Biochem J* (1993); **292**: 873-876.
- [95] Hauner H, Entenmann G. 'Regional variation of adipose differentiation in cultured stromal-vascular cells from the abdominal and femoral adipose tissue of obese women'. *Int J Obes Relat Metab Disord* (1991); **15**: 121-126.
- [96] Kirkland JL, Hollenberg CH, Gillon WS. 'Effects of fat depot site on differentiation-dependent gene expression in rat preadipocytes'. *Int J Obes Relat Metab Disord* (1996); **20**: S102-S107.
- [97] Hauner H, Wabitsch M, Pfeiffer EF. 'Differentiation of adipocyte precursor cells from obese and nonobese adult women and from different adipose tissue sites'. *Horm Metab Res* (1988); **19**: 35-39.

- [98] National Institute of Health (Kirschstein R, Skirboll LR.). (2001) Stem cells: Scientific progress and future research directions. <http://www.nih.gov/news/stemcell/scireport.htm>.
- [99] Caplan AI, Bruder SP. 'Mesenchymal stem cells: building blocks for molecular medicine in the 21st century'. *Trends Mol Med* (2001); **7**: 259-264.
- [100] Friedenstein AJ, Piatetzky-Shapiro II, Petrakova KV. 'Osteogenesis in transplants of bone marrow cells'. *J Embryol Exp Morphol* (1966); **16**: 381-390.
- [101] Owen M. 'Marrow stromal stem cells'. *J Cell Sci Suppl* (1988); **10**: 63-76.
- [102] Pittenger MF, Mackay AM, Beck SC, Jaiswal RK, Douglas R, Mosca JD, Moorman MA, Simonetti DW, Craig S, Marshak DR. 'Multilineage potential of adult human mesenchymal stem cells'. *Science* (1999); **284**: 143-147.
- [103] Gritti A, Vescovi AL, Galli R. 'Adult neural stem cells: plasticity and developmental potential'. *J Physiol* (2002); **96**: 81-90.
- [104] O'Brien K, Muskiewicz K, Gussoni E. 'Recent advances in and therapeutic potential of muscle-derived stem cells'. *J Cell Biochem* (2002); 80-87.
- [105] Gimble JM. 'Adipose tissue-derived therapeutics'. *Expert Opin Biol Ther* (2003); **3**: 705-713.
- [106] Kuznetsov SA, Mankani MH, Gronthos S, Satomura K, Bianco P, Robey PG. 'Circulating Skeletal Stem Cells'. *J Cell Biol* (2001); **153**: 1133-1140.
- [107] Forbes S, Vig P, Poulsom R, Thomas H, Alison M. 'Hepatic stem cells'. *J Pathol* (2002); **197**: 510-518.
- [108] Janes SM, Lowell S, Hutter C. 'Epidermal stem cells'. *J Pathol* (2002); **197**: 479-491.
- [109] Bianco P, Riminucci M, Gronthos S, Robey PG. 'Bone Marrow Stromal Stem Cells: Nature, Biology, and Potential Applications'. *Stem Cells* (2001); **19**: 180-192.
- [110] Friedenstein AJ, Chailakhjan RK, Lalykina KS. 'The development of fibroblast colonies in monolayer cultures of guinea-pig bone marrow and spleen cells'. *Cell Tissue Kinet* (1970); **3**: 393-403.
- [111] Owen ME, Cave J, Joyner CJ. 'Clonal analysis *in vitro* of osteogenic differentiation of marrow CFU-F'. *J Cell Sci* (1987); **87**: 731-738.
- [112] Devine SM. 'Mesenchymal stem cells: will they have a role in the clinic?'. *J Cell Biochem* (2002); 73-79.
- [113] Deans RJ, Moseley AB. 'Mesenchymal stem cells. Biology and potential clinical uses'. *Exp Hematol* (2000); **28**: 875-884.

- [114] Friedenstein AJ, Deriglasova UF, Kulagina NN, Panasuk AF, Rudakowa SF, Luria EA, Ruadkow IA. 'Precursors for fibroblasts in different populations of hematopoietic cells as detected by the *in vitro* colony assay method'. *Exp Hematol* (1974); **2**: 83-92.
- [115] Gronthos S, Graves SE, Ohta S, Simmons PJ. 'The STRO-1+ fraction of adult human bone marrow contains the osteogenic precursors'. *Blood* (1994); **84**: 4164-4173.
- [116] Colter DC, Sekiya I, Prockop DJ. 'Identification of a subpopulation of rapidly self-renewing and multipotential adult stem cells in colonies of human marrow stromal cells'. *Proc Natl Acad Sci USA* (2001); **98**: 7841-7845.
- [117] Gronthos S, Franklin DM, Leddy HA, Robey PG, Storms RW, Gimble JM. 'Surface protein characterization of human adipose tissue-derived stromal cells'. *J Cell Physiol* (2001); **189**: 54-63.
- [118] Zuk PA, Zhu M, Mizuno H, Huang J, Futrell JW, Katz AJ, Benhaim P, Lorenz HP, Hedrick MH. 'Multilineage cells from human adipose tissue: Implications for cell-based therapies'. *Tissue Eng* (2001); **7**: 211-228.
- [119] Bruder SP, Jaiswal N, Haynesworth SE. 'Growth kinetics, self-renewal, and the osteogenic potential of purified human mesenchymal stem cells during extensive subcultivation and following cryopreservation'. *J Cell Biochem* (1997); **64**: 278-294.
- [120] Satomura K, Derubeis AR, Fedarko NS, Ibaraki-O'Connor K, Kuznetsov SA, Rowe DW, Young MF, Robey PG. 'Receptor tyrosine kinase expression in human bone marrow stromal cells'. *J Cell Physiol* (2001); **177**: 426-438.
- [121] Kuznetsov SA, Friedenstein AJ, Robey PG. 'Factors required for bone marrow stromal fibroblast colony formation *in vitro*'. *Br J Haematol* (1997); **97**: 561-570.
- [122] van den Bos C, Mosca JD, Winkles J, Kerrigan L, Burgess WH, Marshak DR. 'Human mesenchymal stem cells respond to fibroblast growth factors'. *Hum Cell* (2002); **10**: 45-50.
- [123] Locklin RM, Oreffo ROC, Triffitt JT. 'Effects of TGF β and bFGF on the differentiation of human bone marrow stromal fibroblasts'. *Cell Biol Int* (1999); **23**: 185-194.
- [124] Scutt A, Bertram P. 'Basic fibroblast growth factor in the presence of dexamethasone stimulates colony formation, expansion, and osteoblastic differentiation by rat bone marrow stromal cells'. *Calcif Tissue Int* (1999); **64**: 69-77.
- [125] Tsutsumi S, Shimazu A, Miyazaki K, Pan H, Koike C, Yoshida E, Takagishi K, Kato Y. 'Retention of multilineage differentiation potential of mesenchymal cells during proliferation in response to FGF'. *Biochem Biophys Res Commun* (2001); **288**: 413-419.

- [126] Martin I, Muraglia A, Campanile G, Cancedda R, Quarto R. 'Fibroblast growth factor-2 supports *ex vivo* expansion and maintenance of osteogenic precursors from human bone marrow'. *Endocrinology* (1997); **138**: 4456-4462.
- [127] Mastrogiacomo M, Cancedda R, Quarto R. 'Effect of different growth factors on the chondrogenic potential of human bone marrow stromal cells'. *Osteoarthritis and Cartilage* (2001); **9**: S36-S40.
- [128] Gronthos S, Simmons PJ. 'The growth factor requirements of STRO-1-positive human bone marrow stromal precursors under serum-deprived conditions *in vitro*'. *Blood* (1995); **85**: 929-940.
- [129] Cassiede P, Dennis JE, Ma F, Caplan AI. 'Osteochondrogenic potential of marrow mesenchymal progenitor cells exposed to TGF- β 1 or PDGF-BB as assayed *in vivo* and *in vitro*'. *J Bone Miner Res* (1996); **11**: 1264-1273.
- [130] Tanaka H, Liang CT. 'Effect of platelet-derived growth factor on DNA synthesis and gene expression in bone marrow stromal cells derived from adult and old rats'. *J Cell Physiol* (1995); **164**: 367-375.
- [131] Lisignoli G, Remiddi G, Cattini L, Cocchini B, Zini N, Fini M, Grassi F, Piacentini A, Facchini A. 'An elevated number of differentiated osteoblast colonies can be obtained from rat bone marrow stromal cells using a gradient isolation procedure'. *Connect Tissue Res* (2001); **42**: 49-58.
- [132] Cassiede P, Dennis JE, Ma F, Caplan AI. 'Osteochondrogenic potential of marrow mesenchymal progenitor cells exposed to TGF- β 1 or PDGF-BB as assayed *in vivo* and *in vitro*'. *J Bone Miner Res* (1996); **11**: 1264-1273.
- [133] Bianchi G, Banfi A, Mastrogiacomo M, Notaro R, Luzzatto L, Cancedda R, Quarto R. 'Ex vivo enrichment of mesenchymal cell progenitors by fibroblast growth factor 2'. *Exp Cell Res* (2003); **287**: 98-105.
- [134] Stenderup K, Justesen J, Clausen C, Kassem M. 'Aging is associated with decreased maximal life span and accelerated senescence of bone marrow stromal cells'. *Bone* (2003); **33**: 919-926.
- [135] Zimmermann S, Voss M, Kaiser S, Kapp U, Waller CF, Martens UM. 'Lack of telomerase activity in human mesenchymal stem cells'. *Leukemia* (2003); **17**: 1146-1149.
- [136] Simonsen JL, Rosada C, Serakinci N, Justesen J, Stenderup K, Rattan SIS, Jensen TG, Kassem M. 'Telomerase expression extends the proliferative life-span and maintains the osteogenic potential of human bone marrow stromal cells'. *Nat Biotechnol* (2002); **20**: 592-596.

- [137] Mihara K, Imai C, Coustan-Smith E, Dome JS, Dominici M, Vanin E, Campana D. 'Development and functional characterization of human bone marrow mesenchymal cells immortalized by enforced expression of telomerase'. *Br J Haematol* (2003); **120**: 846-849.
- [138] Minguell JJ, Erices A, Conget P. 'Mesenchymal stem cells'. *Exp Biol Med* (2001); **226**: 507-520.
- [139] Clarke D, Frisen J. 'Differentiation potential of adult stem cells'. *Curr Opin Genet Dev* (2001); **11**: 575-580.
- [140] Verfaillie CM. 'Adult stem cells: assessing the case for pluripotency'. *Trends Cell Biol* (2002); **12**: 502-508.
- [141] Jiang Y, Jahagirdar BN, Reinhardt RL, Schwartz RE, Keene CD, Ortiz-Gonzalez XR, Reyes M, Lenvik T, Lund T, Blackstad M, Du J, Aldrich S, Lisberg A, Low WC, Largaespada DA, Verfaillie CM. 'Pluripotency of mesenchymal stem cells derived from adult marrow'. *Nature* (2002); **418**: 41-49.
- [142] Muraglia A, Cancedda R, Quarto R. 'Clonal mesenchymal progenitors from human bone marrow differentiate *in vitro* according to a hierarchical model'. *J Cell Sci* (2000); **113**: 1161-1166.
- [143] Nuttall ME, Patton AJ, Olivera DL, Nadeau DP, Gowen M. 'Human trabecular bone cells are able to express both osteoblastic and adipocytic phenotype: implications for osteopenic disorders'. *J Bone Miner Res* (1998); **13**: 371-382.
- [144] Janderova L, McNeil M, Murrell AN, Mynatt RL, Smith SR. 'Human mesenchymal stem cells as an *in vitro* model for human adipogenesis'. *Obes Res* (2003); **11**: 65-74.
- [145] Gimble JM, Robinson CE, Wu X, Kelly KA, Rodriguez BR, Kliewer SA, Lehmann JM, Morris DC. 'Peroxisome proliferator-activated receptor- γ activation by thiazolidinediones induces adipogenesis in bone marrow stromal cells'. *Mol Pharmacol* (1996); **50**: 1087-1094.
- [146] Sottile V, Seuwen K. 'Bone morphogenetic protein-2 stimulates adipogenic differentiation of mesenchymal precursor cells in synergy with BRL 49653 (rosiglitazone)'. *FEBS Lett* (2000); **475**: 201-204.
- [147] Sen A, Lea-Currie YR, Sujkowska D, Franklin DM, Wilkison WO, Halvorsen YD, Gimble JM. 'Adipogenic potential of human adipose derived stromal cells from multiple donors is heterogeneous'. *J Cell Biochem* (2001); **81**: 312-319.
- [148] Haynesworth SE, Reuben D, Caplan AI. 'Cell-based tissue engineering therapies: the influence of whole body physiology'. *Adv Drug Deliv Rev* (1998); **33**: 3-14.
- [149] Wobus AM. 'Potential of embryonic stem cells'. *Mol Aspects Med* (2001); **22**: 149-164.
- [150] Pedersen RA. 'Embryonic stem cells for medicine'. *Sci Am* (1999); **280**: 68-73.

- [151] Evans MJ, Kaufman MH. 'Establishment in culture of pluripotential cells from mouse embryos'. *Nature* (1981); **292**: 154-156.
- [152] Thomson JA, Itskovitz-Eldor J, Shapiro SS, Waknitz MA, Swiergiel JJ, Marshall VS, Jones JM. 'Embryonic Stem Cell Lines Derived from Human Blastocysts'. *Science* (1998); **282**: 1145-1147.
- [153] Bishop AE, Buttery LDK, Polak JM. 'Embryonic stem cells'. *J Pathol* (2002); **197**: 424-429.
- [154] Prella K, Zink N, Wolf E. 'Pluripotent stem cells--model of embryonic development, tool for gene targeting, and basis of cell therapy'. *Anat Histol Embryol* (2002); **31**: 169-186.
- [155] Rohwedel J, Guan K, Wobus AM. 'Induction of cellular differentiation by retinoic acid *in vitro*'. *Cells Tissues Organs* (1999); **165**: 190-202.
- [156] Dani C, Smith AG, Dessolin S, Leroy P, Staccini L, Villageois P, Darimont C, Ailhaud G. 'Differentiation of embryonic stem cells into adipocytes *in vitro*'. *J Cell Sci* (1997); **110**: 1279-1285.
- [157] Dani C. 'Embryonic stem cell-derived adipogenesis'. *Cells Tissues Organs* (1999); **165**: 173-180.
- [158] Denker H. 'Embryonic stem cells: An exciting field for basic research and tissue engineering, but also an ethical dilemma?'. *Cells Tissues Organs* (1999); **165**: 246-249.
- [159] Vats A, Tolley NS, Polak JM, Gough JE. 'Scaffolds and biomaterials for tissue engineering: a review of clinical applications'. *Clin Otolaryngol* (2003); **28**: 165-172.
- [160] Hutmacher DW. 'Scaffold design and fabrication technologies for engineering tissues. State of the art and future perspectives'. *J Biomat Sci Polym Ed* (2001); **12**: 107-124.
- [161] Liu X, Ma P, X. 'Polymeric scaffolds for bone tissue engineering'. *Ann Biomed Eng* (2004); **32**: 477-486.
- [162] Yang S, Leong KF, Du Z, Chua CK. 'The design of scaffolds for use in tissue engineering. Part I. Traditional factors'. *Tissue Eng* (2001); **7**: 679-689.
- [163] Lucke A, Kiermaier J, Gopferich A. 'Peptide acylation by poly(alpha-hydroxy esters)'. *Pharm Res* (2002); **19**: 175-181.
- [164] Cai K, Yao K, Cui Y, Yang Z, Li X, Xie H, Qing T, Gao L. 'Influence of different surface modification treatments on poly(D,L-lactic acid) with silk fibroin and their effects on the culture of osteoblast *in vitro*'. *Biomaterials* (2002); **23**: 1603-1611.
- [165] Suh H, Hwang YS, Lee JE, Han CD, Park JC. 'Behavior of osteoblasts on a type I atelocollagen grafted ozone oxidized poly L-lactic acid membrane'. *Biomaterials* (2001); **22**: 219-230.

- [166] Nobs L, Buchegger F, Gurny R, Allemann E. 'Surface modification of poly(lactic acid) nanoparticles by covalent attachment of thiol groups by means of three methods'. *Int J Pharm* (2003); **250**: 327-337.
- [167] Badylak SF. 'The extracellular matrix as a scaffold for tissue reconstruction'. *Semin Cell Dev Biol* (2002); **13**: 377-383.
- [168] Lee KY, Mooney DJ. 'Hydrogels for Tissue Engineering'. *Chem Rev* (2001); **101**: 1869-1879.
- [169] Sultzbaugh KJ, Speaker TJ. 'A method to attach lectins to the surface of spermine alginate microcapsules based on the avidin biotin interaction'. *J Microencapsul* (1996); **13**: 363-376.
- [170] Friess W. 'Collagen - biomaterial for drug delivery'. *Eur J Pharm Biopharm* (1998); **45**: 113-136.
- [171] Mizuno M, Shindo M, Kobayashi D, Tsuruga E, Amemiya A, Kuboki Y. 'Osteogenesis by bone marrow stromal cells maintained on type I collagen matrix gels *in vivo*'. *Bone* (1997); **20**: 101-107.
- [172] Miller WH, Jr., Faust IM, Hirsch J. 'Demonstration of de novo production of adipocytes in adult rats by biochemical and radioautographic techniques'. *J Lipid Res* (1984); **25**: 336-347.
- [173] Kawaguchi N, Toriyama K, Nicodemou-Lena E, Inou K, Torii S, Kitagawa Y. '*De novo* adipogenesis in mice at the site of injection of basement membrane and basic fibroblast growth factor'. *Proc Natl Acad Sci USA* (1998); **95**: 1062-1066.
- [174] Kimura Y, Ozeki M, Inamoto T, Tabata Y. 'Time course of *de novo* adipogenesis in matrigel by gelatin microspheres incorporating basic fibroblast growth factor'. *Tissue Eng* (2002); **8**: 603-613.
- [175] Tabata Y, Miyao M, Inamoto T, Ishii T, Hirano Y, Yamaoki Y, Ikada Y. '*De novo* formation of adipose tissue by controlled release of basic fibroblast growth factor'. *Tissue Eng* (2000); **6**: 279-289.
- [176] Yuksel E, Weinfeld AB, Cleek R, Waugh JM, Jensen J, Boutros S, Shenaq SM, Spira M. '*De novo* adipose tissue generation through long-term, local delivery of insulin and insulin-like growth factor-1 by PLGA/PEG microspheres in an *in vivo* rat model: a novel concept and capability'. *Plast Reconstr Surg* (2000); **105**: 1721-1729.
- [177] Masuda T, Furue M, Matsuda T. 'Photocured, styrenated gelatin-based microspheres for *de novo* adipogenesis through corelease of basic fibroblast growth factor, insulin, and insulin-like growth factor I'. *Tissue Eng* (2004); **10**: 523-535.

- [178] Toriyama K, Kawaguchi N, Kitoh J, Tajima R, Inou K, Kitagawa Y, Torii S. 'Endogenous adipocyte precursor cells for regenerative soft-tissue engineering'. *Tissue Eng* (2002); **8**: 157-165.
- [179] Fukumura D, Ushiyama A, Duda DG, Xu L, Tam J, Krishna V, Chatterjee K, Garkavtsev I, Jain RK. 'Paracrine regulation of angiogenesis and adipocyte differentiation during *in vivo* adipogenesis'. *Circ Res* (2003); **93**: e88-e97.
- [180] Rupnick MA, Panigrahy D, Zhang CY, Dallabrida SM, Lowell BB, Langer R, Folkman MJ. 'From the Cover: Adipose tissue mass can be regulated through the vasculature'. *Proc Natl Acad Sci USA* (2002); **99**: 10730-10735.
- [181] Cao R, Brakenhielm E, Wahlestedt C, Thyberg J, Cao Y. 'Leptin induces vascular permeability and synergistically stimulates angiogenesis with FGF-2 and VEGF'. *Proc Natl Acad Sci USA* (2001); **98**: 6390-6395.
- [182] Hutley LJ, Herington AC, Shurety W, Cheung C, Vesey DA, Cameron DP, Prins JB. 'Human adipose tissue endothelial cells promote preadipocyte proliferation'. *Am J Physiol Endocrinol Metab* (2001); **281**: E1037-E1044.
- [183] Varzaneh FE, Shillabeer G, Wong KL, Lau DC. 'Extracellular matrix components secreted by microvascular endothelial cells stimulate preadipocyte differentiation *in vitro*'. *Metabolism* (1994); **43**: 906-912.
- [184] Aoki S, Toda S, Sakemi T, Sugihara H. 'Coculture of endothelial cells and mature adipocytes actively promotes immature preadipocyte development *in vitro*'. *Cell Struct Funct* (2003); **28**: 55-60.
- [185] Dolderer JH, Findlay MW, Cooper-White J, Thompson EW, Trost N, Hennessy O, Penington A, Morrison WA. 'Making tissue engineering for breast reconstruction a reality'. *Cytotherapy* (2004); **3**: 263-263.
- [186] Borges J, Mueller MC, Padron NT, Tegtmeier F, Lang EM, Stark GB. 'Engineered adipose tissue supplied by functional microvessels'. *Tissue Eng* (2003); **9**: 1263-1270.
- [187] Abbott A. 'Cell culture: biology's new dimension'. *Nature* (2003); **424**: 870-872.
- [188] Hishikawa K, Miura S, Marumo T, Yoshioka H, Mori Y, Takato T, Fujita T. 'Gene expression profile of human mesenchymal stem cells during osteogenesis in three-dimensional thermoreversible gelation polymer'. *Biochem Biophys Res Commun* (2004); **317**: 1103-1107.
- [189] Huang W, Carlsen B, Wulur I, Rudkin G, Ishida K, Wu B, Yamaguchi DT, Miller TA. 'BMP-2 exerts differential effects on differentiation of rabbit bone marrow stromal cells

grown in two-dimensional and three-dimensional systems and is required for *in vitro* bone formation in a PLGA scaffold'. *Exp Cell Res* (2004); **299**: 325-334.

[190] McBeath R, Pirone DM, Nelson CM, Bhadriraju K, Chen CS. 'Cell shape, cytoskeletal tension, and RhoA regulate stem cell lineage commitment'. *Dev Cell* (2004); **6**: 483-495.

[191] Nakajima I, Yamaguchi T, Ozutsumi K, Aso H. 'Adipose tissue extracellular matrix: newly organized by adipocytes during differentiation'. *Differentiation* (1998); **63**: 193-200.

[192] Ibrahim A, Bonino F, Bardon S, Ailhaud G, Dani C. 'Essential role of collagens for terminal differentiation of preadipocytes'. *Biochem Biophys Res Commun* (1992); **187**: 1314-1322.

[193] Hausman GJ, Wright JT, Richardson RL. 'The influence of extracellular matrix substrata on preadipocyte development in serum-free cultures of stromal-vascular cells'. *J Anim Sci* (1996); **74**: 2117-2128.

[194] Patrick CW, Jr., Wu X. 'Integrin-mediated preadipocyte adhesion and migration on laminin-1'. *Ann Biomed Eng* (2003); **31**: 505-514.

[195] Boo JS, Yamada Y, Okazaki Y, Hibino Y, Okada K, Hata KI, Yoshikawa T, Sugiura Y, Ueda M. 'Tissue-engineered bone using mesenchymal stem cells and a biodegradable scaffold'. *J Craniofac Surg* (2002); **13**: 231-239.

[196] Bruder SP, Kurth AA, Shea M, Hayes WC, Jaiswal N, Kadiyala S. 'Bone regeneration by implantation of purified, culture-expanded human mesenchymal stem cells'. *J Orthop Res* (1998); **16**: 155-162.

[197] Lisignoli G, Zini N, Remiddi G, Piacentini A, Puggioli A, Trimarchi C, Fini M, Maraldi NM, Facchini A. 'Basic fibroblast growth factor enhances *in vitro* mineralization of rat bone marrow stromal cells grown on non-woven hyaluronic acid based polymer scaffold'. *Biomaterials* (2001); **22**: 2095-2105.

[198] Lisignoli G, Fini M, Giavaresi G, Nicoli AN, Toneguzzi S, Facchini A. 'Osteogenesis of large segmental radius defects enhanced by basic fibroblast growth factor activated bone marrow stromal cells grown on non-woven hyaluronic acid-based polymer scaffold'. *Biomaterials* (2002); **23**: 1043-1051.

[199] Quarto R, Mastrogiacomo M, Cancedda R, Kutepov SM, Mukhachev V, Lavroukov A, Kon E, Marcacci M. 'Repair of large bone defects with the use of autologous bone marrow stromal cells'. *N Engl J Med* (2001); **344**: 385-386.

[200] van den Dolder J, Farber E, Spauwen PHM, Jansen JA. 'Bone tissue reconstruction using titanium fiber mesh combined with rat bone marrow stromal cells'. *Biomaterials* (2003); **24**: 1745-1750.

- [201] Temenoff JS, Park H, Jabbari E, Sheffield TL, LeBaron RG, Ambrose CG, Mikos AG. 'In vitro osteogenic differentiation of marrow stromal cells encapsulated in biodegradable hydrogels'. J Biomed Mater Res (2004); **70A**: 235-244.
- [202] Johnstone B, Hering TM, Caplan AI, Goldberg VM, Yoo JU. 'In vitro chondrogenesis of bone marrow-derived mesenchymal progenitor cells'. Exp Cell Res (1998); **238**: 265-272.
- [203] Martin I, Padera RF, Vunjak-Novakovic G, Freed LE. 'In vitro differentiation of chick embryo bone marrow stromal cells into cartilaginous and bone-like tissues'. J Orthop Res (1998); **16**: 181-189.
- [204] Li W-JW-J, Tuli R, Okafor C, Derfoul A, Danielson KGK, Hall DJD, Tuan RSR. 'A three-dimensional nanofibrous scaffold for cartilage tissue engineering using human mesenchymal stem cells'. Biomaterials (2005); **26**: 599-609.
- [205] Lee JW, Kim YH, Kim SH, Han SH, Hahn SB. 'Chondrogenic differentiation of mesenchymal stem cells and its clinical applications'. Yonsei Med J (2004); **45**: 41-47.
- [206] Young RG, Butler DL, Weber W, Caplan AI, Gordon SL, Fink DJ. 'Use of mesenchymal stem cells in a collagen matrix for Achilles tendon repair'. J Orthop Res (1998); **16**: 406-413.
- [207] Borges J, Mueller MC, Padron NT, Tegtmeier F, Lang EM, Stark GB. 'Engineered adipose tissue supplied by functional microvessels'. Tissue Eng (2003); **9**: 1263-1270.
- [208] Neels JG, Thinnis T, Loskutoff DJ. 'Angiogenesis in an *in vivo* model of adipose tissue development'. FASEB J (2004); **18**: 983-985.

Chapter 2

Goals of the Thesis

A plethora of research approaches towards the engineering of bone, cartilage, liver, skin, and other tissues has been performed since the beginning of the 1990s. However, the generation of adipose tissue equivalents is still an orphan discipline and a challenge (**chapter 1**). To date, exclusively mature adipocytes and preadipocytes have been used in the field of adipose tissue engineering. The overall goal of this thesis was to evaluate the potential of bone marrow-derived mesenchymal stem cells (MSCs) as alternative cell source.

This work can be subdivided into three main parts:

1. Establishment of a stem cell-based adipogenic 2-D cell culture and thorough investigation of the effect of basic fibroblast growth factor (bFGF) on the adipogenesis of MSCs
2. Generation of adipocyte constructs using MSCs in 3-D cell culture
3. Utilization of biomimetic polymers for tissue engineering applications

1. 2-D cell culture

So far, MSCs have been used exclusively for engineering of bone, cartilage, and tendon. As a first step towards adipose tissue engineering, the establishment of an adipogenic cell culture based on MSCs was performed and various candidates of adipogenic inducers were tested in conventional 2-D cell culture. Furthermore, the growth factors epidermal growth factor (EGF), platelet-derived growth factor-BB (PDGF-BB), and basic fibroblast growth factor (bFGF) were evaluated with regard to their potential to modulate the proliferation, differentiation, and the cell shape of MSCs (**chapter 3**). The first goal of the next chapter was to investigate the effects of bFGF on the adipogenic differentiation of MSCs induced by an adipogenic hormonal cocktail in detail. Basic FGF was supplemented in different phases of the culture and adipogenesis was characterized on the cellular and the molecular level. A special focus was set on the effects of bFGF on the expression of a key transcription factor in adipogenesis, the peroxisome proliferator-activated receptor γ (PPAR γ), and the modulation of the responsiveness of MSCs to PPAR γ ligands by bFGF (**chapter 4**). In a follow-up study, the effect of bFGF on the adipogenesis of MSCs was investigated under clonal conditions because MSCs represent an inhomogeneous cell population. The responsiveness of single cells to bFGF was determined in order to distinguish between two different possible mechanisms of action of bFGF: (a) the preferential proliferation of a subpopulation of MSCs prone to differentiate into adipocytes and (b) the exertion of direct effects on the commitment

level of MSCs. Therefore, an appropriate medium for the cloning experiments was determined and bFGF was supplemented in different phases of the clone culture (**chapter 5**).

2. 3-D cell culture

The main goal of this part was to transfer the established adipogenic protocol from 2-D to 3-D cell culture applying tissue engineering techniques. In general, three major components have been adopted for the generation of artificial tissues: cells, scaffolds, and growth factors. First, scaffolds with different pore size ranges were tested for their potential use in tissue engineering approaches in combination with MSCs (**chapter 6**). In chapters 3 and 4, MSCs and bFGF have been demonstrated to be suitable for an adipogenic cell culture in 2-D cell culture. Consequently, combining the three components cells, scaffolds, and growth factors, the potential of MSCs was evaluated, for the first time, for a long-term adipose tissue engineering approach *in vitro*. The aims of this approach were an efficient differentiation of MSCs into mature adipocytes and a characterization of the differentiation processes on the histological and molecular level (**chapter 7**).

3. Biomimetic polymers

Biomimetic polymers for tissue engineering applications have been recently developed in order to control the cellular behavior at the molecular level. In our laboratory, a diblock copolymer consisting of a PLA and a PEG moiety was designed whereby the latter component can be modified in order to covalently bind peptides and proteins containing free, primary amine groups. These polymers can be processed into 3-D scaffolds which allow for an instant surface modification. A main goal of this project was to demonstrate the feasibility of the instant surface modification of these 3-D scaffolds with the angiogenic growth factor bFGF, that is, the covalent binding of bFGF to the scaffolds. As a first step, the adsorption of bFGF to a PEG-PLA polymer derivative was determined in comparison to PLA. Furthermore, a protocol was established to efficiently desorb bFGF from polymer surfaces which allowed for the determination of the absolute amounts of covalently bound bFGF (**chapter 8**). In a follow-up study, the covalent immobilization of bFGF to the scaffolds was characterized in detail, and furthermore, the stability of the linkage of bFGF to the scaffolds was tested *in vivo*. Finally, the potential of the scaffolds with tethered bFGF to induce angiogenesis was evaluated *in vivo* in comparison to scaffolds with adsorbed bFGF and injected bFGF (**chapter 9**).

Chapter 3

Modulators of the Adipogenesis of Mesenchymal Stem Cells

Markus Neubauer, Achim Göpferich, Torsten Blunk

Department of Pharmaceutical Technology, University of Regensburg,
Universitaetsstrasse 31, D-93040 Regensburg, Germany

Abstract

The differentiation of precursor cells into adipocytes, termed adipogenesis, is a complex process that is affected by a wide variety of environmental conditions. Growth factors such as epidermal growth factor (EGF), platelet-derived growth factor (PDGF), transforming growth factor- β (TGF- β), and basic fibroblast growth factor (bFGF) and drugs such as insulin, glucocorticoids, cAMP-elevating substances, and peroxisome proliferator-activated receptor γ ligands are known to influence the differentiation of mesenchymal stem cells (MSCs) into various lineages.

In this study, the ability of a variety of growth factors (EGF, PDGF-BB, bFGF) and drugs (dexamethasone, IBMX, indomethacin, insulin) to enhance the adipogenesis of MSCs was tested in conventional 2-D cell culture. To this end, different concentrations and combinations were administered and their success assessed by means of Red Oil O staining of differentiated adipocytes and by the measurement of a marker enzyme of adipogenesis, glycerol-3-phosphate dehydrogenase. Basic fibroblast growth factor in combination with the hormonal cocktail consisting of dexamethasone, insulin, indomethacin, and IBMX exerted the strongest adipogenic conversion of MSCs among all tested systems.

The growth factors EGF, PDGF-BB, and bFGF were further investigated to determine their influence on the modulation of the proliferation of MSCs. EGF and bFGF led to a stimulation, whereas PDGF-BB decreased the proliferation of MSCs, as assessed by the colony forming unit (CFU) assay. The cell shape and the cytoskeletal organization of MSCs after expansion in the absence or presence of growth factors was mostly similar irrespective of the treatment, however, in PDGF-treated and bFGF-treated cultures very small, round, and unspread MSCs were found and visualized by staining the actin filaments using a phalloidin toxin.

Introduction

Adipogenesis, the conversion of precursor cells into adipocytes, is a complex process, which is affected by environmental conditions. Precursor cells of the adipocyte, that is preadipocytes and immature stem cells, have been reported to be capable to undergo adipogenesis [1]. Adipogenic processes have been studied mainly using preadipocytes and preadipocytic cell lines such as the 3T3-L1 and the 3T3-F442A cell lines [2]. Recently, several studies on the adipogenesis of stem cells, especially of the bone marrow-derived multipotent mesenchymal stem cells (MSCs), have contributed to the knowledge in this field [3-6]. To date, a wide variety of extracellular cues, consisting of low molecular weight drugs and growth factors, have been found to influence adipogenesis [2].

The most abundantly employed and most intensively researched prodifferentiative agents include insulin, glucocorticoids applied in the form of dexamethasone, hydrocortisone, and corticosterone, respectively, and compounds leading to elevated cAMP levels such as 3-isobutyl-1-methylxanthine (IBMX) [2]. In addition, ligands of a key transcription factor in adipogenesis, the peroxisome proliferator-activated receptor γ (PPAR γ) [7], are known to act as strong inducers and are administered solely or in combinations with the aforementioned inducers. Examples of PPAR γ ligands include anti-diabetic drugs and the thiazolidinediones, such as troglitazone, pioglitazone, and rosiglitazone [8], as well as anti-inflammatory drugs, such as indomethacin [9]. The combination of IBMX with insulin and glucocorticoids, frequently named adipogenic hormonal cocktails, have reproducibly produced the strongest effects in various culture systems including 3T3-L1 cells, the system investigated most intensively [2]. In studies on the adipogenic conversion of MSCs of various species and MSC cell lines, hormonal cocktails consisting of various combinations of IBMX (0.5 mM), insulin (10 μ g/ml), dexamethasone (10-1000 nM), and indomethacin (60-200 μ M) were used [6,10-15]. Thiazolidinediones were administered in the micromolar range [6,16]. For the adipogenic conversion of embryonic stem cells, retinoic acid administered in a specific scheme has been shown to play a critical role [17].

Growth factors also possess the capacity to modulate the differentiation of MSCs and preadipocytes. Transforming growth factor β (TGF β) has been repeatedly described to promote osteogenesis, but inhibit adipogenesis of MSCs [10,11]. Basic fibroblast growth factor (bFGF) has been recognized as a promoter of osteogenesis [6,18,19], but has been controversially discussed in regard to adipogenesis of MSCs. It has been reported to exert no influence [14], an acceleration [11], and an enhancing effect [10] on the fat cell formation of

MSCs. Basic FGF slightly suppressed adipogenic differentiation of primary human preadipocytes [20]. Bone morphogenetic protein-2 (BMP-2) is acknowledged as a potent inducer of osteogenesis in MSCs [21] and as an inhibitor of adipogenesis [5]. However, BMP-2 has also been reported to promote adipogenesis in combination with the thiazolidinedione rosiglitazone [16]. EGF is known to enhance osteogenic differentiation of purified MSCs [22], the differentiation of MSCs into neurons [23], and the differentiation of MSCs into photoreceptors [24], however, there is no data available on the influence of EGF on the adipogenic differentiation of MSCs. EGF showed a biphasic effect on the adipogenesis of 3T3-L1 preadipocytes: it inhibited adipogenesis of undifferentiated preadipocytes, but enhanced progression of adipogenesis of differentiated adipocytes [25]. Using primary human preadipocytes, EGF exerted an inhibitory effect on the adipogenesis [20]. PDGF-BB has been reported to exert no effect on the osteochondrogenic differentiation of MSCs *in vitro* and *in vivo* [26,27], however, to date, information concerning the influence of PDGF-BB on the adipogenesis of MSCs is not available. Regarding primary preadipocytes, PDGF-BB, similarly to bFGF, led to a suppression of the adipogenic differentiation [20].

In this study, various combinations of inducing cocktails and the growth factors epidermal growth factor (EGF), platelet-derived growth factor BB (PDGF-BB), and basic fibroblast growth factor (bFGF) were tested in order to assess their prodifferentiative properties. In addition, the modulation of the proliferation of MSCs by the growth factors was determined by the colony forming unit assay (CFU assay). Beyond the modulation of the proliferation and the differentiation potential of MSCs by growth factors, the cell shape and the cytoskeletal organization of cells can also be influenced by growth factors [28]. Remarkably, the differentiation of MSCs into a certain lineage is known to be modulated by the cell shape [29]. Both the cell shape and the actin filaments were visualized with phalloidin coupled to a fluorescent dye [28].

Materials and Methods

Materials

If not otherwise stated, chemicals were obtained from Sigma, Steinheim, Germany. Basic FGF and PDGF-BB were obtained from PeproTec (Rocky Hill, NJ, USA). EGF was purchased from Biomol (Hamburg, Germany). Insulin was kindly provided by Hoechst Marion Roussel (Frankfurt am Main, Germany). Cell culture plastics were purchased from Corning Costar (Bodenheim, Germany).

Cell culture

Marrow stromal cells were obtained from six-week old male Sprague Dawley rats (weight: 170 - 180 g, Charles River, Sulzfeld, Germany). MSCs were flushed from the tibiae and femora according to the protocol of Ishaug [30]. Cells were centrifuged at 1,200 rpm for 5 min. The resulting cell pellet was resuspended in basal medium consisting of DMEM (Biochrom, Berlin, Germany), 10% fetal bovine serum (Gemini Bio-Products Inc., Calabasas, CA, USA), 1% penicillin/streptomycin (Invitrogen, Karlsruhe, Germany), and 50 µg/ml ascorbic acid. Cells were seeded in T75 flasks and cultured at 37°C and 5% CO₂. Cells were allowed to adhere to the substrate for three days. The flasks were rinsed twice with phosphate-buffered saline (PBS, Invitrogen, Karlsruhe, Germany) in order to remove non-adherent cells. In the experiments conducted to determine the influence of different growth factors and combinations of inducers, adherent cells were exposed to either basal medium (designated as “w/o GF”), to basal medium supplemented with 3 ng/ml EGF (“EGF”), 3 ng/ml PDGF-BB (“PDGF”), or 3 ng/ml bFGF (“bFGF”) from day 3 after the cell isolation until the end of the culture, that is, until the end of the differentiation period. In addition, the same experiment was performed with a growth factor dose of 10 ng/ml instead of 3 ng/ml. Furthermore, to elucidate the influence of bFGF in a more detailed manner, concentrations of 0, 0.1, 1, and 3 ng/ml bFGF were administered after the cell isolation until the end of the culture.

Culturing the adherent cells, 12 ml of basal medium with or without growth factors were exchanged every 2-3 days until confluence was reached after 12 days. Cells were passaged once with 0.25% trypsin and EDTA (Invitrogen, Karlsruhe, Germany). For adipogenic differentiation, cells were seeded at a density of 30,000 cells/cm² in 24-well plates and grown to postconfluence for 3 days with or without growth factors. Subsequently, cells were differentiated for 8 days either in the presence or absence of growth factors. In detail, to induce adipogenic differentiation, cultures were treated for 3 days with dexamethasone and 3-isobutyl-1-methylxanthine (IBMX, Serva Electrophoresis, Heidelberg, Germany,

(“Dex/IBMX”), IBMX and indomethacin (“IBMX/Indo”), or dexamethasone, IBMX, indomethacin, and insulin (“Dex/IBMX/Indo/Ins”). The concentrations were: 0.5 mM IBMX, 10 nM dexamethasone, 60 μ M indomethacin and 10 μ g/ml insulin. Subsequently, all cultures, irrespective of the inducer combination used, were maintained for 5 more days in differentiation medium consisting of basal medium supplemented with 10 μ g/ml insulin. Thus, MSCs underwent an 8-day differentiation phase consisting of a three day induction phase and a five day maintenance phase. A chart of the supplementation schedule is published in Figure 1 of Chapter 4.

Oil Red O staining

Cells were washed once with PBS and fixed with 10% formaldehyde (Merck, Darmstadt, Germany) overnight. Cells were covered with 3 mg/ml Oil Red O for 2h. Excess dye was removed with PBS and cells were fixed with 10% formaldehyde.

Glycerol-3-phosphate dehydrogenase (GPDH) activity measurement

The activity of GPDH, a key enzyme in lipid biosynthesis, was measured using a protocol adapted from Pairault and Green [31]. In brief, cells washed with PBS were scraped in lysis buffer containing 50 mM Tris, 1 mM EDTA, and 1 mM β -mercaptoethanol on ice. Subsequently, the resulting suspension was sonicated with a digital sonifier (Branson Ultrasonic Corporation, Danburg, CT, USA). Cell lysates were centrifuged for 5 min at 13,200 rpm at 4°C. Aliquots of the supernatant were mixed with a solution containing 0.1 M triethanolamine, 2.5 mM EDTA, 0.5 mM β -mercaptoethanol, 120 μ M reduced nicotinamide adenine dinucleotide (NADH) (Roche, Mannheim, Germany), and 200 μ M dihydroxyacetonephosphate. Enzyme activity was monitored by measurement of the disappearance of NADH at 340 nm over 4.2 min. Enzyme activity was normalized to the protein content of each sample. Proteins were determined by the method of Lowry et al. [32]. Proteins were precipitated using 12% trichloroacetic acid. Proteins were solubilized in an alkaline solution and complexed with a mixture of disodium tartrate, copper sulfate and folin-ciocalteu reagent (all Merck, Darmstadt, Germany). Absorption was measured at 546 nm after 30 min incubation.

Actin staining

Actin staining was conducted with fluorescein-phalloidin (Molecular Probes, Leiden, The Netherlands) at room temperature using a protocol adapted from Martin et al. [28]. MSCs were isolated and propagated to confluence as described above. Cells were passaged once

with 0.25% trypsin and EDTA and were seeded at a density of 4,000 cells/cm² in 24-well plates and grown for 48 to 72 hours with or without growth factor supplements. Subsequently, cells were washed with PBS and fixed using 3.7% formaldehyde for 10 minutes at room temperature. After washing the cells twice with PBS, the cells were permeabilized by a 0.1% Triton X-100 (Merck, Darmstadt, Germany) solution in PBS for 5 minutes. To reduce nonspecific background staining with the fluorescein-phalloidin conjugates, a 1% bovine serum albumin (BSA) solution in PBS was added for 30 minutes, followed by two washing steps with PBS. Subsequently, in each well, 5 μ l of the methanolic stock solution of fluorescein-phalloidin (200U/ml; 6.6 μ M) was diluted with 200 μ l of 1% BSA in PBS and the cells were covered for 20 minutes in the dark. Excess dye was removed by washing twice with PBS. For storage, the stained cells were mounted using Vectashield H-1000 (Vector Laboratories, Burlingame, CA, USA) and kept at 4°C in the dark. Stained cells were photographed on the Zeiss Axiovert 200M microscope coupled to scanning device LSM 510 (Zeiss, Jena, Germany) at 100-fold magnification (Ex = 496 nm, Em = 516 nm).

Colony forming unit (CFU) assay

The CFU assay was performed according to protocols adapted from Martin et al. [33] and Bianchi et al. [34]. After the isolation of the cells, which was performed as described above, a small sample of the cell suspension was treated with an equal volume of 4% acetic acid in order to lyse red blood cells. Mononucleated cell counts were determined with a hemacytometer following the staining of the cells with crystal violet in 0.1 M citric acid [35]. Subsequently, 64,000 mononucleated cells were seeded per T75-flask (75 cm²) and cells were left undisturbed for three days to allow for cell attachment. All experimental groups were maintained in basal medium for the first three days. Thereafter, adherent cells were propagated in basal medium (designated as “w/o GF”), in basal medium supplemented with 3 ng/ml EGF (“EGF”), 3 ng/ml PDGF-BB (“PDGF”), or 3 ng/ml bFGF (“bFGF”). Medium was exchanged every two to three days. After 11 days of proliferation in the distinct media, cells were fixed with 10% formaldehyde, stained with 3 ml 1% methylene blue solution in 10 mM borate buffer, pH 8.8, for 30 minutes. Cells were washed three times with water. After complete drying, the cells were stored in the flasks. Colonies were counted under an inverse light microscope (Leica DM IRB, Leica Microsystems, Wetzlar, Germany). One colony was defined as a confluent area covered by at least 50 cells [36].

Statistics

GPDH data are expressed as means \pm standard deviation. Single-factor analysis of variance (ANOVA) was used in conjunction with a multiple comparison test (Tukey's test) to assess statistical significance.

Results*Combinations of inducing agents for the adipogenesis of MSCs*

In preliminary experiments, dexamethasone (Dex, 10 nM), IBMX (0.5 mM), insulin (Ins, 10 μ g/ml), and indomethacin (60 μ M) were applied in all possible combinations. The addition of single inducers did not induce adipogenic differentiation (data not shown). Minimum requirements were the combinations of Dex/IBMX or IBMX/Indo in order to obtain a detectable degree of differentiation (data not shown).

Influence of growth factors and combinations of inducers on the adipogenesis of MSCs

MSCs cultured in the absence of a growth factor ("w/o GF") and in presence of 3 ng/ml EGF ("EGF"), 3 ng/ml PDGF-BB ("PDGF"), and 3 ng/ml bFGF ("bFGF") were exposed to the inducing cocktails Dex/IBMX, IBMX/Indo, and Dex/IBMX/Indo/Ins. Figure 1 shows histological pictures after Oil Red O staining of intracellular lipid droplets of differentiated adipocytes. Dex/IBMX exerted a very weak adipogenesis in groups "w/o GF" and "EGF" and a moderate differentiation in the group "PDGF" (Fig. 1). In contrast, this combination was sufficient for a clear differentiation in presence of bFGF (Fig. 1). Measurement of the glycerol-3-phosphate dehydrogenase (GPDH) activity confirms the histological observations (Fig. 2). The highest activity was detected in the presence of bFGF as compared to all other groups. PDGF treatment yielded a GPDH activity significantly elevated to the groups "w/o GF" and "EGF". Supplementation of the combination IBMX/Indo resulted in a very weak differentiation of cells grown in the presence of EGF and no growth factor, but clearly induced adipogenesis in the presence of PDGF and bFGF (Fig. 1). Again, the Oil Red O staining could be confirmed by the values of the corresponding GPDH activities (Fig. 2). The strongest prodifferentiative effect on MSCs was obtained after induction with the hormonal cocktail consisting of Dex/IBMX/Indo/Ins. In the groups "w/o GF" and "EGF", the number of differentiated adipocytes was clearly increased as compared to cells induced by Dex/IBMX and IBMX/Indo. This cocktail also produced the highest number of adipocytes in the groups "PDGF" and "bFGF". In the "PDGF" group, this cocktail yielded adipocytes with distinctly

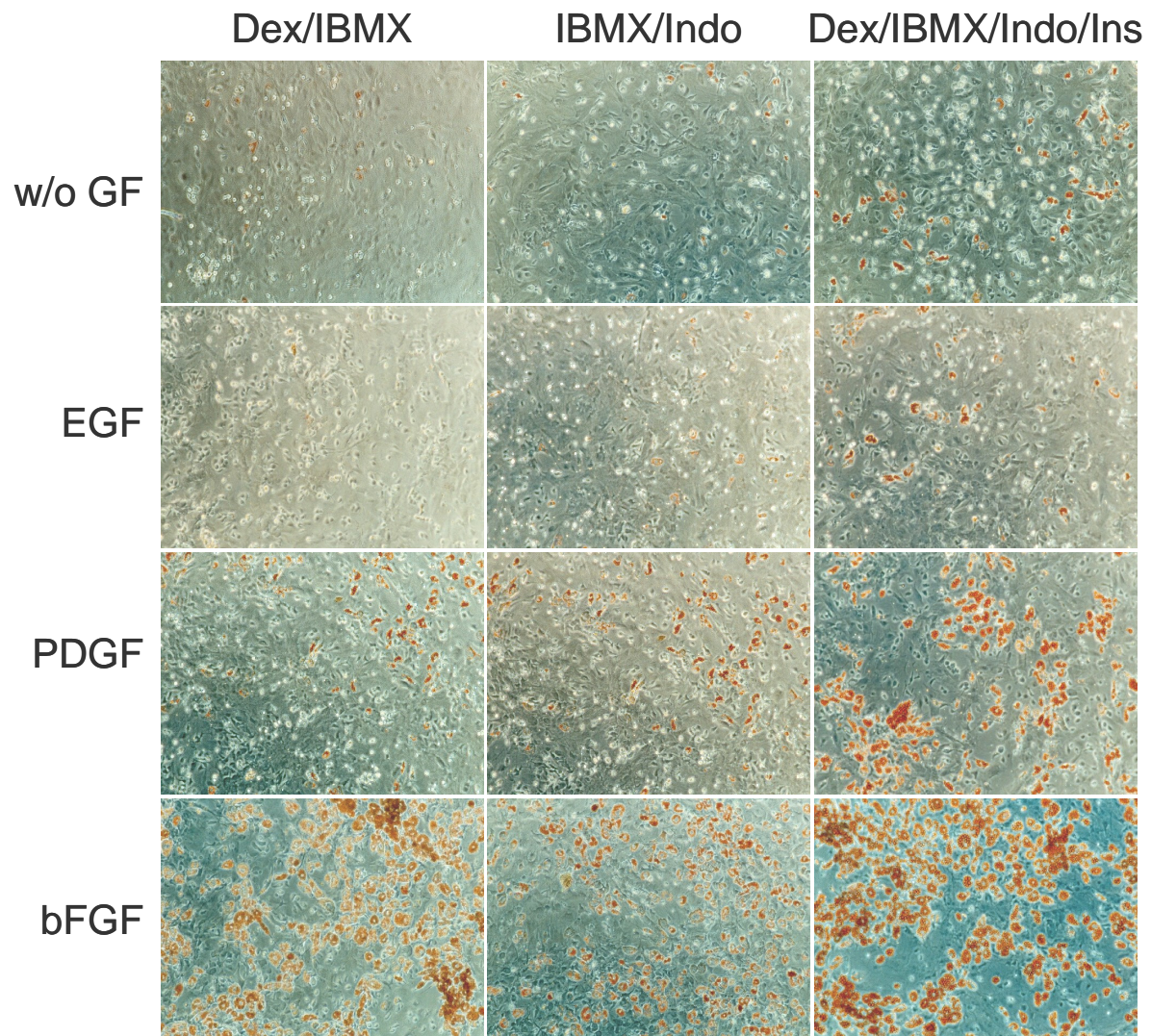


Fig. 1 Adipogenesis of MSCs monitored by Oil Red O staining of lipid droplets on day 8 after induction. Growth factors were administered at a concentration of 3 ng/ml. Induction occurred by addition of the inducer combinations dexamethasone/IBMX, IBMX/indomethacin, and dexamethasone, IBMX, indomethacin, and insulin.

larger lipid droplets as compared to cells induced by Dex/IBMX, IBMX/Indo, and the control group irrespective of the inducing regimen. In the case of bFGF, the size of the lipid droplets was increased following induction with Dex/IBMX and Dex/IBMX/Indo/Ins as compared to IBMX/Indo treatment; Dex/IBMX/Indo/Ins even yielded adipocytes with larger lipid inclusions than any other group. Using the latter cocktail, the GPDH activities of the groups “PDGF” and “bFGF” were significantly higher than the activities of the groups “w/o GF” and “EGF”.

The following paragraph briefly summarizes the results with regard to the growth factors’ effects. Basic FGF-treated MSCs appeared to be most sensitive to adipogenic inducers, an effect that was most pronounced after administration of the hormonal cocktail consisting of Dex/IBMX/Indo/Ins. The clearest differences relative to the groups with EGF, PDGF, and the

control were obtained following the exposure of MSCs to the weakest induction cocktail, the combination of Dex and IBMX. PDGF-BB also exerted an enhancing effect on the adipogenesis, but attenuated as compared to bFGF. In contrast, EGF had no stimulatory effect on the adipogenic differentiation of MSCs.

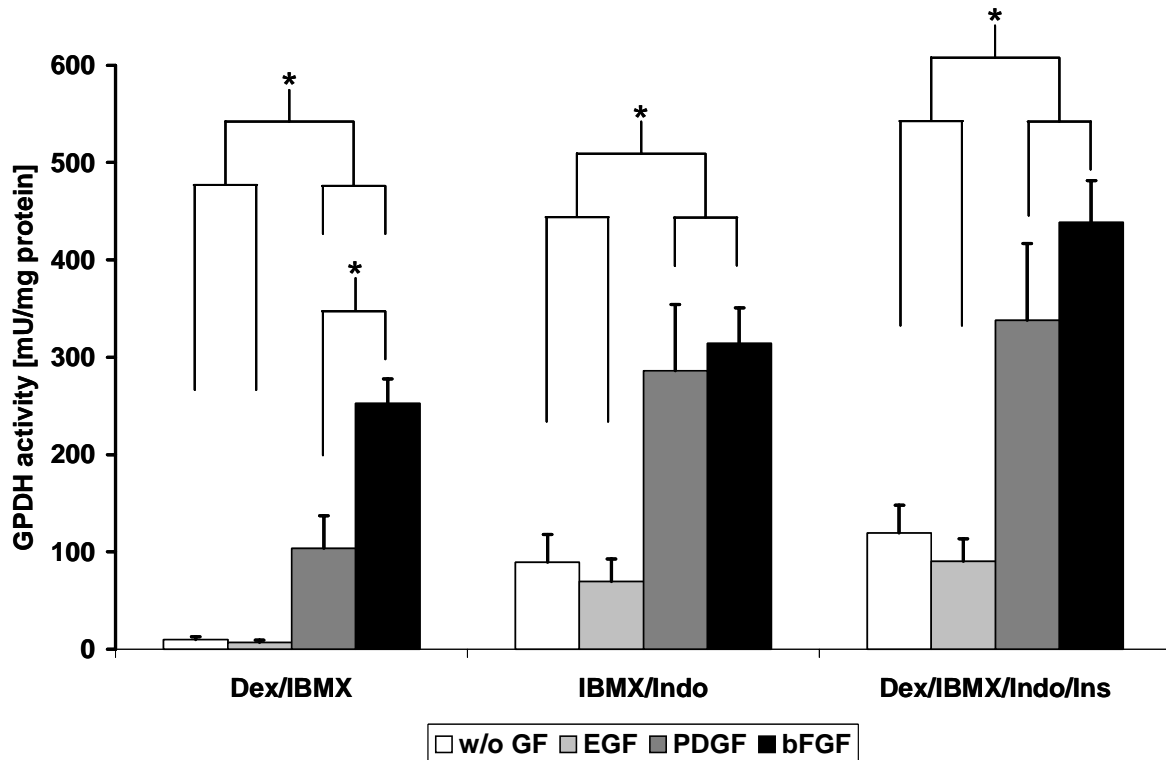


Fig. 2 Adipogenesis of MSCs monitored by GPDH measurement on day 3 after induction. Growth factors were administered at a concentration of 3 ng/ml. Induction occurred by addition of the inducer combinations dexamethasone/IBMX, IBMX/indomethacin, and dexamethasone, IBMX, indomethacin, and insulin. Asterisks indicate statistically significant differences at a level of $p < 0.01$ ($n=3$).

Adipogenesis of MSCs was additionally assessed using the growth factors at a concentration of 10 ng/ml and, again, exposed to the inducing cocktails Dex/IBMX, IBMX/Indo, and Dex/IBMX/Indo/Ins. Cells grown in the absence of a growth factor served as a control group and were the same as the control group shown in Figs. 1 and 2. In general, the three different combinations influenced the adipogenesis of MSCs in the presence of 10 ng/ml growth factors similarly to the way they did in the presence of 3 ng/ml growth factors. Exceptions presented themselves in two groups especially: PDGF-treated and bFGF-treated cells exhibited a decreased differentiation after induction with IBMX/Indo as compared to the corresponding groups using 3 ng/ml growth factors (Figs. 1 and 3), most pronouncedly in the “PDGF” group. Remarkably, in presence of 10 ng/ml bFGF and the Dex/IBMX/Indo/Ins combination,

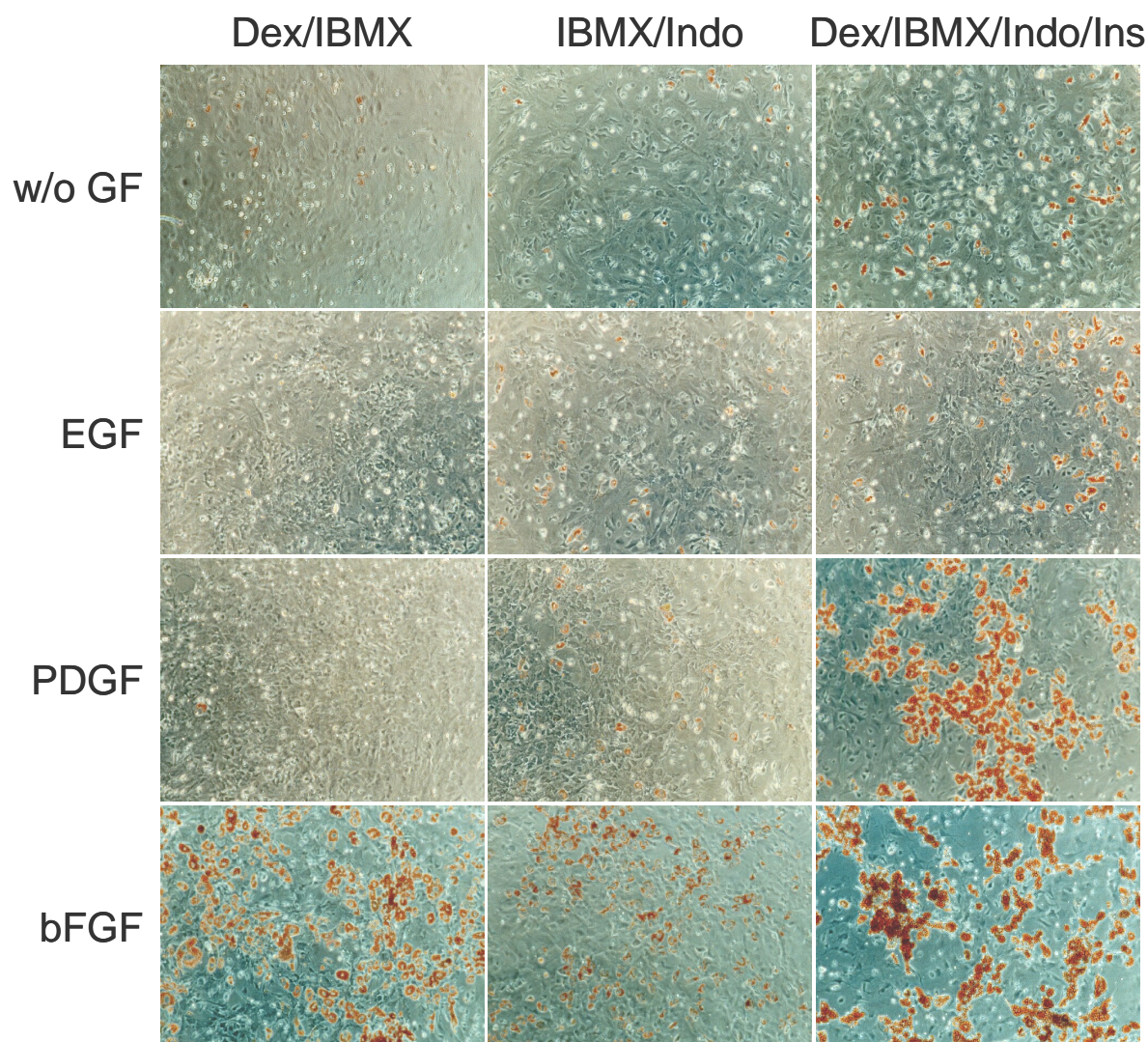


Fig. 3 Adipogenesis of MSCs monitored by Oil Red O staining of lipid droplets on day 8 after induction. Growth factors were administered at a concentration of 10 ng/ml. Induction occurred with addition of the inducer combinations dexamethasone/IBMX, IBMX/indomethacin, and dexamethasone, IBMX, indomethacin, and insulin.

differentiated adipocytes appear in clusters with a high density of adipocytes exhibiting large lipid droplets (Fig. 3). EGF administered at 10 ng/ml had no prodifferentiative effect on MSCs (Fig. 3). Values of the GPDH activity revealed no elevation after supplementation of 10 ng/ml EGF as compared to 3 ng/ml EGF (Fig. 4). GPDH activities of the groups “PDGF” and “bFGF” were distinctly lower in presence of Dex/IBMX and IBMX/Indo after addition of 10 ng/ml growth factors as compared to the values obtained by supplementation of 3 ng/ml growth factors (Fig. 4). In the case of PDGF, the GPDH activity was not significantly higher than the activities measured for the groups “EGF” and “w/o GF”. In contrast, GPDH activities of 10 ng/ml PDGF and bFGF supplementation were not decreased following the induction

with Dex/IBMX/Indo/Ins as compared to the supplementation with 3 ng/ml growth factors (Figs. 2 and 4).

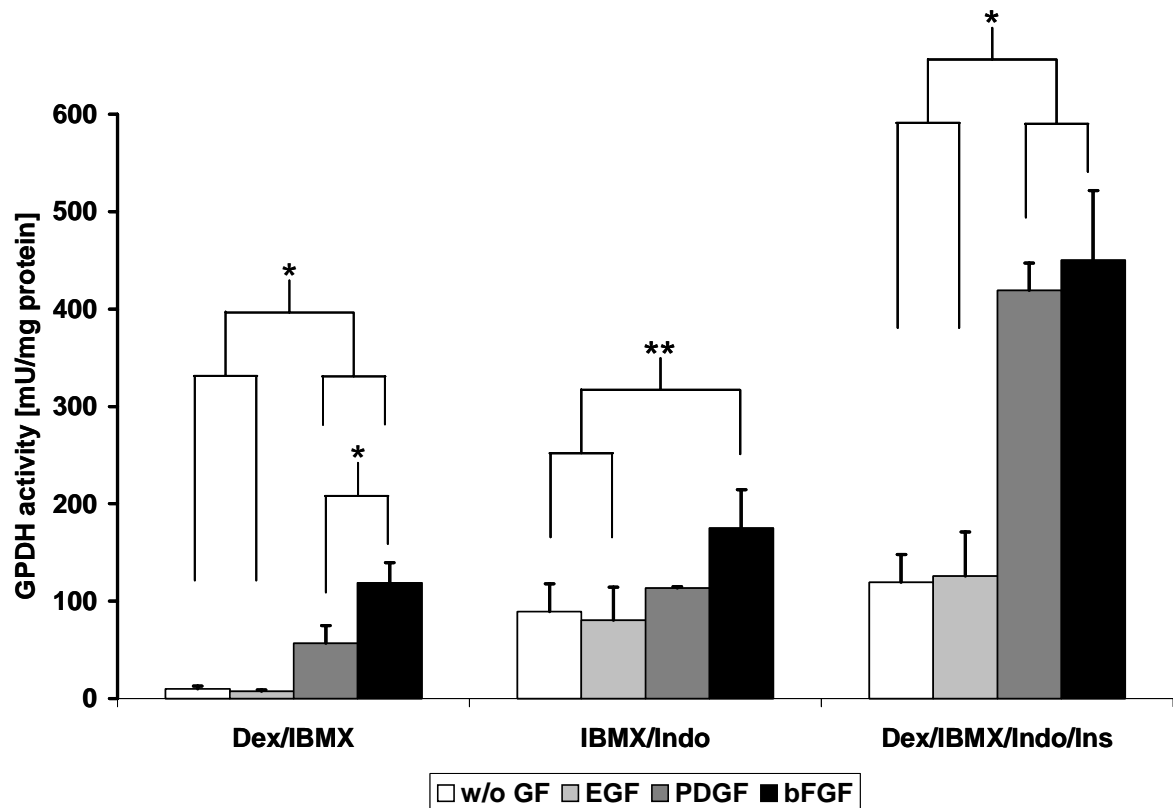


Fig. 4 Adipogenesis of MSCs monitored by GPDH measurement on day 3 after induction. Growth factors were administered at a concentration of 10 ng/ml. Induction occurred by addition of the inducer combinations dexamethasone/IBMX, IBMX/indomethacin, and dexamethasone, IBMX, indomethacin, and insulin. Asterisks indicate statistically significant differences at a level of $p < 0.01$ (*) or $p < 0.05$ (**) ($n=3$).

Determination of the effects of bFGF concentrations ranging from 0 to 3 ng/ml

The aforementioned data suggest that bFGF exerts the strongest enhancement of the adipogenesis of MSCs among the three growth factors. Supplementation of 10 ng/ml bFGF did not lead to an increase of adipogenic differentiation as compared to the addition of 3 ng/ml bFGF (Figs. 1-4).

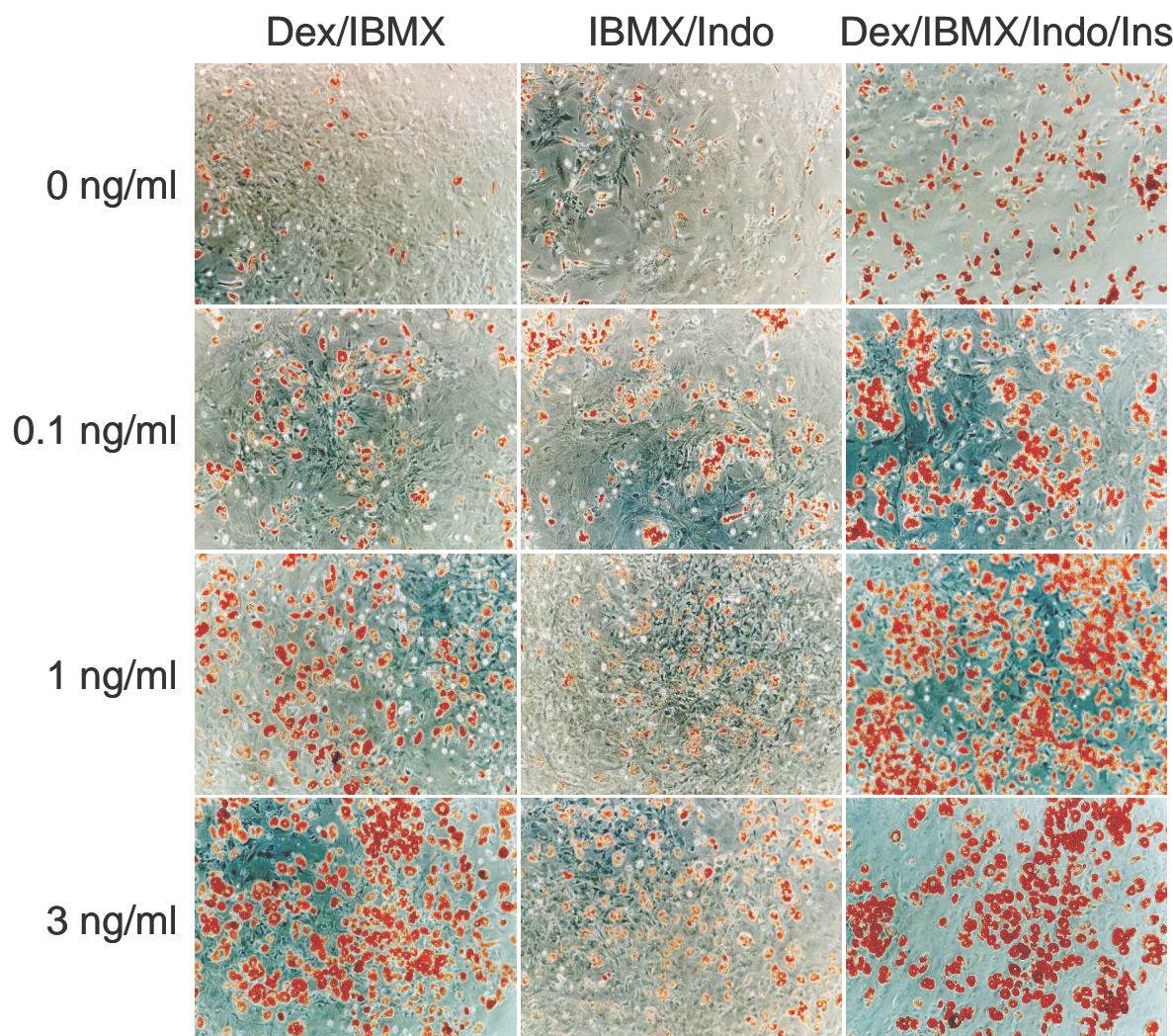


Fig. 5 Adipogenesis of MSCs monitored by Oil Red O staining of lipid droplets on day 8 after induction. Basic FGF was administered at concentrations ranging from 0 to 3 ng/ml. Induction occurred by the addition of the inducer combinations dexamethasone/IBMX, IBMX/indomethacin, and dexamethasone, IBMX, indomethacin, and insulin.

For the determination of the most potent concentration of bFGF, the effect of bFGF concentrations of 0, 0.1, 1, and 3 ng/ml were assessed by Oil Red O staining and GPDH activity measurement. In all experimental groups, the cocktail consisting of Dex/IBMX/Indo/Ins provoked, again, the strongest adipogenic differentiation as compared to

the inducer combinations Dex/IBMX and IBMX/Indo (Fig. 5), confirmed by a clearly elevated GPDH activity in the group with Dex/IBMX/Indo/Ins (Fig. 6). Irrespective of the inducer combination, the differentiation of MSCs was enhanced with increasing concentrations of bFGF (Fig. 5). When Dex/IBMX was used as the inducing cocktail, there was, beyond the increased number of differentiated adipocytes, an augmentation of the size of the intracellular lipid droplets observable with increasing bFGF doses (Fig. 5), again reflected in the GPDH activity. The highest values of the GPDH activity were obtained using 3 ng/ml in all cases (Fig. 6). In regard to the cocktail Dex/IBMX/Indo/Ins, the size of lipid droplets was similar in all groups receiving bFGF, but clearly increased as compared to the control group (Fig. 5). Remarkably, the lipid droplet sizes were decreased after induction with IBMX/Indo as compared to Dex/IBMX and Dex/IBMX/Indo/Ins using 1 ng/ml and 3 ng/ml bFGF (Fig. 5).

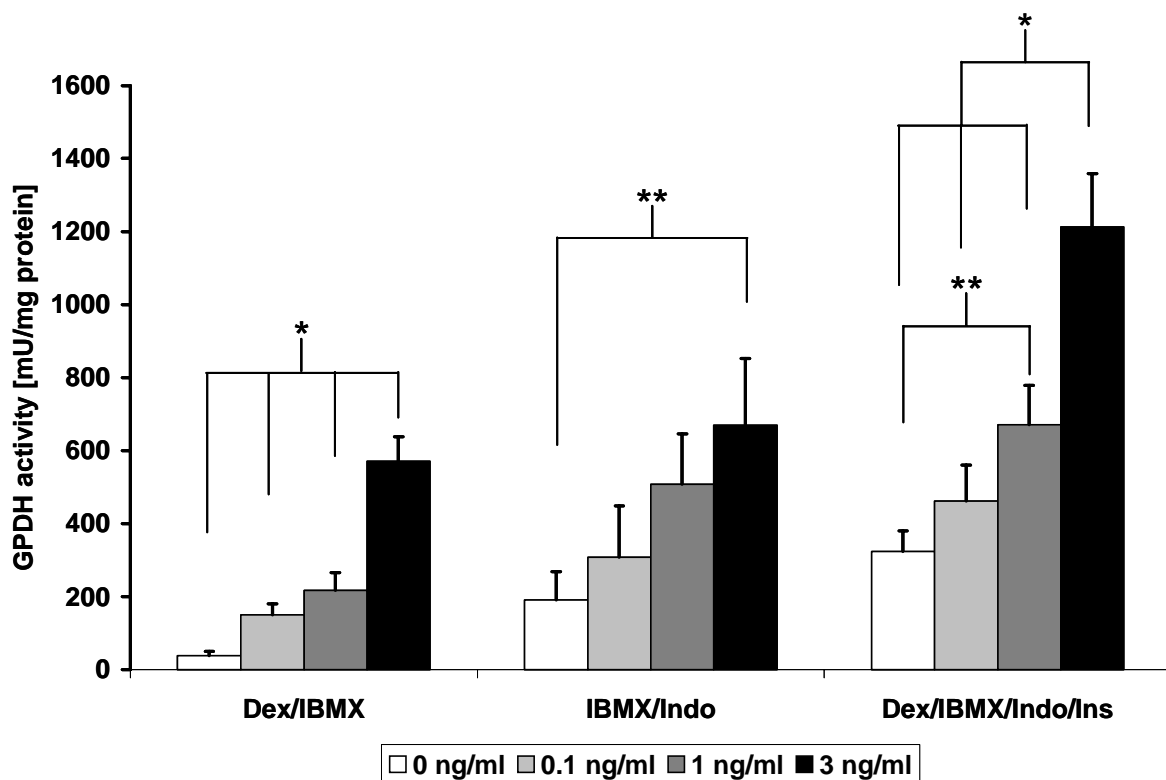


Fig. 6 Adipogenesis of MSCs monitored by GPDH measurement on day 3 after induction. Basic FGF was administered at concentrations ranging from 0 to 3 ng/ml. Induction occurred by addition of the inducer combinations dexamethasone/IBMX, IBMX/indomethacin, and dexamethasone, IBMX, indomethacin, and insulin. Asterisks indicate statistically significant differences at a level of $p < 0.01$ (*) or $p < 0.05$ (**) ($n=3$).

Actin organization and cell shape

MSCs seeded at a low density of 4,000 cells/cm² were stained with fluorescein-phalloidin in order to assess the actin filament organization and the cell shape. Cells of all groups mainly exhibited long and thick actin filaments and wide-spread and flattened phenotype; only a few cells showed a diffuse actin labeling accompanied by a more spindle-like shape. In the groups “PDGF” and “bFGF”, a higher number of small, round, non-spread cells appeared as compared to “w/o GF” and “EGF”.

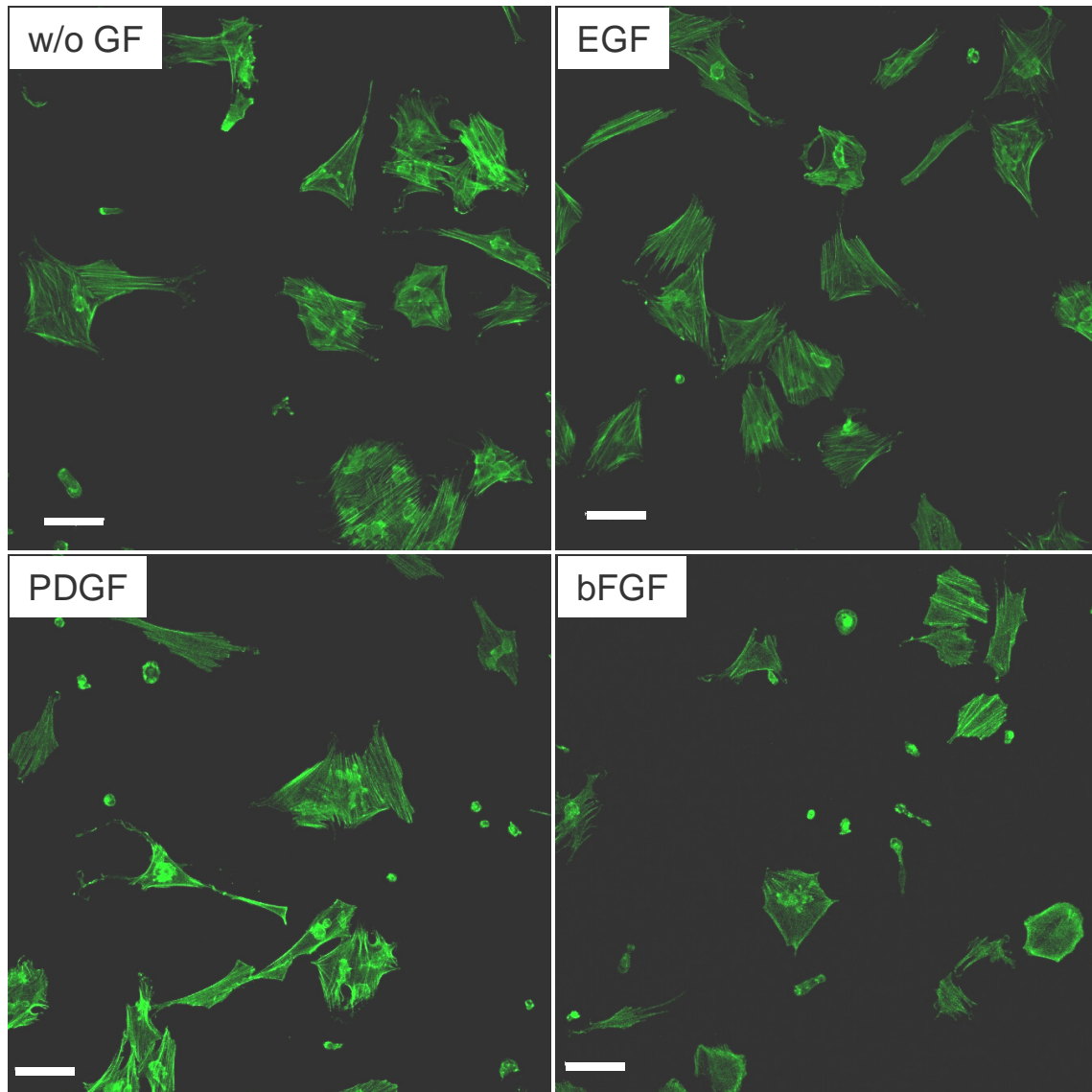


Fig. 7 Staining of the actin filaments of MSCs. Cells were propagated under the influence of the growth factors EGF, PDGF-BB, and bFGF and under control conditions (“w/o GF”). Scale bars: 100 μm.

Colony forming unit (CFU) assay

The number of developed colonies was counted in order to evaluate the effects of different growth factors on the initial expansion of MSCs. Cells were seeded at a very low density, about the tenth part of the density in the conventional culture, and proliferated over 14 days. The control group without supplementation of a growth factor yielded 88 ± 4 colonies per T75 flask (Fig. 8). EGF and bFGF clearly stimulated the growth of colonies and resulted in 114 ± 16 and 118 ± 6 colonies, respectively (Fig. 8). In contrast, the administration of PDGF statistically significantly inhibited the colony development and resulted in 70 ± 7 colonies per flask (Fig. 8).

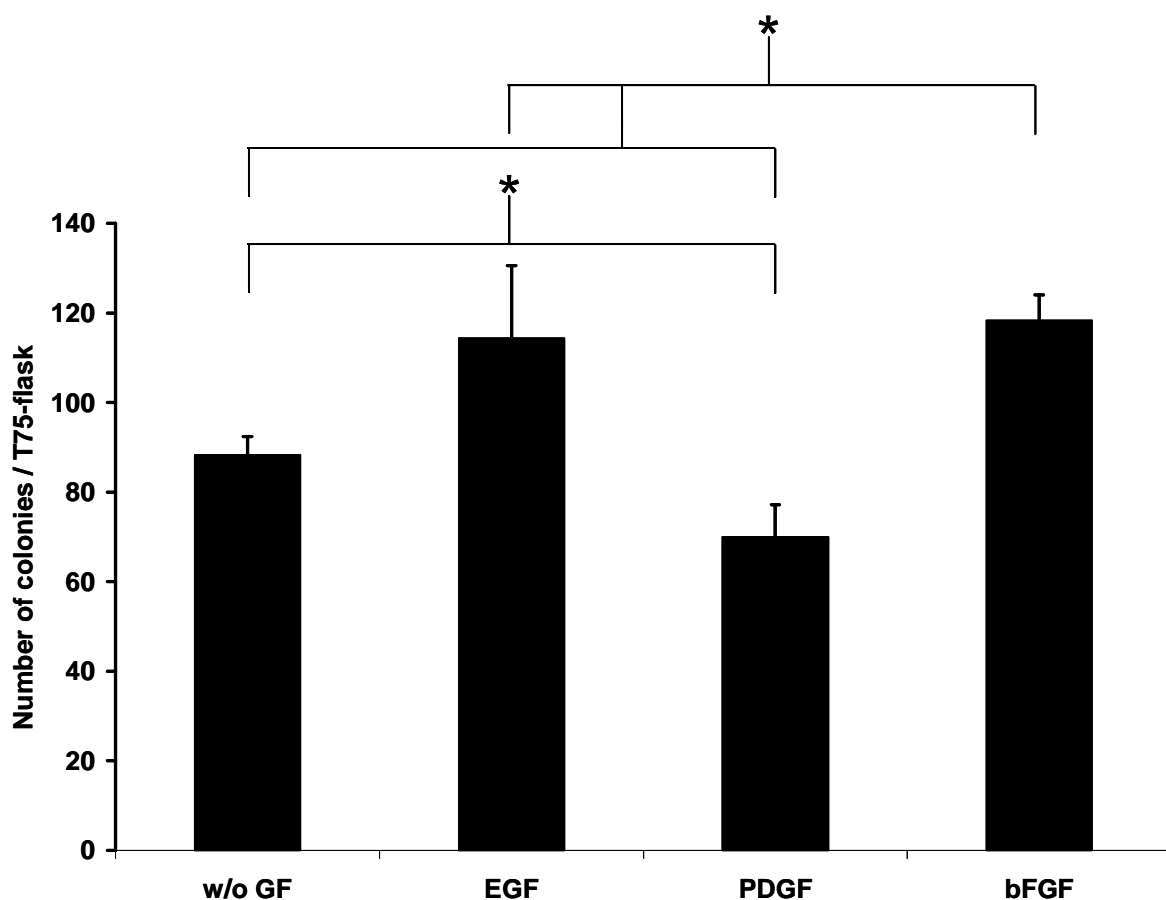


Fig. 8 Effects of different growth factors on the formation of MSC colonies. Data represent mean \pm standard deviation values. Asterisks indicate significantly elevated values ($n=3$, $p < 0.05$).

Moreover, the portion of large colonies is strikingly elevated in cultures in presence of PDGF; that is, the number of grown colonies was decreased as compared to the other experimental groups, but the cells that did respond to PDGF proliferated extensively (Fig. 9). Cultures with EGF, and especially with bFGF, displayed a bigger proportion of smaller colonies than cultures treated with no growth factor or PDGF (Fig. 9).

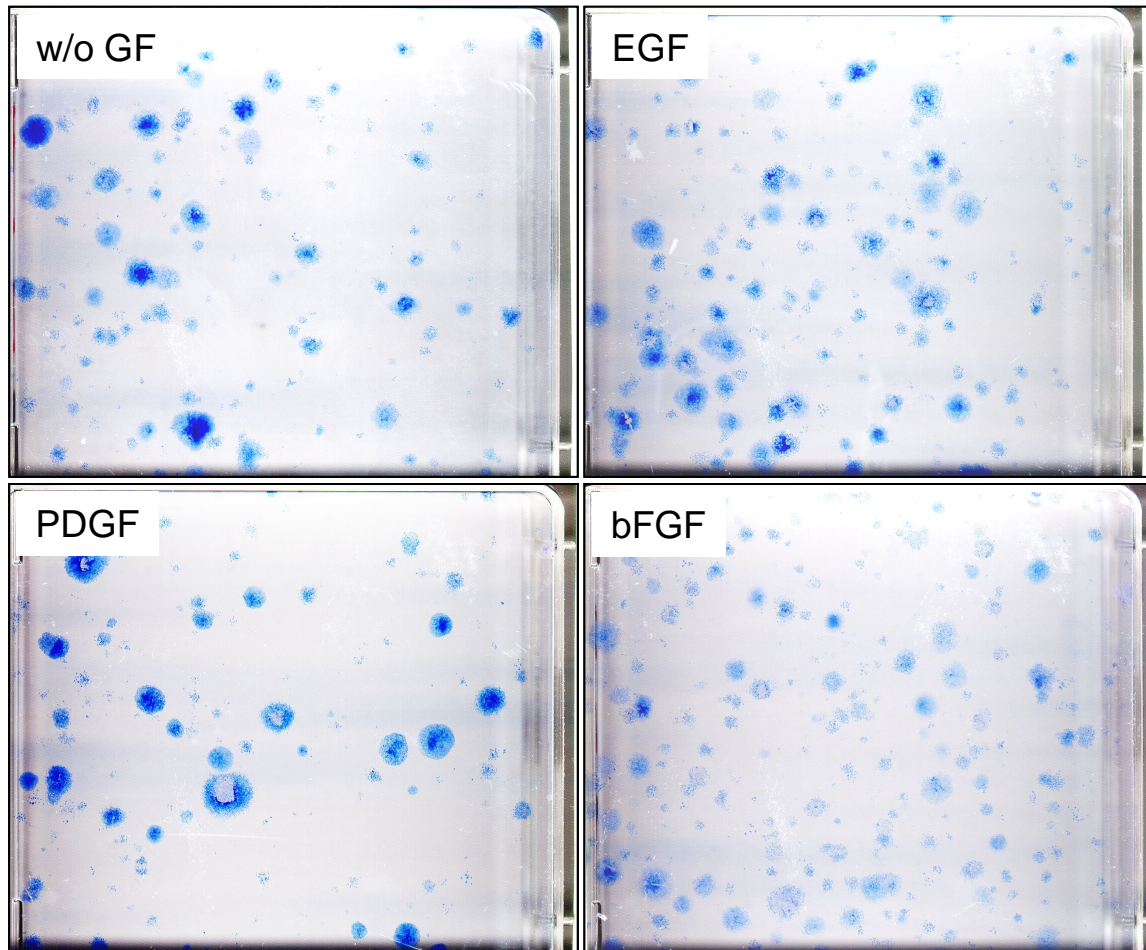


Fig. 9 Stained colonies after 14 days of proliferation. The data presented in Fig. 8 are confirmed by these stainings. The size of the colonies can be estimated using these pictures. PDGF-treated cultures contained a bigger proportion of large colonies, whereas EGF-treated and especially bFGF-treated cultures yielded a bigger portion of smaller colonies as compared to the control group without a growth factor and the PDGF group.

Discussion

This study provides data about the adipogenic differentiation of rat MSCs and its modulation by inducing agents, including dexamethasone (Dex), IBMX, indomethacin (Indo), and insulin (Ins), and growth factors, such as EGF, PDGF-BB, and bFGF. The differentiation process was monitored by staining of developed adipocytes and measurement of GPDH, a key enzyme in lipid biosynthesis that converts dihydroxyacetonephosphate into glycerol-3-phosphate and is a late marker of adipogenesis [37]. The results obtained by these analytical tools were in strong agreement with each other. In addition, the influence of the growth factors EGF, PDGF-BB, and bFGF on the expansion and cell shape of MSCs was investigated.

Dex/IBMX and IBMX/Indo were demonstrated to be the minimal requirement for the induction of adipogenesis in absence of growth factors (data not shown). The combination Dex/IBMX/Indo/Ins exerted the strongest effects on the adipogenic conversion as compared to the other combinations (Figs. 1-4). In regard to the influence of the growth factors, EGF had no effect on the adipogenesis of MSCs and PDGF clearly stimulated adipogenesis, however, bFGF enhanced adipogenesis the most strikingly, especially after the induction using the weak inducer combination Dex/IBMX (Figs. 1-4). Supplementation of any of the growth factors at 3 ng/ml led to stronger or at least similar effects as the addition of 10 ng/ml of the same growth factor. The most potent growth factor, bFGF, was additionally supplemented in the range from 0 to 3 ng/ml (Figs. 5,6). 0.1 ng/ml bFGF clearly increased the adipogenic differentiation as compared to the control. The differentiation was further enhanced by 1 ng/ml and 3 ng/ml bFGF. Consequently, 3 ng/ml bFGF appears to be the optimum concentration for the enhancement of the adipogenic differentiation of MSCs and was, therefore, administered in all following experiments (Chapters 4-7). 3 ng/ml bFGF in combination with Dex/IBMX/Indo/Ins led to the development of the most numerous and most mature adipocytes, that is, to adipocytes with the largest intracellular lipid droplets.

The lack of responsiveness of MSCs to a certain growth factor in regard to the adipogenic differentiation may be due to the absence of cell surface receptors for the growth factors. However, Satomura et al. and Pittenger et al. previously demonstrated the expression of the receptors for EGF, PDGF-BB, and bFGF, the receptor tyrosine kinases EGF-R, PDGF-R β isoform, and FGF-R1 on the surface of MSCs [12,38]. Furthermore, the MSCs used in this study responded to all growth factors in the differentiation experiments and/or in the CFU assay. Gronthos et al. previously reported that EGF and PDGF-BB turned out to be essential and the most potent growth factors for the initial stimulation of the growth of purified MSCs under serum-free conditions, however, bFGF played a secondary role [39]. In the present

study, EGF provoked no effect on the adipogenesis of MSCs, irrespective of the administered inducing cocktail, but increased the colony number in the CFU assay as compared to the control group (Figs. 1-4, 8, and 9). PDGF-BB exerted a clear effect on the adipogenic conversion and simultaneously decreased the colony number accompanied by a striking increase in the portion of large colonies. Basic FGF enhanced, similarly to PDGF-BB, the adipogenic differentiation, but increased, in contrast to PDGF-BB and similarly to EGF, the colony formation.

Regarding these data, an association of the stimulatory effects on the proliferation and the stimulatory effects on the differentiation appears to be unlikely. The stimulation of the proliferation was not a requirement for the stimulation of the differentiation. In contrast, the stimulators of the differentiation of MSCs, PDGF-BB and bFGF, appear to influence the proliferation of different MSC subsets; this is recognizable by the different number and different sizes of developed colonies. As a possible mechanism for the effects of bFGF on the modulation of the differentiation of human MSCs, Bianchi et al. discussed the preferential proliferation and the inhibition of the proliferation of a subpopulation of the MSCs by bFGF [34].

Another mechanism that may clarify the modulation of the MSC behavior by growth factors is the change of the MSC shape after exposure to the growth factors. Martin et al. reported that human MSCs adopt different cell shapes dependent on the presence of bFGF; a large, flattened phenotype in the absence of bFGF and a fibroblastic, more spindle-like shape in presence of bFGF [33]. The osteogenic potential of MSCs cultivated with bFGF was strongly increased and the retention of the differentiation potential was maintained after extensive proliferation with bFGF. Similar observations have been made using bovine chondrocytes in a tissue engineering approach. Chondrocytes expanded in presence of bFGF also adopted a spindle-like shape in contrast to flattened, large cells cultivated in absence of bFGF and, finally, bFGF treatment led to an improvement in the quality of the engineered cartilage [28]. In the present study, the cell shape and the cytoskeletal organization of MSCs expanded under the influence of basal medium; EGF, PDGF-BB, and bFGF showed similar results: large, spread cells with thick actin fibers (Fig. 7). This finding is not in agreement with the two aforementioned studies using human MSCs and bovine chondrocytes under the influence of bFGF [28,33]. The culture conditions of the study using hMSCs are similar to those of the present study in that the MSCs were cultivated on conventional culture plastic with 3 ng/ml bFGF and the human MSCs were cultivated on conventional cell culture plastic using 1 ng/ml

bFGF. However, chondrocytes were cultivated on glass with 5 ng/ml bFGF supplementation. The different surface materials, glass and culture plastics, may explain to the different results. Remarkably, there was one observable difference between the groups “PDGF” and “bFGF” and the groups “w/o GF” and “EGF”. In the groups “PDGF” and “bFGF”, very small cells were observed, which were characterized by their round, non-spread shape. In another study using human MSCs, cells which were flattened and spread underwent osteogenesis, while unspread, round cells became adipocytes [29]. McBeath et al. demonstrated that the cell shape regulated the switch in lineage commitment by modulating endogenous RhoA activity; inhibition of RhoA promotes adipogenesis and activation of RhoA supports osteogenesis. This RhoA commitment signal required actin-myosin-generated tension. A further investigation of the subpopulation characterized by the small and round cells in the present study may give more detailed information about their properties and behavior with regard to the results from McBeath et al [29]. However, it appears to be unlikely that the small round cells are involved in the bFGF-influenced adipogenic differentiation of the MSCs, since the growth of large cell colonies preferably start from large, spread cells (unpublished data).

In conclusion, PDGF-BB and bFGF appear to be enhancers of the adipogenic conversion of MSCs, whereas EGF has no effect in this respect. The highest degree of adipogenesis, the highest numbers of and the most mature adipocytes were obtained after induction with a hormonal cocktail consisting of dexamethasone, IBMX, indomethacin, and insulin in presence of bFGF. The growth factors have different effects on the initial proliferation of MSCs, inhibitory effects were provoked by PDGF-BB, whereby stimulatory effects were induced by EGF and bFGF. Most of the cells propagated either with or without growth factors phenotypically appear to be large and spread cells, however, in presence of PDGF-BB and bFGF a considerable portion of very small, unspread, and round MSCs were observed. Further data and discussion on possible mechanisms of effects of bFGF on the adipogenesis of MSCs are provided in chapters 4 and 5 of this thesis.

References

- [1] Gregoire FM, Smas CM, Sul HS. 'Understanding adipocyte differentiation'. *Physiol Rev* (1998); **78**: 783-809.
- [2] Rosen ED, Spiegelman BM. 'Molecular Regulation of Adipogenesis'. *Annu Rev Cell Dev Biol* (2000); **16**: 145-171.
- [3] Dani C, Smith AG, Dessolin S, Leroy P, Staccini L, Villageois P, Darimont C, Ailhaud G. 'Differentiation of embryonic stem cells into adipocytes in vitro'. *J Cell Sci* (1997); **110**: 1279-1285.
- [4] Gimble JM, Dorheim MA, Cheng Q, Medina K, Wang CS, Jones R, Koren E, Pietrangeli C, Kincade PW. 'Adipogenesis in a murine bone marrow stromal cell line capable of supporting B lineage lymphocyte growth and proliferation: biochemical and molecular characterization'. *Eur J Immunol* (1990); **20**: 379-387.
- [5] Gimble JM, Morgan C, Kelly K, Wu X, Dandapani V, Wang CS, Rosen V. 'Bone morphogenetic proteins inhibit adipocyte differentiation by bone marrow stromal cells'. *J Cell Biochem* (1995); **58**: 393-402.
- [6] Gimble JM, Robinson CE, Wu X, Kelly KA, Rodriguez BR, Kliewer SA, Lehmann JM, Morris DC. 'Peroxisome proliferator-activated receptor- γ activation by thiazolidinediones induces adipogenesis in bone marrow stromal cells'. *Mol Pharmacol* (1996); **50**: 1087-1094.
- [7] Tontonoz P, Hu E, Spiegelman BM. 'Stimulation of adipogenesis in fibroblasts by PPAR γ 2, a lipid-activated transcription factor'. *Cell* (1994); **79**: 1147-1156.
- [8] Kliewer SA, Willson TM. 'The nuclear receptor PPAR γ -bigger than fat'. *Curr Opin Genet Dev* (1998); **8**: 576-581.
- [9] Lehmann JM, Lenhard JM, Oliver BB, Ringold GM, Kliewer SA. 'Peroxisome Proliferator-activated receptors α and γ are activated by indomethacin and other non-steroidal anti-inflammatory drugs'. *J Biol Chem* (1997); **272**: 3406-3410.
- [10] Locklin RM, Williamson MC, Beresford JN, Triffitt JT, Owen ME. 'In vitro effects of growth factors and dexamethasone on rat marrow stromal cells'. *Clin Orthop* (1995); **313**: 27-35.
- [11] Locklin RM, Oreffo ROC, Triffitt JT. 'Effects of TGF β and bFGF on the differentiation of human bone marrow stromal fibroblasts'. *Cell Biol Int* (1999); **23**: 185-194.
- [12] Pittenger MF, Mackay AM, Beck SC, Jaiswal RK, Douglas R, Mosca JD, Moorman MA, Simonetti DW, Craig S, Marshak DR. 'Multilineage potential of adult human mesenchymal stem cells'. *Science* (1999); **284**: 143-147.
- [13] Muraglia A, Cancedda R, Quarto R. 'Clonal mesenchymal progenitors from human bone marrow differentiate in vitro according to a hierarchical model'. *J Cell Sci* (2000); **113**: 1161-1166.

- [14] Tsutsumi S, Shimazu A, Miyazaki K, Pan H, Koike C, Yoshida E, Takagishi K, Kato Y. 'Retention of multilineage differentiation potential of mesenchymal cells during proliferation in response to FGF'. *Biochem Biophys Res Commun* (2001); **288**: 413-419.
- [15] Janderova L, McNeil M, Murrell AN, Mynatt RL, Smith SR. 'Human mesenchymal stem cells as an in vitro model for human adipogenesis'. *Obes Res* (2003); **11**: 65-74.
- [16] Sottile V, Seuwen K. 'Bone morphogenetic protein-2 stimulates adipogenic differentiation of mesenchymal precursor cells in synergy with BRL 49653 (rosiglitazone)'. *FEBS Lett* (2000); **475**: 201-204.
- [17] Dani C. 'Embryonic stem cell-derived adipogenesis'. *Cells Tissues Organs* (1999); **165**: 173-180.
- [18] Hanada K, Dennis JE, Caplan AI. 'Stimulatory effects of basic fibroblast growth factor and bone morphogenetic protein-2 on osteogenic differentiation of rat bone marrow-derived mesenchymal stem cells'. *J Bone Miner Res* (1997); **12**: 1606-1614.
- [19] Pitaru S, Kotev-Emeth S, Noff D, Kaffuler S, Savion N. 'Effect of basic fibroblast growth factor on the growth and differentiation of adult stromal bone marrow cells: enhanced development of mineralized bone-like tissue in culture'. *J Bone Miner Res* (1993); **8**: 919-929.
- [20] Hauner H, Roehrig K, Petruschke T. 'Effects of epidermal growth factor (EGF), platelet-derived growth factor (PDGF) and fibroblast growth factor (FGF) on human adipocyte development and function'. *Eur J Clin Invest* (1995); **25**: 90-96.
- [21] Kim MK, Niyibizi C. 'Interaction of TGF- β 1 and rhBMP-2 on human bone marrow stromal cells cultured in collagen gel matrix'. *Yonsei Med J* (2001); **42**: 338-344.
- [22] Lisignoli G, Remiddi G, Cattini L, Cocchini B, Zini N, Fini M, Grassi F, Piacentini A, Facchini A. 'An elevated number of differentiated osteoblast colonies can be obtained from rat bone marrow stromal cells using a gradient isolation procedure'. *Connect Tissue Res* (2001); **42**: 49-58.
- [23] Sanchez-Ramos J, Song S, Cardozo-Pelaez F, Hazzi C, Stedeford T, Willing A, Freeman TB, Saporta S, Janssen W, Patel N. 'Adult bone marrow stromal cells differentiate into neural cells *in vitro*'. *Exp Neurol* (2000); **164**: 247-256.
- [24] Kicic A, Shen WY, Wilson AS, Constable IJ, Robertson T, Rakoczy PE. 'Differentiation of marrow stromal cells into photoreceptors in the rat eye'. *J Neurosci* (2003); **23**: 7742-7749.
- [25] Adachi H, Kurachi H, Homma H, Adachi K, Imai T, Morishige K, Matsuzawa Y, Miyake A. 'Epidermal growth factor promotes adipogenesis of 3T3-L1 cell in vitro'. *Endocrinology* (1994); **135**: 1824-1830.
- [26] Cassiede P, Dennis JE, Ma F, Caplan AI. 'Osteochondrogenic potential of marrow mesenchymal progenitor cells exposed to TGF- β 1 or PDGF-BB as assayed in vivo and in vitro'. *J Bone Miner Res* (1996); **11**: 1264-1273.

- [27] Chaudhary LR, Hofmeister AM, Hruska KA. 'Differential growth factor control of bone formation through osteoprogenitor differentiation'. *Bone* (2004); **34**: 402-411.
- [28] Martin I, Vunjak-Novakovic G, Yang J, Langer R, Freed LE. 'Mammalian chondrocytes expanded in the presence of fibroblast growth factor 2 maintain the ability to differentiate and regenerate three-dimensional cartilaginous tissue'. *Exp Cell Res* (2001); **253**: 681-688.
- [29] McBeath R, Pirone DM, Nelson CM, Bhadriraju K, Chen CS. 'Cell shape, cytoskeletal tension, and RhoA regulate stem cell lineage commitment'. *Dev Cell* (2004); **6**: 483-495.
- [30] Ishaug SL, Crane GM, Miller MJ, Yasko AW, Yaszemski MJ, Mikos AG. 'Bone formation by three-dimensional stromal osteoblast culture in biodegradable polymer scaffolds'. *J Biomed Mater Res* (1997); **36**: 17-28.
- [31] Pairault J, Green H. 'A study of the adipose conversion of suspended 3T3 cells by using glycerophosphate dehydrogenase as differentiation marker'. *Proc Natl Acad Sci USA* (1979); **76**: 5138-5142.
- [32] Lowry OH, Rosebrough NJ, Farr AL, Randall RJ. 'Protein measurement with the Folin phenol reagent'. *J Biol Chem* (1951); **193**: 265-275.
- [33] Martin I, Muraglia A, Campanile G, Cancedda R, Quarto R. 'Fibroblast Growth Factor-2 Supports ex Vivo Expansion and Maintenance of Osteogenic Precursors from Human Bone Marrow'. *Endocrinology* (1997); **138**: 4456-4462.
- [34] Bianchi G, Banfi A, Mastrogiacomo M, Notaro R, Luzzatto L, Cancedda R, Quarto R. 'Ex vivo enrichment of mesenchymal cell progenitors by fibroblast growth factor 2'. *Exp Cell Res* (2003); **287**: 98-105.
- [35] Lennon DP, Haynesworth SE, Young RG, Dennis JE, Caplan AI. 'A chemically defined medium supports in vitro proliferation and maintains the osteochondral potential of rat marrow-derived mesenchymal stem cells'. *Exp Cell Res* (1995); **219**: 211-222.
- [36] Bianco P. 'Personal communication' (2004)
- [37] Sottile V, Seuwen K. 'A high-capacity screen for adipogenic differentiation'. *Anal Biochem* (2001); **293**: 124-128.
- [38] Satomura K, Derubeis AR, Fedarko NS, Ibaraki-O'Connor K, Kuznetsov SA, Rowe DW, Young MF, Robey PG. 'Receptor tyrosine kinase expression in human bone marrow stromal cells'. *J Cell Physiol* (2001); **177**: 426-438.
- [39] Gronthos S, Simmons PJ. 'The growth factor requirements of STRO-1-positive human bone marrow stromal precursors under serum-deprived conditions in vitro'. *Blood* (1995); **85**: 929-940.

Chapter 4

Basic Fibroblast Growth Factor Enhances PPAR γ Ligand-induced Adipogenesis of Mesenchymal Stem Cells

Markus Neubauer, Claudia Fischbach , Petra Bauer-Kreisel, Esther Lieb, Michael Hacker,
Joerg Tessmar, Michaela B Schulz, Achim Goepferich, Torsten Blunk

Department of Pharmaceutical Technology, University of Regensburg,
Universitaetsstrasse 31, D-93040 Regensburg, Germany

FEBS Letters (2004); **577**: 277-283.

Abstract

Mesenchymal stem cells (MSCs) are capable of differentiating into a variety of lineages including bone, cartilage, or fat depending on the inducing stimuli and specific growth and differentiation factors. It is widely acknowledged that basic fibroblast growth factor (bFGF) modulates chondrogenic and osteogenic differentiation of MSCs, but thorough investigations of its effects on adipogenic differentiation are lacking.

In this study, we demonstrate on the cellular and molecular level that supplementation of bFGF in different phases of cell culture leads to a strong enhancement of adipogenesis of MSCs, as induced by an adipogenic hormonal cocktail. In cultures receiving bFGF, mRNA expression of peroxisome proliferator-activated receptor γ 2 (PPAR γ 2), a key transcription factor in adipogenesis, was upregulated even prior to adipogenic induction. In order to investigate the effects of bFGF on PPAR γ ligand-induced adipogenic differentiation, the thiazolidinedione troglitazone was administered as a single adipogenic inducer. Basic FGF was demonstrated to also strongly increase adipogenesis induced by troglitazone, that is, bFGF clearly increased the responsiveness of MSCs to a PPAR γ ligand.

Introduction

Multipotent mesenchymal stem cells (MSCs) are present in a variety of tissues including bone marrow, blood, muscle, and adipose tissue [1-4]. MSCs were found to differentiate into cartilage, bone, fat, muscle, and other connective tissues [5,6] depending on culture conditions, which include supplementation of lineage-specific inducing agents as well as hormones and growth factors.

Basic fibroblast growth factor (bFGF) belongs to the family of heparin-binding growth factors [7]. To date, more than twenty FGFs have been discovered and FGFs are known to induce chemotactic, angiogenic, and mitogenic activity and play an important role in early differentiation and developmental processes [8,9]. Basic FGF was reported to influence differentiation of MSCs of various species towards different lineages. Addition of bFGF was shown to enhance chondrogenic and osteogenic differentiation of avian MSCs [10] and to retain the differentiation potential of extensively expanded human MSCs towards both the chondrogenic and osteogenic lineage [11]. Using rat MSCs cultivated under varying conditions, the stimulatory effects of bFGF were repeatedly shown to promote differentiation towards the osteogenic lineage [12-14]. In contrast, the effect of bFGF on the adipogenesis of MSCs is controversially discussed [11,15,16]. However, those studies were not focused on adipogenesis; instead experimental conditions were adjusted to the investigation of osteogenesis or chondrogenesis and adipogenic differentiation was mainly assessed by morphology.

Thus, the first goal of this study was to investigate the effects of bFGF on the adipogenic differentiation of rat MSCs induced by an adipogenic hormonal cocktail consisting of dexamethasone, insulin, 3-isobutyl-1-methylxanthine (IBMX) and indomethacin. bFGF was supplemented in different phases of the culture and adipogenesis was characterized on the cellular and the molecular level. Remarkably, in these experiments mRNA expression of the peroxisome proliferator-activated receptor $\gamma 2$ (PPAR $\gamma 2$), a key transcription factor in adipogenesis in vitro and in vivo [17], was elevated in the bFGF group not only during the course of differentiation, but already prior to adipogenic induction. From this result, it was hypothesized that bFGF can also enhance adipogenesis that is solely induced by a PPAR γ ligand. Therefore, the second goal was to determine the effects of bFGF on adipogenic differentiation induced by the thiazolidinedione troglitazone, an acknowledged synthetic ligand of PPAR γ [18].

Materials and Methods

Materials

If not otherwise stated, chemicals were obtained from Sigma, Steinheim, Germany. Basic FGF was obtained from R&D Systems (Minneapolis, MN, USA). Troglitazone and insulin were kindly provided by Dr. T. Skurk (Deutsches Diabetes Forschungsinstitut, Duesseldorf, Germany) and Hoechst Marion Roussel (Frankfurt am Main, Germany), respectively. Cell culture plastics were purchased from Corning Costar (Bodenheim, Germany).

Cell Culture

Marrow stromal cells were obtained from six-week old male Sprague Dawley rats (weight: 170 - 180 g, Charles River, Sulzfeld, Germany). MSCs were flushed from the tibiae and femora according to the protocol of Ishaug [19]. Cells were centrifuged at 1,200 rpm for 5 min. The resulting cell pellet was resuspended in basal medium consisting of DMEM (Biochrom, Berlin, Germany), 10% fetal bovine serum (Gemini Bio-Products Inc., Calabasas, CA, USA), 1% penicillin/streptomycin (Invitrogen, Karlsruhe, Germany), and 50 μ g/ml ascorbic acid. Cells were seeded in T75 flasks and cultured at 37°C and 5% CO₂. Cells were allowed to adhere to the substratum for three days. The flasks were rinsed twice with phosphate-buffered saline (PBS, Invitrogen, Karlsruhe, Germany) in order to remove non-adherent cells. In the following experiments, bFGF was supplemented during different periods of the culture (Fig. 1). Culturing the adherent cells, 12 ml of basal medium with or without 3 ng/ml bFGF were exchanged every 2-3 days until confluence was reached (proliferation phase I, Fig. 1). Cells were passaged once with 0.25% trypsin and EDTA (Invitrogen, Karlsruhe, Germany). For adipogenic differentiation, cells were seeded at a density of 30,000 cells/cm² in either six-well plates (RT-PCR) or 24-well plates (GPDH activity assay, flow cytometry and histological staining) and grown to postconfluence for 3 days with or without bFGF (proliferation phase II, Fig. 1). Subsequently, cells were differentiated for 8 days either in the presence or absence of bFGF (differentiation phase, Fig. 1). In detail, to induce adipogenic differentiation, cultures were treated for 3 days with a hormonal cocktail containing 0.5 mM 3-isobutyl-1-methylxanthine (IBMX) (Serva Electrophoresis, Heidelberg, Germany), 10 nM dexamethasone, 60 μ M indomethacin and 10 μ g/ml insulin, which was added to the basal medium. Subsequently, cultures were maintained for 5 more days in differentiation medium consisting of basal medium supplemented with 10 μ g/ml insulin. Alternatively, cells treated with or without bFGF were differentiated by adding exclusively 5 μ M troglitazone (instead of the hormonal cocktail) to basal medium. For this purpose, troglitazone was dissolved in

dimethylsulfoxide as a 1000-fold stock solution, which was administered with each medium change during the complete course of differentiation (i.e. 8 days) [20].

The supplementation scheme of bFGF is depicted in Fig. 1. Briefly, medium supplemented with bFGF is abbreviated with “F”, basal medium without bFGF with “B”. Cultures treated with bFGF only in proliferation phase II for 3 days are designated as BFB. Addition of the factor during proliferation phases I and II for 15 days is indicated as FFB. Supplementation of bFGF exclusively in differentiation phase is abbreviated as BBF and bFGF treatment during complete time of cell culture as FFF. Cells grown in complete absence of bFGF (BBB) served as control. In preliminary experiments (assessment of adipogenesis by Oil Red O staining), bFGF was additionally supplemented only in the proliferation phase I for 12 days. This condition yielded results similar to those of the group receiving bFGF during proliferation phases I and II for 15 days (data not shown); consequently, in order to simplify the experimental design, this group (bFGF in proliferation phase I only) was omitted in the presented study.

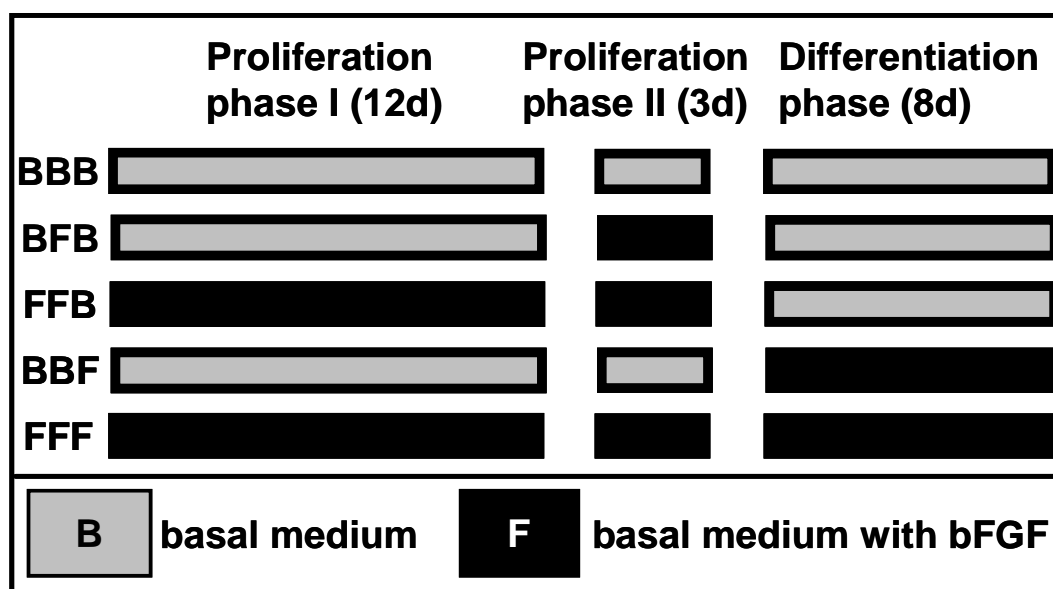


Fig.1 Basic FGF supplementation in different periods of the cell culture. MSCs were exposed to bFGF only in proliferation phase II for 3 days (BFB), only in both proliferation phases I and II for 15 days (FFB), only in the differentiation phase (BBF), or throughout the complete culture period (FFF). Cells grown in the absence of bFGF (BBB) served as a control. Grey boxes represent basal media without bFGF (B), black boxes represent basal medium supplemented with bFGF (F).

GPDH activity assay

Glycerol-3-phosphate dehydrogenase (GPDH) activity was measured using a protocol adapted from Paircault and Green [21]. In brief, cells washed with PBS were scraped in lysis buffer containing 50 mM Tris, 1 mM EDTA, and 1 mM β -mercaptoethanol on ice. Subsequently, the resulting suspension was sonicated with a digital sonifier (Branson Ultrasonic Corporation, Danburg, CT, USA). Cell lysates were centrifuged for 5 min at 13,200 rpm at 4°C. Aliquots of the supernatant were mixed with a solution containing 0.1 M triethanolamine, 2.5 mM EDTA, 0.5 mM β -mercaptoethanol, 120 μ M reduced nicotinamide adenine dinucleotide (NADH) (Roche, Mannheim, Germany), and 200 μ M dihydroxyacetonephosphate. Enzyme activity was monitored by measurement of the disappearance of NADH at 340 nm over 4.2 min. Enzyme activity was normalized to the protein content of each sample. Proteins were determined by the method of Lowry et al. [22]. Proteins were precipitated using 12% trichloroacetic acid. In alkaline solution, proteins were solubilized and complexed with a mixture of disodium tartrate, copper sulfate and folin-ciocalteu reagent (all Merck, Darmstadt, Germany). Absorption was measured at 546 nm after 30 min incubation.

Oil Red O staining

Cells were washed once with PBS and fixed with 10% formaldehyde (Merck, Darmstadt, Germany) overnight. Cells were covered with 3 mg/ml Oil Red O for 2h. Excess dye was removed with PBS and finally, cells were fixed with 10% formaldehyde.

Flow cytometry

This method was carried out using a protocol adapted from Gimble et al. [23]. Cells were carefully harvested by treatment with 0.25% trypsin/EDTA and centrifuged at 200 g at 4°C for 5 min. After washing the pellet with PBS, cells were centrifuged as described above and resuspended in PBS containing the lipophilic fluorescent dye Nile Red. Cells were incubated for 30 min on ice. Samples were analyzed with a FACSCalibur flow cytometer (Becton Dickinson, Heidelberg, Germany). Nile Red fluorescence was measured on the FL2 emission channel through a 585 \pm 21 nm band pass filter, following excitation with an argon ion laser source at 488 nm. For each sample, 10⁴ cells were collected. To determine the number of adipocytes in each sample, a selection marker M1 was set in histograms. The amount of adipocytes was assessed by determining the percentage of cells within the M1 region.

Reverse transcription-polymerase chain reaction (RT-PCR)

Total RNA was harvested from the cells with Trizol reagent (Invitrogen, Karlsruhe, Germany) and isolated according to the manufacturer's instructions. First-strand cDNA was synthesized from total RNA by using random hexamers (Roche Diagnostics, Mannheim, Germany) and Superscript II RNase H Reverse Transcriptase (Invitrogen, Karlsruhe, Germany). Samples were incubated at 42°C for 50 min and heated afterwards at 70°C for 15 min to inactivate the enzyme. Subsequently, PCR was performed with Sawady Taq-DNA-Polymerase (PeqLab, Erlangen, Germany); initial denaturation occurred at 94°C for 120 s, final extension at 72°C for 30 s for each set of primers. The amplification was carried out using the following specific oligonucleotides:

PPAR γ 2:	5'-GAGCATGGTGCCTTCGCTGA-3' / 5'-AGCAAGGCACTTCTGAAACCGA-3'
GLUT4:	5'-AGCAGCTCTCAGGCATCAAT-3' / 5'-CTCAAAGAAGGCCACAAAGC-3'
SCD-1:	5'-CGGGATCACCGCGCCACCACAAGT-3' / 5'-CCACGGACCCAGGGAAACCAGGATG-3'
18S:	5'-TCAAGAACGAAAGTCGGAGGTTTCG-3' / 5'-TTATTGCTCAATCTCGGGTGGCTG-3'

18S rRNA served as control. Conditions set for the investigated genes were: 94°C for 45 s, 62°C for 45 s, 72°C for 1 min (36 cycles) for PPAR γ 2; 94°C for 45 s, 56 °C for 45 s, 72°C for 1 min (32 cycles) for GLUT4; 94°C for 45 s, 62°C for 45 s, 72°C for 1 min (36 cycles) for SCD-1; and 94°C for 45 s, 56°C for 45 s, 72°C for 1 min (25 cycles) for 18S rRNA. Reverse transcription and PCR were performed using a Mastercycler Gradient (Eppendorf AG, Hamburg, Germany). The PCR products were analyzed by electrophoresis on 2% agarose gels, stained with ethidium bromide. Finally, the gels were subjected to imaging and densitometric scanning of the resulting bands under UV light ($\lambda = 312$ nm) using a Kodak EDAS 290 (Fisher Scientific, Schwerte, Germany).

Statistics

FACS data, GPDH data, and RT-PCR quantification are expressed as means \pm standard deviation. Single-factor analysis of variance (ANOVA) was used in conjunction with a multiple comparison test (Tukey's test) to assess statistical significance at a level of $p < 0.01$ for FACS and GPDH data and of $p < 0.05$ for RT-PCR data.

Results

In cultures that did not receive adipogenesis-inducing agents, no lipid droplets were observed in the absence of bFGF (Fig. 2 “BBB-not induced”, Tab. 1) and only very few lipid droplets were detected in the presence of bFGF (Fig. 2 “FFF-not induced”, Tab. 1). Moreover, the activity of GPDH, a key enzyme in lipid biosynthesis, was virtually undetectable in the absence of inducing agents, irrespective of bFGF supplementation (Fig. 3).

In order to investigate the modulating effects of bFGF, cultures stimulated by hormonal inducers were supplemented with bFGF in different phases of the cell culture (Fig. 1). In cultures without bFGF (BBB-control), MSCs only weakly gave rise to adipocytes after induction with a hormonal cocktail (Fig. 2): Only about 2% of cultured cells differentiated into adipocytes, as determined by FACS analysis (Table 1). Exposure to bFGF enhanced the adipogenesis of MSCs in all cases, as determined 8 days after induction by Oil Red O staining and Nile Red flow cytometry of differentiated adipocytes (Fig. 2). Supplementation with bFGF only during the proliferation phase II (BFB) and during the proliferation phases I and II (FFB) yielded a 2.8-fold and 6-fold increase of the fraction of adipocytes, respectively, as compared to BBB-control (Table 1). The latter resulted in adipocytes containing the largest lipid droplets of all groups investigated (Fig. 2). Addition of bFGF in the differentiation phase only (BBF) resulted in a 2.3-fold increase of the adipocyte fraction (Table 1), whereas bFGF supplementation during the complete culture (FFF) yielded the largest increase, i.e., 9.4-fold.

Experimental group	FACS (% cells in M1)	FACS (relative)
BBB - not induced	0.34 \pm 0.06	-
FFF - not induced	1.43 \pm 0.65	-
BBB (induced) - control	2.23 \pm 0.42	1.00
BFB (induced)	6.21 \pm 0.95 *	2.78
FFB (induced)	13.46 \pm 1.19 **	6.03
BBF (induced)	5.07 \pm 0.64 *	2.27
FFF (induced)	20.90 \pm 1.15 ***	9.36

Table 1 Quantification of flow cytometry analysis. To determine the number of adipocytes in each sample, a selection marker M1 was set in histograms (see Fig. 2). Column 2 represents the quantification of differentiated adipocytes expressed as a percentage of total cells in culture, column 3 shows the relative increase as compared to control group without bFGF (BBB induced-control). Tukey’s test ($n=4$) indicates a statistical significantly increase as compared to control group (BBB) (*), compared to BBB, BFB and BBF (**), and compared to all groups (***).

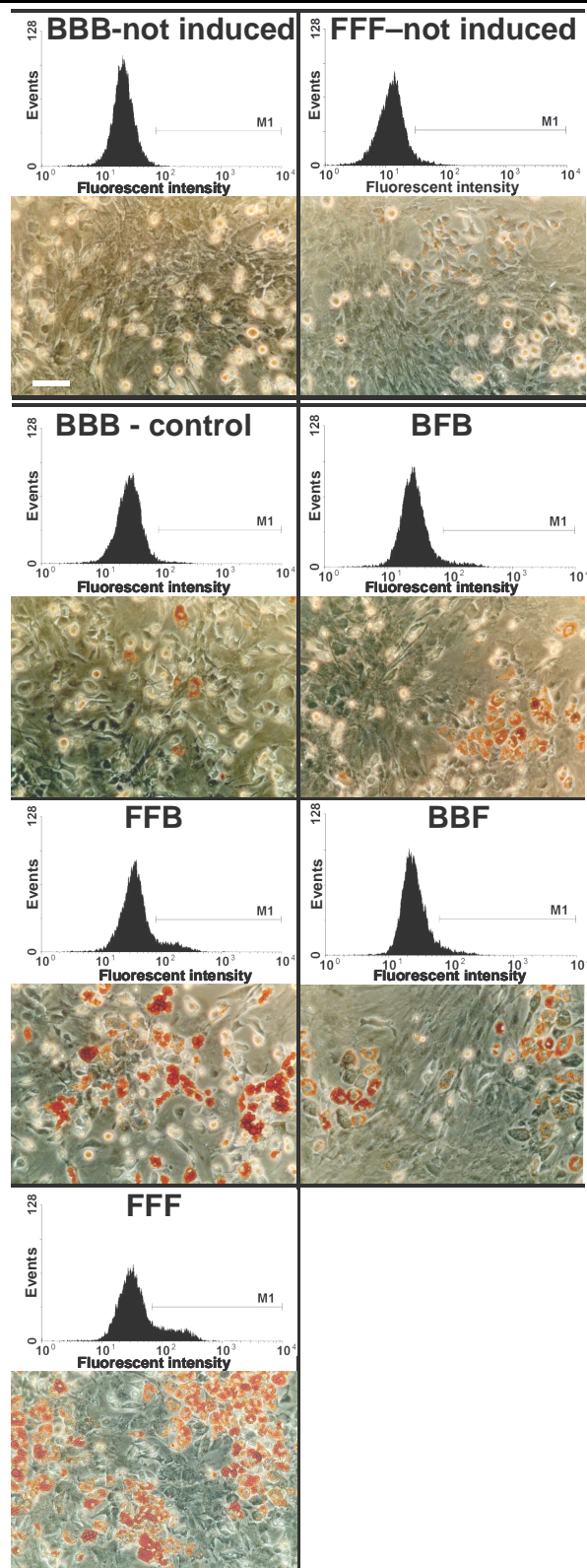


Fig. 2 Adipogenesis of MSCs on day 8 of differentiation: assessment by Oil Red O staining and Nile Red flow cytometry (for quantification data, see Tab. 1). The groups designated as “not induced” were cultivated without induction by the hormonal cocktail (BBB-not induced: in the absence of bFGF; FFF-not induced: in the presence of bFGF). All other groups were hormonally induced. BBB-control was cultivated in the absence of bFGF and served as a control group. Other cultures were treated with bFGF in proliferation phase II for 3 days (BFB), in proliferation phase I and II for 15 days (FFB), in the differentiation phase (BBF), and in complete culture (FFF), respectively. Scale bar: 50 μ m.

Measurement of the GPDH activity supported the observations with regard to effects of bFGF (Fig. 3). In all induced cultures supplemented with bFGF, a significant increase of GPDH activity was detected as compared to the BBB control group. The highest values were again determined for experimental groups FFB and FFF.

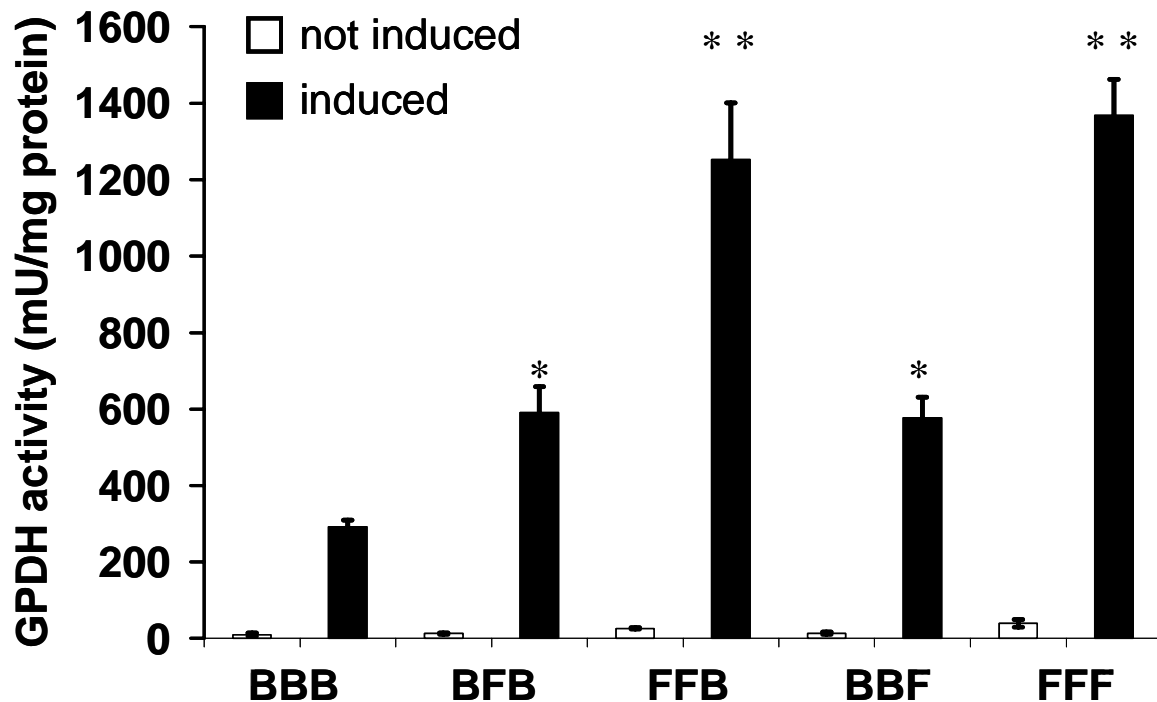


Fig. 3 Measurement of GPDH activity on day 3 of differentiation. Cultures were treated with bFGF in proliferation phase II for 3 days (BFB), in proliferation phase I and II for 15 days (FFB), in the differentiation phase (BBF), and in complete culture (FFF), respectively. Cells grown in absence of bFGF served as control (BBB). GPDH activity was determined in not induced cultures (\square) and in induced cultures (\blacksquare). Tukey's test ($n=4$) indicated a statistically significant increase as compared to control group (BBB) (*) and as compared to BBB, BFB and BBF (**).

Expression of the adipocyte-specific genes PPAR γ 2, a key transcription factor, GLUT4, a glucose transporter and late marker of adipogenesis, and stearoyl-CoA desaturase (SCD-1), a key enzyme in the synthesis of unsaturated fatty acids and also a late marker of adipogenesis, was determined on the mRNA level by RT-PCR (Fig. 4). Selected experimental groups were investigated in order to further elucidate the contribution of bFGF to adipogenic differentiation, i.e., the group receiving bFGF throughout the entire proliferation phase (FFB) was compared to the BBB control group. Gene expression of PPAR γ 2 was assessed one day before induction (cells grown to confluence), one day and three days after induction (Fig. 4B). Expression of PPAR γ 2 was increased on day one and day three after induction, as compared to samples harvested one day prior to induction (Fig. 4A). PPAR γ 2 expression was elevated in

the group receiving bFGF (FFB) as compared to the control group (BBB); this trend was observed not only one day and three days after, but also one day before induction (Fig. 4A). Additionally, gene expression of late markers of adipogenic differentiation, GLUT4 and SCD-1, was assessed on day three after induction (Fig. 4B). Again, quantification showed that differentiation under the influence of bFGF (FFB) led to an increased expression of both markers as compared to the control group (BBB) (Fig. 4B).

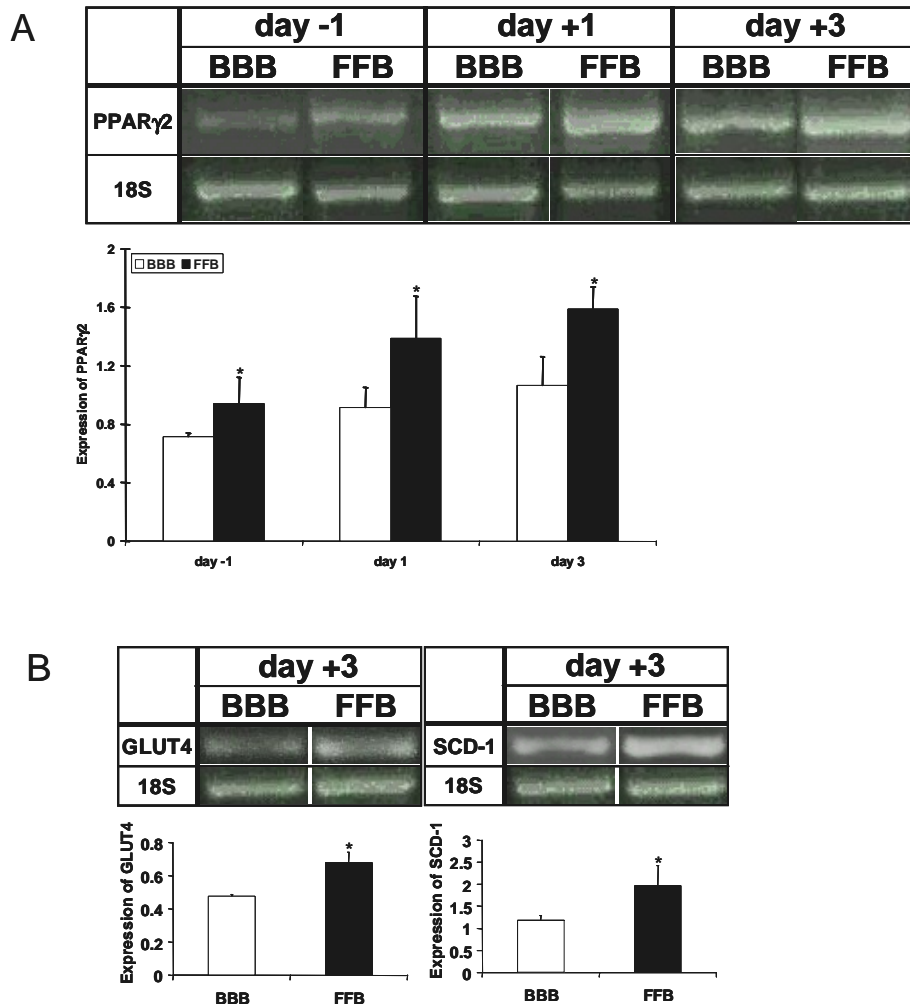


Fig. 4 Assessment of expression of adipocytic genes PPAR γ 2, GLUT4, and SCD-1 using RT-PCR technique. Two experimental groups (BBB and FFB) were exemplarily investigated to demonstrate the effect of bFGF. Three independent experiments were conducted; representative results of one experiment are shown here. Additionally, data from semi-quantitative image analysis are depicted. Statistically significant difference between BBB and FFB group is indicated by *. (A) The expression levels of the transcription factor PPAR γ 2 were determined one day before, one day after and three days after induction with the hormonal cocktail. 18S RNA was used as an internal control. (B) Gene expression of late markers of adipogenic differentiation, GLUT4 and SCD-1 was determined on day 3 after induction.

When using troglitazone as a single inducer (instead of the hormonal cocktail), adipogenic differentiation of MSCs was also observed. In detail, only weak adipogenesis was detected in absence of bFGF (Fig. 5B). Again, the exposure of MSCs to bFGF throughout the entire culture period resulted in a strong enhancement of adipogenesis, which was detected by Oil Red O staining (Fig. 5D) and GPDH activity (Fig. 6). In general, after induction with troglitazone, intracellular lipid droplets were distinctly smaller compared to cultures induced with the hormonal cocktail (Fig. 5), a previously described phenomenon [24]. Apart from that, with regard to Oil Red O staining and GPDH activity, troglitazone cultures were comparable to corresponding cultures employing the hormonal cocktail. Hence, adipogenic differentiation was enhanced by bFGF to the same extent under both inducing conditions (Figs. 5 and 6).

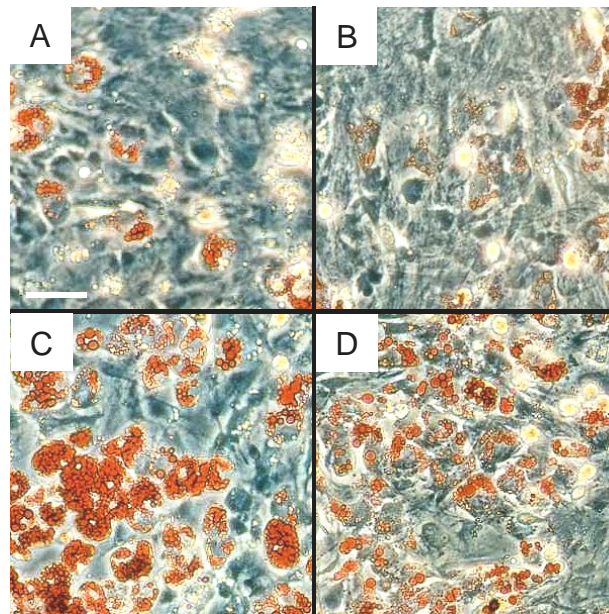


Fig. 5 Oil Red O staining of differentiated adipocytes on day 8 of differentiation. MSCs were induced with the hormonal cocktail in the absence (A) and in the presence of bFGF (during complete culture) (C) or with troglitazone in the absence (B) and the presence of bFGF (during complete culture) (D), respectively. Scale bar: 50 μ m.

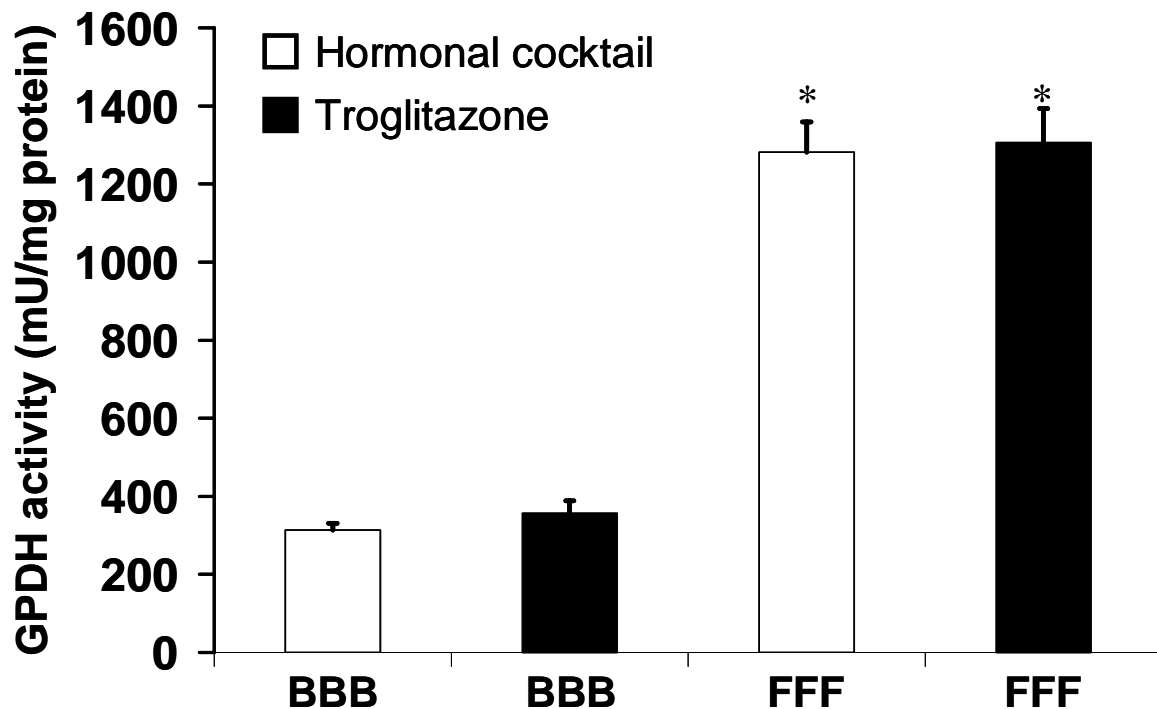


Fig. 6 Measurement of GPDH activity on day 3 of differentiation. MSCs were induced with either the hormonal cocktail (\square) or with troglitazone alone (\blacksquare). For each induction condition, cells were cultivated either in the absence (BBB) or in the presence of bFGF during the entire culture period (FFF). Asterisks indicate significantly elevated values as compared to the control group (BBB) ($n=3$).

Discussion

Adipogenesis is a complex process involving several transcription factors and signal transduction pathways and is affected by a variety of environmental conditions like growth and differentiation factors [17]. In this study, we show that the growth factor bFGF can strongly enhance adipogenesis of MSCs induced by a widely used hormonal cocktail consisting of dexamethasone, IBMX, indomethacin, and insulin.

Besides other features of adipogenic differentiation (Figs. 2,3,4B), bFGF increased the expression of PPAR γ 2, a key transcription factor in adipogenesis [17]. As this effect was observed even prior to adipogenic induction (Fig. 4A), the hypothesis that bFGF can also enhance adipogenic differentiation that is induced by a PPAR γ ligand alone was explored. Indeed, bFGF enhanced adipogenesis solely induced by troglitazone, a commonly recognized PPAR γ ligand, to the same extent as that induced by the hormonal cocktail (Figs. 5-6).

The effects of bFGF on the hormonal cocktail-induced adipogenesis of MSCs is inherently more complex to explain. The inducing effects of dexamethasone and IBMX are still not well understood and are controversially discussed [17]. However, indomethacin is commonly

acknowledged to be a PPAR γ ligand [25]. Furthermore, other experiments using only IBMX and indomethacin as adipogenic inducers showed enhancing effects of bFGF similar to those observed in the experiments employing the complete hormonal cocktail (data not shown). Therefore, the function of indomethacin as PPAR γ ligand suggests that, again, the increase of PPAR γ 2 levels by bFGF likely contributed to the observed effects.

The obtained results are in agreement with earlier morphological observations using rat MSCs [16]. The seemingly contradictory results of a different report obtained with human MSCs showing no effect of bFGF treatment may be reasonably explained by distinctly different adipogenic inducing schemes [11]. In contrast to our induction phase of 3 days, Tsutsumi et al. used a similar hormonal cocktail for 25 days and determined comparable results for groups with and without bFGF supplement [11]. Additionally, preliminary experiments in our laboratory using human MSCs yielded results similar to our data from the rat MSCs, suggesting that the effects of bFGF on adipogenic differentiation are not species-specific.

In the following, possible mechanisms are discussed through which bFGF may enhance adipogenesis and result in elevated PPAR γ 2 expression levels, respectively. First, bFGF may cause a preferential proliferation of a subpopulation of MSCs [26,27], e.g., one with enhanced expression of PPAR γ 2. In this regard, the theoretically possible contribution of differentiated adipocytes, which are present in the bone marrow [28], can be excluded: Mature adipocytes do not attach to the substratum during cell isolation due to their buoyancy [29] and, in the case they did so nonetheless, they would be identified by their typical phenotype (lipid droplets); furthermore, they have been demonstrated to be virtually unable to proliferate on culture plastic substrate [30]. An alternative explanation for enhanced adipogenesis is that bFGF may exert a direct effect on differentiation or commitment level [26,27], e.g., by directly inducing or at least maintaining expression levels of PPAR γ 2 mRNA of MSCs. Basic FGF elevated adipogenesis the most following supplementation throughout the complete culture period. However, the addition of bFGF only during the proliferation phase (3 days or 15 days) also resulted in a distinct increase in differentiation. These data may be explained with both hypotheses, either the preferential proliferation of a subpopulation or by direct effects on the commitment level. However, the enhancing effects of bFGF on adipogenesis after supplementation to postconfluent cells (BBF) (Figs. 2-3) rather supports the idea that a direct effect on the commitment level of MSCs contributes, at least in part, to the observed extent of adipogenesis.

As a possible mechanism for a direct effect on the commitment level, Prusty et al. have suggested the MEK/ERK signalling pathway to play an important role in adipogenesis [31].

Basic FGF is known to be a potent activator of the MEK/ERK pathway [8]. Short-term exposure of bFGF (6 hours) to 3T3-L1 preadipocytes promoted adipogenesis by phosphorylation of ERK1/2 and resulting enhanced PPAR γ and C/EBP α gene expression, irrespective of the presence of MEK1 inhibitors [31]. However, long-term treatment (more than 12-24 hours) of these cells with bFGF, as done in this study, led to a inhibition of adipogenic differentiation of 3T3-L1 cells [31]. Overall, the identification of the mechanism(s) by which bFGF exerts its effects on adipogenesis of MSCs may only be elucidated in full by cloning MSCs. Separated MSCs might allow the exact determination of the response of different subsets of cells to bFGF and adipogenic inducers.

Nevertheless, this study underlines the outstanding role of PPAR γ in the adipogenic conversion of MSCs, demonstrated by the distinct responsiveness of MSCs to the PPAR γ ligand troglitazone and the strikingly increased responsiveness provoked by bFGF. This finding is unexpected because thiazolidinediones alone are not sufficient to stimulate efficient differentiation, but require to be associated with glucocorticoids, insulin and/or IBMX in most culture systems including preadipocytic systems [32-35]. Thus, MSCs and especially bFGF-treated MSCs appear to respond in a different way to PPAR γ activators such as troglitazone as compared to preadipocytic cells.

Moreover, bFGF may play a crucial role in the fate of bone marrow cells: It has been previously shown that under appropriate culture conditions bFGF can enhance osteogenic differentiation [12-14], and it is demonstrated here that given the required adipogenic environment bFGF also enhances adipogenesis. Thus, depending on microenvironmental stimuli and status of lineage-specific transcription factors, bFGF present in bone marrow [36] may function as a regulator in the control of adipogenesis and osteogenesis of MSCs. Furthermore, in several studies an inverse relationship between adipogenic and osteogenic differentiation in MSC cultures was demonstrated [37-39]. Therefore, bFGF may modulate the origin and progression of osteoporosis due to its capability to sensitize MSCs for an enhanced differentiation into either osteoblasts or adipocytes.

References

- [1] Pittenger, MF, Mackay, AM, Beck, SC, Jaiswal, RK, Douglas, R, Mosca, JD, Moorman, MA, Simonetti, DW, Craig, S, Marshak, DR. 'Multilineage potential of adult human mesenchymal stem cells'. *Science* (1999); **284**: 143-147.
- [2] Kuznetsov, SA, Mankani, MH, Gronthos, S, Satomura, K, Bianco, P, Robey, PG. 'Circulating skeletal stem cells'. *J Cell Biol* (2001); **153**: 1133-1140.
- [3] O'Brien, K, Muskiewicz, K, Gussoni, E. 'Recent advances in and therapeutic potential of muscle-derived stem cells'. *J Cell Biochem Suppl* (2002); **38**: 80-87.
- [4] Gronthos, S, Franklin, DM, Leddy, HA, Robey, PG, Storms, RW, Gimble, JM. 'Surface protein characterization of human adipose tissue-derived stromal cells'. *J Cell Physiol* (2001); **189**: 54-63.
- [5] Owen, M. 'Marrow stromal stem cells'. *J Cell Sci Suppl* (1988); **10**: 63-76.
- [6] Dennis, JE, Merriam, A, Awadallah, A, Yoo, JU, Johnstone, B, Caplan, AI. 'A quadripotential mesenchymal progenitor cell isolated from the marrow of an adult mouse'. *J Bone Miner Res* (1999); **14**: 700-709.
- [7] Gospodarowicz, D, Ferrara, N, Schweigerer, L, Neufeld, G. 'Structural characterization and biological functions of fibroblast growth factor'. *Endocr Rev* (1987); **8**: 95-114.
- [8] Powers, CJ, McLeskey, SW, Wellstein, A. 'Fibroblast growth factors, their receptors and signaling'. *Endocr Relat Cancer* (2000); **7**: 165-197.
- [9] Burgess, WH, Maciag, T. 'The heparin-binding (fibroblast) growth factor family of proteins'. *Annu Rev Biochem* (1989); **58**: 575-606.
- [10] Martin, I, Padera, RF, Vunjak-Novakovic, G, Freed, LE. 'In vitro differentiation of chick embryo bone marrow stromal cells into cartilaginous and bone-like tissues'. *J Orthop Res* (1998); **16**: 181-189.
- [11] Tsutsumi, S, Shimazu, A, Miyazaki, K, Pan, H, Koike, C, Yoshida, E, Takagishi, K, Kato, Y. 'Retention of Multilineage Differentiation Potential of Mesenchymal Cells during Proliferation in Response to FGF'. *Biochem Biophys Res Commun* (2001); **288**: 413-419.
- [12] Hanada, K, Dennis, JE, Caplan, AI. 'Stimulatory effects of basic fibroblast growth factor and bone morphogenetic protein-2 on osteogenic differentiation of rat bone marrow-derived mesenchymal stem cells'. *J Bone Miner Res* (1997); **12**: 1606-1614.
- [13] Pitaru, S, Kotev-Emeth, S, Noff, D, Kaffuler, S, Savion, N. 'Effect of basic fibroblast growth factor on the growth and differentiation of adult stromal bone marrow cells: enhanced development of mineralized bone-like tissue in culture'. *J Bone Miner Res* (1993); **8**: 919-929.
- [14] Scutt, A, Bertram, P. 'Basic fibroblast growth factor in the presence of dexamethasone stimulates colony formation, expansion, and osteoblastic differentiation by rat bone marrow stromal cells'. *Calcif Tissue Int* (1999); **64**: 69-77.

- [15] Locklin, RM, Oreffo, ROC, Triffitt, JT. 'In vitro effects of growth factors and dexamethasone on rat marrow stromal cells'. *Cell Biol Int* (1999); **23**: 185-194.
- [16] Locklin, RM, Williamson, MC, Beresford, JN, Triffitt, JT, Owen, ME. 'Effects of TGF beta and bFGF on the differentiation of human bone marrow stromal fibroblasts'. *Clin Orthop* (1995); **313**: 27-35.
- [17] Rosen, ED, Spiegelman, BM. 'Molecular regulation of adipogenesis'. *Annu Rev Cell Dev Biol* (2000); **16**: 145-171.
- [18] Kliewer, SA, Willson, TM. 'The nuclear receptor PPAR γ - bigger than fat'. *Curr Opin Genet Dev* (1998); **8**: 576-581.
- [19] Ishaug, SL, Crane, GM, Miller, MJ, Yasko, AW, Yaszemski, MJ, Mikos, AG. 'Bone formation by three-dimensional stromal osteoblast culture in biodegradable polymer scaffolds'. *J Biomed Mater Res* (1997); **36**: 17-28.
- [20] Kim, YC, Gomez, FE, Fox, BG, Ntambi, JM. 'Differential regulation of the stearoyl-CoA desaturase genes by thiazolidinediones in 3T3-L1 adipocytes'. *J Lipid Res* (2000); **41**: 1310-1316.
- [21] Pairault, J, Green, H. 'A study of the adipose conversion of suspended 3T3 cells by using glycerophosphate dehydrogenase as differentiation marker'. *Proc Natl Acad Sci USA* (1979); **76**: 5138-5142.
- [22] Lowry, OH, Rosebrough, NJ, Farr, AL, Randall, RJ. 'Protein measurement with the Folin phenol reagent'. *J Biol Chem* (1951); **193**: 265-275.
- [23] Gimble, JM, Morgan, C, Kelly, K, Wu, X, Dandapani, V, Wang, CS, Rosen, V. 'Bone morphogenetic proteins inhibit adipocyte differentiation by bone marrow stromal cells'. *J Cell Biochem* (1995); **58**: 393-402.
- [24] Okuno, A, Tamemoto, H, Tobe, K, Ueki, K, Mori, Y, Iwamoto, K, Umesono, K, Akanuma, Y, Fujiwara, T, Horikoshi, H, Yazaki, Y, Kadowaki, T. 'Troglitazone increases the number of small adipocytes without the change of white adipose tissue mass in obese Zucker rats'. *J Clin Invest* (1998); **101**: 1354-1361.
- [25] Lehmann, JM, Lenhard, JM, Oliver, BB, Ringold, GM, Kliewer, SA. 'Peroxisome proliferator-activated receptors α and γ are activated by indomethacin and other non-steroidal anti-inflammatory drugs'. *J Biol Chem* (1997); **272**: 3406-3410.
- [26] Martin, I, Muraglia, A, Campanile, G, Cancedda, R, Quarto, R. 'Fibroblast growth factor-2 supports ex vivo expansion and maintenance of osteogenic precursors from human bone marrow'. *Endocrinology* (1997); **138**: 4456-4462.
- [27] Bianchi, G, Banfi, A, Mastrogiacomo, M, Notaro, R, Luzzatto, L, Cancedda, R, Quarto, R. 'Ex vivo enrichment of mesenchymal cell progenitors by fibroblast growth factor 2'. *Exp Cell Res* (2003); **287**: 98-105.

- [28] Deans, RJ, Moseley, AB. 'Mesenchymal stem cells. Biology and potential clinical uses'. *Exp Hematol* (2000); **28**: 875-884.
- [29] Shigematsu, M, Watanabe, H, Sugihara, H. 'Proliferation and differentiation of unilocular fat cells in the bone marrow'. (1999); *Cell Struct Funct* **24**: 89-100.
- [30] Ailhaud, G, Grimaldi, P, Negrel, R. 'Cellular and molecular aspects of adipose tissue development'. *Annu Rev Nutr* (1992); **12**: 207-233.
- [31] Prusty, D, Park, BH, Davis, KE, Farmer, SR. 'Activation of MEK/ERK signaling promotes adipogenesis by enhancing peroxisome proliferator-activated receptor γ (PPAR γ) and C/EBP α gene expression during the differentiation of 3T3-L1 preadipocytes'. *J Biol Chem* (2002); **277**: 46226-46232.
- [32] Tafuri, SR. 'Troglitazone enhances differentiation, basal glucose uptake, and Glut1 protein levels in 3T3-L1 adipocytes'. *Endocrinology* (1996); **137**: 4706-4712.
- [33] Sottile, V, Seuwen, K. 'Bone morphogenetic protein-2 stimulates adipogenic differentiation of mesenchymal precursor cells in synergy with BRL 49653 (rosiglitazone)'. *FEBS Lett* (2000); **475**: 201-204.
- [34] Tonotonoz, P, Hu, E, Spiegelman, BM. 'Stimulation of adipogenesis in fibroblasts by PPAR γ 2, a lipid-activated transcription factor'. (1994); *Cell* **79**: 1147-1156.
- [35] Gimble, JM, Robinson, CE, Wu, X, Kelly, KA, Rodriguez, BR, Kliewer, SA, Lehmann, JM, Morris, DC. 'Peroxisome proliferator-activated receptor- γ activation by thiazolidinediones induces adipogenesis in bone marrow stromal cells'. *Mol Pharmacol* (1996); **50**: 1087-1094.
- [36] Yoon, SY, Tefferi, A, Li, CY. 'Cellular distribution of platelet-derived growth factor, transforming growth factor-beta, basic fibroblast growth factor, and their receptors in normal bone marrow'. (2000); *Acta Haematol* **104**: 151-157.
- [37] Beresford, JN, Bennett, JH, Devlin, C, Leboy, PS, Owen, ME. 'Evidence for an inverse relationship between the differentiation of adipocytic and osteogenic cells in rat marrow stromal cell cultures'. (1992); *J Cell Sci* **102**: 341-351.
- [38] Kelly, KA, Gimble, JM. '1,25-Dihydroxy vitamin D3 inhibits adipocyte differentiation and gene expression in murine bone marrow stromal cell clones and primary cultures'. *Endocrinology* (1998); **139**: 2622-2628.
- [39] Okazaki, R, Toriumi, M, Fukumoto, S, Miyamoto, M, Fujita, T, Tanaka, K, Takeuchi, Y. 'Thiazolidinediones inhibit osteoclast-like cell formation and bone resorption in vitro'. *Endocrinology* (1999); **140**: 5060-5065.

Chapter 5

A Study on the Mechanisms of the Effect of bFGF on the Adipogenesis of MSCs under Clonal Conditions

Markus Neubauer,¹ Leoni Kunz-Schughart,² Marit Hoffmann,² Achim Goepferich,¹ Torsten Blunk¹

¹ Department of Pharmaceutical Technology, University of Regensburg, Universitätsstrasse 31, 93040 Regensburg, Germany

² Department of Pathology, University of Regensburg, Franz-Josef-Strauß-Allee 11, 93053 Regensburg, Germany

Abstract

Mesenchymal stem cells (MSCs) are multipotent stem cells capable of differentiating at least towards the osteogenic, chondrogenic, and adipogenic lineage. Modulators of the differentiation are a wide variety of growth factors such as transforming growth factor- β , bone morphogenetic proteins, and basic fibroblast growth factor (bFGF). Recently, we demonstrated the enhancing effect of bFGF on the adipogenic conversion of MSCs in 2-D and 3-D cell culture (see chapters 4 and 7). However, mechanisms by which bFGF exerts its effects on MSCs are poorly investigated.

The presence of multiple cell populations in the MSC culture renders the determination of the underlying mechanism more difficult and requires a system with which single cells can be investigated under clonal conditions. The first goals of this study was to evaluate the potential of different media to stimulate the growth of MSCs under clonal conditions. A medium consisting of α -MEM, fetal bovine serum, ascorbic acid, and the B27 supplement, denoted as the cloning medium, was found to be suitable for the expansion of MSCs under cloning condition. This medium ensured the maintenance of the differentiation potential and the responsiveness to bFGF as enhancer of the adipogenesis of MSCs. Administration of the cloning medium allowed for the investigation of the mechanism of action of bFGF on the adipogenesis of MSCs under clonal conditions. In conclusion, differentiation experiments under clonal conditions in which bFGF was supplemented either only in the single cell culture or in the entire culture suggests bFGF to act mainly via the preferential proliferation of a subset of the MSCs capable of undergoing adipogenesis.

Introduction

Mesenchymal stem cells (MSCs) represent intensively investigated stem cells which have the capacity of multipotential differentiation into at least chondrocytes, osteoblasts, and adipocytes [1]. The fate of MSCs depends on the microenvironmental conditions such as absence or presence of inducing stimuli and differentiation and growth factors such as transforming growth factors [2], bone morphogenic proteins [2-4], and basic fibroblast growth factor (bFGF) [5-7].

Recently, we could demonstrate the enhancing effect of bFGF on the adipogenesis of MSCs in 2-D (Chapter 4) and 3-D cell culture (Chapter 7). Basic FGF increases the number of differentiated adipocytes and their maturation and yields elevated expression levels of adipogenic markers such as glycerol-3-phosphate dehydrogenase (GPDH), glucose transporter 4 (GLUT4), and peroxisome proliferator-activated receptor γ (PPAR γ) at the molecular level following the administration of hormonal induction regimen (Chapter 4). In 2-D cell culture, supplementation of bFGF leads to an increased expression of PPAR γ even prior to adipogenic induction accompanied by a very high responsiveness of bFGF-treated MSCs to a PPAR γ ligand, the thiazolidinedione troglitazone.

Principally, two possible mechanisms of the action of bFGF are discussed [5,6]: (1) Basic FGF leads to preferential proliferation of a subset of the MSC population which is responsible for the increased PPAR γ message and (2) supplementation of bFGF exerts direct effects on the commitment level of MSCs, that is, bFGF induces the expression of PPAR γ in certain cells.

Bone marrow is composed of at least three cellular systems: haematopoietic, endothelial and stromal. In adult bone marrow, macrophages, adipocytes, osteogenic cells, haematopoietic cells, cells originating from blood vessels and “reticular” cells coexist and partially cooperate [8]. When MSCs are isolated by adherence to cell culture plastics, as was the case in the studies mentioned above, the adherent cells represent a mixture of different cell types. The presence of multiple cell populations renders the determination of the underlying mechanism more difficult and requires a system with which single cells can be investigated under clonal conditions.

In this study, single cells were sorted with means of FACS analysis. As reasonable clonal growth of certain cell types often is hard to achieve, the first goal of this study was to evaluate an appropriate growth medium for the clonal expansion of MSCs by testing different commonly used cell culture media: Dulbecco’s modified Eagle’s medium (DMEM), modified

Eagle's medium (α -modification) (α -MEM), and RPMI supplemented with additives such as the B27 supplement and conditioned media. The optimum medium revealed to be α -MEM, 10% FBS, 1% antibiotics, 50 μ g/ml ascorbic acid, and the B27 supplement, in the following referred to as cloning medium. The cloning medium was used in the further experiment in order to study the mechanisms of the effect of bFGF on the adipogenesis of MSCs. Basic FGF was administered either (1) in the complete culture, that is, during the proliferation phase and in the subsequent single cell culture, or (2) only in the single cell culture, or (3) not at all as a control group. Supplementation of bFGF only in the single cell culture might be effective if bFGF is capable to exert direct effects on the commitment level, whereas bFGF also in the proliferation phase might support the preferential proliferation of a distinct cell subset which are prone to undergo adipogenic conversion.

Materials and Methods

Materials

If not otherwise stated, chemicals were obtained from Sigma (Steinheim, Germany). The B27 Supplement (in the following abbreviated as B27) was obtained as a 50-fold concentrate from Invitrogen (Karlsruhe, Germany). Basic FGF was obtained from PeproTec (Rocky Hill, NJ, USA). Insulin was kindly provided by Hoechst Marion Roussel (Frankfurt am Main, Germany). Cell culture plastics were purchased from Corning Costar (Bodenheim, Germany).

Evaluation of the cloning medium: Cell isolation and expansion in the proliferation phase

Marrow stromal cells were obtained from six-week old male Sprague Dawley rats (weight: 170 - 180 g, Charles River, Sulzfeld, Germany). MSCs were flushed from the tibiae and femora according to the protocol of Ishaug [9]. Cells were centrifuged at 1,200 rpm for 5 min. The resulting cell pellet was resuspended in basal medium consisting of DMEM (Biochrom, Berlin, Germany), 10 % fetal bovine serum (FBS, Gemini Bio-Products Inc., Calabasas, CA, USA), 1% penicillin/streptomycin (Invitrogen, Karlsruhe, Germany), and 50 μ g/ml ascorbic acid (Fig. 1c). Cells were seeded in T75 flasks and cultured at 37°C and 5% CO₂. Cells were allowed to adhere to the substratum for three days. The flasks were rinsed twice with phosphate-buffered saline (PBS, Invitrogen, Karlsruhe, Germany) in order to remove non-adherent cells. In the following experiments, cells were expanded (proliferation phase) with media based on either α -MEM, DMEM (Biochrom, Berlin, Germany), or RPMI 1640 (BioWhittaker Europe, Verviers, Belgium) respectively, supplemented with 10 % fetal bovine serum (Gemini Bio-Products Inc., Calabasas, CA, USA), 1% penicillin/streptomycin

(Invitrogen, Karlsruhe, Germany), and 50 µg/ml ascorbic acid (Table 1). In some cases, B27 (50-fold concentrate) was additionally supplemented (Table 1). RPMI 1640 was generally supplemented with L-glutamine, MEM sodium pyruvate (C.C. Pro, Neustadt, Germany), MEM non-essential amino acids, and MEM vitamin solution according to the manufacturers' instructions. After reaching confluence, cells were passaged with 0.25% trypsin and EDTA (Invitrogen, Karlsruhe, Germany) and resuspended in DMEM without any other additives at a density of 1.5 to 2 million cells/ml for cell sorting. Cell suspensions were stored on ice until the cell sorting was performed. In the following, the culture phase from day 3 after cell isolation to the time point of the passage is designated as proliferation phase (PP) (Fig. 1a).

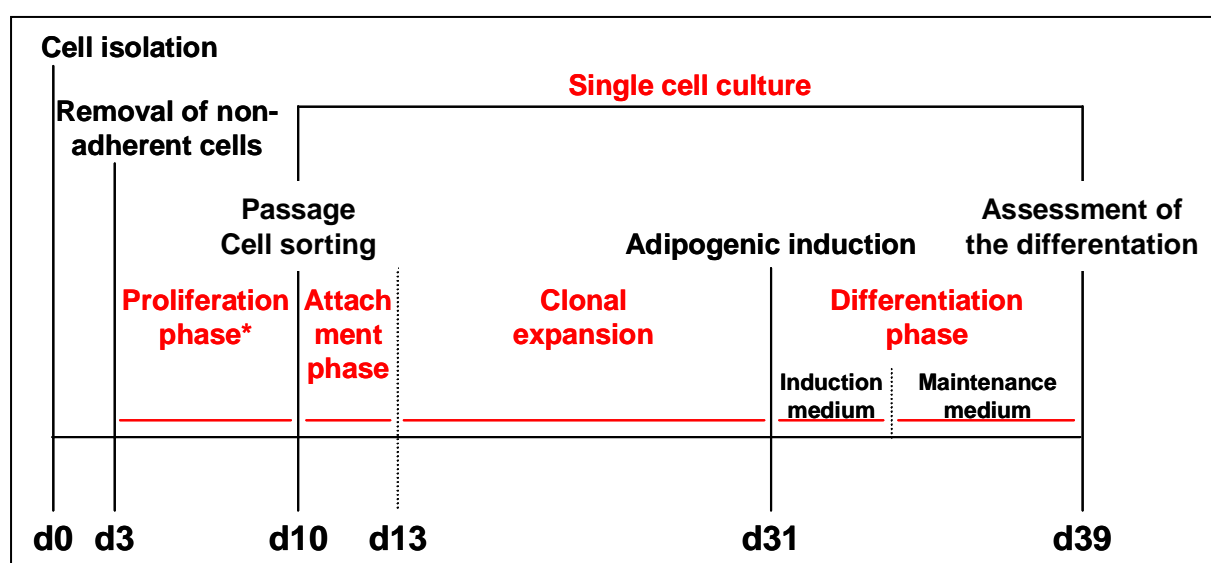


Fig. 1a: Time scheme of the cell culture. For the evaluation of the cloning medium, cells were propagated in the proliferation phase, sorted following the passage, and expanded under clonal conditions using various media (Table 1). Subsequently, the number of grown clones was determined. The most favorable cloning medium (Fig. 1c) was used in all further experiments: For the mechanistic investigation of the effect of bFGF on the adipogenesis of MSCs, cells were propagated using the cloning medium during the proliferation phase, the attachment phase, and the cloning expansion. Adipogenic differentiation was induced with the induction medium and MSCs were differentiated five more days with the maintenance medium (Fig. 1c). After 39 days, the number of grown and differentiated clones was determined. (* The proliferation phase lasted seven days in the presence of the cloning medium, but required up to twelve days with other media depending on their composition.)

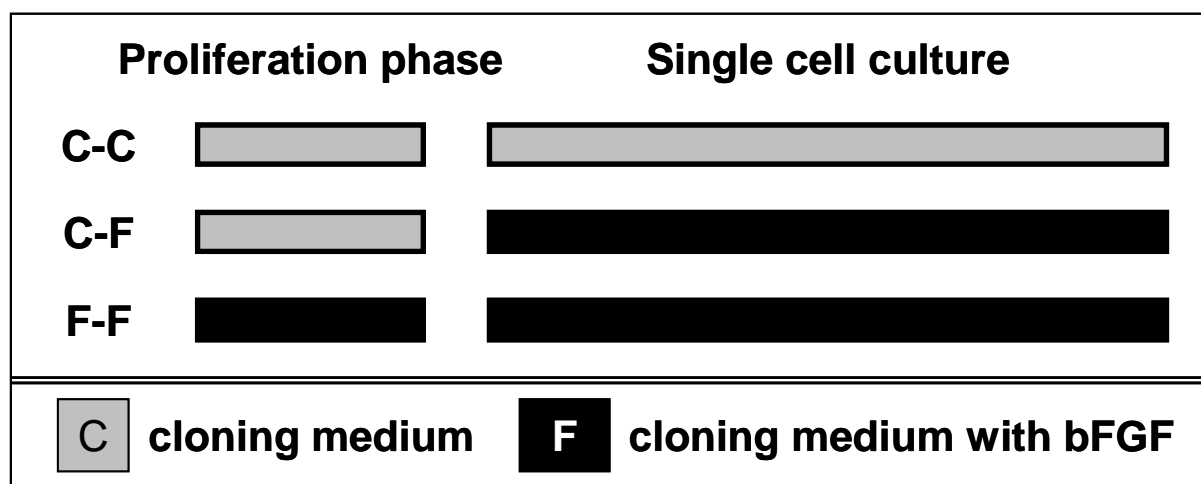


Fig.1b Basic FGF supplementation in different periods of the cell culture. MSCs were exposed to bFGF only in the single cell culture (C-F) or throughout the complete culture period, that is, in the proliferation phase and in the single cell culture (F-F). Cells grown in the absence of bFGF (C-C) served as a control. Grey boxes represent cloning medium without bFGF (C), black boxes represent cloning medium supplemented with bFGF (F).

Media	Description
Basal medium	DMEM, 10% FBS, 1% PS, 50 µg/ml ascorbic acid
Cloning medium	α-MEM, 10% FBS, 1% PS, 50 µg/ml ascorbic acid, B27
Induction medium	clonal conditions: cloning medium supplemented with the hormonal cocktail (10 nM dexamethasone, 0.5 mM IBMX, 60 µM indomethacin, 10 µg/ml insulin) non-clonal conditions: basal medium supplemented with the hormonal cocktail
Maintenance medium	clonal conditions: cloning medium supplemented with 10 µg/ml insulin non-clonal conditions: basal medium supplemented with 10 µg/ml insulin

Fig. 1c: Definition of important and frequently used terms concerning the composition of various media.

Evaluation of the cloning medium: Cell sorting and expansion under clonal conditions

Propidium iodide (PI, 1 µg/ml) was added to the cell suspensions in order to exclude dead cells from the sorting procedure. Cells were monitored in the FACS analysis (FACStar, Beckton Dickinson, Heidelberg, Germany) in two-parameter dot plots, forward scatter (FSC) against sideward scatter (SSC) in order to observe the cell population(s), and FSC against the fluorescence channel 3 (FL3) in order to exclude dead cells which were stained with PI. PI fluorescence was measured on the FL3 emission channel through a 670 nm longpass filter, following excitation with an argon ion laser source at 488 nm. The cells to be sorted were gated in the region 2 (R2). Single cells were sorted in one well each of a 96-well plate. 94

cells were sorted per group. The well plates were pre-filled with the medium (100 μ l/well) used for the attachment phase (Table 1). Cells were left undisturbed for three days for cell attachment. Subsequently, media used during the clonal expansion were added and exchanged every two to three days. In the following, the first three days after the sorting procedure is designated as attachment phase (AP) and the expansion phase under cloning conditions is designated as clonal expansion (CE) (Fig. 1a). In some cases, conditioned media were supplemented to the culture media. Conditioned media were collected in the proliferation phase of corresponding cells, frozen at -20°C , and thawed immediately before use. The pH of the conditioned media was adjusted to pH 7.4 with sterile 0.1 N hydrochloric acid. Cells propagated for about three weeks were fixed with 10% formaldehyde in PBS (Merck, Darmstadt, Germany) and grown clones were counted under an inverse light microscope (Leica DM IRB, Leica Microsystems, Wetzlar, Germany).

Mechanistic investigation of the effects of bFGF: Cell isolation and expansion in the proliferation phase

MSCs were isolated and seeded into T75 flasks as described above. Adherent cells were expanded using cloning medium (α -MEM, 10% FBS, 1% penicillin/streptomycin, 50 μ g/ml ascorbic acid, and B27) in the proliferation phase. After about seven days, cells were passaged and prepared for the cell sorting procedure as described above.

Mechanistic investigation of the effects of bFGF: Cell sorting and expansion under clonal conditions

Cells were sorted with means of FACS analysis as described above. 282 cells were sorted per group. 96-well plates were pre-filled with cloning medium (100 μ l/well) which was exchanged every two to three days for about three weeks. The phase of the culture is designated as single cell culture in the following (Fig. 1a).

Mechanistic investigation of the effects of bFGF: Supplementation of bFGF

Basic FGF was supplemented in two different experimental groups (Fig. 1b). On the one hand, bFGF was added to the cloning medium during the entire culture period: from three days after the cell isolation until the end of single cell culture, that is, during the proliferation phase, attachment phase, clonal expansion, and differentiation phase. This group is designated as “F-F” in the following. On the other hand, bFGF was supplemented to the cloning medium exclusively in the single cell culture, that is, during the attachment phase, clonal expansion, and differentiation phase but not during the initial proliferation phase. This group is

abbreviated as “C-F”. The control group including cells that were cultivated in absence of bFGF is designated as “C-C”. “C” represents the cloning medium, whereas “F” represents the cloning medium supplemented with 3 ng/ml bFGF (Fig. 1b).

Mechanistic investigation of the effects of bFGF: Adipogenic induction and differentiation

After cells were propagated in the clonal expansion phase over three weeks, clones were exposed to a hormonal cocktail in order to induce adipogenic differentiation. Cultures were treated for three days with an induction medium (Fig. 1c) consisting of the hormonal cocktail (0.5 mM 3-isobutyl-1-methylxanthine (IBMX) (Serva Electrophoresis, Heidelberg, Germany), 10 nM dexamethasone, 60 μ M indomethacin and 10 μ g/ml insulin) which was added to the cloning medium. Subsequently, cultures were maintained for five more days in maintenance medium consisting of cloning medium supplemented with 10 μ g/ml insulin (Fig. 1c).

Histological staining of clones

After eight days of differentiation, clones were rinsed with PBS and fixed with 10% formaldehyde. First, differentiated clones were stained with Oil Red O. Cells were covered with 3 mg/ml Oil Red O (100 μ l/96-well) for 2h. Excess dye was removed with PBS and finally, cells were fixed with 10% formaldehyde. Subsequently, clones were stained with 1% methylene blue in 10 mM borate buffer, pH 8.8 (100 μ l/96-well) for 30 minutes. Excess dye was removed with PBS. The buffer was completely removed and clones were counted under an inverse light microscope (Leica DM IRB, Leica Microsystems, Wetzlar, Germany). Pictures were taken on a Minolta camera (Dynax 600 si classic, Minolta Europe, Langehagen, Germany) connected to the inverse light microscope. Thereafter, clones were covered again with 10% formaldehyde for storage.

Differentiation of MSCs under non-clonal conditions

As mechanisms of action of bFGF were investigated using the cloning medium, it had to be ensured that cells cultured with this medium responded to bFGF and adipogenic inducers in the same as in cultures using the basal medium (Chapters 3 and 4). Cells were isolated, propagated, and passaged as described in the second subchapter. Basal medium and cloning medium were used as culture media. Cells were passaged and seeded into 24-well plates at a density of 30,000 cells/cm² as described in Chapter 4 in detail. After a proliferation phase of three days, cells were exposed to the induction medium for further three days (Fig. 1c). Subsequently, cells were treated with the maintenance medium for five more days (Fig. 1c).

After this, cells were rinsed with PBS, fixed with 10% formaldehyde, and Red Oil O staining was performed as described above.

Cells were cultivated in complete absence of bFGF (“without bFGF”) and in presence of 3 ng/ml bFGF from the time point of the cell seeding after the passage to the end of the culture period (“with bFGF”).

Results

Evaluation of a suitable cloning medium

In the conventional 2-D and 3-D cell culture (chapters 3,4,6,7), MSCs were grown and differentiated using the basal medium consisting of DMEM, 10%FBS, 1% antibiotics, and 50 µg/ml ascorbic acid. However, this medium is not sufficient for the stimulation of the growth of MSCs under clonal conditions. Different media based on α -MEM, DMEM, and RPMI were tested in combination with the B27 and conditioned media as shown in (Table 1). The equality of attached cells after the cell isolation among all experimental groups was guaranteed by using the same medium, basal medium, for the first three days in all experimental groups shown in Table 1.

#	Medium in PP	B27	CM	Medium in AP	Medium in CE	B27	CM
1	RPMI	-	-	Medium in CP	RPMI	-	-
2	RPMI	-	-	Medium in CP	RPMI	-	+
3	DMEM	-	-	Medium in CP	DMEM	-	-
4	DMEM	+	-	Medium in CP	DMEM	+	+
5	DMEM	-	-	Medium in CP	α -MEM	+	-
6	DMEM	-	-	Medium in CP	α -MEM	+	+
7	α -MEM	-	-	Medium in CP	α -MEM	-	-
8	α -MEM	-	-	Medium in CP	α -MEM	-	+
9	α -MEM	+	-	α -MEM w/o B27	α -MEM	+	-
10	α -MEM	+	-	Medium in CP	α -MEM	+	+
11	α -MEM	+	-	Medium in CP	α -MEM	+	-
12	α -MEM	+	-	Medium in CP	DMEM	-	-
13	α -MEM	+	-	Medium in CP	DMEM	-	+

Table 1: Cell culture conditions during the entire culture period. After cell isolation, MSCs were allowed to attach to the substratum over three days in basal medium. Thereafter, MSCs were propagated in different media in the proliferation phase (PP) until cells were passaged and sorted for single cell culture. In the attachment phase (AP) after the sorting procedure, cells were already incubated in the medium in which they were subsequently expanded in the clonal expansion (CE), except of MSCs in group 9. Media were partially supplemented with B27 and conditioned medium (CM). DMEM, RPMI, and α -MEM were supplemented with FBS, antibiotics, and ascorbic acid. RPMI was additionally supplemented with L-glutamine, MEM sodium pyruvate, MEM non-essential amino acids, and MEM vitamin solution (see Materials and Methods).

Figure 2 shows the number of grown clones per 96-well plate of all experimental groups. There was virtually no development of clones detectable following the application of media based on either RPMI, DMEM, or α -MEM without further supplementation of B27 or conditioned media (Fig. 2, groups 1, 3, and 7, respectively). Addition of conditioned media in the single cell culture to RPMI-based and α -MEM-based media did not yield a higher number of clones (Fig. 2, groups 2 and 8).

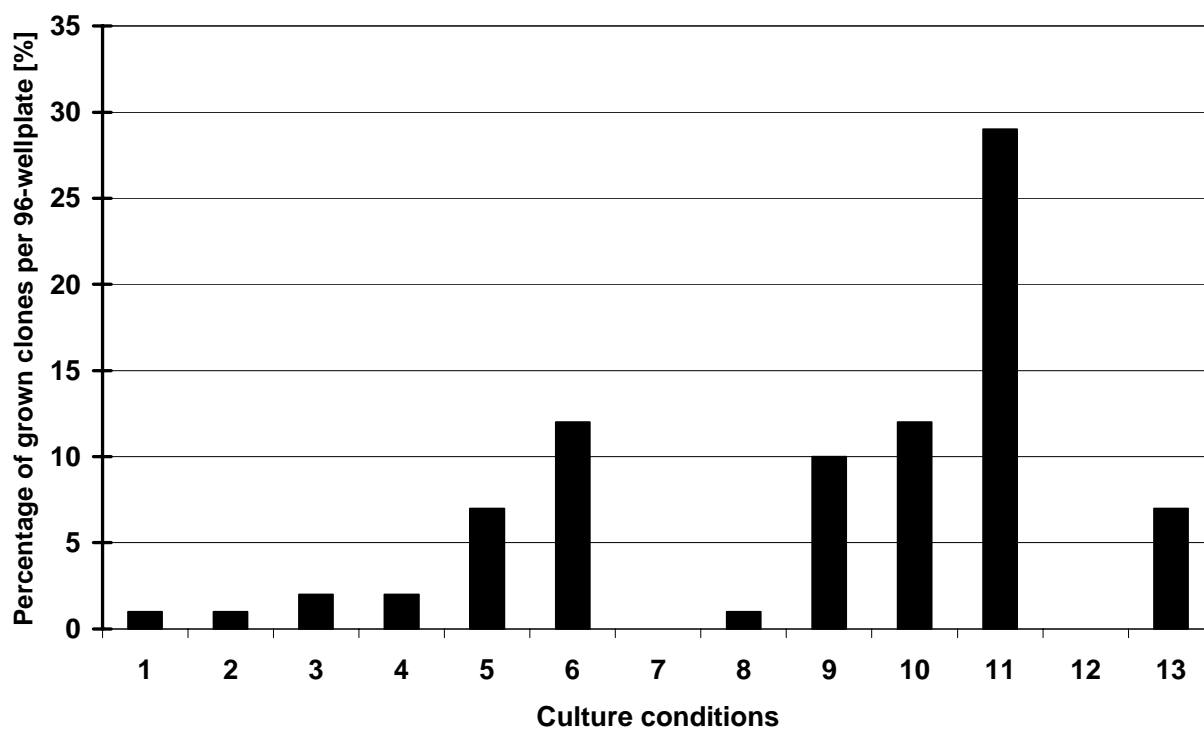


Fig. 2 Grown clones under different culture conditions. MSCs were cultivated with different media and supplements as shown in Table 1. The percentage of developed clones per 96-wellplate is shown here.

Using DMEM-based media, addition of B27 in the entire culture combined with conditioned medium during the clonal expansion led to no improvement (Fig. 2, group 4). However, treatment of MSCs propagated with basal medium in the proliferation phase (Fig. 2, group 5) and with the α -MEM and B27-based medium supplemented with conditioned medium (Fig. 2, group 6) during the clonal expansion clearly improved the growth of clones: 7 clones for group 5 and 12 clones for group 6 as compared to 2 clones for group 3. These results show that the α -MEM and B27-based medium strongly influenced the growth of MSC clones, that is, both α -MEM and B27 are required to obtain a reasonable number of clones for further experiments. Thus, the α -MEM and B27-based medium was applied both in the proliferation phase and during the clonal expansion. Using the α -MEM and B27-based medium in the entire culture except for the attachment phase resulted in ten clones per 96-well plate. Here, a

medium without B27 addition was used in the attachment phase (Fig. 2, group 9). In group 10, the same conditions were used as in group 9 with an additional supplementation of conditioned medium in the clonal expansion phase (Table 1). Group 10 resulted in twelve clones per well plate (Fig. 2). Exclusion of B27 in the attachment phase was tested because the influence of B27 on the attachment of MSC to the cell culture plastic had been unknown. A striking effect on the growth of clones was achieved by using the α -MEM and B27-based medium during the entire period of the culture (Fig. 2, group 11). 29 clones in a 96-well plate were obtained with this culture condition. Using cloning medium in the proliferation phase and basal medium (Fig. 2, group 12, 0 clones) or basal medium supplemented with conditioned medium (Fig. 2, group 13, 7 clones) during the clonal expansion again demonstrated the important influence of the α -MEM and B27-based medium. The most favorable medium for the clonal growth of MSCs consisting of α -MEM, 10% FBS, antibiotics, 50 μ g/ml ascorbic acid, and B27 is termed cloning medium in the following. The size of the grown clones was estimated for the most suitable culture condition using the cloning medium in the entire culture (Fig. 2, group 11). Figure 3 shows the sizes of the clones, categorized in clones covering the area of a well up to 20%, up to 40 %, and from 40 to 100%, as estimated by eye. Approx. 45% of the clones fitted in the lowest category, about 20% in the middle category, and 35% covered at least 40% of the well area.

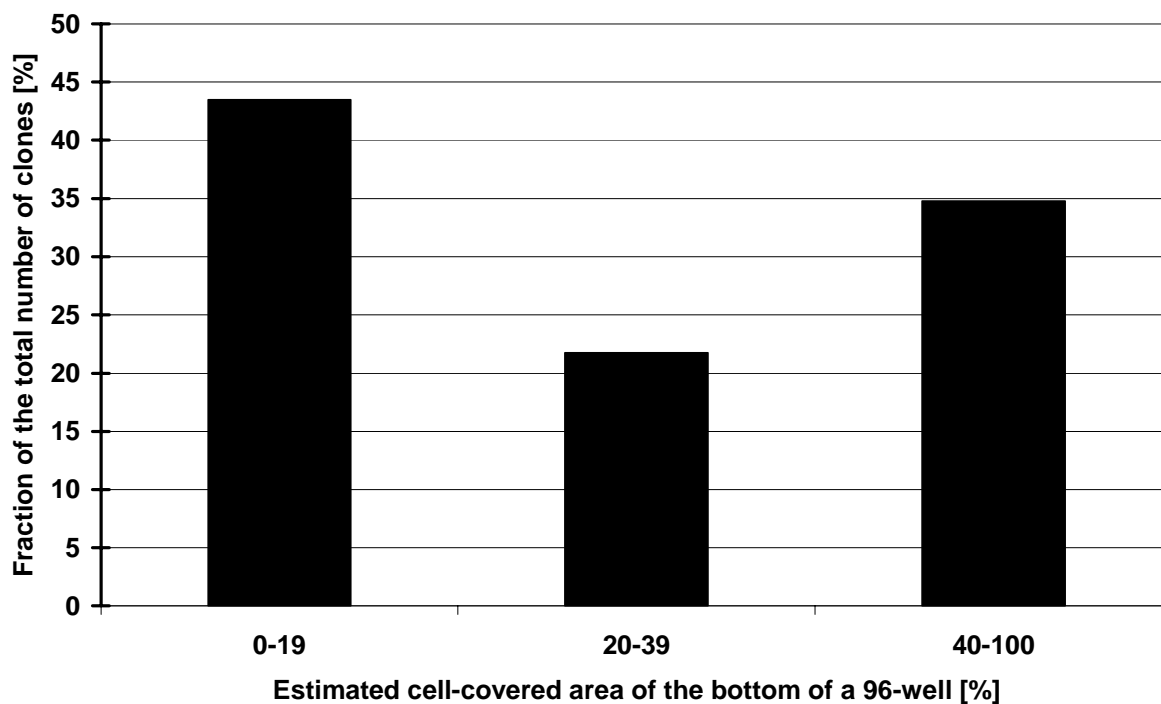


Fig. 3 Size of the grown clones cultivated with the cloning medium (α -MEM, 10% FBS, 1% antibiotics, and B27).

In summary, the cloning medium component α -MEM seems to be superior as compared to DMEM, a component of the basal medium, in regard to the stimulation of clone growth. Table 2 compares the compositions of α -MEM and DMEM subdivided in the categories inorganic salts, amino acids, vitamins, and others. The composition of inorganic salts is quite similar, except for the component ferric nitrate that is part of the DMEM mixture but absent in α -MEM. Remarkably, α -MEM contains a wider variety of amino acids and vitamins than DMEM. Alanine, asparagine, aspartate, cystine, glutamate, proline, biotin, vitamin B12 are exclusively parts of α -MEM but not compounds of the DMEM mixture, all other components are present in both basic media. Strikingly, components with different concentrations in the media are mostly at a lower concentration in α -MEM as compared to DMEM (18 components). Only arginine, cysteine, and glycine are present at a higher concentration in α -MEM as compared to DMEM.

Components	DMEM	α -MEM	Components	DMEM	α -MEM
Inorganic salts	[mg/l]	[mg/l]			
CaCl ₂ 2H ₂ O		265	Methionine	30	15
CaCl ₂	200		Phenylalanine	66	32
Ca ²⁺ , pure	72.2	72.2	Proline		40
MgSO ₄		97.67	Serine	42	25
MgSO ₄ 7H ₂ O	200		Threonine	95	48
Mg ²⁺ , pure	19.7	19.7	Tryptophan	16	10
Fe(NO ₃) ₃ 9H ₂ O	0.1		Tyrosine 2Na H ₂ O		51.9
KCl	400	400	Tyrosine	72	
NaCl	6400	6800	Tyrosine, pure	72	38.4
NaH ₂ PO ₄	124	122	Valine	94	46
NaHCO ₃	3700	2200	Vitamins	[mg/l]	[mg/l]
Amino acids	[mg/l]	[mg/l]	Ascorbic acid Na		50
Alanine		25	Biotin		0.1
Arginine HCl	84	126	Coline chloride	4	1
Asparagine H ₂ O		50	Folic acid	4	1
Aspartate		30	myo-Inositol		2
Cysteine HCl H ₂ O		100	i-Inositol	7.2	
Cysteine	48		Niacinamide	4	1
Cysteine, pure	48	69.5	Pantothenate 1/2Ca	4	1
Cystine 2HCl		31.3	Pyridoxal HCl	4	1
Glutamate		75	Riboflavin	0.4	0.1
Glutamine	580	292	Thiamine HCl	4	1
Glycine	30	50	Vitamin B12		1.36
Histidine HCl H ₂ O	42	42	Others	[mg/l]	[mg/l]
Isoleucine	105	52	Glucose	1000	1000
Leucine	105	52	Phenolred Na	15	11
Lysine HCl	146	72.5	Pyruvate Na	110	110
			Lipoic acid		0.2

Table 2: Composition of DMEM and α -MEM.

The second pivotal component of the cloning medium is the B27 supplement of which the composition is specified in Table 3. B27 is a complex mixture of vitamins, fatty acids, hormones, proteins, and other components. Several antioxidative agents such as tocopherol and retinyl acetate, the reduced form of glutathione, and the enzymes catalase and superoxide dismutase are included in the mixture.

Vitamins	Superoxid dismutase
Biotin	Transferrin
DL-alpha-tocopherol	Insulin
DL-alpha-tocopherol acetate	Fatty acids
Retinyl acetate	Linoleic acid
Hormones	Linolenic acid
Corticosterone	Other components
Progesterone	Ethanolamine HCl
Triodo-1-thyronine	D-Galaktose
Proteins	Glutathione (reduced)
Albumin, bovine	Putrescine 2HCl
Catalase	Selenium

Table 3: Composition of the B27 supplement.

FACS analysis for the cell sorting procedure

MSCs were subjected to FACS analysis after trypsinization in order to sort single cells into 96-wells. In Fig. 4, MSCs expanded with the basal medium and the cloning medium were compared in two-parameter dot plots, forward scatter (FSC) against sideward scatter (SSC) and FSC against fluorescence channel 3 (FL3). The main population of the MSCs of both groups appeared at the same position in the FSC-SSC-dot plots gated in the region 1 (R1), whereas the distribution of the cells was denser in the dot plot of cells propagated in the presence of the cloning medium. 92-94% of all cells were gated in the R1 under both conditions (data not shown). In the FSC-FL3-dot plots, the main population (colored red) can be seen around the region 2 (R2) in which about 68-74% of all cells were gated (data not shown). The cell populations located between 10^3 and 10^4 fluorescence units represent dead cells stained with the fluorescent dye propidium iodide. The portion of dead cells amounted to about 3-5% of all cells (data not shown). With this method, all dead cells could be excluded from the sorting procedure by restricting the cells to be sorted to the cells within R2. Single cells were sorted into one well each of a 96-well plate.

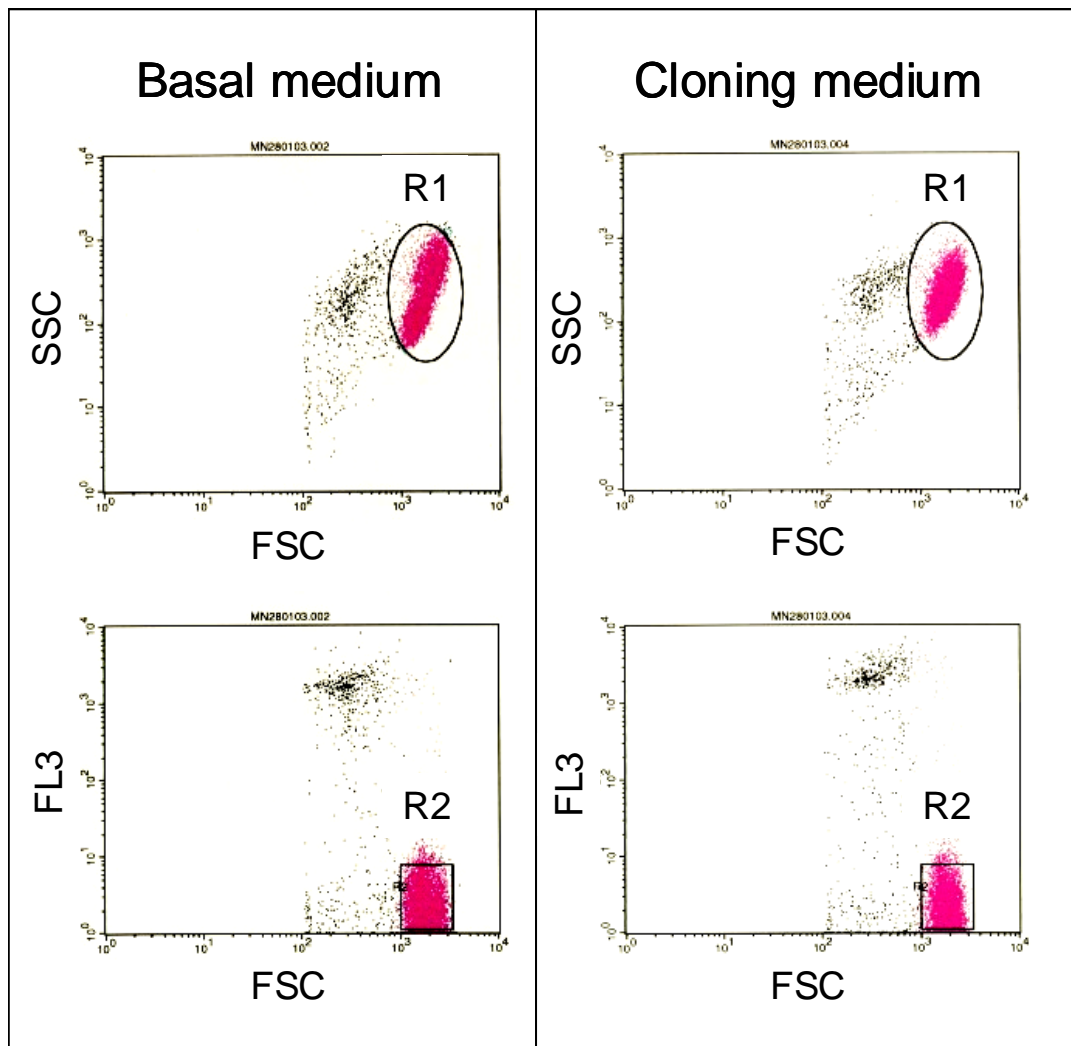


Fig. 4 FACS analysis of MSCs for the cell sorting procedure. Two-parameter dot plots show cells in forward scatter (FSC) against sideward scatter (SSC) in the upper row, and FSC against fluorescence channel 3 (FL3) in the lower row. The propidium iodide staining allowed for the exclusion of dead cells. Viable cells were sorted from the region 2 (R2) which represents cells of the main population as marked in the R1 in the FSC-SSC-dot plots.

Differentiation of MSCs under non—clonal conditions

The first goal of this study was to find a cloning medium for MSCs in order to investigate the effects of bFGF on the adipogenesis of MSCs under clonal conditions. The cloning medium (Fig. 2, group 11) was demonstrated to be a suitable medium for MSC cloning. The next step was to also prove the suitability of the cloning medium for the differentiation of MSCs under non-clonal conditions in comparison to the basal medium which had been used in previous studies in 2-D and 3-D cell culture (chapters 3,4,6,7).

After induction of the adipogenic differentiation by the hormonal cocktail, MSCs weakly gave rise to adipocytes in presence of both the basal and the cloning medium (Fig. 5). Under both conditions, MSCs responded to bFGF that enhanced the adipogenesis of MSCs (as also described in chapter 4 in detail). Basic FGF increased the number of differentiated adipocytes as shown by Red Oil O staining of the lipid inclusions (Fig. 5). Thus, the cultivation of MSCs in the cloning medium did not appear to have a modulating influence on the adipogenic differentiation and on the responsiveness of the MSCs to bFGF under non-clonal conditions as compared to the cultivation of MSCs with the basal medium.

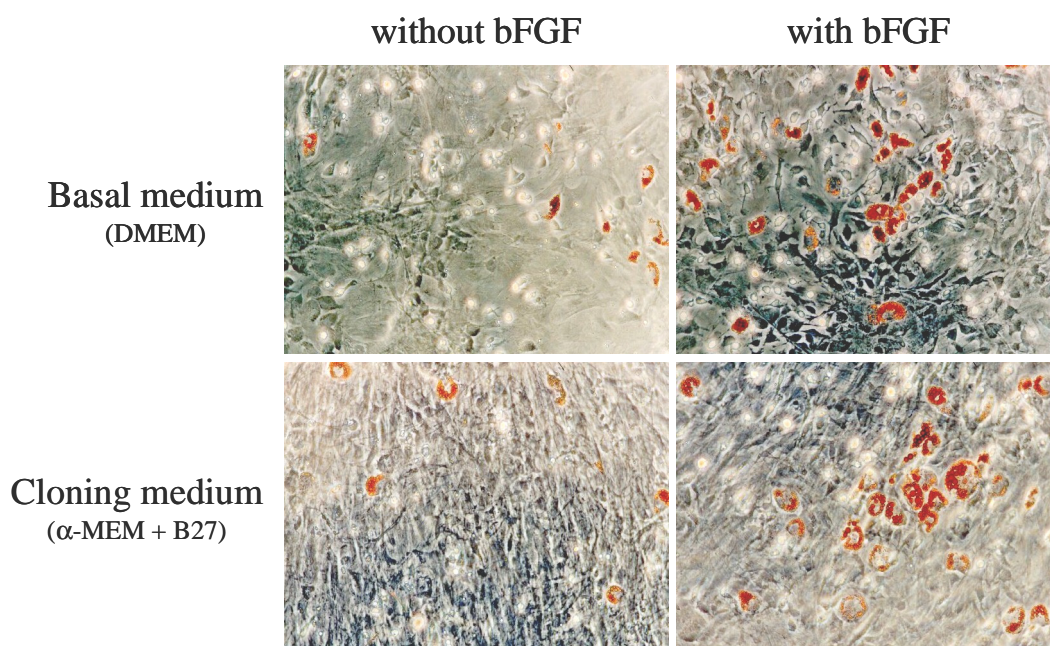


Fig. 5: Adipogenesis of MSCs cultured in basal medium and in cloning medium under non-clonal conditions. MSCs weakly differentiated in absence of bFGF, whereas supplementation of bFGF enhanced the adipogenic differentiation of MSCs under both conditions.

Mechanistic investigation of the effects of bFGF

The aforementioned experiments suggested the cloning medium to be an appropriate medium with which the effects of bFGF on the adipogenesis of MSCs could be investigated under clonal conditions. Basic FGF was supplemented either only in the single cell culture, abbreviated as C-F, or in the entire culture period, that is, during the proliferation phase and in the single cell culture, abbreviated as F-F. Cells cultivated in absence of bFGF (C-C) served as control. The number of grown clones was similar in the groups C-C (48 clones) and F-F (56 clones). In contrast, the number of the clones was clearly elevated in the group C-F (103 clones), as shown in Fig. 6.

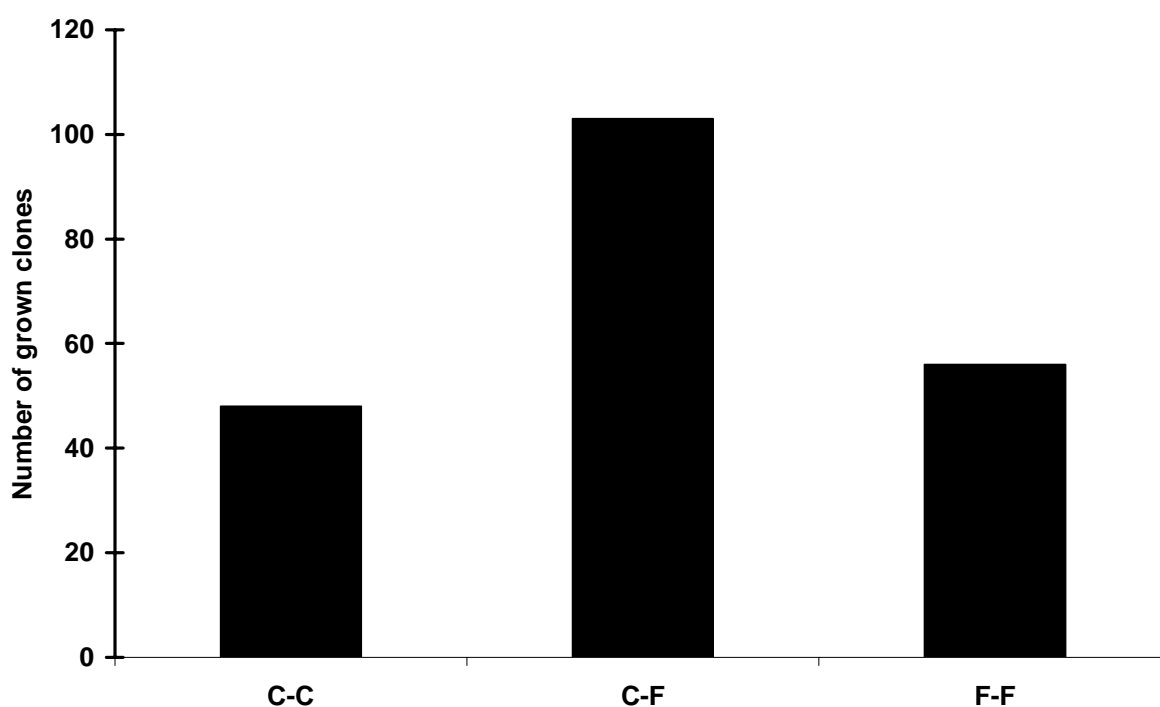


Fig. 6: The growth of clones under different conditions. Basic FGF was supplemented either only in the single cell culture (C-F) or in the entire culture period (F-F). Cells cultivated in absence of bFGF (C-C) served as a control. The total number of wells in the single cell culture was 282.

The number of differentiated clones was similar in the groups C-C (9 clones) and C-F (8 clones) but strikingly increased in the group F-F (25 clones) as compared to C-C and C-F (Fig. 7). Normalized to the number of grown clones under the corresponding conditions (Fig. 6), 19% of the clones were capable to undergo adipogenesis under the condition C-C, 8% under C-F, and remarkable 45% under F-F (Fig. 7).

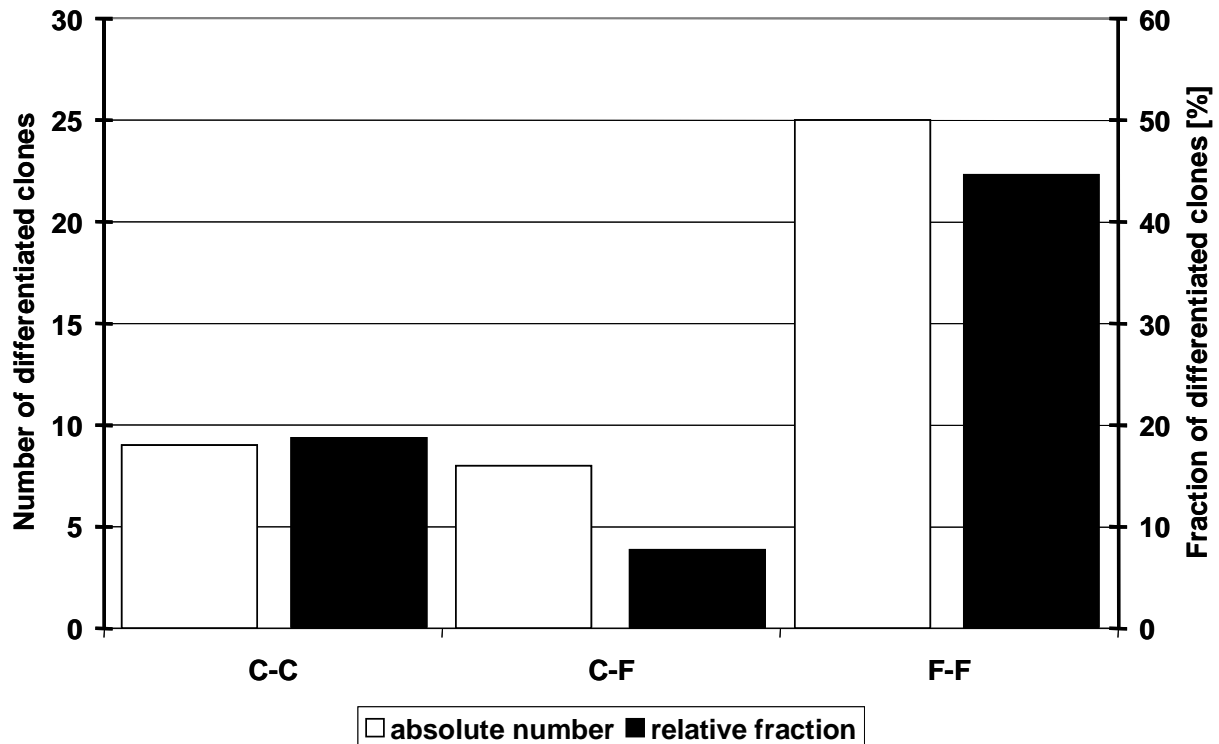


Fig. 7: The adipogenic differentiation of grown clones. Basic FGF was supplemented either only in the single cell culture (C-F) or in the entire culture period (F-F). Cells cultivated in absence of bFGF (C-C) served as a control. White bars show the absolute number of differentiated clones, black bars show the fraction of differentiated clones normalized to the number of grown clones (see Fig. 6) under the corresponding condition.

Figure 8 exemplarily shows a section of a differentiated clone from the group F-F. Adipogenesis was induced in almost all cells of the clone. Lipid droplets were stained red by Oil Red O.

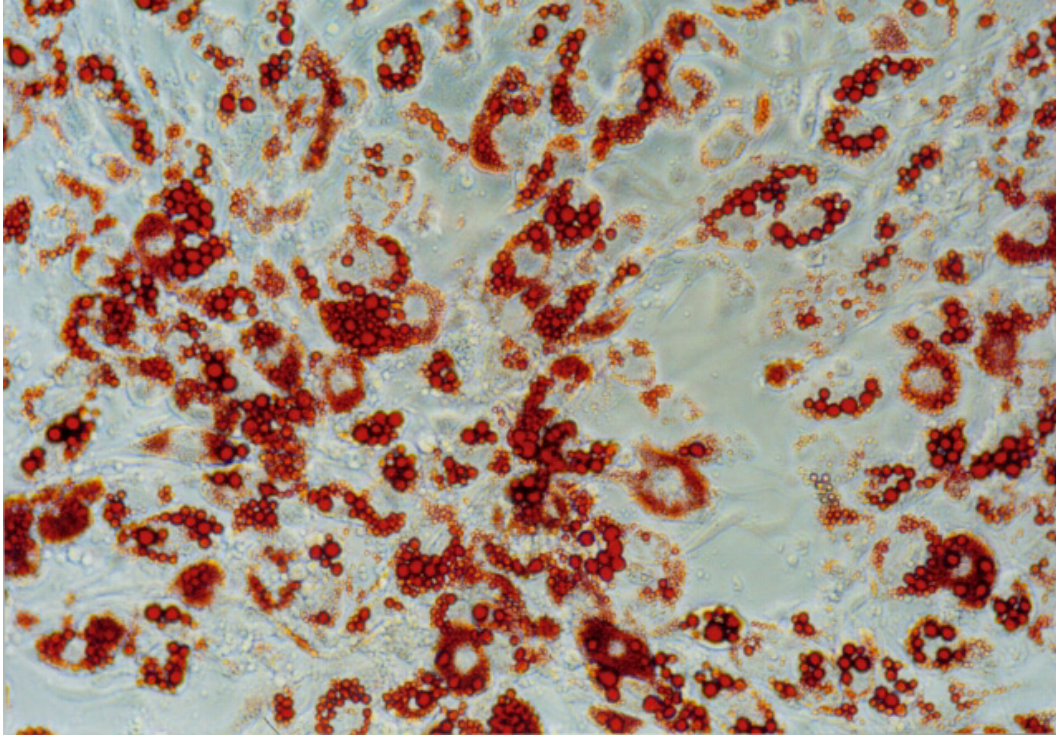


Fig.8: Oil Red O staining of a differentiated clone of the F-F group.

Discussion

Evaluation of a suitable cloning medium

The cloning medium consisting of α -MEM, 10% FBS, 1% antibiotics, 50 μ g/ml ascorbic acid, and B27 turned out to be the most effective medium for the expansion of MSCs under clonal conditions (Table 2, Fig. 2). In addition, the application of the cloning medium retained the responsiveness of MSCs to the hormonal cocktail and to bFGF (Fig. 5). All media, α -MEM, DMEM, and RPMI, were not useful to initiate the clonal growth without any further supplementation of additives. The addition of conditioned media collected in the proliferation phase of the culture had no effect on the clone growth. In contrast, addition of B27 resulted in the most efficient growth stimulation, especially in combination with α -MEM. The use of the cloning medium in the entire culture without any interruption was most effective, any modification led to a decrease of the developed clone number. In preliminary experiments, it was shown that the medium components proline and glutamate, both included in the α -MEM

mixture but excluded in the DMEM mixture, stimulated the proliferation of MSCs under non-clonal conditions if supplemented to the DMEM medium (data not shown). However, virtually no clonal growth was obtained in absence of B27. The B27 supplement in combination with DMEM was originally developed and optimized for the cultivation of hippocampal neurons by Brewer et al. [10]. In that study was shown that the reduction of the concentration of glutamine and the elimination of the toxic ferric sulphate in the DMEM mixture are superior to the original medium. Interestingly, the concentration of glutamine is strikingly lower in α -MEM (292 mg/l) than in DMEM (580 mg/l) and the iron salt ferric nitrate is included in DMEM but not element of α -MEM. Maybe, these components also contribute to the growth and survival of MSCs in the single cell culture. Using the cloning medium, about one third of all plated single cells were stimulated to grow under clonal conditions which partially developed large clones (Figs. 2,3). The high efficacy of the clone growth may allow for the performance of high numbers of differentiation experiments starting at a reasonable number of cells to be sorted and the development of large clones and may allow for further differentiation experiments where the cloned cells are subjected to differential differentiation combined with the application of a wide range of analytical methods.

Cell sorting procedure

Conventional methods for the cloning of MSCs include the cloning ring technique [1] and the limiting dilution technique [11]. These methods represent technical challenges and are time consuming. A preferable technique is provided by the flow cytometry technique. Single cells can be sorted by fluorescence-activated cell sorting (FACS) [12] and magnetic activated cell sorting (MACS) [13], respectively. In this study, we sorted single MSCs using FSC-SSC and FSC-FL3 two-parameter dot plots which facilitate the sorting of cells from the main population with a simultaneous exclusion of propidium iodide-stained dead cells (Fig. 4).

Mechanistic investigation of the effects of bFGF

Basic FGF is a known modulator of the differentiation of MSCs towards the adipogenic [14], osteogenic [6,7,14-19], and chondrogenic [7,15] lineage. Beyond this, bFGF is a useful tool for the extensive expansion, the elongation of the life span, accompanied by the retention of the differentiation potential [5,7]. These aspects emphasize the outstanding role of bFGF for the application of MSCs in the field of tissue engineering. However, mechanisms by which bFGF exerts its effects on MSCs are poorly investigated. To date, a variety of possible mechanisms of the modulation of cellular differentiation by bFGF is discussed in the

literature. For instance, it has been suggested that bFGF exerts its effects via the modulation of the cell shape and the resulting cytoskeletal organization [20] as well as the alteration of the synthesis and the organization of the extracellular matrix and the resulting changes in the cell shape [6]. Mc Beath et al. reported that unspread and round human MSCs preferably underwent adipogenic differentiation due to an inhibition of the RhoA pathway involving actin-myosin-generated tensions [20]. Martin et al. demonstrated human MSCs to exhibit an alternative phenotype in presence of bFGF, elongated and spindle-like, as compared to the absence of bFGF, flattened and spread [6]. Basic FGF-treated MSCs maintained their original elongated shape during extensive expansion and showed an increased osteogenic differentiation. However, a contribution of the cell shape to the effect of bFGF in our cell culture system appears to be unlikely as discussed in chapter 3 of this thesis (Chapter 3, fig. 8). A further discussed mechanism involves bFGF in the exertion of a preferential proliferation of a distinct subset of the MSCs [5,6]. Basic FGF has been shown to select a MSC subpopulation with a distinctly longer life span caused by an increased telomere length of these cells [5]. That study suggested bFGF to exert a bimodal effect: the negative selection of cells already committed to the osteogenic lineage and the stimulation of the proliferation of immature MSCs. Last but not least, bFGF may influence the behavior of MSCs by a direct modulation of their commitment state [6]. In regard to the adipogenesis of cells, bFGF has been demonstrated to directly increase the expression of peroxisome proliferator-activated receptor γ (PPAR γ) and the expression of CCAAT/enhancer-binding protein α (C/EBP α), both key transcription factors in adipogenesis [21], via the MEK/ERK signaling pathway in 3T3-L1 cells [22].

Furthermore, we have demonstrated bFGF to enhance adipogenesis of MSCs. Basic FGF supplemented in different phases of the culture resulted in an elevated adipogenesis in any case and interestingly, PPAR γ mRNA was expressed at higher levels even prior to adipogenic induction in the presence of bFGF as compared to cells cultivated in the absence of bFGF (Chapter 4, Figs. 2-4). This effect of bFGF may be provoked by a preferential proliferation of a subpopulation of MSCs responsible for the elevated PPAR γ message and/or may be caused by a direct effect on the commitment level of MSCs. The present study utilizing clonal conditions was performed in order to address this issue. The mechanistic investigation of the bFGF-influenced adipogenesis of MSCs is rendered more difficult due to the inhomogeneous mixture of different cell subpopulations. The single cell culture allows the investigation of the (bFGF-influenced) differentiation process of clones derived from a single cell.

Surprisingly, bFGF supplemented in the single cell culture (C-F) yielded about double the number of grown clones than the control group without bFGF (C-C) and the group with bFGF in the entire culture (F-F) (Fig. 6). However, clones of the C-F group differentiated to the same extent that the control group but clearly weaker than the clones of the F-F group (Fig. 7). Clones derived from the C-F group respond to bFGF, that is, the number of grown clones is clearly elevated than in the control group, but the addition of bFGF in the single cell culture had no promoting effect in regard to the differentiation of MSCs. Thus, a direct commitment of single MSCs towards the adipogenic lineage exerted by bFGF appears to be unlikely in this study. In contrast, addition of bFGF in the proliferation phase and in the single cell culture yielded 25 differentiated clones, i.e. 45% of all grown clones underwent adipogenesis, a clear increase as compared to the B-B group (9 differentiated clones, 19% of all clones) and the C-F group (8 differentiated clones, 8% of all clones) (Fig. 7). Thus, it seems that the supplementation of bFGF in the proliferation phase led to preferential proliferation of a subpopulation of the MSCs which possess a high capacity to give rise to adipocytes. A preferential proliferation of this subset would result in a high number of these cells present at the time point of the passage and subsequently, a higher probability to recover these cells in the single cell culture following the cell sorting procedure.

With regard to the groups C-F and F-F, the responsiveness of the MSCs of these groups to bFGF in the different culture phases should be discussed. Obviously, a higher number of cells of the C-F respond to bFGF in the single cell culture as compared to the F-F group in respect to the initiation of the clone growth (Fig. 6). However, the cells of the C-F group failed to undergo adipogenesis (Fig. 7). In contrast, approx. 50% of the grown clones of the F-F group gave rise to adipocytes (Fig. 7) and these cells were stimulated during the proliferation phase and during the single cell culture by bFGF. A possible explanation may be the existence of at least two cellular subpopulations which are both proliferatively stimulated by bFGF but only one certain subpopulation is capable of differentiating into adipocytes. To explain the obtained results, a subpopulation incapable of undergoing adipogenesis might be primarily propagated in absence of bFGF during the proliferation phase (C-F), whereas the subpopulation with the potential of adipogenic differentiation might be predominantly expanded in presence of bFGF during the proliferation phase (F-F).

This study suggests bFGF to exert its effect on the adipogenesis of MSCs predominantly through the preferential proliferation of a subpopulation of MSCs which is capable of differentiating into adipocytes. However, the enhancement of the adipogenesis of MSCs by bFGF supplemented only during the differentiation phase in the conventional 2-D cell culture

is hardly to explain with this mechanism. In this case, bFGF was added to postconfluent cells in combination with the hormonal cocktail, that is, bFGF could not stimulate the proliferation of MSCs (Chapter 4, Figs. 2-4, experimental group “BBF”). The fraction of MSCs which differentiated in this group was about 5%. Probably, the number of cells committed by this way is too low to be recovered in the present study and a higher number of single cells has to be tested in future experiments. For this group, a direct effect of bFGF on the commitment level of the MSCs is more likely, for instance, a mechanism such as the one proposed by Prusty et al. [22], as discussed above.

In conclusion, a medium, denoted as the cloning medium, was found to be suitable for the expansion of MSCs under cloning condition. This medium ensured the maintenance of the differentiation potential and the responsiveness to bFGF as enhancer of the adipogenesis of MSCs. Differentiation experiments under clonal conditions in which bFGF was supplemented either only in the single cell culture phase or in the entire culture, respectively, suggests bFGF to act mainly via the preferential proliferation of a subset of the MSCs capable of undergoing adipogenesis.

References

- [1] Pittenger MF, Mackay AM, Beck SC, Jaiswal RK, Douglas R, Mosca JD, Moorman MA, Simonetti DW, Craig S, Marshak DR. 'Multilineage potential of adult human mesenchymal stem cells'. *Science* (1999); **284**: 143-147.
- [2] Kim MK, Niyibizi C. 'Interaction of TGF-beta1 and rhBMP-2 on human bone marrow stromal cells cultured in collagen gel matrix'. *Yonsei Med J* (2001); **42**: 338-344.
- [3] Sottile V, Seuwen K. 'Bone morphogenetic protein-2 stimulates adipogenic differentiation of mesenchymal precursor cells in synergy with BRL 49653 (rosiglitazone)'. *FEBS Lett* (2000); **475**: 201-204.
- [4] Gimble JM, Morgan C, Kelly K, Wu X, Dandapani V, Wang CS, Rosen V. 'Bone morphogenetic proteins inhibit adipocyte differentiation by bone marrow stromal cells'. *J Cell Biochem* (1995); **58**: 393-402.
- [5] Bianchi G, Banfi A, Mastrogiacomo M, Notaro R, Luzzatto L, Cancedda R, Quarto R. '*Ex vivo* enrichment of mesenchymal cell progenitors by fibroblast growth factor 2'. *Exp Cell Res* (2003); **287**: 98-105.
- [6] Martin I, Muraglia A, Campanile G, Cancedda R, Quarto R. 'Fibroblast growth factor-2 supports *ex vivo* expansion and maintenance of osteogenic precursors from human bone marrow'. *Endocrinology* (1997); **138**: 4456-4462.
- [7] Tsutsumi S, Shimazu A, Miyazaki K, Pan H, Koike C, Yoshida E, Takagishi K, Kato Y. 'Retention of multilineage differentiation potential of mesenchymal cells during proliferation in response to FGF'. *Biochem Biophys Res Commun* (2001); **288**: 413-419.
- [8] Deans RJ, Moseley AB. 'Mesenchymal stem cells. Biology and potential clinical uses'. *Exp Hematol* (2000); **28**: 875-884.
- [9] Ishaug SL, Crane GM, Miller MJ, Yasko AW, Yaszemski MJ, Mikos AG. 'Bone formation by three-dimensional stromal osteoblast culture in biodegradable polymer scaffolds'. *J Biomed Mater Res* (1997); **36**: 17-28.
- [10] Brewer GJ, Torricelli JR, Evege EK, Price PJ. 'Optimized survival of hippocampal neurons in B27-supplemented Neurobasal, a new serum-free medium combination'. *J Neurosci Res* (1993); **35**: 567-576.
- [11] Muraglia A, Cancedda R, Quarto R. 'Clonal mesenchymal progenitors from human bone marrow differentiate *in vitro* according to a hierarchical model'. *J Cell Sci* (2000); **113**: 1161-1166.

- [12] Suzuki A, Zheng YW, Kaneko S, Onodera M, Fukao K, Nakauchi H, Taniguchi H. 'Clonal identification and characterization of self-renewing pluripotent stem cells in the developing liver'. *J Cell Biol* (2002); **156**: 173-184.
- [13] Ahdjoudj S, Lasmoles F, Oyajobi BO, Lomri A, Delannoy P, Marie PJ. 'Reciprocal control of osteoblast/chondroblast and osteoblast/adipocyte differentiation of multipotential clonal human marrow stromal F/STRO-1+ cells'. *J Cell Biochem* (2001); **81**: 23-38.
- [14] Locklin RM, Oreffo ROC, Triffitt JT. 'Effects of TGF.β. and bFGF on the differentiation of human bone marrow stromal fibroblasts'. *Cell Biol Int* (1999); **23**: 185-194.
- [15] Martin I, Padera RF, Vunjak-Novakovic G, Freed LE. '*In vitro* differentiation of chick embryo bone marrow stromal cells into cartilaginous and bone-like tissues'. *J Orthop Res* (1998); **16**: 181-189.
- [16] Locklin RM, Williamson MC, Beresford JN, Triffitt JT, Owen ME. '*In vitro* effects of growth factors and dexamethasone on rat marrow stromal cells'. *Clin Orthop* (1995); 27-35.
- [17] Hanada K, Dennis JE, Caplan AI. 'Stimulatory effects of basic fibroblast growth factor and bone morphogenetic protein-2 on osteogenic differentiation of rat bone marrow-derived mesenchymal stem cells'. *J Bone Miner Res* (1997); **12**: 1606-1614.
- [18] Pitaru S, Kotev-Emeth S, Noff D, Kaffuler S, Savion N. 'Effect of basic fibroblast growth factor on the growth and differentiation of adult stromal bone marrow cells: enhanced development of mineralized bone-like tissue in culture'. *J Bone Miner Res* (1993); **8**: 919-929.
- [19] Scutt A, Bertram P. 'Basic fibroblast growth factor in the presence of dexamethasone stimulates colony formation, expansion, and osteoblastic differentiation by rat bone marrow stromal cells'. *Calcif Tissue Int* (1999); **64**: 69-77.
- [20] McBeath R, Pirone DM, Nelson CM, Bhadriraju K, Chen CS. 'Cell shape, cytoskeletal tension, and RhoA regulate stem cell lineage commitment'. *Dev Cell* (2004); **6**: 483-495.
- [21] Ailhaud G. 'Cell surface receptors, nuclear receptors and ligands that regulate adipose tissue development'. *Clin Chim Acta* (1999); **286**: 181-190.
- [22] Prusty D, Park BH, Davis KE, Farmer SR. 'Activation of MEK/ERK signaling promotes adipogenesis by enhancing peroxisome proliferator-activated receptor γ (PPAR γ) and C/EBP α gene expression during the differentiation of 3T3-L1 preadipocytes'. *J Biol Chem* (2002); **277**: 46226-46232.

Chapter 6

Stem Cell Seeding and Proliferation on Scaffolds with Different Pore Sizes

Markus Neubauer,¹ Michael Hacker,¹ Carlos Garcia-Lopez,^{1,2} Michaela B. Schulz,¹ Achim Göpferich,¹ Torsten Blunk¹

¹ Department of Pharmaceutical Technology, University of Regensburg, Universitaetsstrasse 31, 93040 Regensburg, Germany

² Department of Pharmacy and Pharmaceutical Technology, University of Santiago de Compostela, Universitario Sur, 15782 Santiago de Compostela (A Coruna), Spain

Abstract

Mesenchymal stem cells represent a promising potential cell source for tissue engineering strategies including approaches towards adipose tissue engineering. Beyond an appropriate cell source, suitable biomaterials for the fabrication of cell carriers are required in tissue engineering.

In this study, the potential of a diblock copolymer consisting of poly(ethylene glycol) (PEG) and poly(lactic acid) (PLA) components, abbreviated as MeO-PEG₂PLA₄₀, was evaluated for the use in tissue engineering. This polymer consists of a 2kDa PEG chain and a 40 kDa PLA compound. A novel solid lipid templating technique allowed for the fabrication of custom-made scaffolds with various ranges of pore sizes: 100-300 μm , 300-500 μm , and 500-710 μm . Cell attachment and proliferation of MSCs on 3-D cell carriers was investigated in regard to effects of the different pore size ranges over a time course of two weeks.

MSCs were harvested from rat bone marrow and dynamically seeded onto the polymer scaffolds. Cellular distribution and cell shape were monitored by H&E histology and scanning electron microscopy. The proliferation of MSCs on the scaffolds was assessed by measurement of the cell number with means of DNA assay. MSCs were uniformly distributed within all scaffolds. The initial seeding density of MSCs onto the different scaffolds was equal in all groups whereas the cell number varied over the course of time.

The scaffolds with pore sizes from 100 to 300 μm allowed for cell penetration throughout the entire scaffold and the cell number was maintained over two weeks. Thus, this scaffold type appears to be most suitable for tissue engineering applications among the tested scaffolds in regard to tissue development.

Introduction

Conventional surgical techniques do not represent the optimum option for the supply with adipose tissue surrogates in reconstructive and plastic surgery [1,2]. Recently, promising new therapy strategies based on tissue engineering techniques have been developed which comprise *de novo* adipogenesis and cell-based therapy approaches [3]. In general, three critical components have emerged in tissue engineering approaches: cells, scaffolds, and growth factors [4]. In this study, mesenchymal stem cells (MSCs) and a derivative of PEG-PLA diblock copolymers as a scaffold material were used in order to investigate their potential for (adipose) tissue engineering applications.

In the field of adipose tissue engineering, the cell source is mainly restricted to preadipocytes [5-16]. However, MSCs represent a potential cell source for tissue engineering approaches towards various tissues [17-23]. MSCs can be easily isolated and allow for a billion-fold expansion. Moreover, these stem cells possess the capacity for multipotent differentiation [20]. In detail, MSCs are capable to undergo differentiation at least towards the bone, cartilage, fat, muscle, tendon, skin, and marrow stroma lineage [22,24]. To date, MSCs are applied to tissue engineering approaches in the field of bone [25-30], cartilage [31,32], and tendon [33] regeneration *in vitro* and *in vivo*. The potential of MSCs for adipose tissue engineering has been evaluated in the study presented in Chapter 7 of this thesis.

To date, for cell-based strategies, preadipocytes are used as cell source in combination with cell carriers made from a wide range of materials. Preadipocytes have been cultivated on porous scaffolds made from synthetic, protein-coated polytetrafluoroethylene [5] or synthetic, biodegradable PLGA [6,11] and polyglycolic acid [15,16]. Furthermore, natural biomaterials such as collagen [7,9,10,13], hyaluronic acid [9,14], (RGD-modified) alginate gels [12], and fibrin glue [8] in the form of sponges and hydrogels have been shown to function as applicable carriers for preadipocytes. In those studies, scaffolds with pore sizes in the range of 40 to 633 μm were used.

In our laboratory, various poly(ethylene glycol)-block-poly(D,L-lactic acid) polymers have been synthesized and characterized as described in [34-36]. These polymers with varying ratios of the PEG and the PLA components have been shown to suppress unspecific protein adsorption and cell attachment and to modulate the osteogenic differentiation of MSCs in 2-D cell culture. In addition, by derivatization of the PEG compound, biomimetic polymers can be synthesized to which bioactive molecules such as peptides and proteins can be covalently bound in order to control the cellular behavior (see chapter 9) [37,38]. In this study, MeO-PEG₂PLA₄₀, a diblock copolymer with a hydrophilic 2 kDa poly(ethylene glycol) (PEG) chain

and a lipophilic 40 kDa poly(lactic acid) compound was used. This biodegradable PEGPLA polymer can be processed into 3-D cell carriers by a solid lipid templating technique as described by Hacker et al. [39]. With this method, the pore size of the scaffolds can be controlled by the size of the porogen microparticles which consist of lipids. Architectural features of scaffolds such as the pore size and the interconnectivity of the pores have been shown to influence cell seeding, distribution, migration, and growth, the transport of nutrients and oxygen into the scaffolds, and the removal of metabolites out of the scaffold [40,41]. These processes strongly contribute to the development and maintenance of new tissues [42]. The aim of this study was to demonstrate the attachment and proliferation of MSCs in regard to the influence of different pore sizes of the scaffolds. Therefore, scaffolds used in this study are characterized by different ranges of pore sizes: 100-300 μm , 300-500 μm , and 500-710 μm .

Materials and Methods

Materials

If not otherwise stated, chemicals were obtained from Sigma (Steinheim, Germany). Basic FGF was obtained from PeproTec (Rocky Hill, NJ, USA). Cell culture plastics were purchased from Corning Costar (Bodenheim, Germany).

The polymer MeO-PEG₂PLA₄₀ was synthesized in our laboratory as previously described [36]. The structure of the polymer is shown in Figure 1.

Spinner flasks were self-made (250 ml volume, 6 cm bottom diameter, side arms for gas exchange). Silicon stoppers were obtained from Schuber & Weiss (München, Germany); needles were from Unimed (Lausanne, Switzerland).

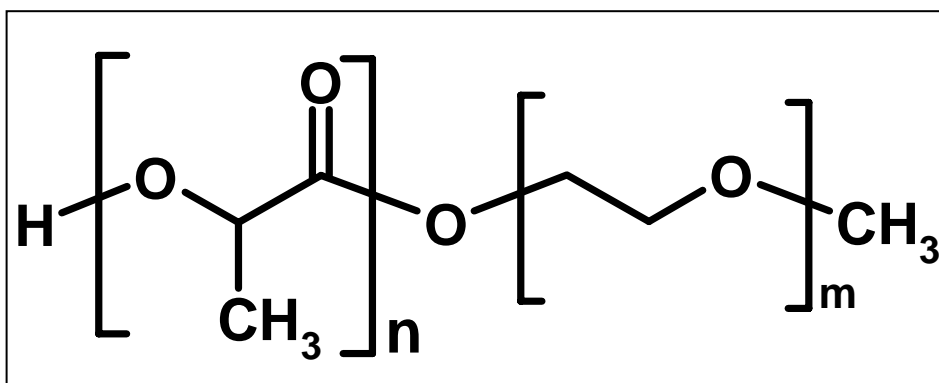


Fig. 1 Structure of the polymer used for the fabrication of the scaffold, a poly(D,L-lactic acid)-block-poly(ethylene glycol)-monomethylether consisting of a 2 kDa PEG chain and a 40 kDa PLA block, abbreviated as MeO-PEG₂PLA₄₀.

Scaffold fabrication

Scaffolds were fabricated using a protocol adapted from Hacker et al. [39]. Briefly, the scaffolds were fabricated from 30% MeO-PEG₂PLA₄₀ polymer dissolved in a methyl ethyl ketone-tetrahydrofurane-mixture (59:41 (v/v)) and 70% lipid microparticles made from Softisan[®] 154 and Witepsol[®] H42 (ratio 1:1; kindly provided by SASOL Germany (Witten, Germany)) were weighed into a separate vial. The size of porogen particles ranged from 100 μm to 300 μm, from 300 μm to 500 μm, and from 500 to 710 μm, respectively. After 1 h storage at -20°C the porogen particles were transferred into the polymer solution and mixed for 5 min on ice. The resulting highly viscous dispersion was then transferred into a 10 ml polypropylene syringe and injected into eight cubic Teflon[®] molds (with a cylindrical cavity of 0.8 cm in diameter). After a pre-extraction treatment step in n-hexane at 0°C for 90 min, the filled molds were submerged in warm n-hexane to precipitate the polymer and extract the porogen particles concurrently. This procedure was carried out in two separate n-hexane baths of different temperatures: first, molds were incubated at 45°C for 7.5 min and in a second step at 35°C for 22.5 min. Subsequently, the molds were transferred into a n-hexane bath of 0°C for 5 min. Finally, the porous cylindrical polymer constructs were removed from the molds and vacuum-dried for 48 h. For further investigations the constructs were cut into 2 mm slices which were then addressed as scaffolds.

Cell isolation and expansion

Marrow stromal cells were obtained from six-week old male Sprague Dawley rats (weight: 170 - 180 g, Charles River, Sulzfeld, Germany). MSCs were flushed from the tibiae and femora according to an established protocol published by Ishaug [43]. Cells were centrifuged

at 1200 rpm for 5 min. The resulting cell pellet was resuspended in basal medium (DMEM (Biochrom, Berlin, Germany), 10 % fetal bovine serum (Gemini Bio-Products, Calabasas, CA, USA), 1 % penicillin/streptomycin (Invitrogen, Karlsruhe, Germany), 50 µg/ml ascorbic acid) and seeded in T75 flasks. Cells were cultured in an incubator (37°C, 5% CO₂) and were allowed to adhere to the substratum for three days. The flasks were rinsed twice with phosphate-buffered saline (PBS, Invitrogen, Karlsruhe, Germany) to remove non-adherent cells. 12 ml of basal medium were then exchanged every 2-3 days. After confluence was reached, cells were detached with 0.25 % trypsin and EDTA (Invitrogen, Karlsruhe, Germany). The cell number of the obtained cell suspension was determined in triplicate using a hemacytometer.

3-D cell culture

MeO-PEG₂PLA₄₀ scaffolds were pre-wetted with 70% ethanol and rinsed extensively with PBS. Scaffolds were strung onto needles (10 cm long, 0.5 mm diameter) and located with segments of silicone tubing (1 mm long). Four needles with two scaffolds each were inserted into a silicone stopper; the stopper was in turn placed into the mouth of a spinner flask. A magnetic stir bar was placed at the bottom of the spinner flask. The spinner flasks were filled with 100 ml basal medium and put on a magnetic stir plate (Bellco 10 Glas, Vineland, NJ, USA) at 80 rpm in an incubator (37°C, 5% CO₂). After 24 h, the medium was aspirated and the cell suspension containing 2.5 million cells per scaffold, was filled into the flask. The volume of the medium was filled up with basal medium to 100 ml. Stirring for three days at 80 rpm allowed for cell attachment to the scaffold. At this point of time, cell-polymer constructs were harvested for histology, SEM, and measurement of the cell number. Further scaffolds were cultivated for two weeks in order to determine the cell numbers after 7 days and 14 days (proliferation phase). Day 0 of the proliferation phase was the day the seeding procedure was finished. Cell-polymer constructs were transferred into six-well plates containing one scaffold and 5 ml medium per well. Constructs were cultivated in six-well plates on an orbital shaker at 50 rpm (Dunn Labortechnik, Asbach, Germany) until the time point of harvest. In order to stimulate the proliferation of MSCs on the 3-D cell carriers, the medium was supplemented with a potent mitogen, 3 ng/ml basic fibroblast growth factor (bFGF). Basic FGF has been repeatedly reported to stimulate the proliferation of various cell types [44-46] and has been shown to enhance the proliferation of rat MSCs in Chapter 3 of this thesis.

Histology

After the seeding procedure over three days, on day 0 of the proliferation phase, cell-polymer constructs were washed once with PBS and pre-fixed with 2.5% glutaraldehyde in PBS for 15 min and subsequently with 10% formaldehyde (Merck, Darmstadt, Germany) in PBS for storage. Tissue constructs were dehydrated and embedded in paraffin. Deparaffinized sections (5 µm) were stained with hematoxylin and eosin (H&E). Photographs were taken with a Dynax 600 si classic camera (Minolta Europe GmbH; Langenhagen, Germany) mounted on a Leica DM IRB light microscope (Leica Microsystems AG; Wetzlar, Germany).

Scanning electron microscopy (SEM)

After the seeding procedure over three days, on day 0 of the proliferation phase, cell-polymer constructs were pre-fixed for 15 min with 2.5% glutaraldehyde in PBS and with 10% formaldehyde for storage. Tissue constructs were crosslinked for 30 min with 1% osmium tetroxide. After extensive rinsing and freezing at -80°C, samples underwent lyophilization (Christ Beta 2-16, Martin Christ Gefriertrocknungsanlagen, Osterode am Harz, Germany). Samples were glued on aluminium stubs using conductive carbon tape. Thereafter, cell-polymer constructs were coated with gold-palladium (Polaron SC515, Fisons surface systems, Grinstead, UK). All micrographs were taken at 10 kV on a DSM 950 (Zeiss, Oberkochen, Germany).

DNA assay

On day 0, 7, and 14 of the proliferation phase, a fluorimetric assay was performed in order to determine the total amount of DNA on the cell-polymer constructs and to subsequently assess the cell number [47]. Cell-polymer constructs were washed with PBS and digested with 1 ml of a papainase solution (CellSystem, St. Katharinen, Germany) (3.2 U/ml in buffer) for 18 h at 60 °C. The number of cells per cell-polymer construct was assessed from the DNA content using Hoechst 33258 dye (Polysciences, Warrington, PA, USA) measured on a spectrofluorometer (RF-1501, Shimadzu Deutschland GmbH, Duisburg, Germany). Cell standards and DNA standards (from calf thymus) were prepared in parallel. A conversion factor of 13 pg DNA per MSC was used to calculate the total cell number per scaffold. The factor was obtained by measurement of the DNA content of a cell standard, that is, a certain number of MSCs which number was determined using a hemacytometer, using the same conditions as described for the cell-polymer constructs. The determined number of cells is

expressed as the percentage of initially provided cells in the cell suspension, that is, 2.5 million MSCs per scaffold.

Statistics

DNA data are expressed as means \pm standard deviation (n=3). Single-factor analysis of variance (ANOVA) was used in conjunction with a multiple comparison test (Tukey's test).

Results

Scaffold structure

Custom-made scaffolds were fabricated by a novel solid lipid templating technique [39]. Fig. 2 shows SEM pictures of the microstructure of the scaffolds. The structure characterized by a high porosity and a highly interconnected network of pores was generated by a simultaneous precipitation of the polymer and dissolution of the porogen microparticles. Three ranges of pore sizes in the ranges from 100 to 300 μm , from 300 to 500 μm , and from 500 to 710 μm were chosen for this study.

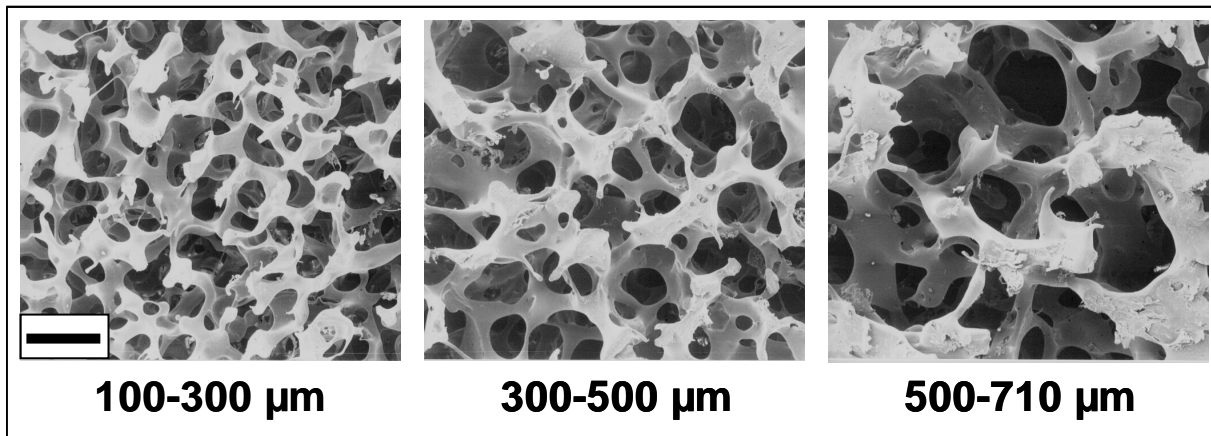


Fig. 2 SEM pictures of blank scaffolds made from MeO-PEG₂PLA₄₀ polymer. Pore sizes ranged from 100-300, 300-500, and 500-710 μm , respectively. Scale bar: 200 μm .

Cell seeding

After the seeding procedure, cross-sections of the scaffolds were stained with H&E in order to observe cellular distribution of the cells within the scaffold. Figure 3 shows scaffolds with different pore sizes which were halved and cross sections were cut. MSCs were uniformly distributed throughout the entire scaffolds in all groups as shown in pictures taken at 40-fold magnification. The cells attached to the scaffold walls and coated the walls. The cavities

within the scaffolds were not filled with cells, thus, the size of the pores can be clearly recognized in the histological sections. At the higher magnification, discrete stem cells and stem cell clusters were observable.

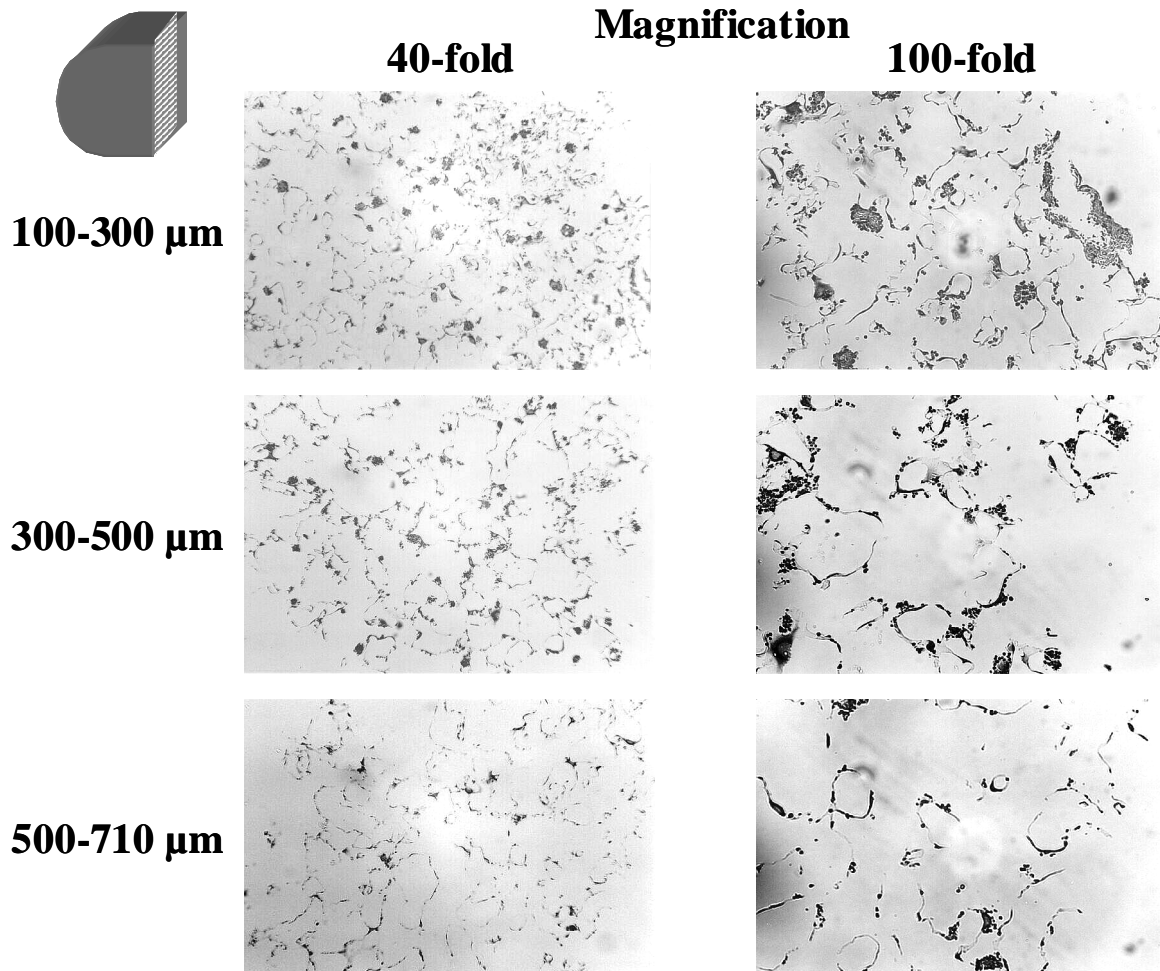


Fig. 3 Histology of the cell-polymer constructs with varying ranges of the pore size at the end of the seeding procedure. Deparaffinized sections (5 μm) were stained with H&E. The cartoon shows a half of a scaffold and the striped area marks the observed area, the interior of a scaffold.

The surface of the scaffolds was additionally examined by SEM at 200-fold and 500-fold magnification (Fig. 4a). At the low magnification, the uniform distribution recognized in histological sections could be confirmed with SEM. Mostly single cells and a few cell clusters were distributed on scaffolds with pore sizes from 100-300 μm and from 300-500 μm .

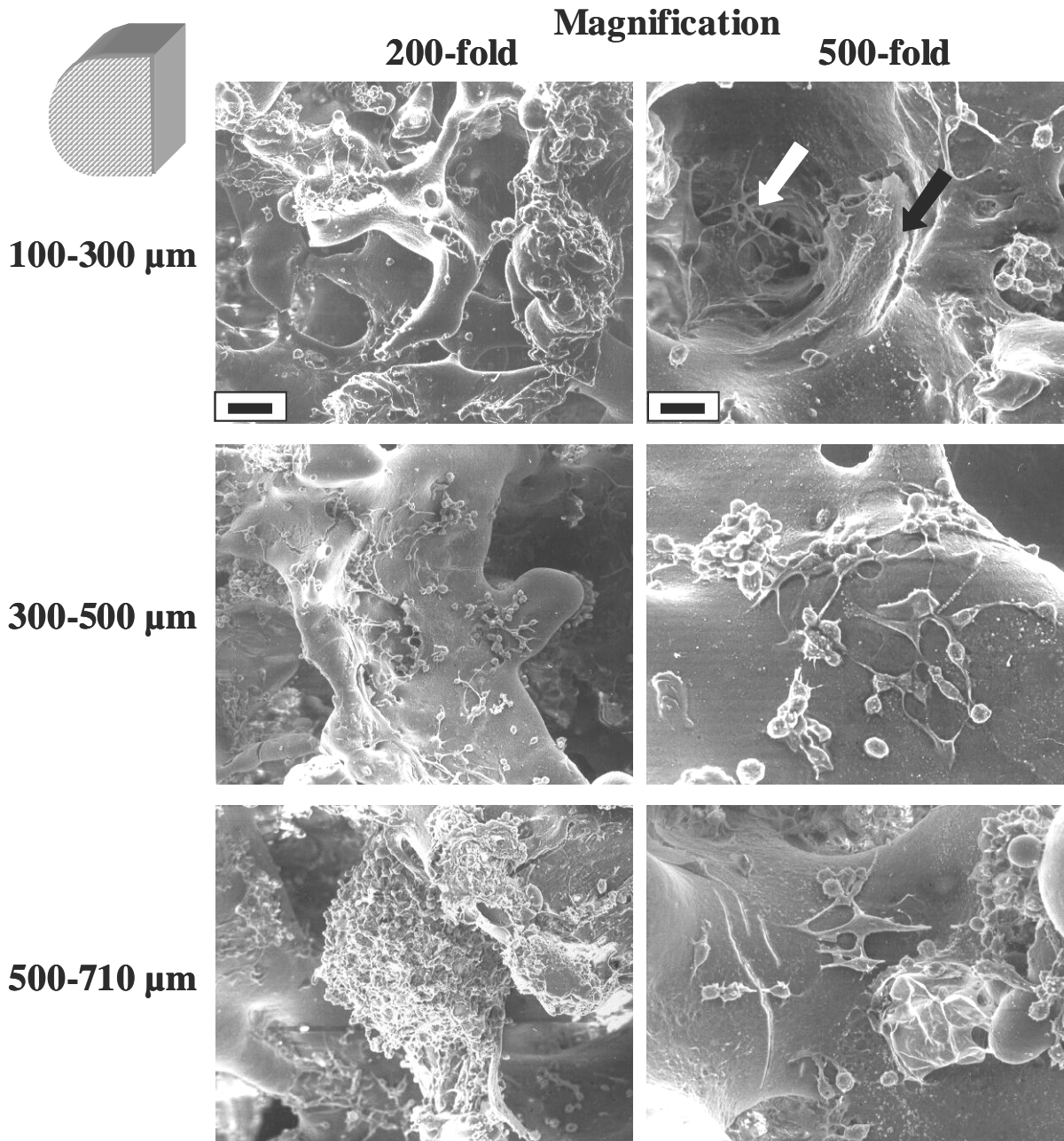


Fig. 4a SEM pictures of MSC-seeded MeO-PEG₂PLA₄₀ scaffolds at the end of the seeding procedure. The surface of the cell-polymer constructs is shown on the photographs. The cartoon shows a half of a scaffold and the striped area marks the observed area, the surface of the scaffolds. Scale bars at 200-fold magnification represent 50 μm and 20 μm at 500-fold magnification, respectively. The black arrow marks a cell-matrix area and the white arrow points to matrix fibrils secreted by MSCs.

However, large cell aggregates were found on scaffolds with 500-710 μm pores. The cell shape and the production of structures considered to be extracellular matrix compounds are recognizable in pictures taken at the high magnification. In all scaffolds, round and unspread as well as flattened and well-spread cells could be seen. Large cell-matrix areas, designated by the black arrow, and matrix fibrils, designated by the white arrow, were exclusively observable on scaffolds with pore sizes from 100 to 300 μm .

Figure 4b gives insights into the interior of the scaffolds. Here, the exact centre of a scaffold is shown at 200-fold and 500-fold magnification. Remarkably, cells could be found in the middle of the scaffolds in all groups. The smallest pore sizes from 100 to 300 μm appeared to be large enough to allow for the penetration of MSCs to the centre of the scaffolds. In regard to cell shape and formation of aggregates, the same tendencies were observed in areas inside the scaffolds at the surface (Fig. 4a,b).

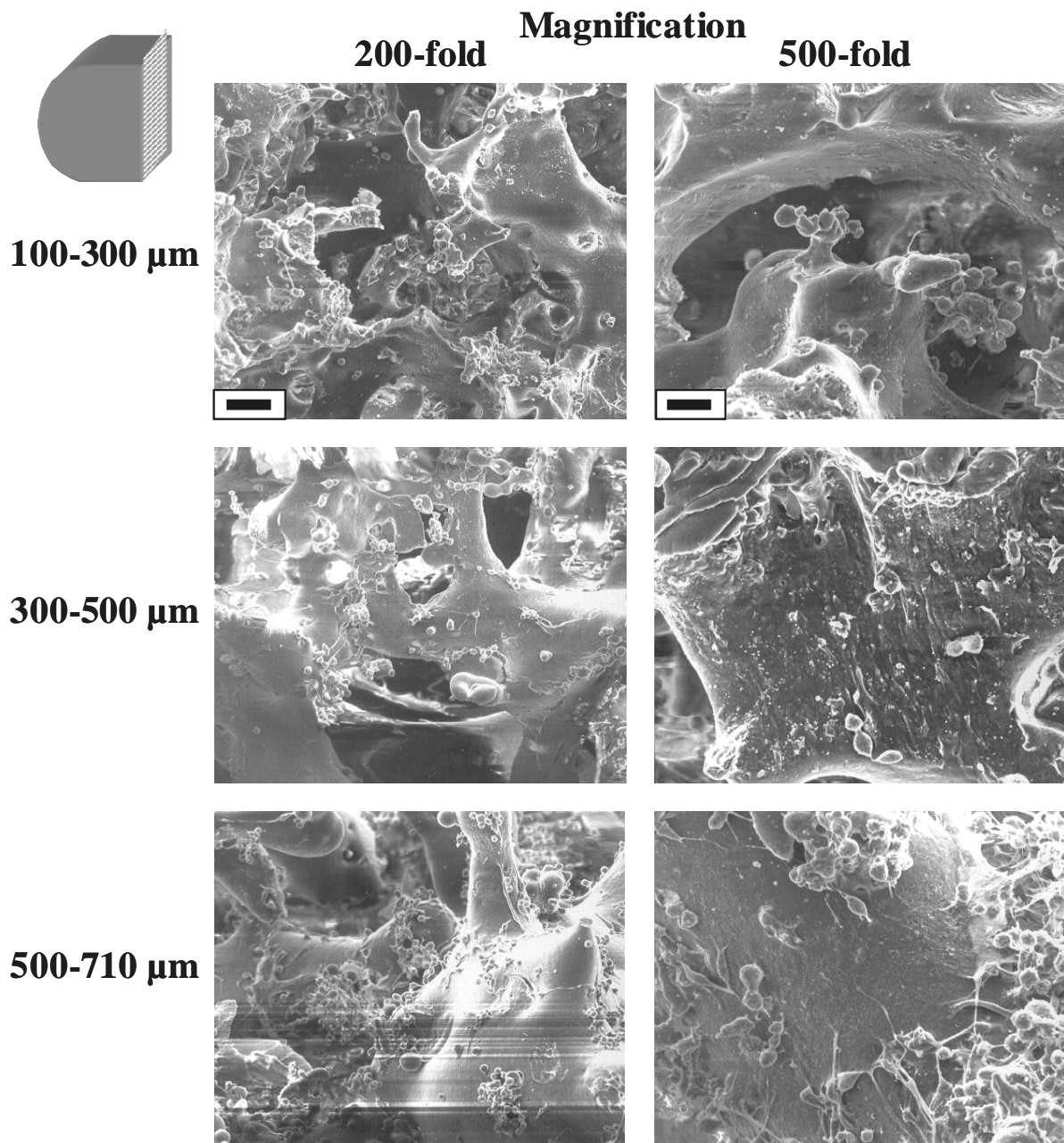


Fig. 4b SEM pictures of MSC-seeded MeO-PEG₂PLA₄₀ scaffolds at the end of the seeding procedure. The inner area of cross-sections of the cell-polymer constructs is shown on the photographs. The cartoon shows a half of a scaffold and the striped area marks the observed area, the interior of a scaffold. Scale bars at 200-fold magnification represent 50 μm, and 20 μm at 500-fold magnification.

Cell number

Beyond the attachment of MSCs onto the scaffolds, the proliferation of MSCs in presence of the mitogenic growth factor basic fibroblast growth factor (bFGF) was investigated. After the seeding procedure, the cell-polymer constructs were cultivated for further 14 days. On day 0, 7, and 14 of the proliferation phase, the total cell number of attached cells was examined by the determination of the total DNA content (Fig. 5).

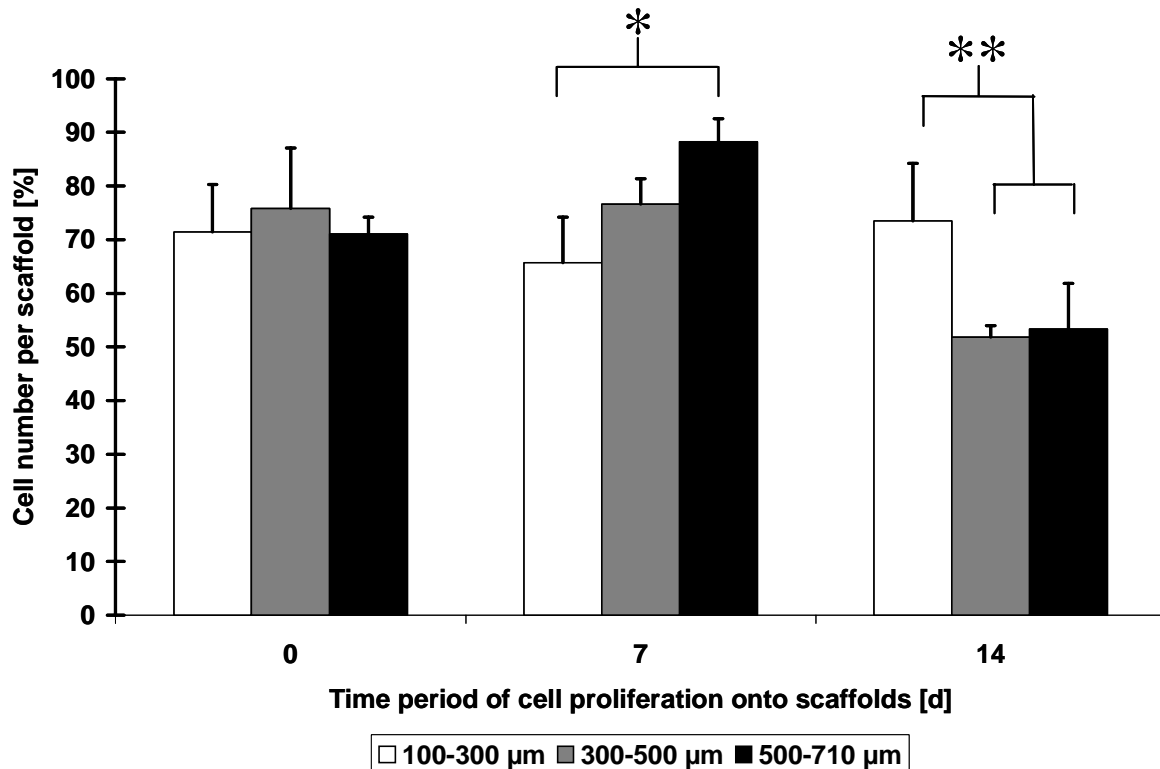


Fig. 5 Determination of the cell number after the three-day seeding procedure (d0), after one week (d7) and after two weeks (d14) of proliferation. Cell number was assessed by measuring the DNA content following enzymatic digestion of the cell-polymer constructs. Values are expressed as mean \pm SD ($n=3$) and are normalized to the initially provided number of MSCs in the cell suspension (2.5 million per scaffold). Statistically significant differences of experimental groups are denoted by * ($p < 0.01$) and ** ($p < 0.05$).

In all groups, a similar number of cells attached to the scaffolds after three days of dynamic cell seeding in spinner flasks, irrespective of the pore sizes. No statistically significant differences were calculated between the different scaffold types at this point of time. About 71% to 76% of initially provided cells in the cell suspension (2.5 million MSCs per scaffold) attached to the scaffolds with various pore sizes. After the proliferation of MSCs for one week, most cells were observed on scaffolds with pores from 500 to 710 μm . A decreased cell number was determined on scaffolds with pores from 300 to 500 μm . The scaffolds with pores from 100 to 300 μm yielded the lowest cell number, significantly different from

scaffolds with 500 to 710 μm pores. However, after two weeks, the highest cell number was determined for scaffolds with 100 to 300 μm large pores. A significantly decreased number of cells was attached to scaffolds with the other pore size ranges. Regarding the course of time, the cell number was not statistically different at all time points on scaffolds with 100 to 300 μm pores. In contrast, the cell number slightly increased on scaffolds with pores sizes ranging from 300 to 500 μm and 500 to 710 μm , respectively, within one week, and strikingly decreased from 77% to 52% and 88% to 53%, respectively, after two weeks. In these groups, a distinctly higher number of cells was attached to the substrate of the well plates as compared to the group with scaffolds with pores from 100 to 300 μm indicating that the MSCs fell off the scaffolds (data not shown).

Discussion

An important requirement for successful cell-based tissue engineering is an uniform distribution of seeded cells throughout the scaffold. High porosity, appropriate pore sizes, and a high interconnectivity of pores facilitate uniform seeding of cells onto scaffolds and subsequently a sufficient supply of cells with oxygen and nutrients as well as the removal of metabolites from the scaffolds [40-42,48].

To date, a wide variety of materials such as tricalcium phosphate, hydroxyapatite, ceramics, hyaluronic acid, titanium, poly(glycolic acid), and collagen as cell carriers for MSCs have been used for tissue engineering approaches towards bone, cartilage, and tendon [25-33]. In this study, we used poly(*D,L*-lactic acid)-*block*-poly(ethylene glycol)-monomethylether, abbreviated as MeO-PEG₂PLA₄₀, as a biomaterial. PEG-PLA polymers have been described to suppress unspecific protein adsorption and cell attachment due to the hydrophilic PEG moiety. By variation of the PEG/PLA ratio, the attachment of MSCs and their differentiation into osteoblasts can be modulated as shown in 2-D cell culture [36]. Lieb et al. demonstrated that MeO-PEG₂PLA₄₀ allowed for a significantly increased MSC attachment as compared to MeO-PEG₅PLA₂₀ and MeO-PEG₅PLA₄₅ derivatives but the cell attachment is strongly suppressed as compared to more lipophilic polymers such as PLA and PLGA [36]. Furthermore, when differentiated towards osteoblasts, MSCs cultivated on MeO-PEG₂PLA₄₀ polymer films increased the mineralization the most, as compared to other PEG-PLA derivatives and the lipophilic polymers [36]. In summary, MeO-PEG₂PLA₄₀ appears to be a suitable polymer for tissue engineering applications since MSCs attach to and proliferate on this polymer to a degree sufficient for the formation of a tissue, thus, the polymer may stimulate the differentiation of MSCs. Hacker et al. developed a process for the manufacture

of scaffolds from the MeO-PEGPLA polymers with a simultaneous polymer preprecipitation and porogen dissolution, designated as solid lipid templating [39]. This scaffold fabrication technique leads to scaffold structures characterized by a high porosity and highly interconnected pores (Fig. 2).

In recently published studies on cell-based adipose tissue engineering, scaffolds with pore sizes from 40 μm to 633 μm have been used. In detail, the pore sizes were: 40 μm [10], 52 μm [5], 50 μm , 50-340 μm , and 100-300 μm [9], 65 and 100 μm [13], 135-633 μm [6,11], and 400 μm [14]. Heimburg et al. stated that an enlargement of the pore size is advantageous since preadipocytes showed a much better differentiation, an improved vascularization, and a more extensive cellular penetration into the sponges with a pore size of 65 and 100 μm respectively, as compared to a pore size of 45 μm [13]. In a further study, hyaluronic acid-based sponges with a pore size of 50-340 μm proved as superior to collagen sponges with a pore size of 50 μm in regard to cellularity [9]. The results of these studies indicate that pore sizes distinctly larger than 50 μm appear to be useful for adipose tissue engineering approaches.

The goal of this study was to assess the potential of scaffolds with different pore sizes for MSC-based tissue engineering approaches. Cell attachment, cellular distribution within the scaffold, and the proliferation of MSCs on the scaffolds was investigated with means of histology, SEM, and cell number determination. The porogen size ranges of the used scaffolds ranged from 100 to 300 μm , 300 to 500 μm , and 500 to 710 μm (Fig. 2).

In summary, all ranges of scaffolds seem to be suitable for tissue engineering applications with regard to the uniform distribution of MSCs throughout the scaffolds (Fig. 3), that is, even the class with the smallest pore sizes (100 to 300 μm) was sufficient for an absolutely uniform cell distribution. In addition, a similar number of MSCs attached to all scaffolds after three days of cell seeding (Fig. 5). These striking observations may be attributed to the high porosity and the high interconnectivity of the pores of the used scaffolds (Fig. 2). Furthermore, the seeding procedure, the dynamic cell seeding of MSCs in spinner flasks, appeared to be appropriate for the combination of MSCs and the used scaffolds.

MSCs seeded onto scaffolds with different pore size ranges adopted cell shapes ranging from absolutely round to well spread, whereby the majority of the cells tend to be round-shaped. This finding is in agreement with the observations in 2-D cell culture experiments using MeO-PEG-PLA polymer films by Lieb et al. [36]. MSCs attached to tissue culture polystyrene in 2-D cell culture exhibited a well-spread and flattened shape. In contrast, MSCs attached to the more hydrophilic PEGPLA polymers were shown to adopt a round shape. This

change of the cell shape was observed to be more pronounced with an increasing ratio of PEG/PLA [36]. Changes of the cell shape might strongly impact the cellular behaviour since it is known that changes in cytoskeletal filament assembly may lead to changes in gene expression and cell function and may lead to the modulation of the MSC differentiation including the adipogenic differentiation [49,50].

A remarkable difference between the experimental groups represents the observed early production of extracellular matrix-like structures in the form of sheets and fibril on scaffolds with pore sizes ranging from 100 to 300 μm (Fig. 4a). The production of matrix is necessary to provide stability and long-term maintenance of the new tissue and to replace the degrading scaffold biomaterial [51]. Furthermore, adipogenic differentiation and adipocyte behaviour are known to be influenced by compounds of the extracellular matrix [52-55]. The adhesion, proliferation, and differentiation of preadipocytes can be modulated in an inhibitory or a stimulatory way depending on the type of the ECM material provided to the cells [53-55]. Furthermore, the production of collagens during the preadipocytic state has been reported to be essential for the terminal adipogenesis of preadipocytes [52].

Unexpectedly, the number of MSCs attached to scaffolds with pore sizes from 300 to 500 μm and from 500 to 710 μm strongly decreased towards the end of the culture (Fig. 5). Living cells fell off the scaffolds with enlarged pore sizes, attached to and proliferated on the culture plastic material (data not shown). In contrast, the cell count was maintained constant on scaffolds with pore sizes from 100 to 300 μm (Fig. 5). With regard to the histology in Fig. 3 and the SEM pictures in Fig. 4a, it is clearly recognizable that cells on the scaffolds with 100 to 300 μm pores were seeded denser than in the other scaffolds and virtually each discrete cell was in contact to the scaffold material. In scaffolds with larger pores, the cells were separated by the wide cavities of the scaffolds and the cells tended to build aggregates, most pronounced in scaffolds with the pore size range 500 to 710 μm . These aggregates reached into the cavity of the scaffolds but a connection to an opposite polymeric scaffold wall is unlikely due to the large pores and thus, the cell aggregates might have fallen off the scaffolds. Apparently, the contrary effects were caused by the probably simultaneously occurring processes: The proliferation of MSCs on the scaffolds led to an elevation of the cell number, whereas the dropping off of the MSCs from the scaffolds decreased the cell number. Probably, the difference of the cell numbers was caused by the difference of the number of MSCs that fell off the scaffolds and there was no difference in the proliferation rate of the MSCs on scaffolds with different pore sizes. An insufficient supply of the MSCs within the scaffolds with nutrients and oxygen which may result in a decreased proliferation of MSCs

appears to be unlikely with regard to the cellular distribution of the cells throughout the scaffolds and the highly interconnected pores (Figs. 2-4). Furthermore, the early production of structures considered to be ECM might have been contributed to the retention of the MSCs on scaffolds with pores from 100 to 300 μm . The cell detachment might have been promoted by the hydrophilic surface of the MeO-PEG₂PLA₄₀ polymer and possibly, the cell detachment would not have occurred on more lipophilic surfaces such as the commonly used materials PLA or PLGA.

In conclusion, scaffolds made from MeO-PEG₂PLA₄₀ seem to be suitable for tissue engineering applications based on MSCs. All ranges of pore sizes allowed for a uniform cellular distribution throughout the entire scaffold. Scaffolds with pore sizes from 100 to 300 μm appeared to be advantageous in comparison to scaffolds with pores from 300 to 500 μm and from 500 to 710 μm , respectively, in regard to cell proliferation and early production of extracellular matrix components.

As a future perspective, this study may provide useful data for the application of biomimetic derivatives of the MeO-PEG₂PLA₄₀ to which peptides and proteins can be covalently bound to in order to control the cellular behaviour. Scaffolds with pore sizes from 100 to 300 μm made from the biomimetic derivatives utilizing the solid lipid templating were used in the study presented in chapter 9 of this thesis.

References

- [1] Katz AJ, Llull R, Hedrick MH, Futrell JW. 'Emerging approaches to the tissue engineering of fat'. *Clin Plast Surg* (1999); **26**: 587-603.
- [2] Patrick CW, Jr. 'Tissue engineering strategies for adipose tissue repair'. *Anat Rec* (2001); **263**: 361-366.
- [3] Beahm EK, Walton RL, Patrick CW, Jr. 'Progress in adipose tissue construct development'. *Clin Plast Surg* (2003); **30**: 547-58.
- [4] Langer R, Vacanti JP. 'Tissue engineering'. *Science* (1993); **260**: 920-926.
- [5] Kral JG, Crandall DL. 'Development of a human adipocyte synthetic polymer scaffold'. *Plast Reconstr Surg* (1999); **104**: 1732-1738.
- [6] Patrick CW, Jr., Chauvin PB, Hobbey J, Reece GP. 'Preadipocyte seeded PLGA scaffolds for adipose tissue engineering'. *Tissue Eng* (2001); **5**: 139-151.
- [7] Huss FR, Kratz G. 'Mammary epithelial cell and adipocyte co-culture in a 3-D matrix: the first step towards tissue-engineered human breast tissue'. *Cells Tissues Organs* (2001); **169**: 361-367.
- [8] Schoeller T, Lille S, Wechselberger G, Otto A, Mowlawi A, Piza-Katzer H. 'Histomorphologic and volumetric analysis of implanted autologous preadipocyte cultures suspended in fibrin glue: a potential new source for tissue augmentation'. *Aesthetic Plast Surg* (2001); **25**: 57-63.
- [9] von Heimburg D, Zachariah S, Low A, Pallua N. 'Influence of different biodegradable carriers on the *in vivo* behavior of human adipose precursor cells'. *Plast Reconstr Surg* (2001); **108**: 411-420.
- [10] von Heimburg D, Zachariah S, Kuhling H, Heschel I, Schoof H, Hafemann B, Pallua N. 'Human preadipocytes seeded on freeze-dried collagen scaffolds investigated *in vitro* and *in vivo*'. *Biomaterials* (2001); **22**: 429-438.
- [11] Patrick CW, Jr., Zheng B, Johnston C, Reece GP. 'Long-term implantation of preadipocyte-seeded PLGA scaffolds'. *Tissue Eng* (2002); **8**: 283-293.
- [12] Halberstadt C, Austin C, Rowley J, Culberson C, Loeb sack A, Wyatt S, Coleman S, Blacksten L, Burg K, Mooney et a. 'A hydrogel material for plastic and reconstructive applications injected into the subcutaneous space of a sheep'. *Tissue Eng* (2002); **8**: 309-319.
- [13] von Heimburg D, Kuberka M, Rendchen R, Hemmrich K, Rau G, Pallua N. 'Preadipocyte-loaded collagen scaffolds with enlarged pore size for improved soft tissue engineering'. *Int J Artif Organs* (2003); **26**: 1064-1076.

- [14] Halbleib M, Skurk T, de Luca C, von Heimburg D, Hauner H. 'Tissue engineering of white adipose tissue using hyaluronic acid-based scaffolds. I: *in vitro* differentiation of human adipocyte precursor cells on scaffolds'. *Biomaterials* (2003); **24**: 3125-3132.
- [15] Fischbach C, Spruss T, Weiser B, Neubauer M, Becker C, Hacker M, Gopferich A, Blunk T. 'Generation of mature fat pads *in vitro* and *in vivo* utilizing 3-D long-term culture of 3T3-L1 preadipocytes'. *Exp Cell Res* (2004); **300**: 54-64.
- [16] Fischbach C, Seufert J, Staiger H, Hacker M, Neubauer M, Gopferich A, Blunk T. 'Three-dimensional *in vitro* model of adipogenesis: Comparison of culture conditions'. *Tissue Eng* (2004); **10**: 215-229.
- [17] Heath CA. 'Cells for tissue engineering'. *Trends Biotechnol* (2000); **18**: 17-19.
- [18] Prockop DJ. 'Marrow stromal cells as stem cells for nonhematopoietic tissues'. *Science* (2001); **276**: 71-74.
- [19] Bianco P, Gehron Robey P. 'Marrow stromal stem cells'. *J Clin Invest* (2000); **105**: 1663-1668.
- [20] Caplan AI, Bruder SP. 'Mesenchymal stem cells: building blocks for molecular medicine in the 21st century'. *Trends Mol Med* (2001); **7**: 259-264.
- [21] Minguell JJ, Erices A, Conget P. 'Mesenchymal stem cells'. *Exp Biol Med* (2001); **226**: 507-520.
- [22] Haynesworth SE, Reuben D, Caplan AI. 'Cell-based tissue engineering therapies: the influence of whole body physiology'. *Adv Drug Deliv Rev* (1998); **33**: 3-14.
- [23] Ringe J, Kaps C, Burmester GR, Sittinger M. 'Stem cells for regenerative medicine: advances in the engineering of tissues and organs'. *Naturwissenschaften* (2002); **89**: 338-351.
- [24] Pittenger MF, Mackay AM, Beck SC, Jaiswal RK, Douglas R, Mosca JD, Moorman MA, Simonetti DW, Craig S, Marshak DR. 'Multilineage potential of adult human mesenchymal stem cells'. *Science* (1999); **284**: 143-147.
- [25] Boo JS, Yamada Y, Okazaki Y, Hibino Y, Okada K, Hata KI, Yoshikawa T, Sugiura Y, Ueda M. 'Tissue-engineered bone using mesenchymal stem cells and a biodegradable scaffold'. *J Craniofac Surg* (2002); **13**: 231-239.
- [26] Bruder SP, Kurth AA, Shea M, Hayes WC, Jaiswal N, Kadiyala S. 'Bone regeneration by implantation of purified, culture-expanded human mesenchymal stem cells'. *J Orthop Res* (1998); **16**: 155-162.
- [27] Lisignoli G, Zini N, Remiddi G, Piacentini A, Puggioli A, Trimarchi C, Fini M, Maraldi NM, Facchini A. 'Basic fibroblast growth factor enhances *in vitro* mineralization of rat bone

marrow stromal cells grown on non-woven hyaluronic acid based polymer scaffold'. *Biomaterials* (2001); **22**: 2095-2105.

[28] Lisignoli G, Fini M, Giavaresi G, Nicoli AN, Toneguzzi S, Facchini A. 'Osteogenesis of large segmental radius defects enhanced by basic fibroblast growth factor activated bone marrow stromal cells grown on non-woven hyaluronic acid-based polymer scaffold'. *Biomaterials* (2002); **23**: 1043-1051.

[29] Quarto R, Mastrogiacomo M, Cancedda R, Kutepov SM, Mukhachev V, Lavroukov A, Kon E, Marcacci M. 'Repair of large bone defects with the use of autologous bone marrow stromal cells'. *N Engl J Med* (2001); **344**: 385-386.

[30] van den Dolder J, Farber E, Spauwen PHM, Jansen JA. 'Bone tissue reconstruction using titanium fiber mesh combined with rat bone marrow stromal cells'. *Biomaterials* (2003); **24**: 1745-1750.

[31] Johnstone B, Hering TM, Caplan AI, Goldberg VM, Yoo JU. '*In vitro* chondrogenesis of bone marrow-derived mesenchymal progenitor cells'. *Exp Cell Res* (1998); **238**: 265-272.

[32] Martin I, Padera RF, Vunjak-Novakovic G, Freed LE. 'In vitro differentiation of chick embryo bone marrow stromal cells into cartilaginous and bone-like tissues'. *J Orthop Res* (1998); **16**: 181-189.

[33] Young RG, Butler DL, Weber W, Caplan AI, Gordon SL, Fink DJ. 'Use of mesenchymal stem cells in a collagen matrix for Achilles tendon repair'. *J Orthop Res* (1998); **16**: 406-413.

[34] Lucke A, Te, Schnell E, Schmeer G, Gopferich A. 'Biodegradable poly(-lactic acid)-poly(ethylene glycol)-monomethyl ether diblock copolymers: structures and surface properties relevant to their use as biomaterials'. *Biomaterials* (2000); **21**: 2361-2370.

[35] Lucke A, Fustella E, Tessmar J, Gazzaniga A, Gopferich A. 'The effect of poly(ethylene glycol)-poly(D,L-lactic acid) diblock copolymers on peptide acylation'. *J Control Release* (2002); **80**: 157-168.

[36] Lieb E, Tessmar J, Hacker M, Fischbach C, Rose D, Blunk T, Mikos AG, Gopferich A, Schulz MB. 'Poly(D,L-lactic acid)-poly(ethylene glycol)-monomethyl ether diblock copolymers control adhesion and osteoblastic differentiation of marrow stromal cells'. *Tissue Eng* (2003); **9**: 71-84.

[37] Tessmar JK, Mikos AG, Gopferich A. 'Amine-reactive biodegradable diblock copolymers'. *Biomacromolecules* (2002); **3**: 194-200.

[38] Tessmar J, Mikos A, Gopferich A. 'The use of poly(ethylene glycol)-block-poly(lactic acid) derived copolymers for the rapid creation of biomimetic surfaces'. *Biomaterials* (2003); **24**: 4475-4486.

- [39] Hacker M, Tessmar J, Neubauer M, Blaimer A, Blunk T, Gopferich A, Schulz MB. 'Towards biomimetic scaffolds: Anhydrous scaffold fabrication from biodegradable amine-reactive diblock copolymers'. *Biomaterials* (2003); **24**: 4459-4473.
- [40] Liu X, Ma P, X. 'Polymeric scaffolds for bone tissue engineering'. *Ann Biomed Eng* (2004); **32**: 477-486.
- [41] Hutmacher DW. 'Scaffold design and fabrication technologies for engineering tissues. State of the art and future perspectives'. *J Biomat Sci Polym Ed* (2001); **12**: 107-124.
- [42] Yang S, Leong KF, Du Z, Chua CK. 'The design of scaffolds for use in tissue engineering. Part I. Traditional factors'. *Tissue Eng* (2001); **7**: 679-689.
- [43] Ishaug SL, Crane GM, Miller MJ, Yasko AW, Yaszemski MJ, Mikos AG. 'Bone formation by three-dimensional stromal osteoblast culture in biodegradable polymer scaffolds'. *J Biomed Mater Res* (1997); **36**: 17-28.
- [44] Butterwith SC, Peddie CD, Goddard C. 'Regulation of adipocyte precursor DNA synthesis by acidic and basic fibroblast growth factors: Interaction with heparin and other growth factors'. *J Endocrinol* (1993); **137**: 369-374.
- [45] Gospodarowicz D, Ferrara N, Schweigerer L, Neufeld G. 'Structural characterization and biological functions of fibroblast growth factor'. *Endocr Rev* (1987); **8**: 95-114.
- [46] van den Bos C, Mosca JD, Winkles J, Kerrigan L, Burgess WH, Marshak DR. 'Human mesenchymal stem cells respond to fibroblast growth factors'. *Hum Cell* (2002); **10**: 45-50.
- [47] Kim YJ, Sah RL, Doong JY, Grodzinsky AJ. 'Fluorometric assay of DNA in cartilage explants using Hoechst 33258'. *Anal Biochem* (1988); **174**: 168-176.
- [48] Vats A, Tolley NS, Polak JM, Gough JE. 'Scaffolds and biomaterials for tissue engineering: a review of clinical applications'. *Clin Otolaryngol* (2003); **28**: 165-172.
- [49] Mooney DJ, Langer R, Ingber DE. 'Cytoskeletal filament assembly and the control of cell spreading and function by extracellular matrix'. *J Cell Sci* (1995); **108**: 2311-2316.
- [50] McBeath R, Pirone DM, Nelson CM, Bhadriraju K, Chen CS. 'Cell shape, cytoskeletal tension, and RhoA regulate stem cell lineage commitment'. *Dev Cell* (2004); **6**: 483-495.
- [51] Bonassar LJ, Vacanti CA. 'Tissue engineering: the first decade and beyond'. *J Cell Biochem* (1998); **Suppl. 30/31**: 297-303.
- [52] Ibrahimi A, Bonino F, Bardon S, Ailhaud G, Dani C. 'Essential role of collagens for terminal differentiation of preadipocytes'. *Biochem Biophys Res Commun* (1992); **187**: 1314-1322.

[53] Hausman GJ, Wright JT, Richardson RL. 'The influence of extracellular matrix substrata on preadipocyte development in serum-free cultures of stromal-vascular cells'. *J Anim Sci* (1996); **74**: 2117-2128.

[54] Nakajima I, Yamaguchi T, Ozutsumi K, Aso H. 'Adipose tissue extracellular matrix: newly organized by adipocytes during differentiation'. *Differentiation* (1998); **63**: 193-200.

[55] Patrick CW, Jr., Wu X. 'Integrin-mediated preadipocyte adhesion and migration on laminin-1'. *Ann Biomed Eng* (2003); **31**: 505-514.

Chapter 7

Adipose Tissue Engineering Based on Mesenchymal Stem Cells and Basic Fibroblast Growth Factor *in vitro*

Markus Neubauer, Michael Hacker, Petra Bauer-Kreisel, Barbara Weiser, Claudia Fischbach,
Michaela B Schulz, Achim Goepferich, Torsten Blunk

Department of Pharmaceutical Technology, University of Regensburg, Universitaetsstrasse
31, D-93040 Regensburg, Germany

submitted to Tissue Engineering

Abstract

Despite the clinical need for reconstructive and plastic surgery, the supply with engineered adipose tissue equivalents still remains a challenge. As yet, preadipocytes have exclusively been applied as a cell material for the tissue engineering of fat. Herein, we report the establishment of a 3-D long-term cell culture using bone marrow-derived mesenchymal stem cells (MSCs) as an alternative cell source and custom-made poly(lactic-co-glycolic)acid (PLGA) scaffolds as a cell carrier. Cell-polymer constructs were cultivated for four weeks in both the absence and presence of basic fibroblast growth factor (bFGF), which was previously shown to strongly enhance adipogenesis of MSCs in conventional 2-D short-term culture. A striking enhancement of the adipogenic differentiation of MSCs and tissue development caused by bFGF in the 3-D culture was observed by osmium tetroxide histology and scanning electron microscopy. On the molecular level, reflecting the increased accumulation of lipids, bFGF increased the enzymatic activity of GPDH, a late marker of adipogenesis, and the expression of the adipocyte-specific genes PPAR γ 2 and GLUT4, as assessed by RT-PCR. This study demonstrates that MSCs, especially in combination with bFGF, may represent a promising approach to adipose tissue engineering.

Introduction

Despite the continuously increasing clinical demand [1], at present, an optimum strategy for the regeneration and replacement of adipose tissue remains elusive [2-4]. Adipose tissue is required in reconstructive, cosmetic, and correctional surgery. Indications for adipose tissue include, for instance, therapies following oncological resections and complex traumata or augmentative surgery of the breast, cheek, chin, or lips [4].

Even though fat functions as a natural filling material, autologous adipose tissue remains minimally effective due to insufficient neovascularization and resultant unpredictable shrinkage of the fat graft. Injection of single cell suspensions of mature adipocytes does not represent an alternative method, because exposure of the fragile adipocytes to the mechanical forces of liposuction results in about 90% traumatized adipocytes [5].

Recently, promising new therapy strategies based on tissue engineering techniques that combine *de novo* adipogenesis and cell-based therapeutic approaches have been developed. *De novo* adipogenesis has been induced by injection of Matrigel and basic fibroblast growth factor (bFGF) [6-8] or long-term local delivery of insulin and insulin-like growth factor-I by poly(lactic-co-glycolic) (PLGA)/polyethyleneglycol (PEG) microspheres [9]. To date, only preadipocytes have been used as a cell source for cell-based strategies, although in combination with cell carriers made from a wide range of materials. Primary preadipocytes or preadipocytic cell lines have been cultivated on porous scaffolds made from synthetic, protein-coated polytetrafluoroethylene [10], synthetic, biodegradable PLGA [11] and polyglycolic acid [12,13]. Furthermore, collagen [14-16] and hyaluronic acid-based scaffolds [14,17] have been shown to function as suitable carriers for preadipocytes. Additionally, recent studies using preadipocytes examined the potential of hydrogel materials for adipose tissue engineering including collagen gels [18], alginate and RGD-modified alginate gels [19], and fibrin glue [20].

Stem cells derived from adult bone marrow, also referred to as mesenchymal stem cells (MSCs), represent a promising alternative cell source for soft tissue engineering [21-24]. The use of MSCs may circumvent some major drawbacks associated with mature adipocytes and precursor cells, i.e., MSCs can be easily isolated and MSCs possess the capacity of a billionfold expansion [21]. Due to their multipotent differentiation capacity [21], MSCs have been applied in many tissue engineering approaches, e.g., in the field of bone [25-30], cartilage [31,32], and tendon [33] regeneration *in vitro* and *in vivo*. However, no study on tissue engineered fat exists using MSCs.

Therefore, the overall aim of this study was to demonstrate, for the first time, the potential of MSCs for the application in adipose tissue engineering. MSCs were seeded on custom-made PLGA scaffolds with a pore size from 100 to 300 μm fabricated using a solid lipid templating technique [34]. Recently, in 2-D cell culture over eight days, we demonstrated a strong enhancement of hormonally induced adipogenesis of MSCs after exposure to bFGF [35]. This study aimed at (a) the transfer of the established adipogenic protocol including the application of bFGF from 2-D to 3-D long-term cell culture, (b) an efficient adipogenic differentiation of MSCs and subsequent maturation, and (c) a characterization of the differentiation processes on the histological and molecular level. Therefore, MSCs were cultivated in both the absence and presence of bFGF over four weeks in 3-D cell culture applying a repeated hormonal induction regimen.

Materials and Methods

Materials

If not otherwise stated, chemicals were obtained from Sigma (Steinheim, Germany). Basic FGF was obtained from PeproTec (Rocky Hill, NJ, USA). Insulin was kindly provided by Hoechst Marion Roussel (Frankfurt am Main, Germany). Cell culture plastics were purchased from Corning Costar (Bodenheim, Germany). Poly(lactic-co-glycolic acid) (PLGA 75:25; approx. 90 kD) was obtained from Boehringer Ingelheim (Ingelheim am Rhein, Germany). Spinner flasks were self-made (250 ml volume, 6 cm bottom diameter, side arms for gas exchange). Silicon stoppers were obtained from Schuber & Weiss (München, Germany); needles were from Unimed (Lausanne, Switzerland).

Scaffold fabrication

Scaffolds were fabricated using a protocol adapted from Hacker et al [34]. Briefly, 0.80 g of PLGA (75:25) polymer was weighed in a glass vial and dissolved in 2.70 ml ethylacetate. 3.20 g of lipid microparticles made from Softisan[®] 154 and Witepsol[®] H42 (ratio 2:1; kindly provided by SASOL Germany (Witten, Germany)) were weighed in a separate vial. The size of porogen particles ranged from 100 μm to 300 μm . After cooling for 1 h at -20°C , the porogen particles were transferred into the polymer solution and mixed for 5 min on ice. The resulting highly viscous dispersion was then transferred into a 10 ml polypropylene syringe and injected into eight cubic Teflon[®] molds with a cylindrical cavity of 0.8 cm in diameter. After a pre-extraction treatment step in n-hexane at 0°C for 15 min, the filled molds were submerged in warm n-hexane to concurrently precipitate the polymer and extract the porogen

particles. This procedure was carried out in two separate n-hexane baths of different temperatures: 52°C for 10 min followed by 40°C for 20 min. Subsequently, the molds were transferred into an n-hexane bath of 0°C for 5 min. Finally, the porous cylindrical polymer constructs were removed from the molds and vacuum-dried for 48 h. For further investigations, the constructs were cut into 2 mm slices, which were then termed scaffolds.

Cell isolation and expansion

Marrow stromal cells were obtained from six-week old male Sprague Dawley rats (weight: 170 - 180 g, Charles River, Sulzfeld, Germany). MSCs were flushed from the tibiae and femora according to an established protocol published by Ishaug [36]. Cells were centrifuged at 1200 rpm for 5 min. The resulting cell pellet was resuspended in basal medium (DMEM (Biochrom, Berlin, Germany), 10 % fetal bovine serum (Gemini Bio-Products, Calabasas, CA, USA), 1 % penicillin/streptomycin (Invitrogen, Karlsruhe, Germany), 50 µg/ml ascorbic acid) and seeded in T75 flasks. Cells were cultured in an incubator (37°C, 5% CO₂) and were allowed to adhere to the substratum for three days. The flasks were rinsed twice with phosphate-buffered saline (PBS, Invitrogen, Karlsruhe, Germany) to remove non-adherent cells. 12 ml of basal medium, either with or without 3 ng/ml bFGF, were then exchanged every 2-3 days. After confluence was reached, cells were detached with 0.25 % trypsin and EDTA (Invitrogen, Karlsruhe, Germany), centrifuged and resuspended in basal medium. The cell number of the obtained cell suspension was determined using a hemocytometer; the cell suspension was used for seeding onto the polymer scaffolds (see below).

3-D cell culture

PLGA scaffolds were pre-wet with 70% ethanol and rinsed extensively with PBS. Scaffolds were strung onto needles (10 cm long, 0.5 mm diameter) and secured with segments of silicone tubing (1 mm long). Four needles with two scaffolds each were inserted into a silicone stopper; the stopper was in turn placed into the mouth of a spinner flask. A magnetic stir bar was placed at the bottom of the spinner flask. The spinner flasks were filled with 100 ml basal medium and placed on a magnetic stir plate (Bellco 10 Glas, Vineland, NJ, USA) at 80 rpm in an incubator (37°C, 5% CO₂). After 24 h, the medium was aspirated and the flask was filled with a cell suspension containing three million cells per scaffold in 100 ml of basal medium. Stirring for three days at 80 rpm allowed for cell attachment to the scaffold. Subsequently, the cell-polymer constructs were transferred into six-well plates containing one scaffold and 5 ml medium per well. From this point in time, cells which had been cultured with bFGF during the proliferation phase in 2-D culture again received bFGF treatment (3

ng/ml) for the entire 3-D culture (including adipogenic induction and maintenance); cells which had been cultured without bFGF during proliferation (2-D) still did not receive any bFGF during 3-D culture. Constructs from both groups (with or without bFGF) were cultivated in six-well plates on an orbital shaker at 50 rpm (Dunn Labortechnik, Asbach, Germany) until they were harvested. Three days after the transfer into six-well plates, adipogenesis was induced by adding the induction medium (a hormonal cocktail containing 0.5 mM 3-isobutyl-1-methylxanthine (IBMX) (Serva Electrophoresis, Heidelberg, Germany), 10 nM dexamethasone, 60 μ M indomethacin, and 10 μ g/ml insulin in basal medium); this point of time was referred to as day 0. After three days (day 3), cells were exposed to an adipogenic maintenance medium consisting of basal medium supplemented with 10 μ g/ml insulin. On day 7, cell-polymer constructs were either harvested and designated as “1 week” or underwent the alternate treatment with induction (for three days each) and maintenance medium (for four days each) a second (“2 weeks”), a third (“3 weeks”), and a fourth time (“4 weeks”) (Fig. 1).

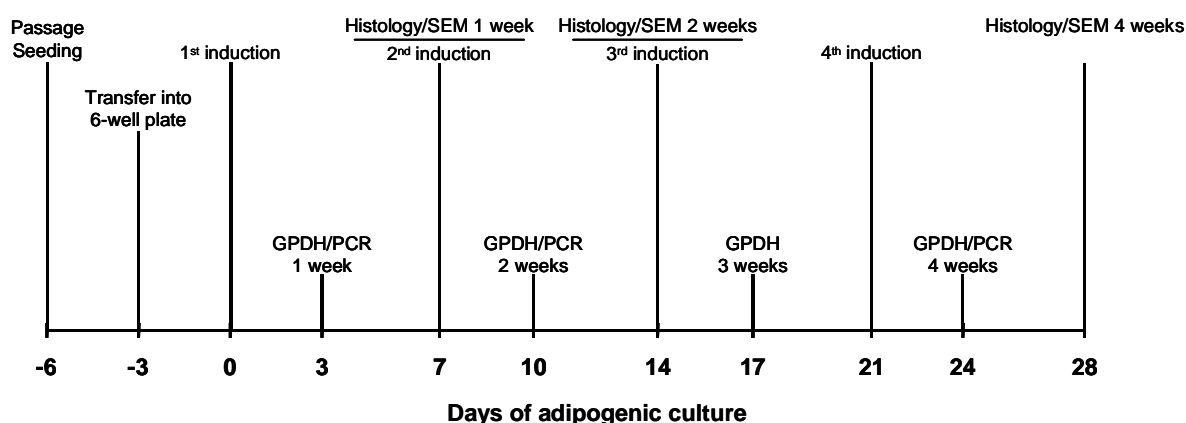


Fig. 1 Time course of adipogenic 3-D cell culture: MSCs were seeded onto scaffolds for three days, followed by a three days lasting proliferation period. Subsequently, cell-polymer constructs were induced weekly, i.e. MSCs were exposed to adipogenic inducer cocktail for three days (on day 0, 7, 14, and 21) and were allowed to differentiate for four more days (on day 3, 10, 17, and 24). The day of the first induction is designated as day 0 of adipogenic culture. Constructs were harvested three days after every induction for GPDH and PCR analysis and eight days after every induction for histology and SEM.

In a previous study investigating the adipogenic differentiation of MSCs in 2-D culture, bFGF was demonstrated to strongly enhance adipogenesis [35]. The application of bFGF over different culture periods led to varying degrees of enhancement, with the largest effect seen when bFGF was applied throughout the entire culture period (proliferation, induction and maintenance of adipogenesis). Therefore, for this study (3-D culture), only the group that

received bFGF throughout the entire culture period (maximum effect in 2-D culture) was compared to a control group receiving no bFGF at all.

The number of MSCs attached to the scaffold after the cell seeding procedure was determined fluorometrically by measuring the amount of DNA using Hoechst 33258 dye (Polysciences, Warrington, PA, USA) [37].

Osmium tetroxide (OsO₄) staining

Lipid staining with OsO₄ was performed by adapting a previously published protocol [38]. After one, two and four weeks of adipogenic culture (Fig. 1), cell-polymer constructs were washed once with PBS and pre-fixed with 2.5% glutaraldehyde in PBS for 15 min and subsequently stored in 10% formaldehyde (Merck, Darmstadt, Germany) in PBS. In order to crosslink intracellular lipids, cell-polymer constructs were covered with a 1% aqueous OsO₄ solution (Carl Roth, Karlsruhe, Germany) for 1 h on ice. Excess OsO₄ was removed with extensive washing with bidistilled water and cells were again fixed with 10% formaldehyde. Tissue constructs were dehydrated and embedded in paraffin. Deparaffinized sections (5 μm) were counterstained with hematoxylin and eosin (H&E). Photographs were taken on a Zeiss Axiovert 200M microscope coupled to a Zeiss LSM 510 scanning device (Zeiss, Jena, Germany). Photographs at 400-fold magnification were obtained with an oil immersion technique using Immersol 518F (Zeiss, Oberkochen, Germany)

Scanning electron microscopy (SEM)

After one, two and four weeks of adipogenic culture (Fig. 1), cell-polymer constructs were pre-fixed for 15 min with 2.5% glutaraldehyde in PBS and stored in 10% formaldehyde. Constructs were then crosslinked for 30 min with 1% osmium tetroxide. After extensive rinsing and freezing at -80°C, samples were subjected to lyophilization (Christ Beta 2-16, Martin Christ Gefriertrocknungsanlagen, Osterode am Harz, Germany). Samples were glued onto aluminum stubs using conductive carbon tape. Thereafter, cell-polymer constructs were coated with gold-palladium (Polaron SC515, Fisons surface systems, Grinstead, UK). All micrographs were taken at 10 kV on a DSM 950 (Zeiss, Oberkochen, Germany).

Glycerol-3-phosphate dehydrogenase (GPDH) activity assay

GPDH activity was measured using a protocol adapted from Pairault and Green [39]. Cell-polymer constructs were harvested weekly three days after each induction and denoted as “1 week” (harvest on day 3), “2 weeks” (harvest on day 10), “3 weeks” (harvest on day 17), and “4 weeks” (harvest on day 24) (Fig. 1). In preliminary experiments employing MSCs, the

maximum GPDH activity was obtained three days after induction, as assessed by kinetic measurements (data not shown). In brief, cell-polymer constructs washed with PBS were cut and put in lysis buffer containing 50 mM Tris, 1 mM EDTA, and 1 mM β -mercaptoethanol on ice. The resulting suspension was subsequently sonicated with a digital sonifier (Branson Ultrasonic Corporation, Danburg, CT, USA). Cell lysates were centrifuged for 5 min at 13,200 rpm at 4°C. Aliquots of the supernatant were mixed with a solution containing 0.1 M triethanolamine, 2.5 mM EDTA, 0.5 mM β -mercaptoethanol, 120 μ M reduced nicotinamide adenine dinucleotide (NADH) (Roche, Mannheim, Germany), and 200 μ M dihydroxyacetonephosphate. Enzyme activity was monitored by measurement of the disappearance of NADH at 340 nm over 4.2 min. Enzyme activity was normalized to the protein content of each sample. Proteins were determined by the method of Lowry et al. [40]. Proteins were precipitated using 12% trichloroacetic acid. In alkaline solution, the proteins were solubilized and complexed with a mixture of disodium tartrate, copper sulfate and folin-ciocalteu reagent (all from Merck, Darmstadt, Germany). Absorption was measured at 546 nm after a 30 min incubation.

Reverse transcription-polymerase chain reaction (RT-PCR)

Cell-polymer constructs were harvested weekly three days after each induction and denoted as “1 week” (harvest on day 3), “2 weeks” (harvest on day 10), and “4 weeks” (harvest on day 24) (Fig. 1). In previous experiments in 2-D culture, gene expression levels of investigated genes reached their maxima three days after induction, as assessed by kinetic measurements (data not shown). Total RNA was harvested from the cells with Trizol reagent (Invitrogen, Karlsruhe, Germany) and isolated according to the manufacturer’s instructions. First-strand cDNA was synthesized from total RNA by using random hexamers (Roche Diagnostics, Mannheim, Germany) and Superscript II RNase H Reverse Transcriptase (Invitrogen, Karlsruhe, Germany). Samples were incubated at 42°C for 50 min and heated afterwards at 70°C for 15 min to inactivate the enzyme. Subsequently, PCR was performed with Sawady Taq-DNA-Polymerase (PeqLab, Erlangen, Germany); initial denaturation occurred at 94°C for 120 sec, final extension at 72°C for 30 sec for each set of primers. The amplification was carried out using the following specific oligonucleotides:

PPAR γ 2: 5'-GAGCATGGTGCCTTCGCTGA-3'/5'-AGCAAGGCACTTCTGAAACCGA-3'

GLUT4: 5'-AGCAGCTCTCAGGCATCAAT-3'/5'-CTCAAAGAAGGCCACAAAGC-3'

18S: 5'-TCAAGAACGAAAGTCGGAGGTTTCG-3'/5'-TTATTGCTCAATCTCGGGTGGCTG-3'

18S rRNA served as control. Appropriate conditions for the investigated genes were: 94°C for 45 s, 62°C for 45 s, 72°C for 1 min (36 cycles) for PPAR γ 2; 94°C for 45 sec, 56 °C for 45 sec, 72°C for 1 min (32 cycles) for GLUT4; and 94°C for 30 sec, 56°C for 45 sec, 72°C for 1 min (25 cycles) for 18s rRNA. Reverse transcription and PCR were performed using a Mastercycler Gradient (Eppendorf AG, Hamburg, Germany). The PCR products were analyzed by electrophoresis on 2% agarose gels stained with ethidium bromide. Finally, the gels were subjected to imaging of the resultant bands under UV light ($\lambda = 312$ nm) using a Kodak EDAS 290 (Fisher Scientific, Schwerte, Germany).

Statistics

GPDH data are expressed as means \pm standard deviation. Single-factor analysis of variance (ANOVA) was used in conjunction with a multiple comparison test (Tukey's test).

Results

Scaffold material and cell seeding

The scaffolds, fabricated from PLGA by a solid lipid templating technique [34] exhibited a structure characterized by a high porosity and a highly interconnected network of pores (pore size 100-300 μm) (Fig. 2). Three million cells per scaffold were used in the dynamic seeding process in spinner flasks. During the three day seeding period, $70.3\pm 8.0\%$ of the cells attached to the scaffolds (data not shown).

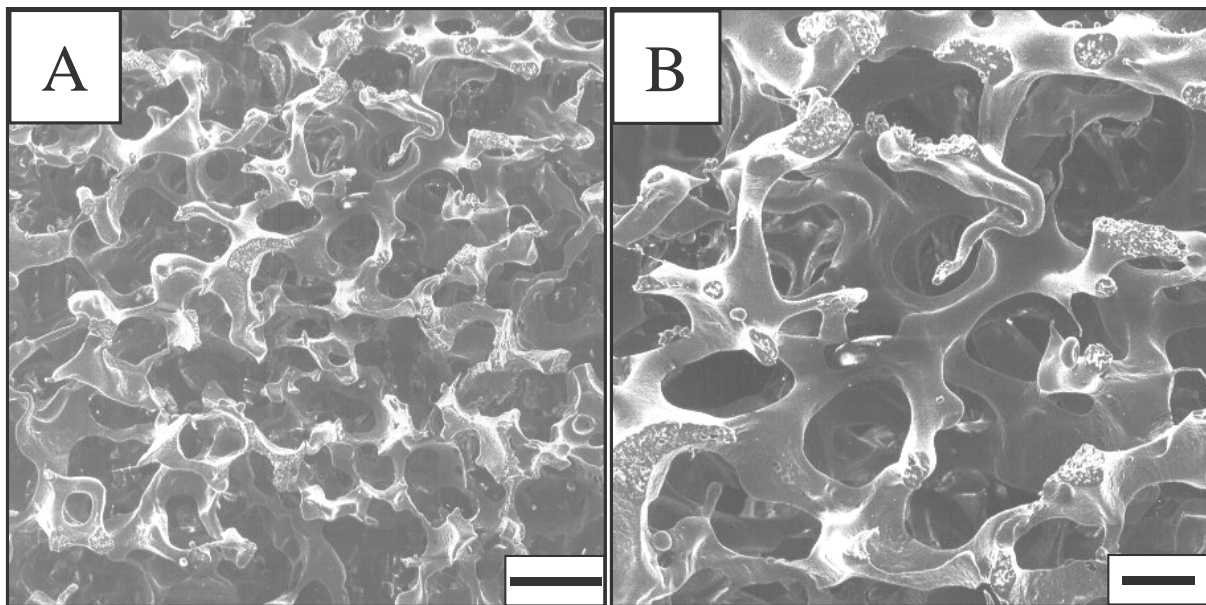


Fig. 2 Scanning electron microscopy of blank PLGA scaffolds without seeded MSCs: scaffolds exhibit a highly porous structure with interconnected pores. Photographs are shown in 100-fold magnification (A) and 200-fold magnification (B). Scale bars: 200 μm (A) and 100 μm (B).

OsO₄ histology

In order to induce adipogenesis, the cell-polymer constructs were treated with a widely used hormonal cocktail [35,41] consisting of dexamethasone, IBMX, indomethacin, and insulin. In the absence of inducing stimuli, no adipocytes developed in either the absence or presence of bFGF (data not shown). In Fig. 3a, induced cell-polymer constructs are shown over a time course of four weeks. Constructs were fixed with OsO₄ resulting in black stained areas, which mark intracellular lipid droplets of differentiated adipocytes.

Cell-polymer constructs cultivated in presence of bFGF clearly yielded a higher number of differentiated adipocytes compared to the control group without bFGF (Fig. 3a). This discrepancy in the differentiation rates was observable at all times. In both groups, a relatively modest increase in the number of adipocytes occurred between 1 and 2 weeks, whereas a

large increase was observed between two and four weeks; the latter was especially pronounced in the presence of bFGF.

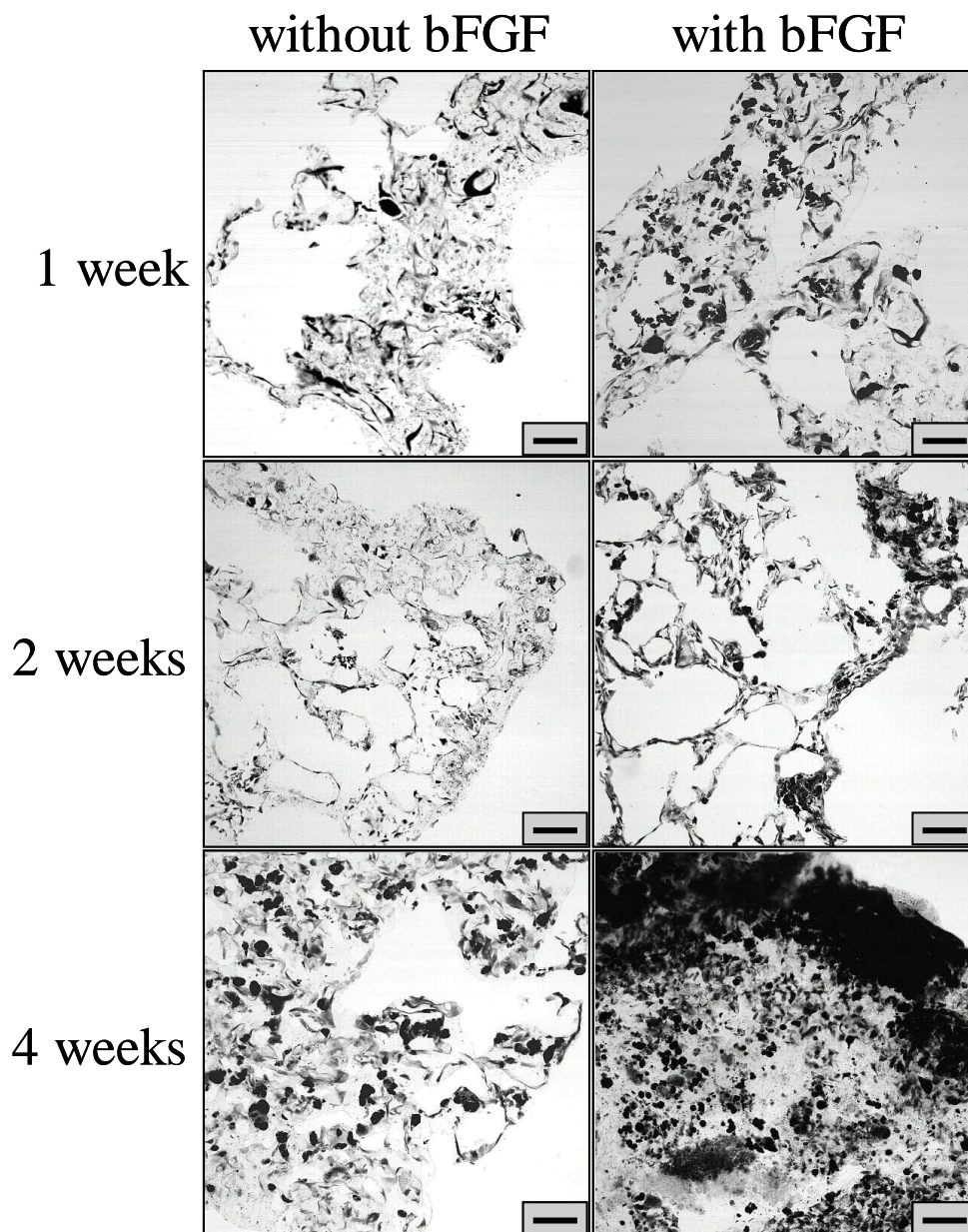


Fig. 3a *OsO₄* histology of cell-polymer constructs (100-fold magnification): Sections of constructs cultivated over 1, 2 and 4 weeks in absence and presence of bFGF. Black stained areas represent *OsO₄*-crosslinked lipid droplets. Histological paraffin sections were counterstained with hematoxylin and eosin (H&E). A clear development of the tissue and the differentiation rate of MSCs was observable in the course of time; more pronounced after treatment of MSCs with bFGF compared to control group. Scale bar: 100 μ m.

Under both culture conditions, the size of lipid droplets increased with time. The size of accumulated lipid droplets was distinctly larger in the presence of bFGF than in the absence of bFGF (Fig. 3b). After four weeks, adipocytes differentiated in presence of bFGF partially exhibited a unilocular phenotype, i.e., one large lipid droplet appears within an adipocyte indicating a high degree of maturation of differentiated MSCs. Multivacuolar adipocytes (several small lipid droplets within a cell) were observed mainly in inner parts of the scaffold (data not shown). Without supplementation of bFGF, only adipocytes with several discrete small lipid droplets per adipocyte were visible in all areas of the scaffold at all points of time (Fig. 3b).

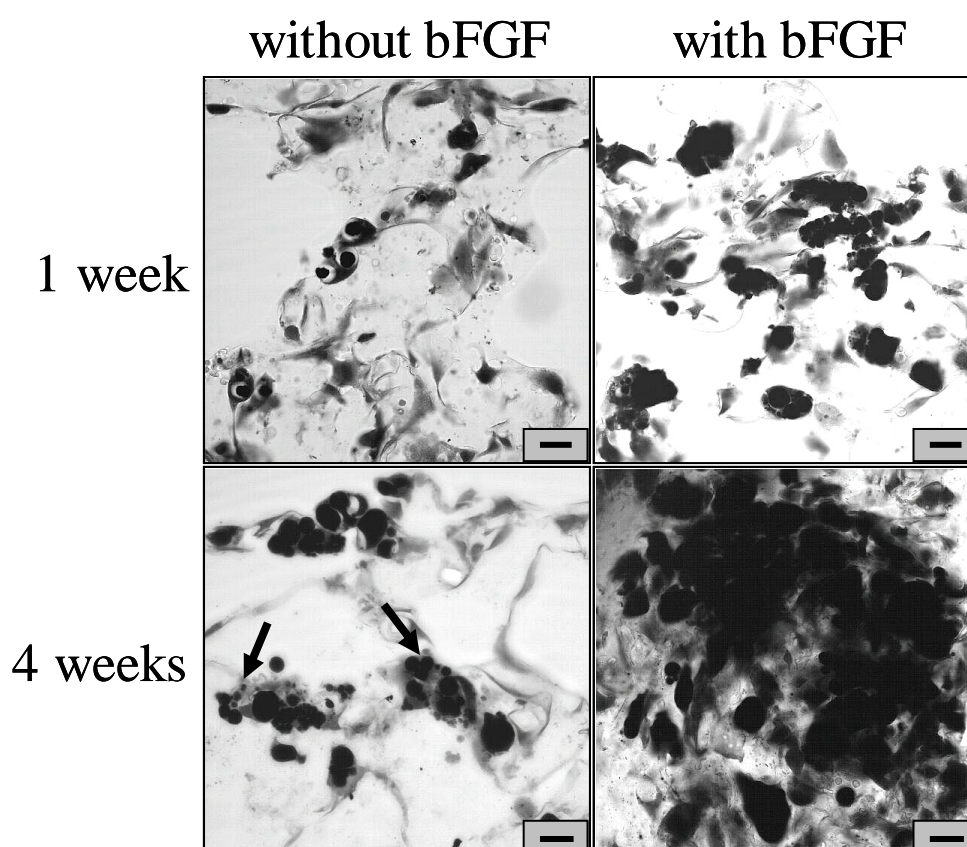


Fig. 3b *OsO₄ histology of cell-polymer constructs (400-fold magnification): Constructs cultivated in absence and presence of bFGF are shown after 1 and 4 weeks. Black stained areas represent OsO₄-crosslinked lipid droplets. Immature, multivacuolar adipocytes are designated by the black arrows. An augmentation of intracellular lipid droplets was observable in the course of time and in presence of bFGF compared to control group. Scale bar: 20 μ m.*

Scanning electron microscopy (SEM)

Tissue development and cellular distribution were monitored on the surface and in the interior of cell-polymer constructs using SEM. In the presence of bFGF, the scaffold surface was partially covered by cells and structured sheets considered to be extracellular matrix (ECM) material after just two weeks and was completely covered after four weeks (Fig. 4a). Thus, discrete adipocytes could not be observed at the surface, but rather only in the interior of the

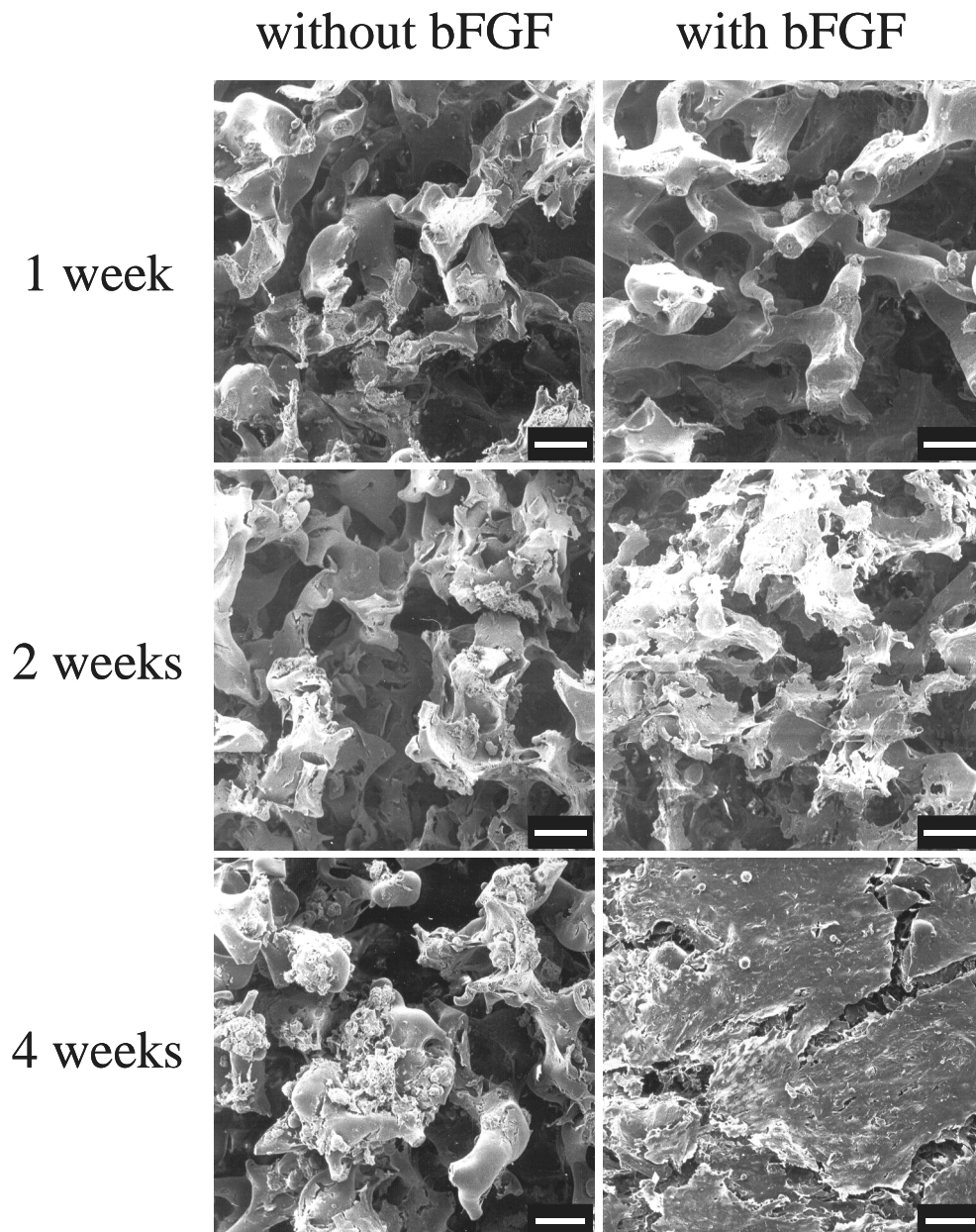


Fig. 4a SEM of the surface of cell-polymer constructs (100-fold magnification): Constructs cultivated over 1, 2, and 4 weeks in absence and presence of bFGF revealed a clear tissue development in the course of time, more pronounced after treatment of MSCs with bFGF compared to control group. Figures show single cells or groups of cells attached to the polymeric scaffold and, at later points of time, figures show cell-extracellular matrix areas covering the scaffold surface. Scale bars: 100 μ m.

scaffold. material after just two weeks and was completely covered after four weeks (Fig. 4a). Thus, discrete adipocytes could not be observed at the surface, but rather only in the interior of the scaffold. In contrast, in the absence of bFGF, the structure of the scaffold (compare Fig. 2) was still clearly identifiable after one and two weeks; after four weeks, the scaffold was only partially covered by cells and sheets (Fig. 4a).

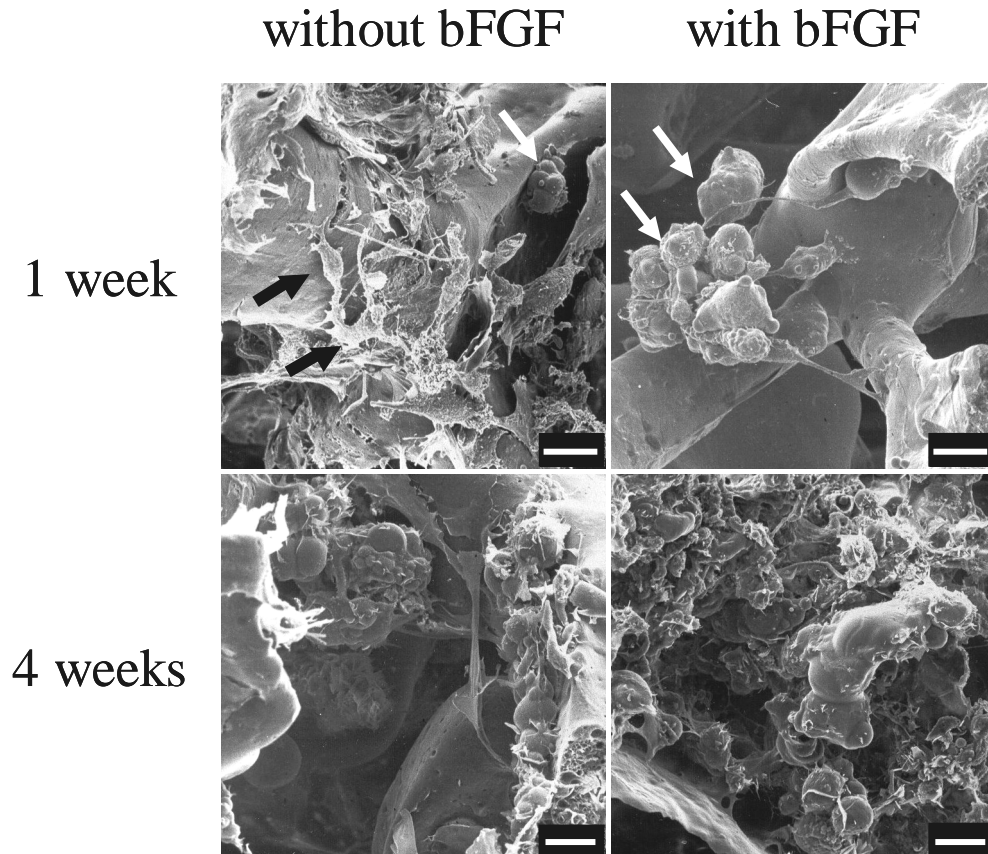


Fig. 4b SEM of the interior of cell-polymer constructs (500-fold magnification): Constructs cultivated in absence and presence of bFGF are shown after 1 and 4 weeks. Undifferentiated MSCs are designated by the black arrow, differentiated adipocytes by the white arrows. An increase in cell size and changes in morphology with bulged cell membranes due to fat storage were observed. An augmentation of intracellular lipid droplets was observable in the course of time and in presence of bFGF compared to control group. Scale bars: 20 μm .

In the interior of the constructs, differentiated adipocytes exhibited a multivacuolar phenotype (Fig. 4b). The size of the adipocytes was increased in bFGF-treated constructs as compared to the control group (Fig. 4b). In the presence of bFGF, groups of adipocytes were observed even after one week, recognizable by the bulged cell membranes, which are caused by lipid droplets. After four weeks, cells were additionally embedded in structures regarded as extracellular matrix. In the absence of bFGF, most cells were undifferentiated MSCs and only a few differentiated adipocytes were observed.

Glycerol-3-phosphate dehydrogenase (GPDH) activity

The degree of adipogenesis of MSCs in the cell-polymer constructs was reflected in measurements of the GPDH activity, which was determined three days after each induction. GPDH is a late marker of adipogenic differentiation, since it is a key enzyme in the biosynthesis of triglycerides. GPDH activity was significantly elevated after supplementation of bFGF compared to the control group after one (6.0-fold), two (3.8-fold), and three (1.8-fold) weeks (Fig. 5). In contrast, values of GPDH activity were equal after four weeks. The kinetics of GPDH activity was different for the two experimental groups. In the absence of bFGF, GPDH activity increased the first three weeks; after that no further increase was observed. In contrast, in the presence of bFGF, GPDH activity reached a maximum after two weeks followed by a steady decrease.

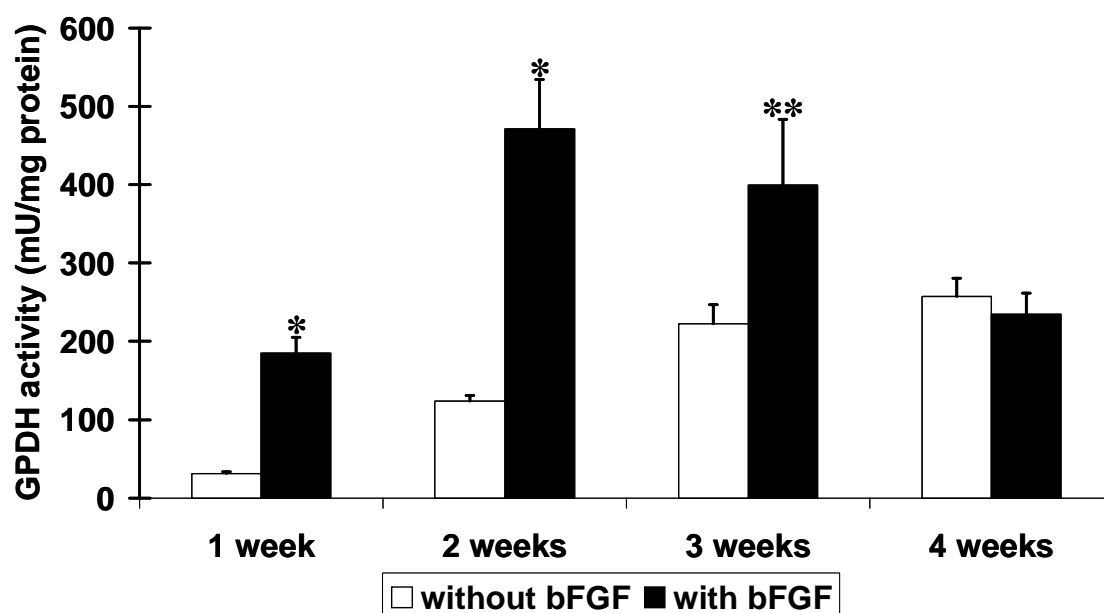


Fig. 5 GPDH activity of cell-polymer constructs: GPDH, a key enzyme involved in triacylglycerol synthesis, was determined at day 3 after each induction of adipogenesis and standardized per mg protein. White bars represent control group without bFGF, gray bars represent bFGF-treated cell-polymer constructs. Values are expressed as mean \pm SD ($n=3$). Statistically significant differences of bFGF treated cell compared to control group are denoted by * ($p < 0.01$) and ** ($p < 0.05$).

Reverse transcription-polymerase chain reaction (RT-PCR)

RT-PCR was performed three days after each induction in order to assess adipocytic gene expression of peroxisome proliferator-activated receptor $\gamma 2$ (PPAR $\gamma 2$), a key transcription factor of adipogenesis, and of glucose transporter 4 (GLUT4), a late marker of adipogenesis. The housekeeping gene 18S served as control gene. Basic FGF-treated cells yielded a clearly higher PPAR $\gamma 2$ expression compared to control without bFGF in the complete time course (Fig. 6). The differential expression was most pronounced after one and two weeks and attenuated after four weeks. In cell-polymer constructs cultivated in the absence of bFGF, PPAR $\gamma 2$ expression steadily increased with time. Basic FGF-treated constructs showed an initially high level of PPAR $\gamma 2$ expression, which was only slightly increased thereafter. GLUT4 expression was elevated in the bFGF group after one and two weeks and similar after four weeks compared to the control group. In the absence of bFGF, similarly to the expression profile of PPAR $\gamma 2$, GLUT4 expression steadily increased with time. In contrast, GLUT4 levels in the presence of bFGF were initially high and were maintained at later time points.

Gene	1 week		2 weeks		4 weeks	
	-bFGF	+bFGF	-bFGF	+bFGF	-bFGF	+bFGF
PPAR$\gamma 2$						
18S						
GLUT4						
18S						

Fig. 6 RT-PCR analysis of cell-polymer constructs: adipocyte-specific gene expression of PPAR γ , a key transcription factor in adipogenesis, and glucose transporter 4 (GLUT4) were evaluated at day 3 after induction of adipogenesis. Gene expression of cells cultured in absence (- bFGF) and presence (+ bFGF) of bFGF were compared in the course of time. The housekeeping gene 18S served as internal standard.

Discussion

To the best of our knowledge, this study reports an adipose tissue engineering approach using mesenchymal stem cells as cell source for the first time. The resulting cell-polymer constructs exhibited characteristics of white adipose tissue, such as lipid droplet-containing adipocytes including unilocular cells, adipocyte-specific enzyme activity and gene expression.

Recently, we found bFGF to enhance adipogenesis of MSCs in 2-D cell culture over eight days [35]. In the present study, the adipogenic protocol was successfully transferred from 2-D short-term to 3-D long-term cell culture. MSCs were seeded onto PLGA scaffolds and repeatedly exposed to the inducing regimen over four weeks. Basic FGF-treated cells on polymeric scaffolds exhibited a clearly enhanced adipogenic differentiation and maturation compared to constructs cultivated in absence of bFGF.

Cellular distribution, the appearance of lipid droplets and development of a tissue-like context were monitored by means of OsO₄ histology and SEM. The results of both techniques were well in agreement with each other, demonstrating an enhanced adipogenesis for the experimental group receiving bFGF. Within this group, a higher number of MSCs that differentiated into adipocytes were observed in all areas of the constructs and at all points of time (Figs. 3a,b and 4b). Furthermore, bFGF supplementation even led to the development of mature unilocular adipocytes in the outer area of the constructs (Fig. 3b). The observation that cells located in the interior of the scaffolds were smaller and multivacuolar may be attributed to the reduced supply of the cells with oxygen, nutrients, and adipogenic stimuli. Oxygen gradients in tissue-engineered constructs have previously been shown, for instance, in cartilage [42]. With regard to the development of tissue-like structures, the addition of bFGF again proved to be advantageous, yielding higher densities of adipocytes embedded in structures regarded as secreted extracellular matrix components.

On the molecular level, differentiation was monitored by measurement of the activity of the enzyme GPDH and of adipocytic gene expression of PPAR γ 2 and GLUT4 over the course of four weeks (Figs. 5 and 6). PPAR γ has been shown to act as the key transcription factor in adipogenesis *in vitro* and *in vivo* and PPAR γ activators like prostaglandin derivatives, anti-inflammatory drugs including indomethacin and the synthetic insulin-sensitizing thiazolidinediones are known as strong inducers of adipogenesis [43]. The GLUT isoform 4 is predominantly expressed in mature muscle and fat tissues and is primarily responsible for the increase in glucose uptake in response to insulin stimulation, which is necessary to generate the substrate glycerol-3-phosphate for the biosynthesis of triglycerides [44]. GPDH is a key

enzyme in lipid biosynthesis, converting dihydroxyacetonephosphate into glycerol-3-phosphate [45]. Both GLUT4 and GPDH are regarded as late markers of adipogenesis.

All three markers were clearly detectable in the 3-D culture system and indicated the process of adipogenesis of MSCs. Strongly supporting the microscopical observations, the cells in the group receiving bFGF in general exhibited higher levels of both adipocyte-specific gene expression and enzyme activity (Figs. 5 and 6). Whereas PPAR γ 2 expression was higher in the bFGF group over the whole course of the experiment (Fig. 6), GLUT4 expression and GPDH activity was distinctly higher especially at early time points, whereas after four weeks levels with and without bFGF were similar (Figs. 5 and 6). Apparently, lipid biosynthesis was initially enhanced in the presence of bFGF; as a result, advanced maturation of adipocytes, indicated by large lipid droplets within differentiated adipocytes (Fig. 3b), led to reduced lipid accumulation at later stages of the culture.

To date, only a few *in vitro* studies investigating adipose tissue engineering have been performed. Mainly using primary preadipocytes seeded onto scaffolds of various materials, most of these studies were restricted to histology and/or SEM for the evaluation of the tissue quality. They did show adipogenic differentiation of preadipocytes, however most of the adipocytes observed exhibited an immature phenotype [10,11,18]. In comparison to the only preadipocyte study that presented a more detailed histological cross-section and GPDH activity measurements [17], the MSC-derived constructs described here exhibited a higher density of differentiated adipocytes within the scaffold and values of GPDH activity that were approx. 5-fold higher at their maximum.

In contrast to all other *in vitro* studies including the one presented here, Fischbach et al. demonstrated the feasibility of engineering a coherent mature fat pad employing the preadipocytic cell line 3T3-L1 in a long-term culture [13]. In order to further improve the quality of tissue constructs generated with MSCs, possible future strategies may be the elevation of the initial cell number and the variation of the induction scheme including further potent inducing agents such as thiazolidinediones, ligands of PPAR γ . Additionally, perfusion cultures may be a tool to circumvent the insufficient supply of cells in the interior of the scaffolds.

In conclusion, we established a 3-D cell culture based on MSCs, PLGA scaffolds, and the growth factor bFGF for stem cell-based adipose tissue engineering. MSCs seem to be a promising alternative cell source that, especially in combination with bFGF, has potential for advanced adipogenic differentiation and tissue development.

References

- [1] American Society of Plastic Surgeons. (2003) Statistics of the American Society of Plastic Surgeons. www.plasticsurgery.org.
- [2] Katz AJ, Llull R, Hedrick MH, Futrell JW. 'Emerging approaches to the tissue engineering of fat'. *Clin Plast Surg* (1999); **26**: 587-603.
- [3] Beahm EK, Walton RL, Patrick CW, Jr. 'Progress in adipose tissue construct development'. *Clin Plast Surg* (2003); **30**: 547-58.
- [4] Patrick CW, Jr. 'Tissue engineering strategies for adipose tissue repair'. *Anat Rec* (2001); **263**: 361-366.
- [5] Patrick CW, Jr., Chauvin PB, Robb G.L. 'Tissue engineered adipose tissue'. In: Patrick CW, Jr., Mikos AG, McIntire L.V., editors. *Frontiers in tissue engineering*. Oxford: Elsevier Science, 1998. p. 369-382.
- [6] Kawaguchi N, Toriyama K, Nicodemou-Lena E, Inou K, Torii S, Kitagawa Y. '*De novo* adipogenesis in mice at the site of injection of basement membrane and basic fibroblast growth factor'. *Proc Natl Acad Sci USA* (1998); **95**: 1062-1066.
- [7] Tabata Y, Miyao M, Inamoto T, Ishii T, Hirano Y, Yamaoki Y, Ikada Y. '*De novo* formation of adipose tissue by controlled release of basic fibroblast growth factor'. *Tissue Eng* (2000); **6**: 279-289.
- [8] Toriyama K, Kawaguchi N, Kitoh J, Tajima R, Inou K, Kitagawa Y, Torii S. 'Endogenous adipocyte precursor cells for regenerative soft-tissue engineering'. *Tissue Eng* (2002); **8**: 157-165.
- [9] Yuksel E, Weinfeld AB, Cleek R, Waugh JM, Jensen J, Boutros S, Shenaq SM, Spira M. '*De novo* adipose tissue generation through long-term, local delivery of insulin and insulin-like growth factor-1 by PLGA/PEG microspheres in an in vivo rat model: a novel concept and capability'. *Plast Reconstr Surg* (2000); **105**: 1721-1729.
- [10] Kral JG, Crandall DL. 'Development of a human adipocyte synthetic polymer scaffold'. *Plast Reconstr Surg* (1999); **104**: 1732-1738.
- [11] Patrick CW, Jr., Chauvin PB, Hobbey J, Reece GP. 'Preadipocyte seeded PLGA scaffolds for adipose tissue engineering'. *Tissue Eng* (2001); **5**: 139-151.
- [12] Fischbach C, Seufert J, Staiger H, Hacker M, Neubauer M, Goepferich A, Blunk T. 'Three-dimensional *in vitro* model of adipogenesis: Comparison of culture conditions'. *Tissue Eng* (2004); **10**: 215-229.

- [13] Fischbach C, Spruss T, Weiser B, Neubauer M, Becker C, Hacker M, Gopferich A, Blunk T. 'Generation of mature fat pads *in vitro* and *in vivo* utilizing 3-D long-term culture of 3T3-L1 preadipocytes'. *Exp Cell Res* (2004); **300**: 54-64.
- [14] von Heimburg D, Zachariah S, Low A, Pallua N. 'Influence of different biodegradable carriers on the *in vivo* behavior of human adipose precursor cells'. *Plast Reconstr Surg* (2001); **108**: 411-420.
- [15] von Heimburg D, Zachariah S, Kuhling H, Heschel I, Schoof H, Hafemann B, Pallua N. 'Human preadipocytes seeded on freeze-dried collagen scaffolds investigated *in vitro* and *in vivo*'. *Biomaterials* (2001); **22**: 429-438.
- [16] von Heimburg D, Kuberka M, Rendchen R, Hemmrich K, Rau G, Pallua N. 'Preadipocyte-loaded collagen scaffolds with enlarged pore size for improved soft tissue engineering'. *Int J Artif Organs* (2003); **26**: 1064-1076.
- [17] Halbleib M, Skurk T, de Luca C, von Heimburg D, Hauner H. 'Tissue engineering of white adipose tissue using hyaluronic acid-based scaffolds. I: *in vitro* differentiation of human adipocyte precursor cells on scaffolds'. *Biomaterials* (2003); **24**: 3125-3132.
- [18] Huss FR, Kratz G. 'Mammary epithelial cell and adipocyte co-culture in a 3-D matrix: the first step towards tissue-engineered human breast tissue'. *Cells Tissues Organs* (2001); **169**: 361-367.
- [19] Halberstadt C, Austin C, Rowley J, Culberson C, Loeb sack A, Wyatt S, Coleman S, Blacksten L, Burg K, Mooney et al. 'A hydrogel material for plastic and reconstructive applications injected into the subcutaneous space of a sheep'. *Tissue Eng* (2002); **8**: 309-319.
- [20] Schoeller T, Lille S, Wechselberger G, Otto A, Mowlawi A, Piza-Katzer H. 'Histomorphologic and volumetric analysis of implanted autologous preadipocyte cultures suspended in fibrin glue: a potential new source for tissue augmentation'. *Aesthetic Plast Surg* (2001); **25**: 57-63.
- [21] Caplan AI, Bruder SP. 'Mesenchymal stem cells: building blocks for molecular medicine in the 21st century'. *Trends Mol Med* (2001); **7**: 259-264.
- [22] Haynesworth SE, Reuben D, Caplan AI. 'Cell-based tissue engineering therapies: the influence of whole body physiology'. *Adv Drug Deliv Rev* (1998); **33**: 3-14.
- [23] Heath CA. 'Cells for tissue engineering'. *Trends Biotechnol* (2000); **18**: 17-19.
- [24] Ringe J, Kaps C, Burmester GR, Sittlinger M. 'Stem cells for regenerative medicine: advances in the engineering of tissues and organs'. *Naturwissenschaften* (2002); **89**: 338-351.

- [25] Boo JS, Yamada Y, Okazaki Y, Hibino Y, Okada K, Hata KI, Yoshikawa T, Sugiura Y, Ueda M. 'Tissue-engineered bone using mesenchymal stem cells and a biodegradable scaffold'. *J Craniofac Surg* (2002); **13**: 231-239.
- [26] Bruder SP, Kurth AA, Shea M, Hayes WC, Jaiswal N, Kadiyala S. 'Bone regeneration by implantation of purified, culture-expanded human mesenchymal stem cells'. *J Orthop Res* (1998); **16**: 155-162.
- [27] Lisignoli G, Zini N, Remiddi G, Piacentini A, Puggioli A, Trimarchi C, Fini M, Maraldi NM, Facchini A. 'Basic fibroblast growth factor enhances *in vitro* mineralization of rat bone marrow stromal cells grown on non-woven hyaluronic acid based polymer scaffold'. *Biomaterials* (2001); **22**: 2095-2105.
- [28] Lisignoli G, Fini M, Giavaresi G, Nicoli AN, Toneguzzi S, Facchini A. 'Osteogenesis of large segmental radius defects enhanced by basic fibroblast growth factor activated bone marrow stromal cells grown on non-woven hyaluronic acid-based polymer scaffold'. *Biomaterials* (2002); **23**: 1043-1051.
- [29] Quarto R, Mastrogiacomo M, Cancedda R, Kutepov SM, Mukhachev V, Lavroukov A, Kon E, Marcacci M. 'Repair of large bone defects with the use of autologous bone marrow stromal cells'. *N Engl J Med* (2001); **344**: 385-386.
- [30] van den Dolder J, Farber E, Spauwen PHM, Jansen JA. 'Bone tissue reconstruction using titanium fiber mesh combined with rat bone marrow stromal cells'. *Biomaterials* (2003); **24**: 1745-1750.
- [31] Johnstone B, Hering TM, Caplan AI, Goldberg VM, Yoo JU. '*In vitro* chondrogenesis of bone marrow-derived mesenchymal progenitor cells'. *Exp Cell Res* (1998); **238**: 265-272.
- [32] Martin I, Padera RF, Vunjak-Novakovic G, Freed LE. 'In vitro differentiation of chick embryo bone marrow stromal cells into cartilaginous and bone-like tissues'. *J Orthop Res* (1998); **16**: 181-189.
- [33] Young RG, Butler DL, Weber W, Caplan AI, Gordon SL, Fink DJ. 'Use of mesenchymal stem cells in a collagen matrix for Achilles tendon repair'. *J Orthop Res* (1998); **16**: 406-413.
- [34] Hacker M, Tessmar J, Neubauer M, Blaimer A, Blunk T, Gopferich A, Schulz MB. 'Towards biomimetic scaffolds: Anhydrous scaffold fabrication from biodegradable amine-reactive diblock copolymers'. *Biomaterials* (2003); **24**: 4459-4473.
- [35] Neubauer M, Fischbach C, Bauer-Kreisel P, Lieb E, Hacker M, Tessmar J, Schulz MB, Gopferich A, Blunk T. 'Basic fibroblast growth factor enhances PPAR γ ligand-induced adipogenesis of mesenchymal stem cells'. *FEBS Lett*, In Press.

- [36] Ishaug SL, Crane GM, Miller MJ, Yasko AW, Yaszemski MJ, Mikos AG. 'Bone formation by three-dimensional stromal osteoblast culture in biodegradable polymer scaffolds'. *J Biomed Mater Res* (1997); **36**: 17-28.
- [37] Kim YJ, Sah RL, Doong JY, Grodzinsky AJ. 'Fluorometric assay of DNA in cartilage explants using Hoechst 33258'. *Anal Biochem* (1988); **174**: 168-176.
- [38] Abramowsky CR, Pickett JP, Goodfellow BC, Bradford WD. 'Comparative demonstration of pulmonary fat emboli by "en bloc" osmium tetroxide and oil red O methods'. *Hum Pathol* (1981); **12**: 753-755.
- [39] Pairault J, Green H. 'A study of the adipose conversion of suspended 3T3 cells by using glycerophosphate dehydrogenase as differentiation marker'. *Proc Natl Acad Sci USA* (1979); **76**: 5138-5142.
- [40] Lowry OH, Rosebrough NJ, Farr AL, Randall RJ. 'Protein measurement with the Folin phenol reagent'. *J Biol Chem* (1951); **193**: 265-275.
- [41] Pittenger MF, Mackay AM, Beck SC, Jaiswal RK, Douglas R, Mosca JD, Moorman MA, Simonetti DW, Craig S, Marshak DR. 'Multilineage potential of adult human mesenchymal stem cells'. *Science* (1999); **284**: 143-147.
- [42] Kellner K, Liebsch G, Klimant I, Wolfbeis OS, Blunk T, Schulz MB, Gopferich A. 'Determination of oxygen gradients in engineered tissue using a fluorescent sensor'. *Biotechnol Bioeng* (2002); **80**: 73-83.
- [43] Rosen ED, Spiegelman BM. 'Molecular regulation of adipogenesis'. *Annu Rev Cell Dev Biol* (2000); **16**: 145-171.
- [44] Michelle Furtado L, Poon V, Klip A. 'GLUT4 activation: thoughts on possible mechanisms'. *Acta Physiol Scand* (2003); **178**: 287-296.
- [45] Sottile V, Seuwen K. 'A high-capacity screen for adipogenic differentiation'. *Anal Biochem* (2001); **293**: 124-128.

Chapter 8

Adsorption, Desorption, and Covalent Binding of bFGF to Derivatives of PEG-PLA Polymers

Markus Neubauer,^{1,2} Makoto Ozeki,² Sigrid Drotleff,¹ Michael Hacker,¹ Jörg Teßmar,¹
Yasuhiko Tabata,² Torsten Blunk,¹ Achim Göpferich¹

¹ Department of Pharmaceutical Technology, University of Regensburg, Universitätsstraße 31, 93040 Regensburg, Germany

² Institute for Frontier Medical Sciences, Field of Tissue Engineering, Department of Biomaterials, Kyoto University, 53 Kawara-cho Shogoin, Sakyo-ku, Kyoto 606-8507, Japan.

Abstract

Biomimetic polymers represent a novel class of biomaterials for the control of the interactions with cells at the molecular level. We have recently fabricated 3-D cell carriers from biomimetic derivatives of poly (ethylene glycol)-poly (lactic acid) (PEG-PLA) diblockcopolymers exhibiting a surface which is modifiable by the covalent binding of bioactive agents such as peptides and proteins. Basic fibroblast growth factor (bFGF) is a potent growth factor which is known to modulate the behavior of a wide range of cell types and to provoke angiogenesis *in vivo* and, therefore, bFGF represents an attractive candidate for the immobilization in biomimetic scaffolds .

The goal of this study was the investigation of the interactions of bFGF and, on the one hand, PEG-PLA derivatives exhibiting a hydrophilic surface and, on the other hand, the more lipophilic polymers poly(lactic acid) (PLA) and poly(lactic-co glycolic acid) (PLGA). The adsorption of radiolabeled bFGF to PEG-PLA polymers was distinctly suppressed in comparison to PLA 2-D films. Furthermore, a protocol was established to efficiently desorb bFGF from 2-D polymer films. The transfer of the desorption protocol to 3-D polymer scaffolds allowed for the determination of the amount of bFGF covalently bound to biomimetic scaffolds.

In conclusion, this study provides data about the adsorption and desorption of bFGF to different polymers and presents the establishment of a protocol for the determination of the amounts of bFGF tethered to biomimetic scaffolds.

Introduction

A wide variety of biomaterials has been developed for tissue engineering applications in recent years [1]. Natural materials such as collagen, hyaluronic acid, and fibrin may well reflect the structure and functional properties of native ECM, have a low toxicity, and exert only a weak chronic inflammatory response [2]. However, many natural materials have disadvantageous properties in regard to a potential use in the field of tissue engineering such as batch-to-batch variations, poor mechanical performance, and a chemical structure difficult to modify [3,4]. In contrast, synthetic polymers can be designed in order to obtain a well-defined, tailor-made structure and functionality. Recently, various synthetic biomaterials have been developed which can be modified in order to mimic the biological environment, termed biomimetic polymers [5]. These biomaterials aim at the generation of an inert surface *per se* which can structurally be modified in a specific manner in order to selectively control the cellular behavior [6]. A possible strategy represents the creation of a highly hydrophilic environment, possibly by the use of poly(ethylene glycols) (PEGs), to suppress unspecific protein adsorption and subsequent unspecific cell attachment [7,8]. In addition, PEGs have been described to be easily modifiable and a plethora of PEG derivatives were developed capable of covalently binding substrates with functional end groups such as amine and thiol groups [9-12].

We previously synthesized diblock copolymers consisting of a MeO-PEG moiety and a PLA moiety which possess protein-resistant properties whereby increasing PEG/PLA ratio have been reported to enhance the protein resistance [13]. Furthermore, these polymers with varying ratios of the PEG and the PLA components have been shown to suppress cell attachment and to modulate the osteogenic differentiation of MSCs in 2-D cell culture [8]. The diblock copolymer consisting of a hydrophilic 2 kDa poly(ethylene glycol) (PEG) block and a 40 kDa lipophilic poly(lactic acid) (PLA) block, abbreviated as MeO-PEG₂PLA₄₀, has been shown to be a suitable polymer for tissue engineering applications with regard to cell attachment, proliferation, and differentiation [8]. The substitution of the MeO-PEG block with a H₂N-PEG block allowed for the attachment of an amine-reactive linker, succinimidyl tartrate (ST), and led to activated derivatives of these polymers, abbreviated as ST-NH-PEG₂PLA₄₀ [14]. These PEG-PLA derivatives can be processed into 3-D scaffolds for tissue engineering applications [15]. In a previous study, cyclic RGD sequences covalently bound to 2-D ST-NH-PEG₂PLA₄₀ polymer films have been demonstrated to enhance the adhesion of osteoblasts [16].

The overall goal of the development of biomimetic scaffolds is to covalently immobilize growth factors to 3-D scaffolds made from ST-NH-PEG₂PLA₄₀ in order to specifically control the cellular behavior and tissue development. Basic FGF represents a potent growth factor which is known to modulate the behavior of a wide variety of cell types and to provoke pro-angiogenic effects *in vivo* [17,18].

The goal of this study, as a first step towards the tethering of bFGF to the ST-NH-PEG₂PLA₄₀ polymer, was to characterize the interactions of the diblock copolymer derivatives and the protein basic fibroblast growth factor (bFGF). The protein-resistant properties of MeO-PEG₂PLA₄₀ were evaluated with regard to the adsorption of bFGF in comparison to bFGF adsorption to the lipophilic polymer poly(lactic acid) (PLA). Furthermore, a protocol for the efficient desorption of bFGF from polymer films was established which is relevant for distinguishing between adsorbed and covalently bound bFGF in order to determine the amount of covalently bound bFGF to the ST-NH-PEG₂PLA₄₀ polymer.

Materials and Methods

Materials

Basic FGF was purchased from Kaken Pharmaceutical, Tokyo, Japan. PEG-PLA diblock copolymers (approx. 42 kDa) were synthesized in our laboratory [8], poly(lactic-glycolic acid) (PLGA 75:25; approx. 90 kD) was obtained from Boehringer Ingelheim (Ingelheim am Rhein, Germany). Poly(lactic acid) (PLA, approx. 130 kDa) was purchased from Medisorb Technology International (Cincinnati, OH, USA). If not otherwise stated, chemicals were obtained from Nacalai Tesque (Kyoto, Japan).

Polymer synthesis

The polymer ST-NH-PEG₂PLA₄₀ was synthesized and characterized as described by Tessmar et al. [14]. Briefly, the precursor H₂N-PEG₂PLA₄₀ was synthesized by a ring-opening polymerization of poly(D,L-lactic acid) with poly(ethylene glycol)-monoamine using stannous 2-ethylhexanoate as catalyst. ST-NH-PEG₂PLA₄₀ was obtained by attachment of disuccinimidyl tartrate to H₂N-PEG₂PLA₄₀ (Fig. 1A). MeO-PEG₂PLA₄₀ was synthesized and characterized as previously described [8] (Fig. 1B).

Fabrication of polymer films

Polymers (1.9 mg/cm² film area) were dissolved in dichloromethane (0.15 ml/cm² film area) and poured into glass petri dishes with an absolutely even bottom. The solvent was evaporated

under a chemical hood at room temperature (RT) and atmospheric pressure. The films were detached from the dish bottom and subsequently, they were dried and stored under vacuum. When required, the films were die-punched or cut into pieces.

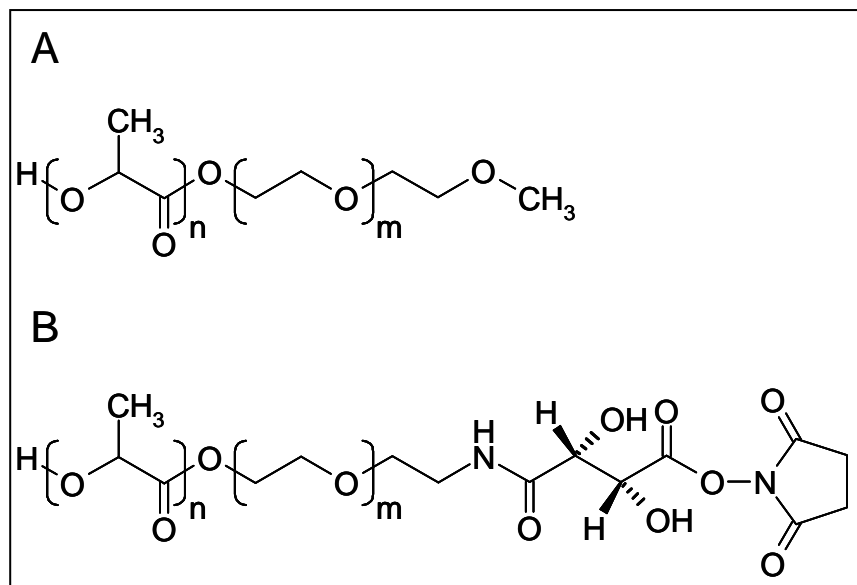


Fig. 1 Structures of the derivatives of poly(*D,L*-lactic acid)-block-poly(ethylene glycol):
A Poly(*D,L*-lactic acid)-poly(ethylene glycol)-monomethyl ether (MeO-PEG₂PLA₄₀),
B Succinimidyl tartrate PEG-PLA (ST-NH-PEG₂PLA₄₀).

Fabrication of scaffolds

Scaffolds were fabricated using a protocol adapted from Hacker et al. [15]. Polymer-specific parameters are shown in Table 1. Briefly, the scaffolds were fabricated from polymer dissolved in a methyl ethyl ketone-tetrahydrofuran-mixture (59:41 (v/v)) and lipid microparticles made from Softisan[®] 154 (S) and Witepsol[®] H42 (H) (kindly provided by SASOL Germany (Witten, Germany)) were weighed into a separate vial. The size of porogen particles ranged from 100 μm to 300 μm . After 1 h storage at -20°C the porogen particles were transferred into the polymer solution and mixed for 5 min on ice. The resulting highly viscous dispersion was then transferred into a 10 ml polypropylene syringe and injected into cubic Teflon[®] molds (with a cylindrical cavity of 0.8 cm in diameter). After a pre-extraction treatment step in *n*-hexane at 0°C for t_0 , the filled molds were submerged in warm *n*-hexane to precipitate the polymer and extract the porogen particles concurrently. This procedure was carried out in two separate *n*-hexane baths of different temperatures: first, molds were incubated at T_1 for t_1 and in a second step at T_2 for t_2 . Subsequently, the molds were transferred into a *n*-hexane bath of 0°C for 5 min. Finally, the porous cylindrical polymer

constructs were removed from the molds and vacuum-dried for 48 h. For further investigations the constructs were cut into 2 mm slices which were then addressed as scaffolds.

Group	Polymer	Lipid mixture (S/H)	t ₀ [min]	T ₁ [°C]/t ₁ [min]	T ₂ [°C]/t ₂ [min]
PLGA	100% PLGA	2:1	15	52/10	40/20
MeO-PEG ₂ PLA ₄₀	100% MeO-PEG ₂ PLA ₄₀	1:1	90	45/7.5	35/22.5
ST-NH-PEG ₂ PLA ₄₀	70% ST-NH-PEG ₂ PLA ₄₀ + 30% MeO-PEG ₂ PLA ₄₀	1:1	90	45/7.5	35/22.5
ST-NH-PEG ₂ PLA ₄₀ /PLA	70% ST-NH-PEG ₂ PLA ₄₀ + 30% PLA	1:1	90	45/7.5	35/22.5

Table 1: Polymer-specific parameters used for the scaffold fabrication.

Contact angle measurements

The wettability of films was measured by the sessile drop method with a contact angle meter (Face, Tokyo, Japan) 0.5 to 10 min after the deposition of droplets (9 µl). The contact angles were determined on three areas of each polymer film (n=3).

Radiolabeling of bFGF

Different amounts of bFGF were labeled using the chloramine T method. In the following, the preparation of 100 µl of a 10 mg/ml bFGF is exemplarily described. 5.00 µl ¹²⁵NaI (3.7 MBq) were added to 100 µl of a 10 mg/ml bFGF solution. After the addition of 100 µl of a 0.2 mg/ml chloramine T solution (710 µM final concentration), the mixture was shaken for 2 min. In order to stop the reaction, 100 µl of a 4 mg/ml sodium metabisulfite solution (21 mM final concentration) was mixed and shaken with the bFGF solution for 2 min. The resulting solution was subjected to a PD-10 column, Sephadex G-25 M (Amersham Biosciences, Uppsala, Sweden) and bFGF was eluted using a phosphate-buffered saline (PBS) pH 8.0. The resultant solution was a 1 mg/ml bFGF solution in PBS, pH 8.0, which was used at different dilutions for all adsorption and binding experiments.

Adsorption of bFGF to polymer films

Polymer films were cut into squares (1 cm x 1 cm). The pieces were incubated in ¹²⁵I-bFGF solutions (pH 8.0) of different concentrations on a shaker (100 min⁻¹) for 2 h at room

temperature (RT). Subsequently, the films were rinsed three times with water and subjected to scintillation (n=3).

Desorption of bFGF from polymer films using different buffer types

Desorption experiments were performed using PLA films because the highest amounts of bFGF adsorbed on PLA films as shown in the adsorption experiment. Six round die-punched PLA films (diameter 0.8 cm) were strung onto a needle (22G) which was located in a reaction tube (2 ml). The films within a tube were separated and secured with segments of silicone tubing (1 mm long). The films were incubated in a ^{125}I -bFGF solution (50 μg in 1.5 ml buffer) for 6 h at RT in order to adsorb bFGF. After rinsing the films with water, they were transferred into 50 ml tubes filled with different desorption solutions: Water, PBS, PBS + 2M NaCl, PBS + 1% SDS, and PBS + 1% SDS in combination with ultrasonic treatment as a positive control. After mild shaking for 5 min at RT, the films were subjected to scintillation.

Desorption of bFGF from polymer films using detergent-containing buffers

Polymer films were treated with different detergent-containing buffers in order to evaluate other agents than SDS for their potential to desorb bFGF. Films were pre-treated as described in the above paragraph. After rinsing the films with water, they were transferred into 50 ml plastic tubes filled with different desorption solutions: Water, PBS + 1% SDS (Nacalai Tesque, Kyoto, Japan), PBS + 1% Tween 80 (Nacalai Tesque, Kyoto, Japan), PBS + 1% Poloxamer 188 (Pluronic F68, Sigma, Steinheim, Germany), and PBS + 1% Triton X-100 (Sigma, Steinheim, Germany). Basic FGF was desorbed on a shaker (100 min^{-1}) at RT. After different time periods, films were subjected to scintillation. In another experiment, bFGF was desorbed using water and PBS + 1% SDS under the above described conditions and additionally at 37°C .

Preparation of scaffolds for adsorption, desorption, and binding experiments

Single scaffolds (diameter 7 mm, height 2 mm) were strung onto a needle each (22G) which was located in a reaction tube (2 ml). The scaffold within a tube was secured with segments of silicone tubing (1 mm long). Scaffolds were pre-wetted in 70% ethanol and extensively rinsed with PBS. Subsequently, scaffolds were subjected to adsorption, desorption, or binding experiments.

Adsorption of bFGF to polymer scaffolds

Scaffolds were prepared as described above. They were incubated in a ^{125}I -bFGF solutions with concentrations ranging from 0.1 to 50 μg (in 1.5 ml buffer) for 2 h at RT on a shaker (20 min^{-1}). Subsequently, the films were rinsed three times with water and subjected to scintillation (n=3).

Desorption of bFGF from polymer scaffolds

Scaffolds were prepared as described above. The most effective buffer to desorb bFGF from polymer films, that is PBS + 1% SDS as determined in the experiment described above, was utilized for the desorption of bFGF from polymer scaffolds. Scaffolds were incubated in a ^{125}I -bFGF solutions (50 μg in 1.5 ml buffer) for 2 h at RT on a shaker (20 min^{-1}). After rinsing the scaffolds with water, for the desorption experiment, they were transferred into 50 ml plastic tubes filled with PBS + 1% SDS which were placed on a shaker (20 min^{-1}). After different time periods, scaffolds were subjected to scintillation (n=3).

Covalent binding of bFGF to ST-NH-PEG₂PLA₄₀ scaffolds

Scaffolds made from MeO-PEG₂PLA₄₀ and ST-NH-PEG₂PLA₄₀ or ST-NH-PEG₂PLA₄₀/PLA were used in this experiment (Table 1). Subsequently, scaffolds were pre-wetted in 70% ethanol and extensively rinsed with PBS pH 8.0. In order to anchor bFGF, scaffolds were incubated in a bFGF solution (dissolved in PBS pH 8.0) at a concentration of 50 μg bFGF (in 1.5 ml buffer) for 2 h (or alternatively for 6 h) at RT on a shaker (20 min^{-1}). After washing the scaffolds in PBS pH 7.4, they were treated with 1% SDS in PBS, pH 7.4, in order to desorb non-covalently bound bFGF for 90 h at RT on a shaker (20 min^{-1}). Finally, the scaffolds were subjected to scintillation (n=3). For the control group which allows the correction for bFGF adsorption, bFGF was adsorbed to and desorbed from MeO-PEG₂PLA₄₀ under the same conditions as described for the covalent binding of bFGF to the ST-NH-PEG₂PLA₄₀. The amount of bFGF covalently bound to ST-NH-PEG₂PLA₄₀ scaffolds was calculated by subtracting the amount associated with MeO-PEG₂PLA₄₀ control scaffolds from that associated with ST-NH-PEG₂PLA₄₀ scaffolds.

Statistics

All data are expressed as means \pm standard deviation. Single-factor analysis of variance (ANOVA) was used in conjunction with a multiple comparison test (Tukey's test) to assess statistical significance at a level of $p < 0.01$ (*) or $p < 0.05$ (**).

Results

Contact angle measurements

Contact angles for PLA and MeO-PEG₂PLA₄₀ films were measured in a course of time from 0.5 to 10 min after droplet deposition in order to measure the wettability of the films. Virtually no differences in contact angles between water and the different polymers were measured in the first minute (Fig. 2). After 3 min onwards, a clear difference between the hydrophobic PLA and the more hydrophilic diblock copolymer was detectable (Fig. 2).

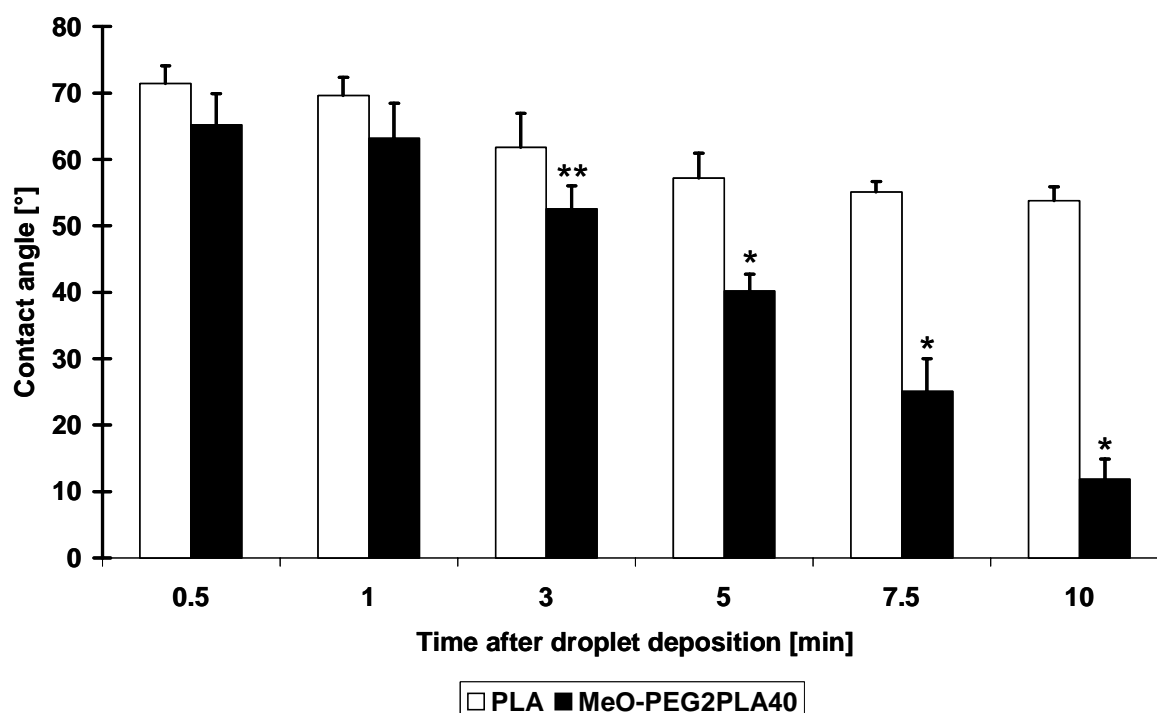


Fig. 2 Measurements of contact angles between water and PLA and MeO-PEG₂PLA₄₀ films, respectively, in a course of time from 0.5 to 10 min after droplet deposition. Data represent mean \pm standard deviation ($n=3$). Asterisks indicate significantly decreased values as compared to PLA films at a level of $p<0.01$ (*) or $p<0.05$ (**).

Adsorption of bFGF to polymer films

In order to test the influence of the differential surface properties on the protein adsorption, different amounts of bFGF were adsorbed to PLA and MeO-PEG₂PLA₄₀ films. Basic FGF adsorbed to both polymers in a dose-dependent manner (Fig. 3). However, MeO-PEG₂PLA₄₀ clearly reduced the adsorption of bFGF as compared to PLA, irrespective of the amount of bFGF in the feed (Fig. 3). The adsorption of bFGF to MeO-PEG₂PLA₄₀ films could not be totally prevented (Fig. 3).

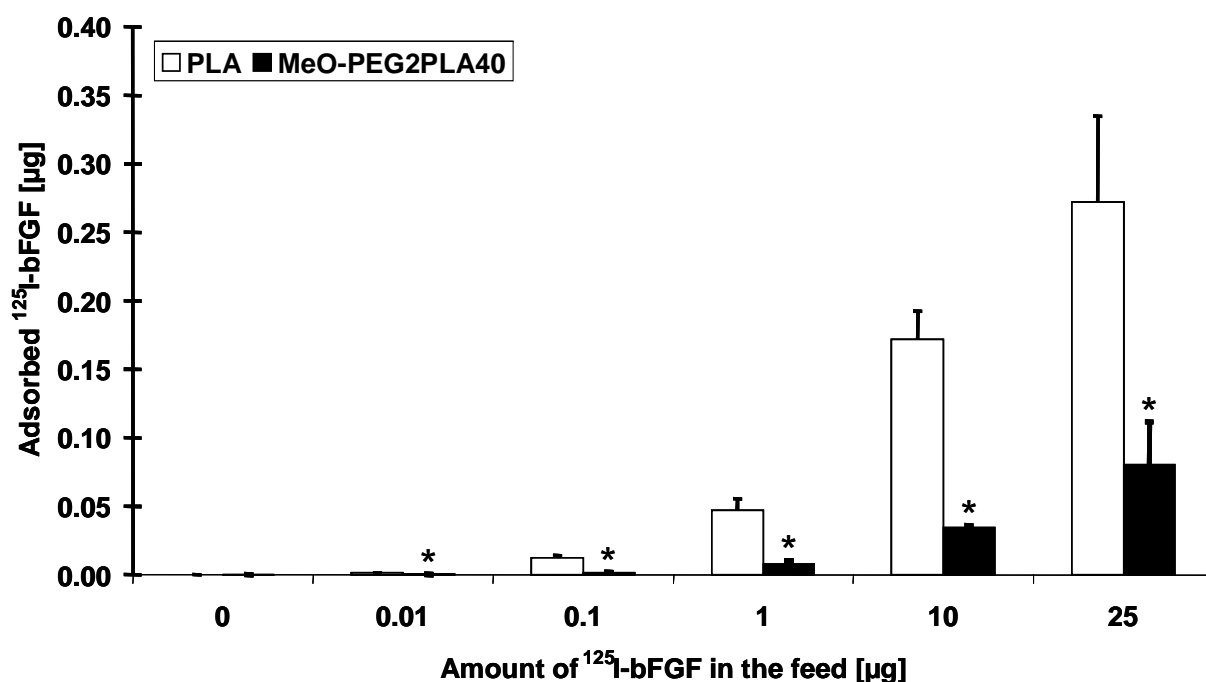


Fig. 3 Adsorption of bFGF to PLA and MeO-PEG₂PLA₄₀ films. Different amounts of bFGF from 0 to 25 µg were provided in the feed. Data represent mean ± standard deviation (n=3). Asterisks indicate significantly decreased values as compared to PLA films at a level of $p < 0.01$ (*) or $p < 0.05$ (**).

Desorption of bFGF from polymer films using different buffer types

As a first step, different types of buffers were used aiming at an efficient desorption of bFGF from the PLA films. PLA was used as a film material because higher amounts of bFGF can be adsorbed to this material as compared to MeO-PEG₂PLA₄₀ (Fig. 3). Films with adsorbed bFGF were treated with PBS, a PBS buffer with a high ionic strength (PBS + 2M sodium chloride), a PBS with a detergent (PBS + 1% SDS), and the SDS-containing buffer combined with an ultrasonic treatment (PBS + 1% SDS + US). The latter combination served as positive control, water as negative control. PBS and PBS + 2M NaCl had no effect on the desorption of bFGF from the PLA films. However, the SDS-containing buffer clearly reduced the amount of bFGF. Approx. 45% of the initially adsorbed bFGF were desorbed from the PLA films after applying the desorption procedure for only 5 min. After treatment of the films with the SDS-containing buffer in combination with ultrasound, approx. 75% of the initially adsorbed bFGF were removed.

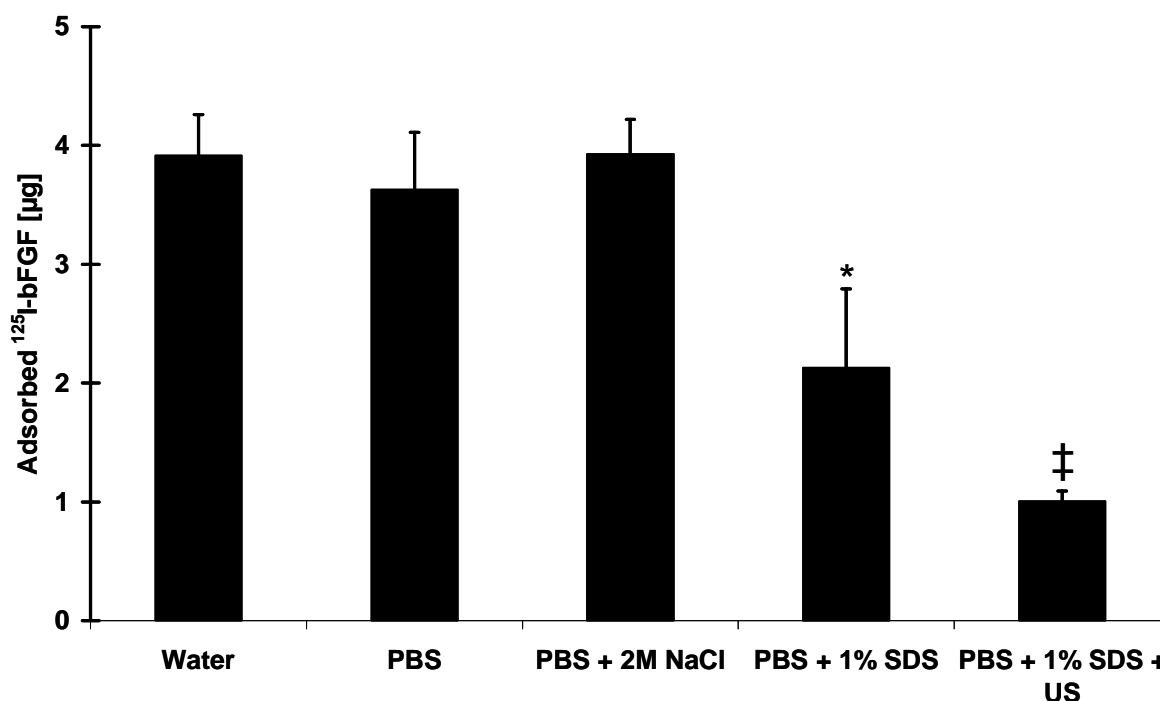


Fig. 4 Desorption of bFGF from PLA films using different types of buffers. The remaining amounts of bFGF after the desorption procedure are shown. Water served as negative control, a detergent-containing buffer in combination with ultrasound as positive control. The tested buffers include PBS, PBS with a high ionic strength (PBS + 2M NaCl), and a detergent containing buffer (PBS + 1% SDS). Data represent mean \pm standard deviation ($n=3$). Tukey's test indicated a statistically significant decrease as compared to the groups with water, PBS, and PBS + 2M NaCl at a level of $p<0.01$ (*). Ultrasonic treatment led to a statistically significant decrease as compared to the group with PBS + 1%SDS at a level of $p<0.05$ and as compared to the groups with water, PBS, and PBS + 2M NaCl at a level of $p<0.01$ (‡).

Desorption of bFGF from polymer films using detergent-containing buffers

In the previous experiment, the detergent-containing buffer proved to be most efficient in the desorption of bFGF from PLA films. Consequently, the potential of further detergents to remove bFGF from polymer films was evaluated: Pluronic F68, Tween 80, and Triton X-100 dissolved in PBS. Surprisingly, Pluronic F68, Tween 80 and Triton X-100 had no statistically significant effect on the desorption of bFGF after 12 h as compared to water (Fig. 5). Only $8.8\pm 6.3\%$, $12.7\pm 1.1\%$, $15.8\pm 1.3\%$, and $20.7\pm 7.3\%$ of the initially adsorbed bFGF were removed by water, Pluronic F68, Tween 80, and Triton X-100, respectively, after 12 h (Fig. 5). In contrast, $88.4\pm 2.3\%$ of the initially adsorbed protein were desorbed after 12 h using the SDS-containing buffer (Fig. 5).

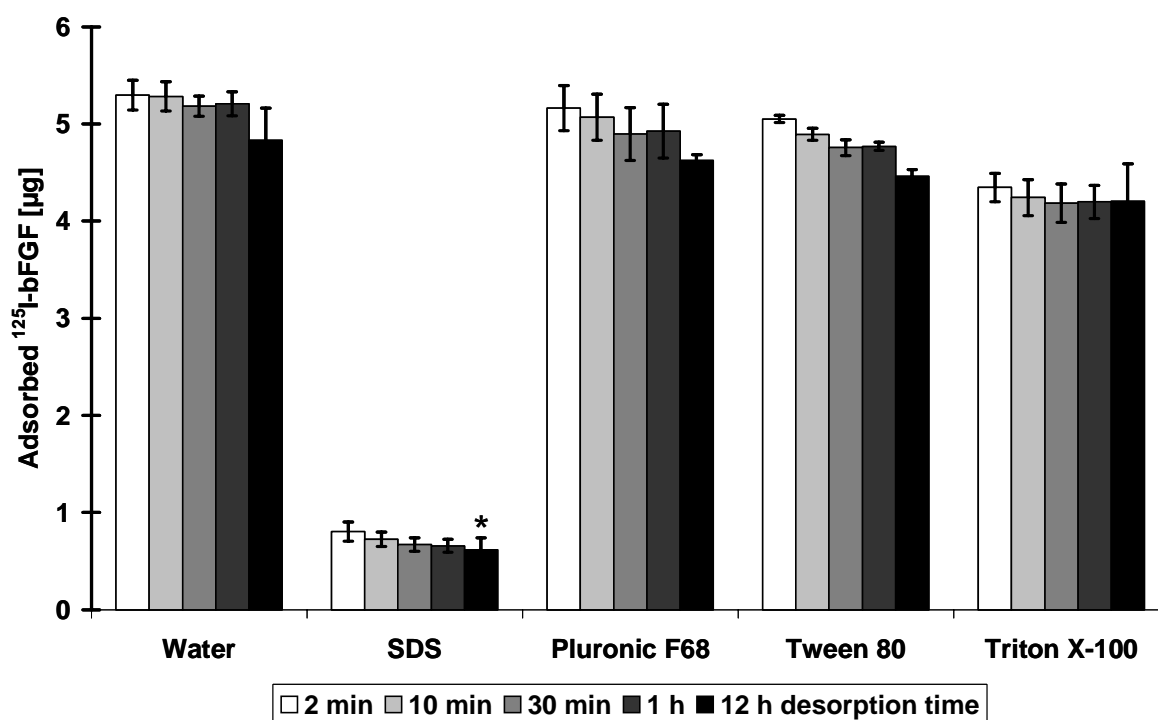


Fig. 5 Desorption of bFGF from PLA films using detergent-containing buffers. The amount of the remaining amounts of bFGF after the desorption procedure is shown. Water served as a control. Data represent mean \pm standard deviation ($n=3$). The asterisk indicates the significantly decreased value after 12 h as compared to all other groups at a level of $p<0.01$.

No further improvement of bFGF desorption from the PLA films was achieved by elevation of the temperature from RT to 37°C during the desorption procedure, irrespective of the presence of the SDS-containing buffer and the time period (Fig. 6).

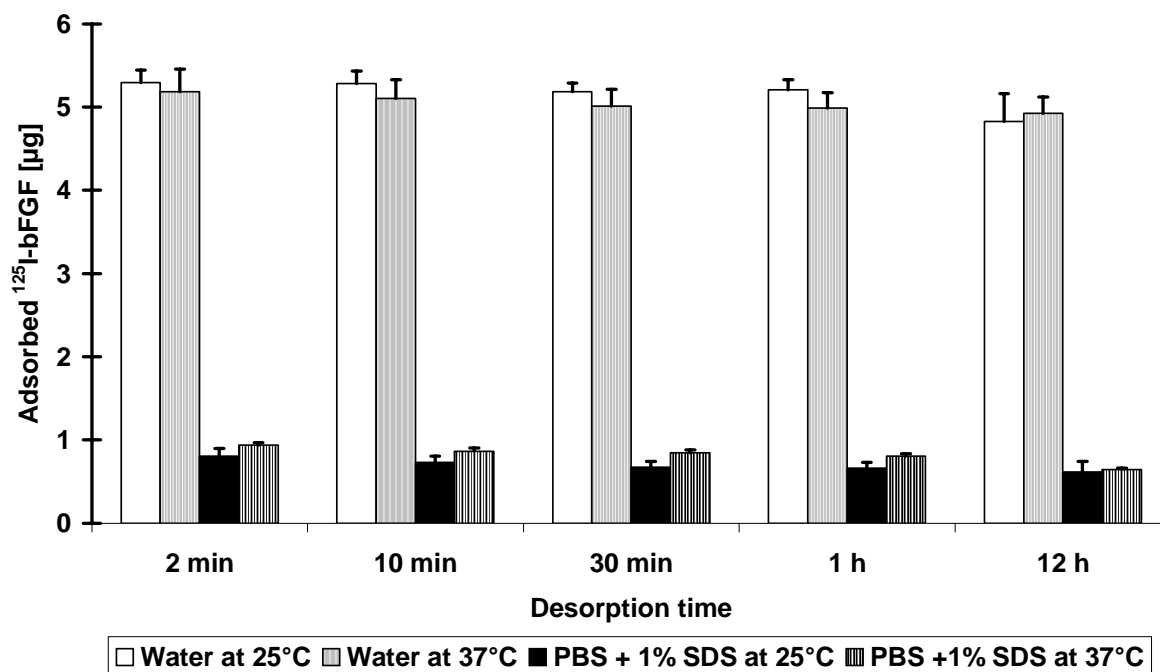


Fig. 6 Desorption of bFGF from PLA films at RT and 37°C. The amount of the remaining amounts of bFGF after the desorption procedure is shown. Water served as a control. Data represent mean \pm standard deviation ($n=3$).

Adsorption of bFGF to polymer scaffolds

In order to test the influence of the differential surface properties on the protein adsorption, different amounts of bFGF were adsorbed to PLGA, MeO-PEG₂PLA₄₀, and ST-NH-PEG₂PLA₄₀ scaffolds. Basic FGF adsorbed to all polymers in a dose-dependent manner (Fig. 7). The protein-resistant property of the PEG moiety of the PEG-PLA derivatives was moderately observable in the scaffold groups receiving 25 or 50 µg bFGF (dissolved in 1.5 ml buffer) in the feed (Fig. 7). However, when lower amounts of bFGF were provided in the feed, no difference in the bFGF adsorption was measured (Fig. 7).

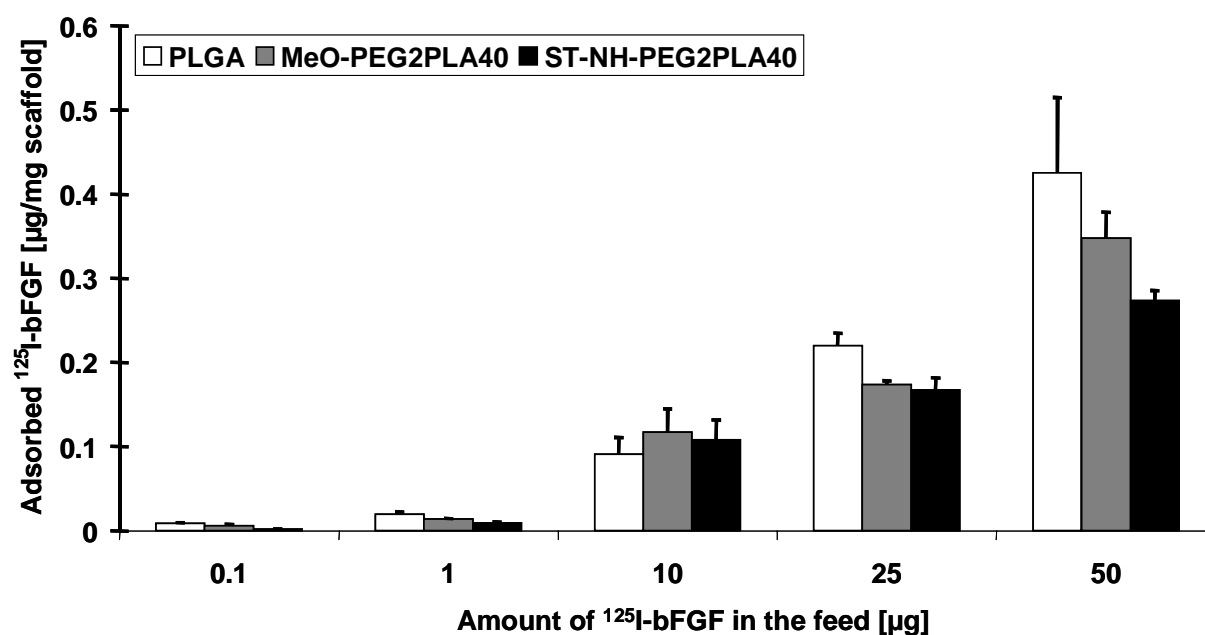


Fig. 7 Adsorption of bFGF to PLGA, MeO-PEG₂PLA₄₀, and ST-NH-PEG₂PLA₄₀ scaffolds. Different amounts of bFGF from 0 to 50 µg were provided in the feed. Data represent mean ± standard deviation (n=3).

Desorption of bFGF from polymer scaffolds

The SDS-containing buffer proved highly efficient for the desorption of bFGF from scaffolds, irrespective of the polymer material. After desorption for 90 h, between 97.7% and 99.5% of the initially adsorbed bFGF was removed from the scaffolds (Fig.8). The amount of bFGF adsorbed to PLGA scaffolds was elevated as compared to the scaffolds made from PEG-PLA derivatives at all points of time (Fig. 8). Although a higher amount of bFGF was initially adsorbed to MeO-PEG₂PLA₄₀ scaffolds than to ST-NH-PEG₂PLA₄₀ scaffolds, the remaining bFGF amount was higher on ST-NH-PEG₂PLA₄₀ scaffolds than on MeO-PEG₂PLA₄₀ scaffolds (Fig. 8). For the understanding of Figure 9, it should be noted that the calculated amount of covalently bound bFGF to ST-NH-PEG₂PLA₄₀ scaffolds was obtained by subtracting the remaining amount of bFGF on ST-NH-PEG₂PLA₄₀ scaffolds from the amount associated with MeO-PEG₂PLA₄₀ scaffolds after 90 h..

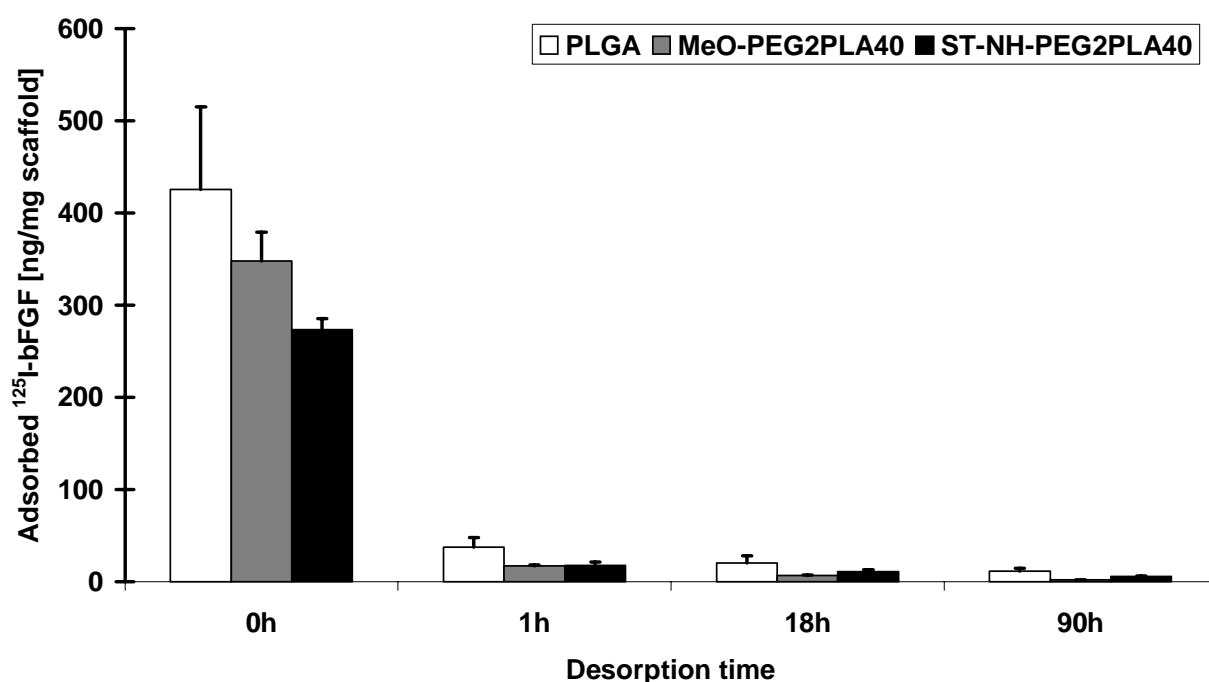


Fig. 8 Desorption of bFGF from PLGA, MeO-PEG₂PLA₄₀, and ST-NH-PEG₂PLA₄₀ scaffolds using PBS + 1% SDS over a maximum of 90 h. The amount of the remaining amounts of bFGF after the desorption procedure is shown. Data represent mean \pm standard deviation ($n=3$).

Covalent binding of bFGF to ST-NH-PEG₂PLA₄₀ scaffolds

As a first step towards the characterization of the covalent immobilization of bFGF in ST-NH-PEG₂PLA₄₀ scaffolds, two blend mixtures were evaluated. The first scaffold material consists of 70% ST-NH-PEG₂PLA₄₀ polymer and 30% MeO-PEG₂PLA₄₀ polymer; these scaffolds were used in the previous experiment (Fig. 8). An alternative blend represents the scaffold material consisting of 70% ST-NH-PEG₂PLA₄₀ polymer and 30% PLA polymer. The ST-NH-PEG₂PLA₄₀/PLA exhibited a higher stability as compared to the ST-NH-PEG₂PLA₄₀/MeO-PEG₂PLA₄₀ blend (upon gross examination), however, the amount of covalently bound bFGF was distinctly lower (Fig. 9).

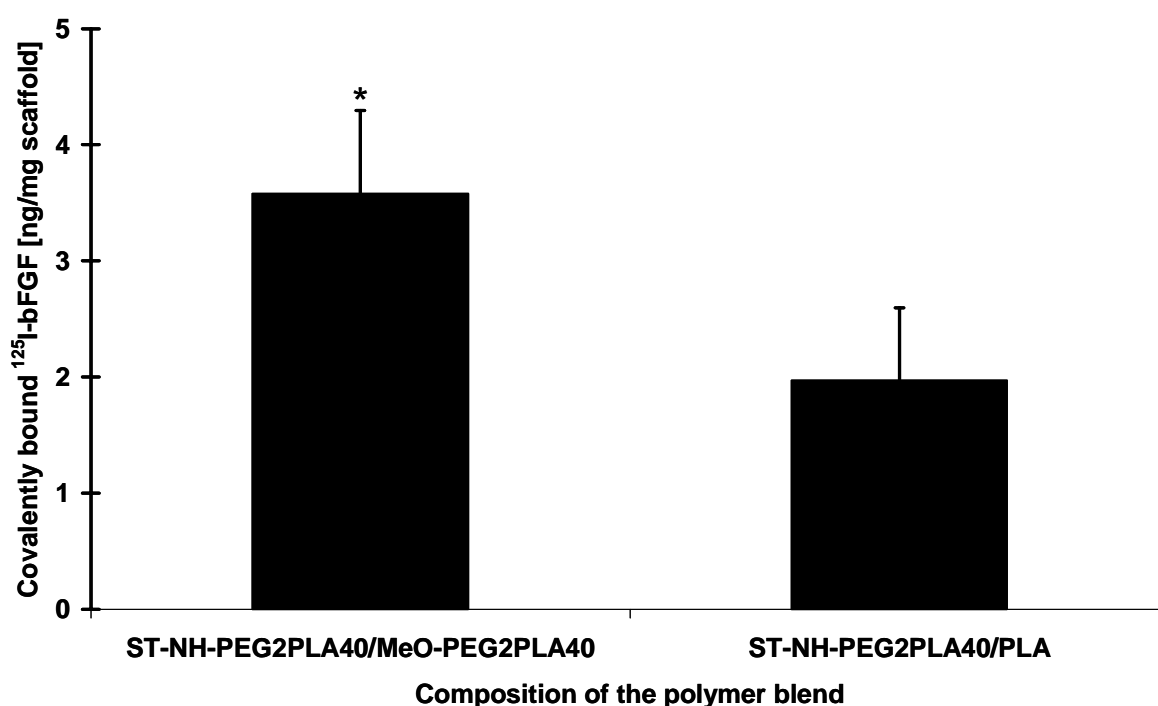


Fig. 9 The influence of the polymer blend on the amount of covalently bound bFGF. Data represent mean \pm standard deviation ($n=3$). The asterisk indicates a significantly elevated value as compared to scaffolds made from the ST-NH-PEG₂PLA₄₀/PLA blend at a level of $p<0.05$.

The next parameter tested was the incubation time of the scaffolds in the bFGF solution in order to anchor bFGF to ST-NH-PEG₂PLA₄₀/MeO-PEG₂PLA₄₀ scaffolds. The scaffolds were exposed to the bFGF solution for two hours and for six hours. The incubation for six hours led to a moderate increase of the amount of tethered bFGF (1.32 ± 0.23 -fold) as compared to an incubation period of two hours (Fig. 10). The difference was not statistically significant.

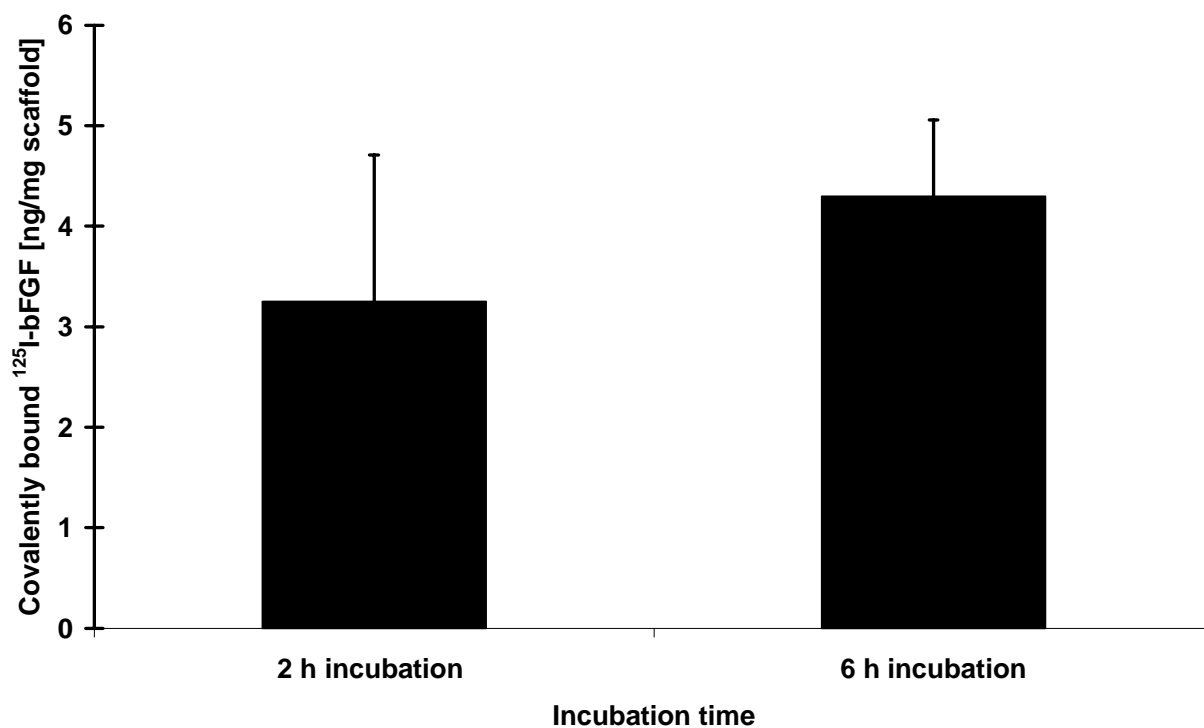


Fig. 10 Comparison of the amounts of tethered bFGF after incubation of the scaffolds (ST-NH-PEG₂PLA₄₀/MeO-PEG₂PLA₄₀) for two hours and for six hours. Data represent mean \pm standard deviation ($n=3$).

Discussion

This study demonstrates the interactions of the growth factor bFGF and, on the one hand, the lipophilic polymers PLA and PLGA and, on the other hand, the more hydrophilic PEG-PLA diblock copolymers with regard to protein adsorption and desorption. Furthermore, a protocol was established in order to determine the absolute amount of bFGF tethered to the amine-reactive polymer ST-NH-PEG₂PLA₄₀.

The contact angle measurements indicated that MeO-PEG₂PLA₄₀ polymer films have a more hydrophilic surface than PLA films. However, the differences of the contact angles of MeO-PEG₂PLA₄₀ and PLA were clearly observable not until 3 min after the droplet deposition (Fig. 2). The lagged feedback might be caused by a required swelling time of the PEG surfaces in the presence of water. The PEG chains might be first hydrated and subsequently erected and then, the PEG chains likely contributed to the elevated hydrophilicity of the MeO-PEG₂PLA₄₀ films. The clearly reduced bFGF adsorption to the MeO-PEG₂PLA₄₀ films, as compared to PLA films, indicated the presence of the PEG chains at the surface of the diblock copolymers (Fig. 3). In previous studies, PEG-PLA polymer derivatives have been shown to reduce the adsorption of the peptides and proteins calcitonin, atrial natriuretic peptide, and fibronectin to polymer films depending on the PEG/PLA ratios [8,13]. In the present study, the effect of the PEG-PLA derivatives on the reduction of bFGF adsorption to 3-D scaffolds was less pronounced than on polymer films (Fig. 7). Hacker et al. recently demonstrated that remnants of porogen material from the scaffold fabrication remain inside the scaffolds in a range from 2.5 to 8% of the scaffold weight [15]. The porogen material might be incorporated in the solid scaffold material or be residual on the surface of the scaffolds. The presence of lipids on the scaffold surface might have promoted the protein adsorption; protein adsorption has previously been demonstrated onto lipid surfaces [19].

Data of the adsorption experiments clearly demonstrated that the presence of PEG chains on the surface of PEG-PLA films or scaffolds reduces the adsorption of bFGF but does not lead to a complete inhibition of bFGF adsorption. In order to be able to distinguish between adsorbed and covalently bound bFGF in binding experiments as shown in Figures 9 and 10, it was absolutely necessary to efficiently remove adsorbed bFGF from the scaffolds. Therefore, a protocol was developed for an efficient desorption of adsorbed bFGF, whereby only a buffer consisting of PBS and 1% SDS was suitable for this purpose (Fig. 5). A desorption of 96 to 99% of the initially adsorbed amounts of bFGF was achieved using the SDS-containing buffer (Fig. 8). A buffer with high ionic strength (PBS + 2M NaCl) had virtually no effect on the desorption of bFGF from the polymer (Fig. 4). Buffers with high ionic strength are commonly

utilized as an eluent in heparin affinity chromatography of bFGF [20] but appear to be ineffective in combination with non-ionic surfaces in this study. Surprisingly, buffers containing the detergents Triton X-100, Tween 80, and Poloxamer 188 also showed roughly weak effects on the desorption of bFGF, similar to the control group using water.

The established desorption protocol allowed for the determination of the amount of bFGF covalently bound to ST-NH-PEG₂PLA₄₀ scaffolds. First, the potential of two polymer blends was evaluated with regard to the amounts of tethered bFGF. ST-NH-PEG₂PLA₄₀ was mixed with either MeO-PEG₂PLA₄₀ or with PLA in the same ratio (70:30). PLA-blended scaffolds appeared to be more stable than the ST-NH-PEG₂PLA₄₀/MeO-PEG₂PLA₄₀ blend (unpublished data). However, the amount of tethered bFGF was decreased in PLA-blended scaffolds as compared to the ST-NH-PEG₂PLA₄₀/MeO-PEG₂PLA₄₀ blend (Fig. 9). Possibly, the presence of PLA polymers in the scaffolds might lead to a partial impairment of the swelling of the PEG chains reducing the number of erected PEG chains protruding into the aqueous environment. Therefore, the possibility of a contact of bFGF molecules in the aqueous solution and activated end groups of the polymer might be reduced. In addition, two time periods were tested for the binding procedure in order to tether a maximum amount of bFGF to the scaffolds. However, incubation of the scaffolds for six hours only moderately increased the amount of tethered bFGF as compared to a two-hour incubation period (Fig. 10).

In conclusion, this study demonstrates the higher hydrophilicity of PEG-PLA polymer film or scaffold surfaces in comparison to PLA polymers without a PEG moiety and the resultant suppression of the adsorption of bFGF. Furthermore, the most favorable desorption buffer consisting of PBS and the detergent SDS allowed for the determination of the amount of bFGF covalently bound to ST-NH-PEG₂PLA₄₀ scaffolds. According to the results of this study, a polymer blend of 70% ST-NH-PEG₂PLA₄₀ and 30% MeO-PEG₂PLA₄₀ appears to be suitable as scaffold material and an incubation time for two hours appears to be suitable for the tethering of a sufficient amount of bFGF.

Acknowledgement

This work was supported by the Deutsche Akademische Austausch Dienst (DAAD) providing a six-month scholarship for Markus Neubauer at the University of Kyoto.

References

- [1] Hubbell JA. 'Biomaterials in tissue engineering'. *Bio/technology* (1995); **13**: 565-576.
- [2] Badylak SF. 'The extracellular matrix as a scaffold for tissue reconstruction'. *Sem Cell Dev Biol* (2002); **13**: 377-383.
- [3] Vats A, Tolley NS, Polak JM, Gough JE. 'Scaffolds and biomaterials for tissue engineering: a review of clinical applications'. *Clin Otolaryngol* (2003); **28**: 165-172.
- [4] Yang S, Leong KF, Du Z, Chua CK. 'The design of scaffolds for use in tissue engineering. Part I. Traditional factors'. *Tissue Eng* (2001); **7**: 679-689.
- [5] Drotleff S, Lungwitz U, Breunig M, Dennis A, Blunk T, Tessmar J, Gopferich A. 'Biomimetic polymers in pharmaceutical and biomedical sciences'. *Eur J Pharm Biopharm* (2004); **58**: 385-407.
- [6] Lutolf MP, Weber FE, Schmoekel HG, Schense JC, Kohler T, Muller R, Hubbell JA. 'Repair of bone defects using synthetic mimetics of collagenous extracellular matrices'. *Nat Biotechnol* (2003); **21**: 513-518.
- [7] Gref R, Luck M, Quellec P, Marchand M, Dellacherie E, Harnisch S, Blunk T, Muller RH. 'Stealth' corona-core nanoparticles surface modified by polyethylene glycol (PEG): influences of the corona (PEG chain length and surface density) and of the core composition on phagocytic uptake and plasma protein adsorption'. *Colloid Surface B* (2000); **18**: 301-313.
- [8] Lieb E, Tessmar J, Hacker M, Fischbach C, Rose D, Blunk T, Mikos AG, Gopferich A, Schulz MB. 'Poly(D,L-lactic acid)-poly(ethylene glycol)-monomethyl ether diblock copolymers control adhesion and osteoblastic differentiation of marrow stromal cells'. *Tissue Eng* (2003); **9**: 71-84.
- [9] Veronese FM. 'Peptide and protein PEGylation: a review of problems and solutions'. *Biomaterials* (2001); **22**: 405-417.
- [10] Roberts MJ, Bentley MD, Harris JM. 'Chemistry for peptide and protein PEGylation'. *Adv Drug Deliv Rev* (2002); **54**: 459-476.
- [11] Veronese FM, Harris JM. 'Introduction and overview of peptide and protein pegylation'. *Adv Drug Deliv Rev* (2002); **54**: 453-456.

- [12] Harris JM, Chess RB. 'Effect of pegylation on pharmaceuticals'. *Nat Rev Drug Discov* (2003); **2**: 214-221.
- [13] Lucke A, Te, Schnell E, Schmeer G, Gopferich A. 'Biodegradable poly(-lactic acid)-poly(ethylene glycol)-monomethyl ether diblock copolymers: structures and surface properties relevant to their use as biomaterials'. *Biomaterials* (2000); **21**: 2361-2370.
- [14] Tessmar JK, Mikos AG, Gopferich A. 'Amine-Reactive Biodegradable Diblock Copolymers'. *Biomacromolecules* (2002); **3**: 194-200.
- [15] Hacker M, Tessmar J, Neubauer M, Blaimer A, Blunk T, Gopferich A, Schulz MB. 'Towards biomimetic scaffolds: Anhydrous scaffold fabrication from biodegradable amine-reactive diblock copolymers'. *Biomaterials* (2003); **24**: 4459-4473.
- [16] Lieb E, Hacker M, Tessmar J, Kunz-Schughart LA, Fiedler J, Dahmen C, Hersel U, Kessler H, Schulz MB, Gopferich A. 'Mediating specific cell adhesion to low-adhesive diblock copolymers by instant modification with cyclic RGD peptides'. *Biomaterials*; in press.
- [17] Gospodarowicz D, Ferrara N, Schweigerer L, Neufeld G. 'Structural characterization and biological functions of fibroblast growth factor'. *Endocr Rev* (1987); **8**: 95-114.
- [18] Nugent MA, Iozzo RV. 'Fibroblast growth factor-2'. *Int J Biochem Cell Biol* (2000); **32**: 115-120.
- [19] Gessner A, Olbrich C, Schroder W, Kayser O, Muller RH. 'The role of plasma proteins in brain targeting: species dependent protein adsorption patterns on brain-specific lipid drug conjugate (LDC) nanoparticles'. *Int J Pharm* (2001); **214**: 87-91.
- [20] Shah D, Johnston TP, Mitra AK. 'Thermodynamic parameters associated with guanidine HCl- and temperature-induced unfolding of bFGF'. *Int J Pharm* (1998); **169**: 1-14.

Chapter 9

Instant Surface Modification of 3-D Polymeric Scaffolds Allows for the Tethering of bFGF and Generation of Vascularized Constructs

Markus Neubauer,^{1,2} Michael Hacker,^{1,3} Sigrid Drotleff,¹ Makoto Ozeki,² Jörg Teßmar,^{1,3}
Michaela B Schulz,¹ Antonios G Mikos,³ Yasuhiko Tabata,² Torsten Blunk,¹ Achim
Göpferich¹

¹ Department of Pharmaceutical Technology, University of Regensburg, Universitätsstraße 31, 93040 Regensburg, Germany

² Institute for Frontier Medical Sciences, Field of Tissue Engineering, Department of Biomaterials, Kyoto University, 53 Kawara-cho Shogoin, Sakyo-ku, Kyoto 606-8507, Japan.

³ Department of Bioengineering, Rice University, MS 142, P.O. Box 1892, Houston, TX, USA

to be submitted to Proc. Natl. Acad. Sci. U.S.A.

Abstract

Biomimetic polymers represent a novel class of biomaterials for the control of the interactions with cells at the molecular level. We have fabricated 3-D cell carriers from derivatives of poly (ethylene glycol)-poly (lactic acid) (PEG-PLA) diblock copolymers exhibiting a protein-resistant surface which is modifiable by the covalent binding of bioactive agents such as peptides and proteins.

In this study, basic fibroblast growth factor (bFGF) was covalently bound to 3-D cell carriers by a simple incubation step. The amounts of covalently immobilized bFGF were determined and radiolabeled bFGF was retained in the scaffolds for three weeks *in vivo*. Tethered bFGF on the surface of the 3-D scaffolds led to vascularization of the scaffolds, in contrast, adsorbed bFGF failed to provoke an ingrowth of fibrovascular tissue. This study demonstrates novel 3-D devices for an instant surface modification to immobilize proteins and peptides such as growth factors for tissue engineering applications .

Introduction

In the field of tissue engineering, the overall goal is the development and the maintenance of functional tissues demanding an optimum combination of cells, cell carriers, and bioactive agents [1]. In recent years a new generation of biomaterials has been designed to modulate the cellular response at the molecular level [2,3]. In this respect, the surface modification of biomaterials used for tissue engineering and implantation applications represents one major tool to control the interactions with attached cells and the surrounding tissue after implantation [4]. The design of low-adhesive “stealth” surfaces modifiable by immobilization of specific agents which can exert desired interactions with target cells or target tissues is one possible way to create biomimetic materials reflecting and mimicking the properties of biological environments [4].

Proteins and peptides represent highly potent agents for the modulation of the tissue development including cellular proliferation, differentiation, motility, adhesion, and angiogenic processes, which have been utilized in tissue engineering approaches, predominantly in the form of growth factors [5,6]. Growth factors generally require to be provided by drug delivery devices for the maintenance of constant concentrations of the factors due to their extremely short half-lives (in the range from minutes to hours) [7,8]. For instance, basic fibroblast growth factor (bFGF) which is known to induce chemotactic, mitogenic, and angiogenic activity and to be involved in differentiation and developmental processes exhibits a plasma half-life of approx. 1.5 minutes [7,9].

Covalent binding of growth factors to polymeric cell carriers is a strategy that combines the delivery of growth factors and the creation of a biomimetic scaffold surface [10,11]. Various strategies have been employed to tether peptides and proteins to biomaterials, mostly conducted in 2-D attempts. For instance, peptide fragments of bone morphogenetic proteins and epidermal growth factor have been tethered to activated glass [10,12] and insulin has been reported to be covalently immobilized onto poly(methyl methacrylate) films [13]; remarkably, the bioactivity of the peptides was retained or even improved after immobilization compared to the soluble form. In 3-D approaches, TGF β 1, TGF β 2, and bFGF have been tethered to PEG hydrogels and injectable collagen gels [14,15]; insulin and RGD peptides have been tethered to non-woven polyester meshes for tissue engineering applications [16]. However, the applied reactions for the surface modification involve laborious procedures due to the absence of functional groups on the scaffold surfaces. Furthermore, the used cell carriers such as hydrogels or fibers lack mechanical strength and stability required in many tissue engineering applications.

Therefore, we have designed a polymer which can be processed into stable sponge-like scaffolds [17] and allows for a surface modification by a simple “instant-like” incubation step [18]. This polymer consists of a 40 kDa lipophilic poly (lactic acid) (PLA) moiety and a hydrophilic asymmetric 2 kDa poly (ethylene glycol) (PEG) moiety coupled to succinimidyl tartrate as an amine-reactive linker, abbreviated as ST-NH-PEG₂PLA₄₀. The PLA chain functions as the backbone responsible for the biodegradability and the stability and the PEG component including the reactive linker represents the protein adsorption-resistant and substrate-binding chain [19,20]. Bioactive molecules bearing free amine groups can be covalently bound to these polymers resulting in a stable amide linkage.

The goal of this study was to demonstrate the feasibility of the instant surface modification of stable 3-D scaffolds with the angiogenic growth factor bFGF [21]. This study provides data about the determination of the amount of covalently immobilized basic fibroblast growth factor (bFGF) onto 3-D scaffolds, the evaluation of the stability of the covalent linkage *in vivo*, and the investigation of angiogenic effects of the growth factor bFGF tethered to 3-D scaffolds in comparison with the adsorbed form after implantation into the subcutis of mice.

Materials and Methods

Materials

Basic FGF was purchased from Kaken Pharmaceutical, Tokyo, Japan. PEG-PLA diblock copolymers (approx. 42 kDa) were synthesized in our laboratory [22], poly(lactic-co-glycolic acid) (PLGA 75:25; approx. 90 kD) was obtained from Boehringer Ingelheim (Ingelheim am Rhein, Germany).

Polymer synthesis

The polymer ST-NH-PEG₂PLA₄₀ was synthesized and characterized as described by Tessmar et al. [19]. Briefly, the precursor H₂N-PEG₂PLA₄₀ was synthesized by a ring-opening polymerization of poly(D,L-lactic acid) with poly(ethylene glycol)-monoamine using stannous 2-ethylhexanoate as catalyst. ST-NH-PEG₂PLA₄₀ was obtained by attachment of disuccinimidyl tartrate to H₂N-PEG₂PLA₄₀ (Fig. 1A). MeO-PEG₂PLA₄₀ was synthesized and characterized as previously described in [22] (Fig. 1B).

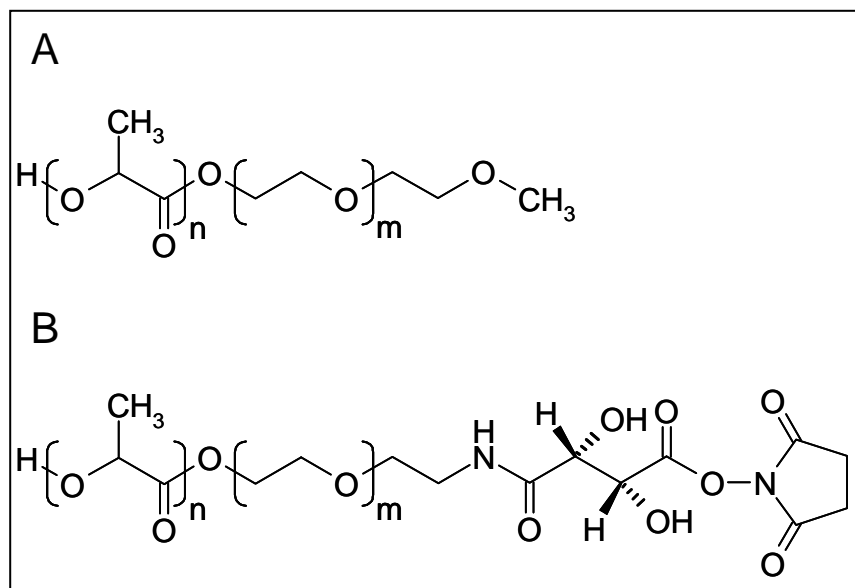


Fig. 1 Structures of the derivatives of poly(D,L-lactic acid)-block-poly(ethylene glycol):
A Poly(D,L-lactic acid)-poly(ethylene glycol)-monomethyl ether (MeO-PEG₂PLA₄₀),
B Succinimidyl tartrate PEG-PLA (ST-NH-PEG₂PLA₄₀).

Scaffold fabrication

Scaffolds were fabricated using a protocol adapted from Hacker et al. [17]. Polymer-specific parameters are shown in Table 1. Briefly, the scaffolds were fabricated from polymer dissolved in a methyl ethyl ketone-tetrahydrofuran-mixture (59:41 (v/v)) and lipid microparticles made from Softisan[®] 154 (S) and Witepsol[®] H42 (H) (kindly provided by SASOL Germany (Witten, Germany)) were weighed into a separate vial. The size of porogen particles ranged from 100 μm to 300 μm . After 1 h storage at -20°C the porogen particles were transferred into the polymer solution and mixed for 5 min on ice. The resulting highly viscous dispersion was then transferred into a 10 ml polypropylene syringe and injected into cubic Teflon[®] molds (with a cylindrical cavity of 0.8 cm in diameter). After a pre-extraction treatment step in n-hexane at 0°C for t_0 , the filled molds were submerged in warm n-hexane to precipitate the polymer and extract the porogen particles concurrently. This procedure was carried out in two separate n-hexane baths of different temperatures: first, molds were incubated at T_1 for t_1 and in a second step at T_2 for t_2 . Subsequently, the molds were transferred into a n-hexane bath of 0°C for 5 min. Finally, the porous cylindrical polymer constructs were removed from the molds and vacuum-dried for 48 h. For further investigations the constructs were cut into 2 mm slices which were then addressed as scaffolds.

Group	Polymer	Lipid mixture (S/H)	t ₀ [min]	T ₁ [°C]/t ₁ [min]	T ₂ [°C]/t ₂ [min]
PLGA	100% PLGA	2:1	15	52/10	40/20
MeO-PEG ₂ PLA ₄₀	100% MeO- PEG ₂ PLA ₄₀	1:1	90	45/7.5	35/22.5
ST-NH- PEG ₂ PLA ₄₀	70% ST-NH- PEG ₂ PLA ₄₀ + 30% MeO-PEG ₂ PLA ₄₀	1:1	90	45/7.5	35/22.5

Table 1: Polymer-specific parameters used for the scaffold fabrication.

Radiolabeling of bFGF

Different amounts of bFGF were labeled using the chloramine T method. In the following, the preparation of 100 µl of a 10 mg/ml bFGF is exemplarily described. 5.00 µl ¹²⁵NaI (3.7 MBq) were added to 100 µl of a 10 mg/ml bFGF solution. After the addition of 100 µl of a 0.2 mg/ml chloramine T solution (710 µM final concentration), the mixture was shaken for 2 min. In order to stop the reaction, 100 µl of a 4 mg/ml sodium metabisulfite solution (21 mM final concentration) was mixed and shaken with the bFGF solution for 2 min. The resulting solution was subjected to a PD-10 column, Sephadex G-25 M (Amersham Biosciences, Uppsala, Sweden) and bFGF was eluted using a phosphate-buffered saline (PBS) pH 8.0. The resultant solution was a 1 mg/ml bFGF solution in PBS, pH 8.0, which was used at different dilutions for all adsorption and binding experiments.

Determination of the amounts of covalently bound bFGF to scaffolds

Scaffolds made from MeO-PEG₂PLA₄₀ and ST-NH-PEG₂PLA₄₀ were strung onto 22G needles and located with small segments of silicone tubing. Subsequently, scaffolds were pre-wetted in 70% ethanol and extensively rinsed with PBS pH 8.0. In order to anchor bFGF, scaffolds were incubated in bFGF solution (in PBS pH 8.0) concentrated from 0 to 100 µg bFGF in 1.5 ml buffer for two hours at room temperature (RT) on a shaker (20 min⁻¹). After washing the scaffolds in PBS pH 7.4, they were treated with 1% sodium dodecyl sulphate (SDS, Nacalai Tesque, Kyoto, Japan) in PBS pH 7.4 in order to desorb non-covalently bound bFGF for 90 h at RT on a shaker (20 min⁻¹). Finally, the scaffolds were subjected to scintillation. Some scaffolds were subjected to scintillation after the treatment with SDS for only 1 h in order to assess the amount of adsorbed/covalently immobilized bFGF prior to implantation. For the control group which allows for the correction for bFGF adsorption, bFGF was adsorbed to and desorbed from MeO-PEG₂PLA₄₀ under the same conditions as

described for the covalent binding of bFGF to the ST-NH-PEG₂PLA₄₀. The amount of bFGF covalently bound to ST-NH-PEG₂PLA₄₀ scaffolds was calculated by subtracting the amount associated with MeO-PEG₂PLA₄₀ control scaffolds from that associated with ST-NH-PEG₂PLA₄₀ scaffolds.

Stability of the linkage in biomimetic scaffolds in vivo

¹²⁵I-bFGF was adsorbed and covalently bound to MeO-PEG₂PLA₄₀ and ST-NH-PEG₂PLA₄₀ scaffolds, respectively, by incubation in 1.5 ml buffer solution containing 50 μg ¹²⁵I-bFGF for 2 h at RT on a shaker (20 min⁻¹). After washing the scaffolds in PBS pH 7.4, they were treated with 1% sodium dodecyl sulphate (SDS) in PBS pH 7.4 in order to desorb bFGF for 1 h at RT on a shaker (20 min⁻¹). The scaffolds with adsorbed and bound ¹²⁵I-bFGF were implanted into the back subcutis of mice (female ddY mice (6 to 8-week-old), Japan SLC, Hamamatsu, Japan) following a washing step with PBS pH 7.4. Additionally, an aqueous solution of ¹²⁵I-bFGF (250 ng/site) was subcutaneously injected into the back of mice. After certain time intervals, the scaffolds or the injection site were excised and the adjacent tissue was wiped off with a tissue. The radioactivity of the residual scaffolds, the skin, and the paper was measured using the gamma counter. The ratio of the thus measured radioactivity to the radioactivity of bFGF initially used were expressed as the percentage of the remaining activity in the *in vivo* bFGF release experiment. Three mice were sacrificed at each point of time and for each experimental condition. Animal experiments were done according to the institutional guidance of Kyoto University on animal experimentation.

Assessment of angiogenesis induced by adsorbed and tethered bFGF in vivo

Basic FGF was adsorbed and covalently bound to PLGA, MeO-PEG₂PLA₄₀ and ST-NH-PEG₂PLA₄₀ scaffolds, respectively, by incubation in a 1.5 ml buffer solution containing 50 μg bFGF for 2 h at RT on a shaker (20 min⁻¹). After washing the scaffolds in PBS pH 7.4, they were treated with 1% sodium dodecyl sulphate (SDS) in PBS pH 7.4 in order to desorb bFGF for 1 h at RT on a shaker (20 min⁻¹). Scaffolds were washed with PBS pH 7.4 and were implanted into the back subcutis of mice. Control scaffolds without bFGF were treated the same way but the incubation buffer contained no bFGF. Three mice were sacrificed for each experimental condition three weeks after implantation and scaffolds were prepared for the evaluation of angiogenic effects and ingrowth of fibrovascular tissue. The scaffolds were excised with the adjacent tissue, rinsed in PBS, and fixed with 2.5 % glutaraldehyde for 15 min. Subsequently, scaffolds were treated with 10% formaldehyde in PBS for storage. Fixed scaffolds were embedded in Tissue Tek. 10 μm thick sections were cut on a cryotome and

were stained with hematoxylin and eosin (H&E). In detail, scaffolds were halved, three sections were cut from the middle of the construct (layer 1), and further three sections were cut each at a distance of approx. 200 μm (layer 2) and 400 μm (layer 3) from layer 1. All capillaries observed in the entire cross-sections were counted under an inverse light microscope. The capillary number of one scaffold was calculated from the mean of the nine values obtained from layers 1-3. The mean for each experimental condition resulted from scaffolds from three mice.

Statistics

All data are expressed as means \pm standard deviation. Single-factor analysis of variance (ANOVA) was used in conjunction with a multiple comparison test (Tukey's test) to assess statistical significance at a level of $p < 0.01$ or $p < 0.05$.

Results

Principle

Scaffolds were fabricated from PLGA and PEG-PLA derivatives. The activated ST-NH-PEG₂PLA₄₀ scaffolds represent an "off-the-shelf" product that is storable over a long time period. When required, the scaffold surface can be modified by simple incubation in a solution of a bioactive agent bearing free amine groups such as bFGF in this study (Fig.2).

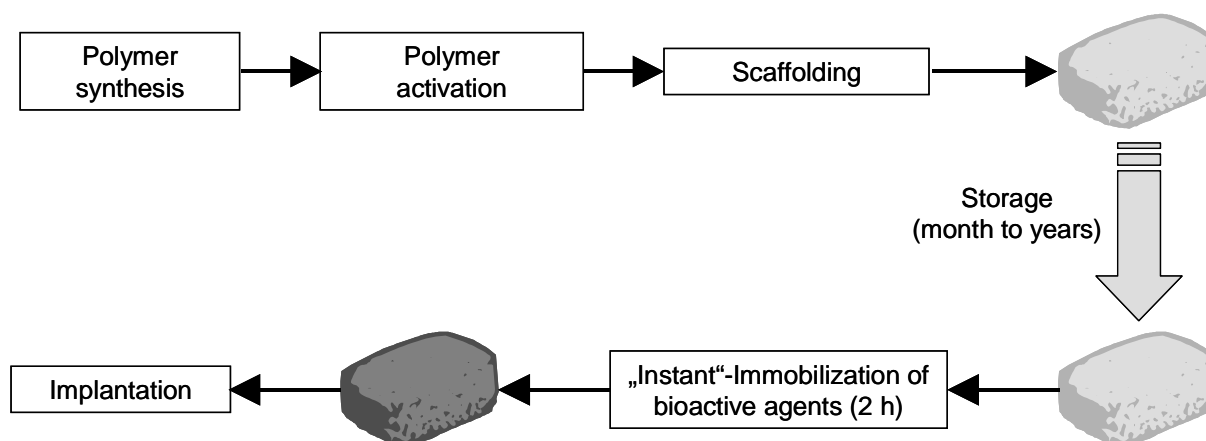


Fig. 2 Principle of the instant surface modification of 3-D polymeric scaffolds. The scaffolds were fabricated from the activated polymer ST-NH-PEG₂PLA₄₀ which can be stored under the exclusion of moisture. When required for implantation, a bioactive compound such as bFGF can be covalently immobilized by a simple incubation of the scaffolds in the bFGF solution for two hours.

Determination of the amounts of covalently bound bFGF to scaffolds

In order to determine the amount of bFGF tethered to the ST-NH-PEG₂PLA₄₀ scaffolds, these scaffolds and MeO-PEG₂PLA₄₀ control scaffolds were incubated for two hours at room temperature in solutions with different bFGF concentrations at pH 8.0. With an increasing amount of bFGF in the incubation solution, the amount of covalently immobilized bFGF could be elevated (Fig. 3). The minimum concentration of bFGF required in the feed was 10 µg in 1.5 ml incubation buffer in order to anchor a detectable amount of bFGF (Fig. 3). Applying 50 µg bFGF in the feed, 3.6±0.7 ng/mg scaffold could be tethered to ST-NH-PEG₂PLA₄₀ scaffolds (Fig. 3). The use of 100 µg bFGF resulted in a similar amount of tethered bFGF as compared to 50 µg (Fig. 3). In the following *in vivo* studies, scaffolds were incubated in a solution of 50 µg bFGF.

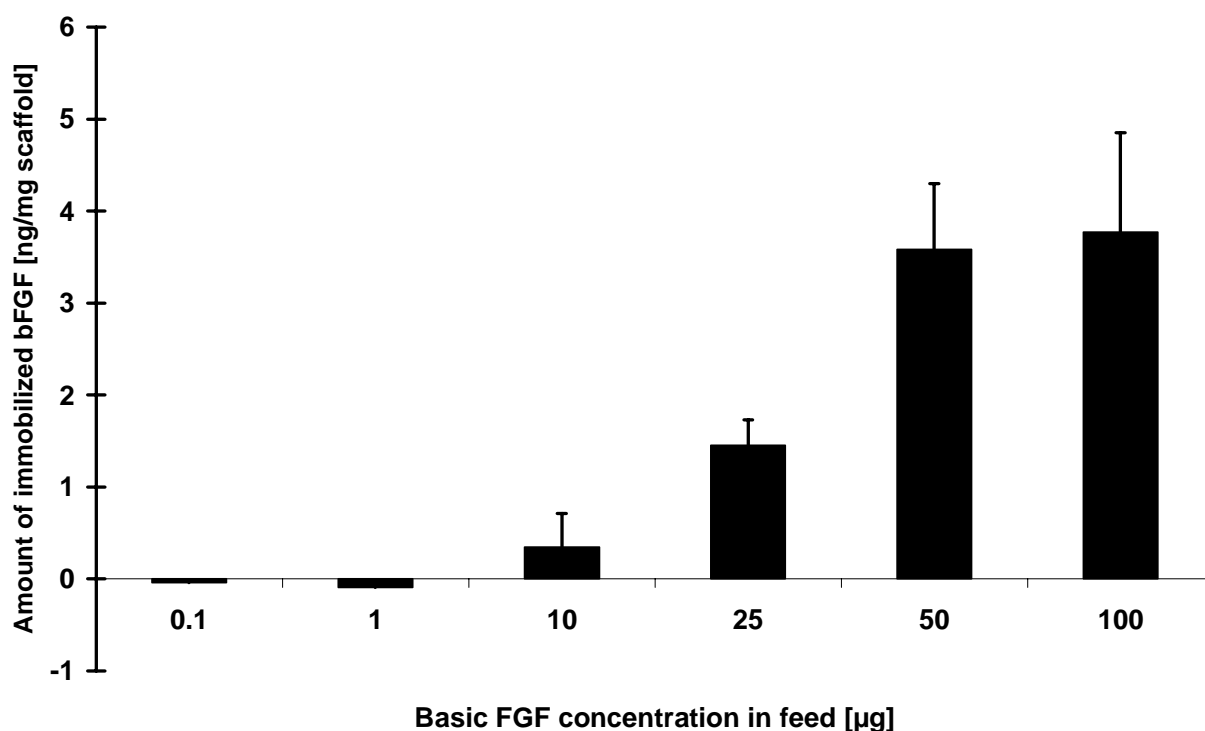


Fig. 3 Determination of the amount of covalently immobilized bFGF. 0.1 to 100 µg bFGF in 1.5 ml incubation buffer were provided in the feed for the binding reaction to ST-NH-PEG₂PLA₄₀ scaffolds. The amount of bFGF covalently bound to ST-NH-PEG₂PLA₄₀ scaffolds was calculated by subtracting the amount associated with MeO-PEG₂PLA₄₀ control scaffolds from that associated with ST-NH-PEG₂PLA₄₀ scaffolds (n=3).

Remaining amount of bFGF after desorption on the scaffolds

In the following *in vivo* experiments, bFGF was desorbed for 1 h before implantation. This short time period was chosen to guarantee the stability of bFGF although it is insufficient to desorb the whole amount of adsorbed protein (Chapter 8, Fig. 8). Figure 4 shows the amounts of adsorbed and/or covalently bound bFGF remaining after desorption for 1 h. Approx. double the amount of bFGF was recovered on PLGA scaffolds (36.95 ± 10.54) as compared to the PEG-PLA derivatives (Fig. 4). A similar amount of bFGF was detected on MeO-PEG₂PLA₄₀ scaffolds (17.12 ± 0.80 ng/mg scaffold) and ST-NH-PEG₂PLA₄₀ scaffolds (17.73 ± 3.44 ng/mg scaffold) (Fig. 4). Scaffolds were implanted with these amounts of bFGF adsorbed/covalently bound to the different scaffold types.

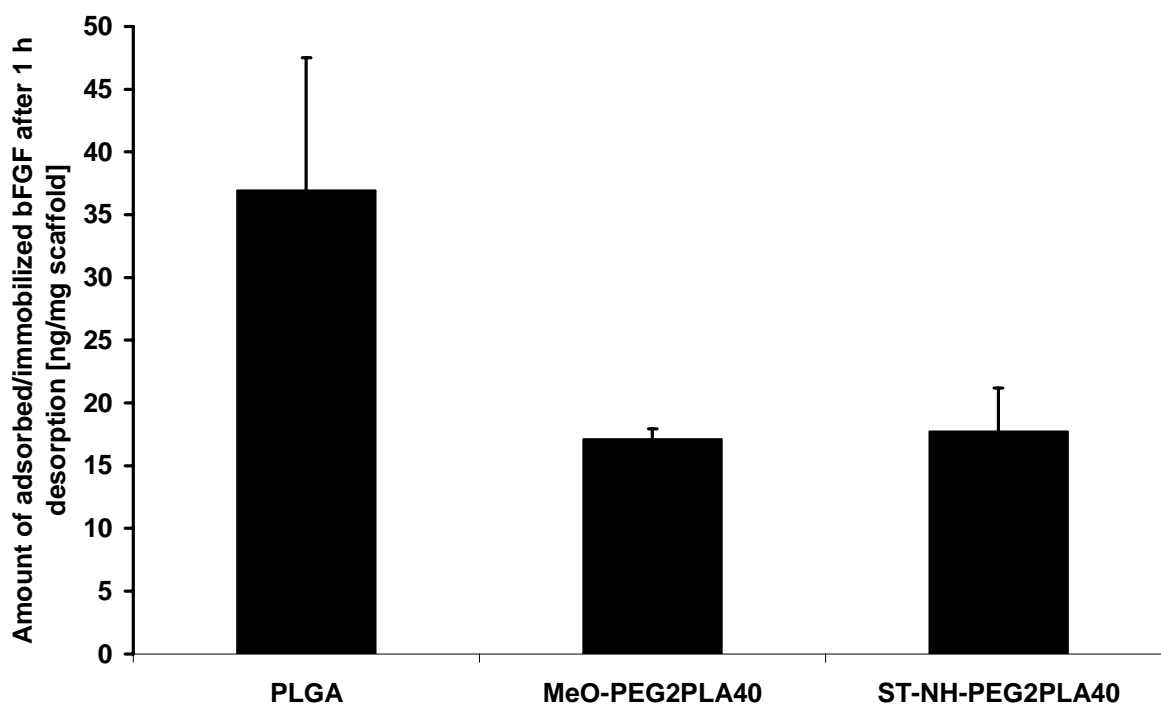


Fig. 4 Remaining amount of bFGF on the scaffolds after desorption for 1 h. The amount of bFGF is normalized to the masses of the scaffolds.

Stability of the linkage of bFGF in biomimetic scaffolds in vivo

The resultant amide linkage between the ST-NH-PEG₂PLA₄₀ polymer and bFGF should be stable under physiological conditions and thus, bFGF should be retained within the scaffold for a certain period of time. In order to test the stability of the linkage, scaffolds with radiolabeled bFGF bound to ST-NH-PEG₂PLA₄₀ scaffolds and adsorbed to MeO-PEG₂PLA₄₀ scaffolds were subcutaneously implanted into mice. As a control group, bFGF was

administered as a s.c. injection into the backs of mice. The amount of injected bFGF rapidly decreased and was significantly different from absorbed and bound bFGF after three days (Fig. 5). Scaffolds with exclusively adsorbed bFGF (MeO-PEG₂PLA₄₀) and scaffolds with adsorbed and bound bFGF (ST-NH-PEG₂PLA₄₀) exhibited similar amounts of remaining bFGF after 1, 3, and 7 days (Fig. 5). During this time period, loosely adsorbed bFGF was released from the scaffolds in the adjacent tissue. The amount of adsorbed bFGF steadily decreased on MeO-PEG₂PLA₄₀ scaffolds until day 21 (Fig. 5). In contrast, a constant amount of bFGF was retained within the ST-NH-PEG₂PLA₄₀ scaffolds from day 7 to day 21 (Fig. 5). Here, 21.3±8.6% of the initially adsorbed/bound bFGF were recovered after three weeks, that is, 3.82±0.33 ng bFGF/mg scaffold. This amount is equal to the amount of bFGF initially tethered to the scaffolds (3.6±0.7 ng bFGF/mg scaffold) as shown in Figure 3.

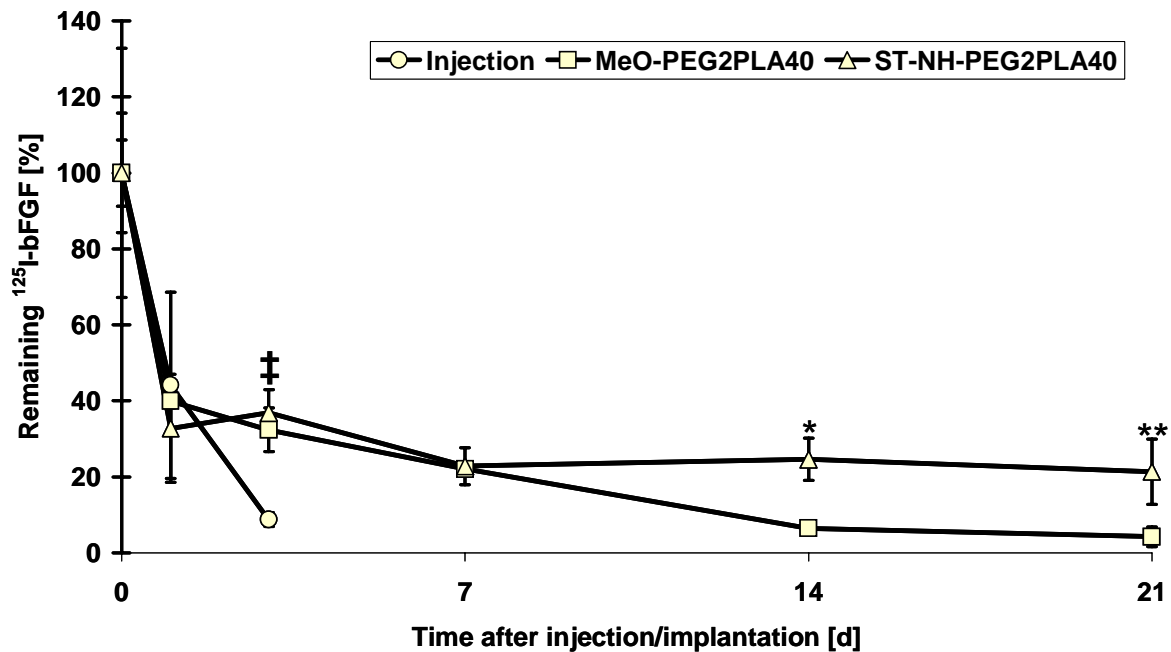


Fig. 5 Stability of the bFGF binding in vivo. Basic FGF was administered in the soluble form as s.c. injection, on MeO-PEG₂PLA₄₀ scaffolds with exclusively adsorbed bFGF, and on ST-NH-PEG₂PLA₄₀ scaffolds with adsorbed and bound bFGF. The amount of remaining bFGF is expressed as the percentage of the amount of bFGF adsorbed/bound to the scaffolds prior to the implantation or as the percentage of the injected amount of bFGF. The statistically significant difference of bFGF delivered by the scaffolds as compared to the injection group is denoted by † ($p < 0.01$). Statistically significant differences of ST-NH-PEG₂PLA₄₀ scaffolds with adsorbed/covalently bound bFGF as compared to MeO-PEG₂PLA₄₀ scaffolds with only adsorbed bFGF are denoted by * ($p < 0.01$) and ** ($p < 0.05$) ($n = 3$).

Assessment of angiogenesis induced by adsorbed and tethered bFGF in vivo

Scaffolds made from PLGA, MeO-PEG₂PLA₄₀, and ST-NH-PEG₂PLA₄₀ were subcutaneously implanted into mice for three weeks, either as blank scaffolds or after adsorption or covalent binding of bFGF (for amounts of bFGF see Fig. 4). The bioactivity and the angiogenic effects of adsorbed or tethered bFGF were determined. The remaining amounts of bFGF after the desorption procedure is shown in Figure 4.

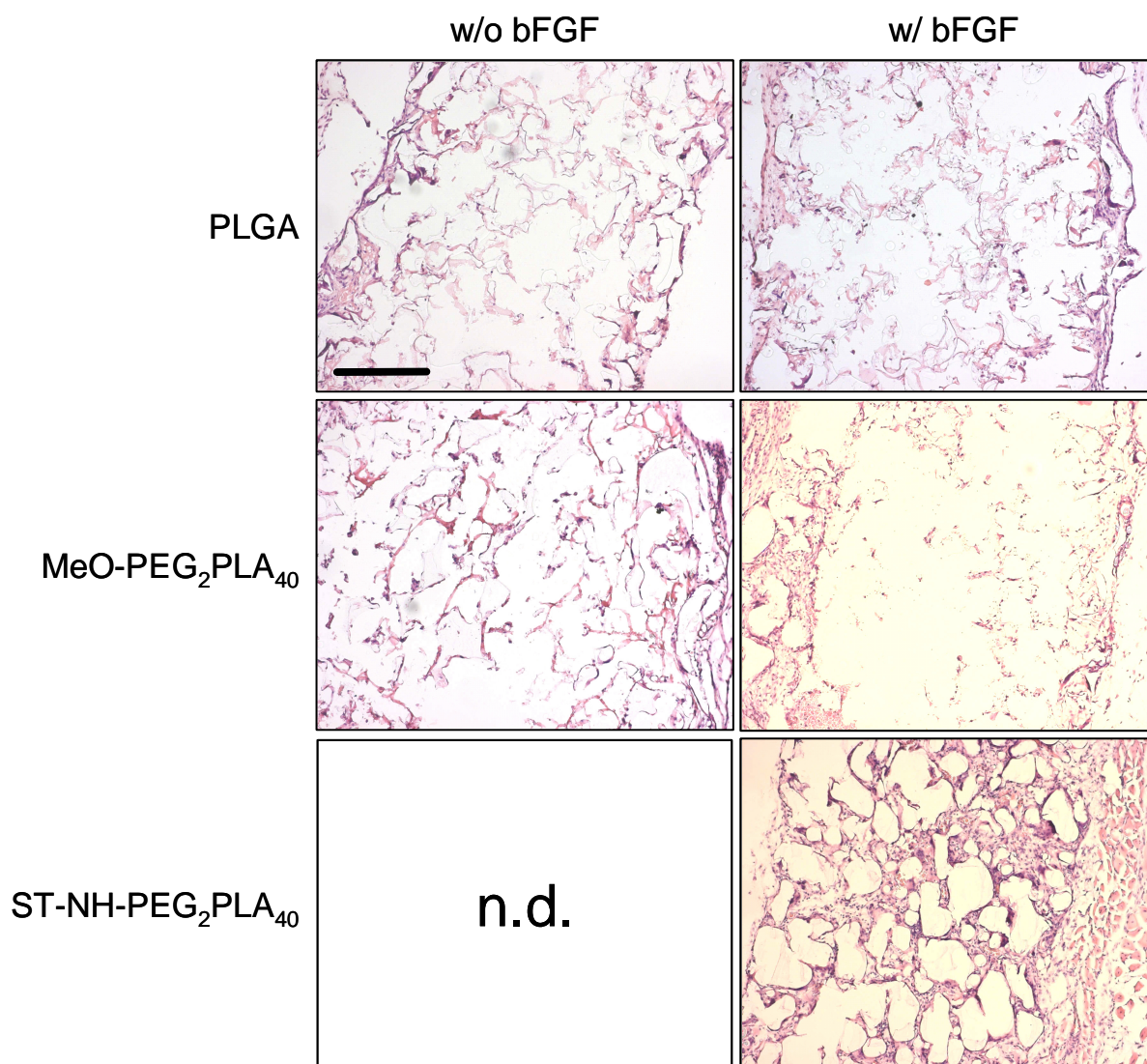


Fig. 6a H&E histology of constructs excised after 3 weeks. Photographs of the scaffolds without and with adsorbed or bound bFGF were taken in 100-fold magnification. Scale bar: 300 μ m. ST-NH-PEG₂PLA₄₀ scaffolds without bFGF could not be evaluated due to instability and shrinkage in vivo.

PLGA and MeO-PEG₂PLA₄₀ constructs exhibited a very low degree of ingrowth of fibrovascular tissue, irrespective of the presence of adsorbed bFGF (Fig. 6a). Only a few blood vessels were observed within these scaffolds, preferably in the regions of the scaffolds

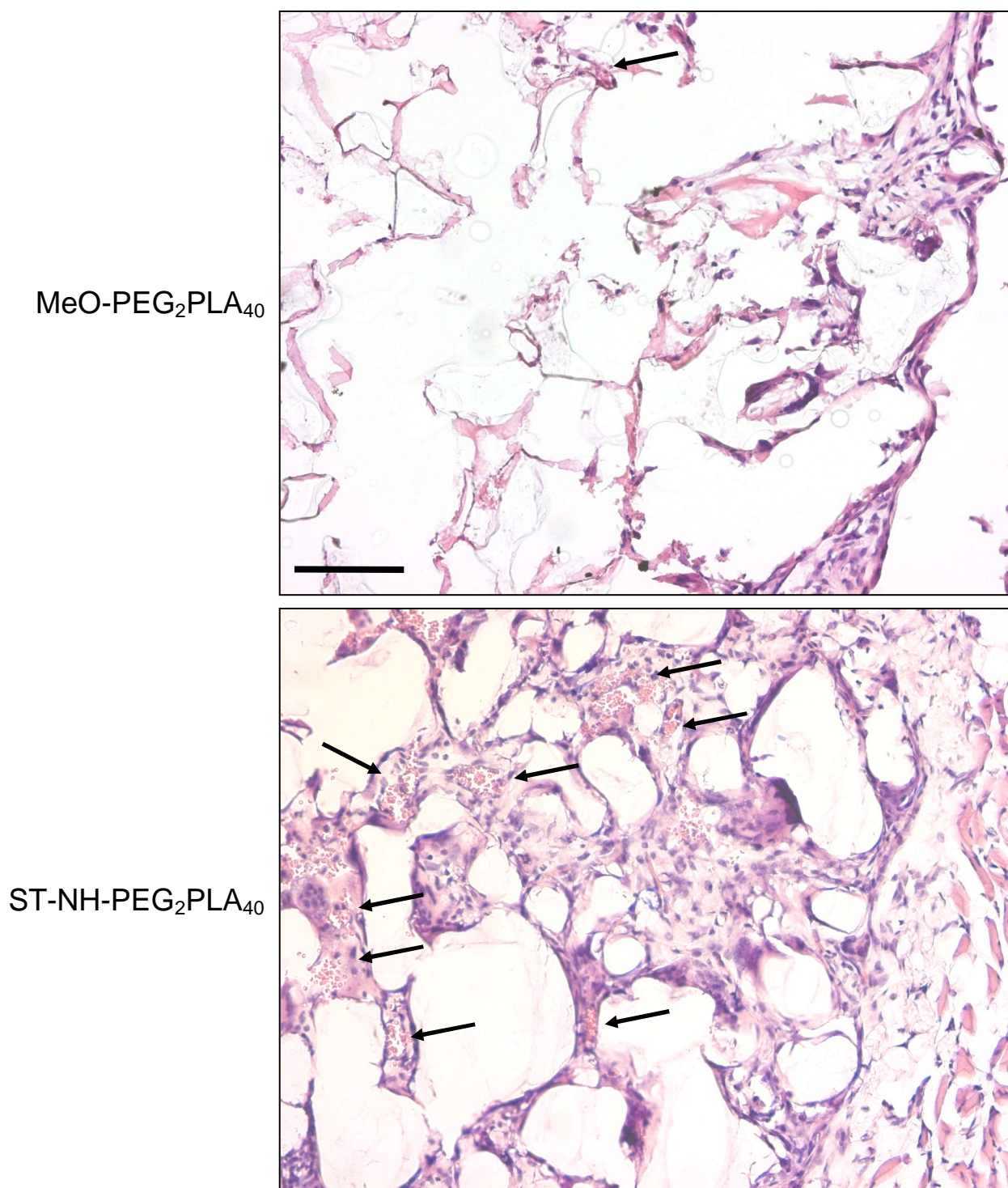


Fig. 6b H&E histology of constructs at higher magnification (200-fold). Two experimental groups, MeO-PEG₂PLA₄₀ and ST-NH-PEG₂PLA₄₀ with bFGF, are exemplarily depicted in order to demonstrate the effect of covalently bound bFGF on the ingrowth of capillaries and connective tissue as compared to adsorbed bFGF. Black arrows mark capillaries within the constructs. Scale bar: 100 μ m.

close to the adjacent tissue. In detail, 5.0 ± 0.4 capillaries were detected within cross-sections of PLGA scaffolds without bFGF, 8.4 ± 5.1 in PLGA scaffolds with bFGF, 3.3 ± 1.9 in MeO-PEG₂PLA₄₀ scaffolds without bFGF, and 5.0 ± 0.4 in MeO-PEG₂PLA₄₀ scaffolds with bFGF

(Fig. 7). In contrast, a significantly higher number of capillaries (40.9 ± 11.5 in cross-sections) penetrated into the ST-NH-PEG₂PLA₄₀ constructs with covalently bound bFGF accompanied by a clearly enhanced ingrowth of connective tissue as compared to all other experimental groups (Figs. 6, 7). ST-NH-PEG₂PLA₄₀ constructs without bFGF could not be evaluated due to their instability and strong shrinkage *in vivo*. Figure 6b exemplarily shows two experimental groups, MeO-PEG₂PLA₄₀ and ST-NH-PEG₂PLA₄₀ with bFGF, at a higher magnification. The density of blood vessels and the ingrowth of connective tissue in ST-NH-PEG₂PLA₄₀ scaffolds with tethered bFGF was strikingly increased as compared to scaffolds with adsorbed bFGF.

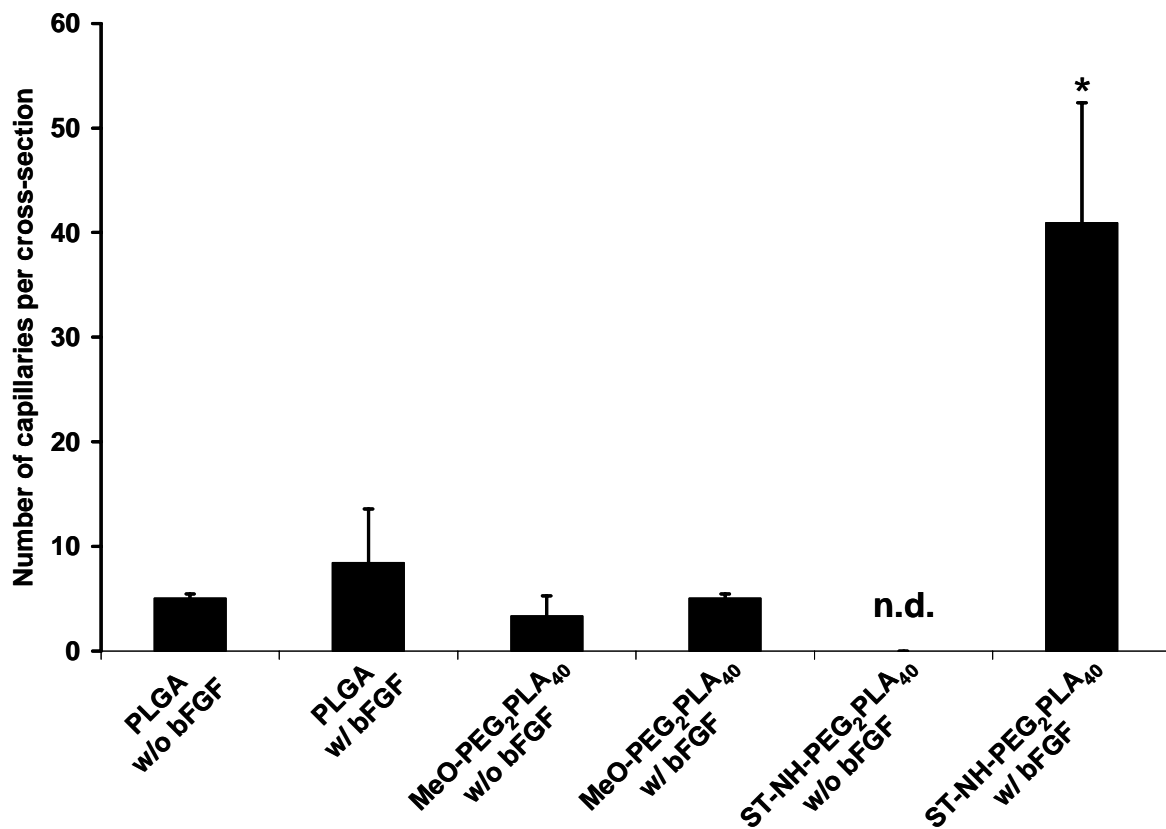


Fig. 7 Determination of the number of capillaries within the constructs. Data represent mean \pm standard deviation. The asterisk indicates a statistically significant difference of the number of capillaries in ST-NH-PEG₂PLA₄₀ scaffolds with covalently immobilized bFGF as compared to all other experimental groups ($p < 0.01$).

Discussion

This study demonstrates a novel principle for the instant surface modification of solid polymeric 3-D scaffolds with the potent growth factor bFGF for tissue engineering applications. Basic FGF could be covalently bound to the scaffolds and was anchored within the scaffolds for at least three weeks *in vivo*. The bioactivity of the tethered growth factor was retained: it strongly promoted angiogenesis in the scaffolds, whereas adsorbed bFGF had no effect on the vascularization. Thus, these constructs represent an “off-the-shelf” product functioning as a solid scaffold-type cell carrier or template for the developing tissue and at the same time, as a delivery device for peptides and growth factors.

Scaffolds and growth factors are known to play an outstanding role in the field of tissue engineering providing a template for a new tissue and modulating the cellular behavior, respectively [1]. However, proteins and peptides have been described as agents susceptible to degradation. They have been reported to exhibit extremely short plasma half-lives, for instance, 1.5 min for bFGF and less than 1 h for vascular endothelial growth factor (VEGF) and absolutely require to be provided by drug delivery devices [7,8]. As yet, polymer devices such as reservoirs, matrices, microspheres, and hydrogels allow for the maintenance of constant local levels of growth factors and consequently for a high efficiency [7]. These systems deliver the protein to the body in the original soluble form which can directly interact with the corresponding receptor on the cell surface in the case of growth factors. The covalent immobilization of proteins may circumvent major drawbacks of the soluble form resulting in the prevention of the internalization of the ligand-receptor-complex and the hindrance of a diffusive spread of the protein [7,10]. Additionally, the tethering of peptides has been shown to prolong the intracellular signaling after binding to cell surface receptors in comparison to factors provided in a soluble, diffusive form and thus, the efficiency of the peptides can be improved [13].

The tethering of a growth factor to a polymer potentially bears the risk of reducing its bioactivity. Physiologically, bFGF binds to high affinity receptors (receptor tyrosine kinases) and to low affinity receptors (heparan-like glycosaminoglycans) located at the cell surface [23]. The structure of bFGF includes both a receptor binding site and a heparin-binding site which are known to be essential for the exertion of its biological activity [24,25]. N-hydroxysuccinimide (NHS) esters as used in this study have been reported to react with primary amines under near-physiological conditions [26]. The bioactivity of tethered bFGF may not or at least only partially be reduced by the covalent binding due to the fact that the primary, higher affinity binding interaction of bFGF with its receptor comprises the amino

acids tyrosine(-24), tyrosine(-103), leucine(-140), and methionine(-142) and thus, this sequence exhibits a lack of primary amines [27]. The retention of the bioactivity was clearly demonstrated in this study since bFGF covalently immobilized in ST-NH-PEG₂PLA₄₀ scaffolds provoked angiogenesis, and in contrast, adsorbed bFGF failed in this regard (Figs. 6,7). A total amount of approx. 17 ng/mg bFGF was detected on these scaffolds prior to implantation (Fig. 4) whereby only approx. 3.6 ng/mg scaffold were covalently bound to the scaffolds (Fig. 3). Basic FGF adsorbed onto the hydrophobic surface of PLGA scaffolds or onto the hydrophilic surface of MeO-PEG₂PLA₄₀ exerted no effects with regard to angiogenesis and tissue ingrowth although the total amount of bFGF was similar in the case of MeO-PEG₂PLA₄₀ or even two-fold increased in the case of the PLGA scaffolds as compared to the ST-NH-PEG₂PLA₄₀ scaffolds (Fig. 4). These observations indicate that the angiogenic effects as shown in Figs. 6 and 7 were exerted exclusively by the covalently immobilized bFGF whereas adsorbed bFGF proved ineffective. Covalently bound bFGF was presented on the surface of the scaffolds at a constant level during three weeks *in vivo*, whereas the amount of adsorbed bFGF strongly decreased after one week (Fig. 5). In detail, the amount of bFGF tethered to the scaffolds prior to implantation was 3.6 ± 0.7 ng bFGF/mg scaffold and three weeks after implantation, the amount was 3.82 ± 0.33 ng bFGF/mg scaffold.

The potential of bFGF to exert angiogenic effects has repeatedly been reported [9,21,28-30]. To induce angiogenesis, bFGF stimulates endothelial cell migration and division, and plays an important role in the remodeling of the extracellular matrix (ECM) [31]. Basic FGF is secreted by cells via a poorly understood mechanism and acts in an autocrine or paracrine manner via its high and low affinity receptors. Furthermore, bFGF can be stored by binding to heparan-like glycosaminoglycans located in the ECM or on the cell surface. When required, bFGF can be released by an enzymatic cleavage of the bFGF/heparin complex [32]. In our study, bFGF was anchored to the scaffolds over the entire period *in vivo* and nevertheless, bFGF strongly provoked an angiogenic effect. Possibly, the immobilization of growth factors also may contribute to a further elucidation of the molecular mechanisms of growth factor-induced angiogenesis.

Other systems using covalently immobilized growth factors or peptides have been developed so far. Non-woven polyester fiber meshes with covalently immobilized RGD peptides and insulin have been reported to promote the adhesion and proliferation of skin fibroblasts *in vitro* and have been utilized to establish a serum-free cell culture [16]. Transforming growth factor- β 1 (TGF- β 1) tethered to acryloyl-PEG hydrogels increased the ECM production of vascular smooth muscle cells *in vitro* similar to incorporated TGF- β 1 [15]. Tethering of TGF-

β 2 to collagen gels has been shown to stabilize the growth factor *in vitro* and to prolong and potentiate the responses to the factor *in vivo* [14]. In contrast to those systems, the polymeric scaffolds used in this study exhibit a solid sponge-like structure which is highly porous and features pores that are highly interconnected [17]. The pore size desired for a certain purpose would easily be variable by the use of different porogen microparticles. Furthermore, the tethering of peptides and proteins had been described as a laborious multi-step chemistry [14-16] whereas the technique described in this study allows for an instant modification of the scaffolds by a simple incubation of the scaffolds in the peptide solution at near-physiological conditions (Fig. 2).

The potential for the promotion of angiogenesis by immobilization of bFGF was shown in this study. Several strategies come into consideration in order to improve the established system or to broaden the spectrum of further applications. The use of RGD peptides may enhance the adhesion of specific cells onto the ST-NH-PEG₂PLA₄₀ scaffolds. Lieb et al. recently demonstrated the positive effects of cyclic RGD sequences covalently immobilized to two-dimensional ST-NH-PEG₂PLA₄₀ films on the adhesion of osteoblasts *in vitro* [18]. In a previous study, DeLong et al. observed an alignment of vascular smooth muscle cells on gradient hydrogels made from acryloyl-PEG with a concentration gradient of covalently immobilized bFGF [33]. Beyond the alignment, these cells showed an increased migration up the concentration gradient as compared to hydrogels with a constant bFGF concentration. The efficiency of the system presented in this study may be increased by the generation of concentration gradients of bFGF in the scaffolds. Possibly, a concentration gradient with increasing bFGF concentrations from the outside to the inside of the scaffolds may result in an enhanced vascularization of the scaffolds. The instant modification method as presented in this study may technically facilitate the generation of concentration gradients in the scaffolds by treatment of different areas of the scaffold with differentially concentrated bFGF solutions. Furthermore, alternative growth factors or growth factor combinations may be utilized for the modulation of the cellular behavior including the proliferation and differentiation of stem cells which have been described to be a promising cell source for tissue engineering [34,35]. In summary, this study demonstrates the feasibility of the surface modification of 3-D scaffolds by a simple instant reaction. The tethering of bFGF to these scaffolds provoked angiogenesis *in vivo*. Thus, this system represents a novel “off-the-shelf” product for tissue engineering applications and potentially facilitates the investigation of angiogenic processes in a novel model system.

Acknowledgement

This work was supported by the Deutsche Akademische Austausch Dienst (DAAD) providing a six-month scholarship for Markus Neubauer at the University of Kyoto.

References

- [1] Langer R, Vacanti JP. 'Tissue engineering'. *Science* (1993); **260**: 920-926.
- [2] Hench LL, Polak JM. 'Third-generation biomedical materials'. *Science* (2002); **295**: 1014-1017.
- [3] Anderson DG, Burdick JA, Langer R. 'Materials science: Smart biomaterials'. *Science* (2004); **305**: 1923-1924.
- [4] Drotleff S, Lungwitz U, Breunig M, Dennis A, Blunk T, Tessmar J, Gopferich A. 'Biomimetic polymers in pharmaceutical and biomedical sciences'. *Eur J Pharm Biopharm* (2004); **58**: 385-407.
- [5] Bonassar LJ, Vacanti CA. 'Tissue engineering: the first decade and beyond'. *J Cell Biochem* (1998); **Suppl. 30/31**: 297-303.
- [6] Tabata Y. 'The importance of drug delivery systems in tissue engineering'. *Pharm Sci Technol Today* (2000); **3**: 80-89.
- [7] Baldwin SP, Mark Saltzman W. 'Materials for protein delivery in tissue engineering'. *Adv Drug Deliv Rev* (1998); **33**: 71-86.
- [8] Bouhadir KH, Mooney DJ. 'Promoting angiogenesis in engineered tissues'. *J Drug Target* (2002); **9**: 397-406.
- [9] Gospodarowicz D, Ferrara N, Schweigerer L, Neufeld G. 'Structural characterization and biological functions of fibroblast growth factor'. *Endocr Rev* (1987); **8**: 95-114.
- [10] Kuhl PR, Griffith-Cima LG. 'Tethered epidermal growth factor as a paradigm for growth factor-induced stimulation from the solid phase'. *Nat Med* (1996); **2**: 1022-1027.
- [11] Ito Y. 'Tissue engineering by immobilized growth factors'. *Mater Sci Eng* (1998); **6**: 267-274.
- [12] Kirkwood K, Rheude B, Kim YJ, White K, Dee KC. '*In vitro* mineralization studies with substrate-immobilized bone morphogenetic protein peptides'. *J Oral Implantol* (2003); **29**: 57-65.
- [13] Ito Y, Zheng J, Imanishi Y, Yonezawa K, Kasuga M. 'Protein-free cell culture on an artificial substrate with covalently immobilized insulin'. *Proc Natl Acad Sci USA* (1996); **93**: 3598-3601.

- [14] Bentz H, Schroeder JA, Estridge TD. 'Improved local delivery of TGF- β .2 by binding to injectable fibrillar collagen via difunctional polyethylene glycol'. *J Biomed Mat Res* (1998); **39**: 539-548.
- [15] Mann BK, Schmedlen RH, West JL. 'Tethered TGF- β increases extracellular matrix production of vascular smooth muscle cells'. *Biomaterials* (2001); **22**: 439-444.
- [16] Gumusderelioglu M, Turkoglu H. 'Biomodification of non-woven polyester fabrics by insulin and RGD for use in serum-free cultivation of tissue cells'. *Biomaterials* (2002); **23**: 3927-3935.
- [17] Hacker M, Tessmar J, Neubauer M, Blaimer A, Blunk T, Gopferich A, Schulz MB. 'Towards biomimetic scaffolds: Anhydrous scaffold fabrication from biodegradable amine-reactive diblock copolymers'. *Biomaterials* (2003); **24**: 4459-4473.
- [18] Lieb E, Hacker M, Tessmar J, Kunz-Schughart LA, Fiedler J, Dahmen C, Hersel U, Kessler H, Schulz MB, Gopferich A. 'Mediating specific cell adhesion to low-adhesive diblock copolymers by instant modification with cyclic RGD peptides'. *Biomaterials*; in press.
- [19] Tessmar JK, Mikos AG, Gopferich A. 'Amine-Reactive Biodegradable Diblock Copolymers'. *Biomacromolecules* (2002); **3**: 194-200.
- [20] Tessmar J, Mikos A, Gopferich A. 'The use of poly(ethylene glycol)-block-poly(lactic acid) derived copolymers for the rapid creation of biomimetic surfaces'. *Biomaterials* (2003); **24**: 4475-4486.
- [21] Bikfalvi A, Savona C, Perollet C, Javerzat S. 'New insights in the biology of fibroblast growth factor-2'. *Angiogenesis* (1997); **1**: 155-173.
- [22] Lieb E, Tessmar J, Hacker M, Fischbach C, Rose D, Blunk T, Mikos AG, Gopferich A, Schulz MB. 'Poly(D,L-lactic acid)-poly(ethylene glycol)-monomethyl ether diblock copolymers control adhesion and osteoblastic differentiation of marrow stromal cells'. *Tissue Eng* (2003); **9**: 71-84.
- [23] Powers CJ, McLeskey SW, Wellstein A. 'Fibroblast growth factors, their receptors and signaling'. *Endocr Relat Cancer* (2000); **7**: 165-197.
- [24] Yayon A, Klagsbrun M, Esko JD, Leder P, Ornitz DM. 'Cell surface, heparin-like molecules are required for binding of basic fibroblast growth factor to its high affinity receptor'. *Cell* (1991); **64**: 841-848.
- [25] Pellegrini L. 'Role of heparan sulfate in fibroblast growth factor signalling: a structural view'. *Curr Opin Struct Biol* (2001); **11**: 629-634.
- [26] Roberts MJ, Bentley MD, Harris JM. 'Chemistry for peptide and protein PEGylation'. *Adv Drug Deliv Rev* (2002); **54**: 459-476.

- [27] Springer BA, Pantoliano MW, Barbera FA, Gunyuzlu PL, Thompson LD, Herblin WF, Rosenfeld SA, Book GW. 'Identification and concerted function of two receptor binding surfaces on basic fibroblast growth factor required for mitogenesis'. *J Biol Chem* (1994); **269**: 26879-26884.
- [28] Nugent MA, Iozzo RV. 'Fibroblast growth factor-2'. *Int J Biochem Cell Biol* (2000); **32**: 115-120.
- [29] Okada-Ban M, Thiery JP, Jouanneau J. 'Fibroblast growth factor-2'. *Int J Biochem Cell Biol* (2000); **32**: 263-267.
- [30] Ornitz DM, Itoh N. 'Fibroblast growth factors'. *Genome Biol* (2001); **2**: Reviews3005.
- [31] Slavin J. 'Fibroblast growth factors: at the heart of angiogenesis'. *Cell Biol Int* (1995); **19**: 431-444.
- [32] Klein S, Roghani M, Rifkin DB. 'Fibroblast growth factors as angiogenesis factors: New insights into their mechanism of action'. In: Goldberg ID, Rosen EM, editors. *Regulation of Angiogenesis*. Basel: Birkhäuser, 1997. p. 159-192.
- [33] DeLong SA, Moon JJ, West JL. 'Covalently immobilized gradients of bFGF on hydrogel scaffolds for directed cell migration'. *Biomaterials*; in press.
- [34] Caplan AI, Bruder SP. 'Mesenchymal stem cells: building blocks for molecular medicine in the 21st century'. *Trends Mol Med* (2001); **7**: 259-264.
- [35] Heath CA. 'Cells for tissue engineering'. *Trends Biotechnol* (2000); **18**: 17-19.

Chapter 10

Summary and Conclusions

Mesenchymal stem cells (MSCs) represent intensively investigated cells with the potential to play an important clinical role in the replacement or regeneration of defect tissues [1-3]. In the field of tissue engineering, MSCs have been utilized in approaches towards bone, cartilage, and tendon [4-7]. However, no study on tissue engineered fat exists using MSCs so far.

The capacity of MSCs to undergo adipogenic differentiation has repeatedly been shown using various inducing stimuli [8-11]. Growth factors including basic fibroblast growth factor (bFGF) have been described to influence the adipogenic differentiation of MSCs. However, the effect of bFGF on the adipogenesis of MSCs has been controversially discussed [8,11,12]. Furthermore, those studies were not focused on adipogenesis with regard to the applied experimental conditions and analytics.

In order to optimize culture conditions for an adipocytic culture of MSCs, adipogenesis-inducing agents such as dexamethasone, IBMX, indomethacin, and insulin were employed in different combinations (**chapter 3**). The combination of all inducers, in the following termed hormonal cocktail, yielded the strongest adipogenic differentiation of MSCs. However, the differentiation rate was still insufficient for tissue engineering applications and, therefore, growth factors known to modulate the differentiation of MSCs were administered. Epidermal growth factor (EGF) had no effect on the adipogenesis of MSCs, whereas platelet-derived growth factor-BB (PDGF-BB) and bFGF strongly enhanced adipogenesis of MSCs. Combined administration of bFGF and the hormonal cocktail led to the strongest enhancement of adipogenesis, that is, the highest number of adipocytes and the most advanced maturation were obtained with this combination.

In a further study, the striking effect of bFGF on the adipogenesis of MSCs was investigated on the cellular and molecular level in detail (**chapter 4**). Supplementation of bFGF in different phases of cell culture and treatment of the cells with the hormonal cocktail led to a strong enhancement of adipogenesis of MSCs. In cultures receiving bFGF, mRNA expression of peroxisome proliferator-activated receptor $\gamma 2$ (PPAR $\gamma 2$), a key transcription factor in adipogenesis, was upregulated even prior to adipogenic induction. In order to investigate the effects of bFGF on PPAR γ ligand-induced adipogenic differentiation, the thiazolidinedione troglitazone was administered as a single adipogenic inducer. Basic FGF was demonstrated to also strongly increase adipogenesis induced by troglitazone, that is, bFGF clearly increased the responsiveness of MSCs to a PPAR γ ligand.

Basic FGF was shown to modulate adipogenesis of MSCs in this study and has been demonstrated to also influence osteogenesis and chondrogenesis of MSCs in other studies [11,13]. However, the mechanism by which bFGF exerts its effects on MSCs are poorly

investigated and understood. Possible mechanisms of action of bFGF include (a) the preferential proliferation of a subpopulation prone to differentiate into adipocytes and (b) the exertion of direct effects on the commitment level of MSCs. The presence of multiple cell populations in the MSC culture renders the determination of the underlying mechanism more difficult. Therefore, a culture was established to investigate the effects of bFGF on the adipogenesis of MSCs under clonal conditions (**chapter 5**). First, a medium consisting of α -MEM, fetal bovine serum, ascorbic acid, and the B27 supplement was found to be suitable for the expansion of MSCs under cloning condition. This medium ensured the maintenance of the differentiation potential and the responsiveness to bFGF of MSCs. Second, differentiation experiments under clonal conditions in which bFGF was supplemented either only in the single cell culture or in the entire culture suggest bFGF to act mainly via the preferential proliferation of a subset of the MSCs capable of undergoing adipogenesis.

In tissue engineering approaches, so far exclusively adipocytes and preadipocytes have been used as cell sources (**chapter 1**). In this thesis, the potential of MSCs for the application in *in vitro* approaches towards adipose tissue engineering was shown for the first time. As a first step, MSCs were seeded onto polymeric scaffolds with different pore size and were cultivated for two weeks on the constructs to observe changes of the cell number (**chapter 6**). Scaffolds with pore sizes from 100 to 300 μm appeared to be most suitable with regard to cellular distribution throughout the scaffold and maintenance of the cell number over the two-week culture period. Scaffolds made from various materials with this pore size range were employed in further studies of this thesis (**chapters 7-9**). The next challenge was the transfer of the adipogenic protocol established in 2-D short-term cell culture to a 3-D long-term cell culture using MSCs and bFGF (**chapter 7**). MSCs were seeded onto poly(lactic-co-glycolic acid) (PLGA) scaffolds and cultivated for four weeks in the absence and in the presence of bFGF. Basic FGF strongly enhanced the adipogenesis of MSCs on the constructs and the development of a tissue-like structure accompanied by an elevation of adipocytic gene and protein expression. Parts of the constructs cultivated in the presence of bFGF for four weeks exhibited highly differentiated and mature adipocytes which were embedded in structures considered to be extracellular matrix.

Recently, a new generation of novel polymers, also termed biomimetic polymers, has been designed in order to control the cellular behavior on the molecular level [14-16]. In our laboratory, poly(ethylene glycol)-poly(lactic acid) (PEG-PLA) polymers have been synthesized to which peptides and proteins can be covalently bound by an instant surface modification [17]. Furthermore, a technique was recently developed to process these polymers

into 3-D scaffolds [18]. As a first step towards the proof of the feasibility of the tethering of bFGF to scaffolds made from a PEG-PLA derivative, the interactions of bFGF with PEG-PLA derivatives were investigated (**chapter 8**). The adsorption of radiolabeled bFGF to PEG-PLA 2-D polymers films was distinctly suppressed in comparison to PLA films. Furthermore, a protocol was established to efficiently desorb radiolabeled bFGF from 2-D polymer films which subsequently, allowed for the determination of the amount of bFGF covalently bound to the scaffolds. In the next study, the tethering of bFGF to the scaffolds was characterized in detail (**chapter 9**). The maximum amount of bFGF which could be covalently immobilized to the scaffolds under appropriate conditions was determined (3.6 ± 0.7 ng bFGF/mg). The stability of the linkage of bFGF to the scaffolds was determined in an *in vivo* experiment. Radiolabeled bFGF could be anchored for at least three weeks within the scaffolds. And last but not least, the bioactivity and the angiogenic effect of tethered bFGF was assessed in a further *in vivo* study. Remarkably, only tethered bFGF strongly induced angiogenesis within the scaffolds, whereas adsorbed bFGF remained ineffective.

In conclusion, this thesis shows the potential of MSCs for adipose tissue engineering applications for the first time. Basic FGF was found to be a suitable growth factor for the enhancement of the adipogenesis of MSCs in 2-D and 3-D cell culture and to strongly improve the generation of engineered adipose tissue-like constructs. In addition, the delivery of bFGF by tethering to 3-D scaffolds allows for the vascularization of tissue constructs *in vivo*. This system represents a novel “off-the-shelf” product for tissue engineering applications. In future studies, a combination of these two strategies may lead to mature vascularized engineered adipose tissue.

References

- [1] Bianco P, Riminucci M, Gronthos S, Robey PG. 'Bone Marrow Stromal Stem Cells: Nature, Biology, and Potential Applications'. *Stem Cells* (2001); **19**: 180-192.
- [2] Caplan AI, Bruder SP. 'Mesenchymal stem cells: building blocks for molecular medicine in the 21st century'. *Trends Mol Med* (2001); **7**: 259-264.
- [3] Devine SM. 'Mesenchymal stem cells: will they have a role in the clinic?'. *J Cell Biochem* (2002); 73-79.
- [4] Lisignoli G, Zini N, Remiddi G, Piacentini A, Puggioli A, Trimarchi C, Fini M, Maraldi NM, Facchini A. 'Basic fibroblast growth factor enhances *in vitro* mineralization of rat bone marrow stromal cells grown on non-woven hyaluronic acid based polymer scaffold'. *Biomaterials* (2001); **22**: 2095-2105.
- [5] Quarto R, Mastrogiacomo M, Cancedda R, Kutepov SM, Mukhachev V, Lavroukov A, Kon E, Marcacci M. 'Repair of large bone defects with the use of autologous bone marrow stromal cells'. *N Engl J Med* (2001); **344**: 385-386.
- [6] Johnstone B, Hering TM, Caplan AI, Goldberg VM, Yoo JU. '*In vitro* chondrogenesis of bone marrow-derived mesenchymal progenitor cells'. *Exp Cell Res* (1998); **238**: 265-272.
- [7] Young RG, Butler DL, Weber W, Caplan AI, Gordon SL, Fink DJ. 'Use of mesenchymal stem cells in a collagen matrix for Achilles tendon repair'. *J Orthop Res* (1998); **16**: 406-413.
- [8] Locklin RM, Oreffo ROC, Triffitt JT. 'In vitro effects of growth factors and dexamethasone on rat marrow stromal cells'. *Clin Orthop* (1995); **313**: 27-35.
- [9] Gimble JM, Robinson CE, Wu X, Kelly KA, Rodriguez BR, Klier SA, Lehmann JM, Morris DC. 'Peroxisome proliferator-activated receptor- γ activation by thiazolidinediones induces adipogenesis in bone marrow stromal cells'. *Mol Pharmacol* (1996); **50**: 1087-1094.
- [10] Pittenger MF, Mackay AM, Beck SC, Jaiswal RK, Douglas R, Mosca JD, Moorman MA, Simonetti DW, Craig S, Marshak DR. 'Multilineage potential of adult human mesenchymal stem cells'. *Science* (1999); **284**: 143-147.
- [11] Tsutsumi S, Shimazu A, Miyazaki K, Pan H, Koike C, Yoshida E, Takagishi K, Kato Y. 'Retention of multilineage differentiation potential of mesenchymal cells during proliferation in response to FGF'. *Biochem Biophys Res Commun* (2001); **288**: 413-419.
- [12] Locklin RM, Oreffo ROC, Triffitt JT. 'Effects of TGF.β and bFGF on the differentiation of human bone marrow stromal fibroblasts'. *Cell Biol Int* (1999); **23**: 185-194.
- [13] Martin I, Muraglia A, Campanile G, Cancedda R, Quarto R. 'Fibroblast Growth Factor-2 Supports ex Vivo Expansion and Maintenance of Osteogenic Precursors from Human Bone Marrow'. *Endocrinology* (1997); **138**: 4456-4462.

- [14] Hench LL, Polak JM. 'Third-generation biomedical materials'. *Science* (2002); **295**: 1014-1017.
- [15] Anderson DG, Burdick JA, Langer R. 'Materials science: Smart biomaterials'. *Science* (2004); **305**: 1923-1924.
- [16] Drotleff S, Lungwitz U, Breunig M, Dennis A, Blunk T, Tessmar J, Gopferich A. 'Biomimetic polymers in pharmaceutical and biomedical sciences'. *Eur J Pharm Biopharm* (2004); **58**: 385-407.
- [17] Tessmar JK, Mikos AG, Gopferich A. 'Amine-Reactive Biodegradable Diblock Copolymers'. *Biomacromolecules* (2002); **3**: 194-200.
- [18] Hacker M, Tessmar J, Neubauer M, Blaimer A, Blunk T, Gopferich A, Schulz MB. 'Towards biomimetic scaffolds: Anhydrous scaffold fabrication from biodegradable amine-reactive diblock copolymers'. *Biomaterials* (2003); **24**: 4459-4473.

Appendices

List of Abbreviations

2-D	two-dimensional
3-D	three-dimensional
α -MEM	Minimum Essential Medium Eagle, alpha-modification
aFGF	acidic fibroblast growth factor
ANOVA	analysis of variance
aP2	adipocyte-specific fatty acid binding protein
ASPS	American Society of Plastic Surgeons
BAT	brown adipose tissue
bFGF	basic fibroblast growth factor
BMP	bone morphogenetic protein
BSA	bovine serum albumin
cAMP	cyclic adenosin 3',5''-monophosphate
CFU	colony forming unit
CD	cluster of differentiation
cDNA	complementary deoxyribonucleic acid
C/EBP	CCAAT/enhancer binding protein
Dex	dexamethasone
DMEM	Dulbecco's Modified Eagle's Medium
DNA	deoxyribonucleic acid
ECM	extracellular matrix
EDTA	ethylenediaminetetraacetic acid
EGF	epidermal growth factor
ERK	extracellular signal-regulated kinase
ES	embryonic stem cell
FACS	fluorescence activated cell sorting (scanning)
FAS	fatty acid synthase
FBS	fetal bovine serum
FL3	fluorescence channel 3
FSC	forward scatter
GAG	glycosaminoglycane
GH	growth hormone
GLUT4	glucose transporter 4

GPDH	glycerol-3-phosphate dehydrogenase
GR	glucocorticoid receptor
HA	hyaluronic acid
H&E	hematoxylin and eosin
hMSC	human mesenchymal stem cell
H ₂ N-PEG ₂ PLA ₄₀	monoamine poly(ethylene glycol)-block-poly(D,L-lactic acid) consisting of a 2 kDa poly(ethylene glycol)-monoamine block and a 40 kDa poly(lactic acid) block
HSC	hematopoietic stem cell
IBMX	3-isobutyl-1-methylxanthine
IGF	insulin-like growth factor
Indo	indomethacin
Ins	insulin
kDa	kilodalton
LIF	leukaemia inhibitory factor
LPL	lipoprotein lipase
MACS	magnetic activated cell sorting
MEF	mouse embryonic feeder
MEK	mitogen-activated protein kinase/extracellular signal-regulated kinase
MeO-PEGPLA	poly(D,L-lactic acid)-poly(ethylene glycol)-monomethyl ether diblock copolymer
MeO-PEG _x PLA _y	poly(D,L-lactic acid)-poly(ethylene glycol)-monomethyl ether diblock copolymer with a PEG block of x kDa and a PLA block of y kDa
mRNA	messenger ribonucleic acid
MSC	mesenchymal stem cell
NaCl	sodium chloride
NADH	reduced nicotinamide adenine dinucleotide
OsO ₄	osmium tetroxide
PBS	phosphate-buffered saline
PCR	polymerase chain reaction
PDGF	platelet-derived growth factor
PEG	poly(ethylene glycol)

PGA	poly(glycolic acid)
PLA	poly(lactic acid)
PLA cell	processed lipoaspirate cells
PLGA	poly(lactic-co-glycolic acid)
PPAR	peroxisome proliferator-activated receptor
Pref-1	preadipocyte factor-1
RGD	peptide sequence Arg-Gly-Asp
rMSC	rat mesenchymal stem cell
rpm	rounds per minute
rRNA	ribosomal ribonucleic acid
RT	room temperature
RT-PCR	reverse transcription-polymerase chain reaction
RXR α	retinoid X receptor α
s.c.	subcutaneous
SCD-1	stearoyl-CoA desaturase-1
SD	standard deviation
SDS	sodium dodecyl sulphate
SEM	scanning electron microscope
SREBP	sterol regulatory element binding protein
SSC	sideward scatter
ST-NH-PEGPLA	N-succinimidyl tartrate monoamine poly(ethylene glycol)-block-poly(D,L-lactic acid)
ST-NH-PEG ₂ PLA ₄₀	N-succinimidyl tartrate monoamine poly(ethylene glycol)-block-poly(D,L-lactic acid) consisting of a 2 kDa poly(ethylene glycol)-monoamine block and a 40 kDa poly(lactic acid) block
T75-flask	75 cm ² cell culture flask
TGF- β	transforming growth factor- β
TNF α	tumor necrosis factor α
Tris	tris(hydroxymethyl)aminomethane buffer
UV	ultraviolet light
VEGF	vascular endothelial growth factor
WAT	white adipose tissue

Curriculum vitae

Name: Markus Neubauer
Date of birth: April 30, 1974
Place of birth: Kolbermoor
Nationality: German
Marital status: married

Education:

09/80-08/84 Elementary School, Thansau
09/84-07/93 Grammar School: Finsterwalder Gymnasium, Rosenheim

Civilian Service:

10/93-10/94 Ambulance man at Ambulanz Rosenheim, Brannenburg

Professional Training and Experience:

11/94-04/99 Study of Pharmacy at the University of Regensburg, Regensburg
05/99-10/99 Traineeship at the "Ahorn-Apotheke", Regensburg
11/99-04/00 Traineeship at Roche Diagnostics GmbH, Penzberg
07/00 Acquisition of the license to practise as pharmacist
05/00-present PhD program at the Department of Pharmaceutical Technology, University of Regensburg, Regensburg, Prof. Achim Göpferich

Scholarship:

05/03-10/03 DAAD scholarship for PhD students at the Department of Biomaterials, Field of Tissue Engineering, Institute for Frontier Medical Sciences, University of Kyoto, Japan, Prof. Yasuhiko Tabata

List of Publications

Publications

Hacker M, Tessmar J, Neubauer M, Blaimer A, Blunk T, Gopferich A, Schulz MB. 'Towards biomimetic scaffolds: Anhydrous scaffold fabrication from biodegradable amine-reactive diblock copolymers'. *Biomaterials* (2003); **24**: 4459-4473.

Fischbach C, Seufert J, Staiger H, Hacker M, Neubauer M, Gopferich A, Blunk T. 'Three-Dimensional in Vitro Model of Adipogenesis: Comparison of Culture Conditions'. *Tissue Eng* (2004); **10**: 215-229.

Fischbach C, Spruß T, Weiser B, Neubauer M, Becker C, Hacker M, Gopferich A, Blunk T. 'Generation of mature fat pads in vitro and in vivo utilizing 3-D long-term culture of 3T3-L1 preadipocytes'. *Exp Cell Res* (2004); **300**: 54-64.

Neubauer, M, Fischbach, C, Bauer-Kreisel, P, Lieb, E, Hacker, M, Tessmar, J, Schulz, MB, Gopferich, A, Blunk, T. 'Basic fibroblast growth factor enhances PPAR γ ligand-induced adipogenesis of mesenchymal stem cells'. *FEBS Lett* (2004); **577**: 277-283. (**Chapter 4**)

Neubauer, M, Hacker, M, Bauer-Kreisel, P, Fischbach, C, Schulz, MB, Gopferich, A, Blunk, T. 'Adipose tissue engineering based on mesenchymal stem cells and basic fibroblast growth factor in vitro'. *Tissue Eng*; submitted. (**Chapter 7**)

Neubauer, M, Fischbach, C, Weiser, B, Gopferich, A, Blunk, T. 'Adipose tissue engineering'. to be submitted to *Tissue Eng* as a review. (**Chapter 1**)

Neubauer, M, Hacker, M, Drotleff, S, Ozeki, M, Teßmar, J, Schulz, MB, Mikos, AG, Tabata, Y, Blunk, T, Gopferich, A. 'Instant Surface Modification of 3-D Polymeric Scaffolds Allows for the Immobilization of bFGF and Generation of Vascularized Constructs'. to be submitted to *Proc Natl Acad Sci USA*. (**Chapter 9**)

Conference abstracts

2001

Neubauer, M, Fischbach, C, Lieb, E, Hacker, M, Tessmar, JK, Schulz, MB, Göpferich, A, Blunk, T. 'Adipogenesis of rat marrow stromal cells in two- and three-dimensional cell culture.' 1st Biennial Meeting of the European Tissue Engineering Society ETES, Freiburg, Germany, 2001 [Tissue Eng. (2001); **7**: 669].

Fischbach, C, Seufert, J, Neubauer, M, Lazariotou, M, Göpferich, A, Blunk, T. '3T3-L1 preadipocytes on three-dimensional polymer scaffolds as a model for fat tissue engineering'. 1st Biennial Meeting of the European Tissue Engineering Society ETES, Freiburg, Germany, 2001 [Tissue Eng. (2001); **7**: 644].

Hacker, M, Tessmar, J, Neubauer, M, Blaimer, A, Blunk, T, Schulz, MB, Göpferich, A. 'Water-free manufacture of Me.PEG-PLA scaffolds for tissue engineering applications'. CRS German Chapter Annual Meeting, Saarbrücken, Germany, 2001.

Hacker, M, Teßmar, J, Lieb, E, Neubauer, M, Blunk, T, Göpferich, A, Schulz, MB. 'Development of a fabrication method for scaffolds used in tissue engineering'. DPhG Jahrestagung, Halle, Germany, 2001.

Hacker, M, Tessmar, J, Neubauer, M, Blunk, T, Schulz, MB, Göpferich, A. 'Towards the manufacture of biomimetic scaffolds'. 1st Biennial Meeting of the European Tissue Engineering Society ETES, Freiburg, Germany 2001 [Tissue Eng. (2001); **7**: 640].

Teßmar, J, Kellner, K, Neubauer, M, Hacker, M, Schulz, MB, Blunk, T, Göpferich, A. 'PEGylation of insulin – towards the synthesis of biomimetic polymers'. 1st Biennial Meeting of the European Tissue Engineering Society ETES, Freiburg, Germany 2001.

Hacker, M, Tessmar, J, Neubauer, M, Lieb, E, Blunk, T, Göpferich, A, Schulz, MB. 'Anhydrous scaffold fabrication from sensitive biodegradable polymers'. MRS 2001 Fall Meeting, Boston, MA; USA, 2001.

2002

Neubauer, M, Fischbach, C, Lieb, E, Hacker, M, Tessmar, J, Schulz, MB, Göpferich, A, Blunk, T. 'Exposure to basic fibroblast growth factor enhances adipogenesis of rat marrow stromal cells *in vitro*'. Keystone Symposium "Molecular Control of Adipogenesis and Obesity", Keystone, CO, USA, 2002.

Neubauer, M, Fischbach, C, Lieb, E, Hacker, M, Tessmar, J, Bauer-Kreisel, P, Schulz, MB, Göpferich, A, Blunk, T. 'Adipogenesis of rat marrow stromal cells in two- and three-dimensional cell culture'. 5th Annual Meeting of the GZG/ETCS, Regensburg, Germany, 2002.

Neubauer, M, Tessmar, J, Hacker, M, Fischbach, C, Schulz, MB, Blunk, T, Göpferich, A. 'Towards engineered adipose tissue using bone marrow stromal cells and basic fibroblast growth factor.' 29th Annual Meeting of the Controlled Release Society, Seoul, Korea, 2002.

Fischbach, C, Seufert, J, Neubauer, M, Lazariotou, M, Göpferich, A, Blunk, T. 'Towards a three-dimensional *in vitro*-model of adipogenesis'. Keystone Symposium "Molecular Control of Adipogenesis and Obesity", Keystone, CO, USA, 2002.

Fischbach, C, Seufert, J, Neubauer, M, Lazariotou, M, Göpferich, A, Blunk, T. 'Towards a three-dimensional *in vitro*-model of adipogenesis'. 5th Annual Meeting of the GZG/ETCS, Regensburg, Germany, 2002.

Hacker, M, Tessmar, J, Neubauer, M, Blunk, T, Göpferich, A, Schulz, MB. 'Macroporous biodegradable scaffolds for controlled surface modification'. 5th Annual Meeting of the GZG/ETCS, Regensburg, Germany, 2002.

Drotleff, S, Tessmar, J, Kellner, K, Hacker, M, Neubauer, M, Schulz, MB, Blunk, T, Göpferich, A. 'Biomimetic polymers for tissue engineering – characterisation of polymers and of proteins for their surface modification'. 5th Annual Meeting of the GZG/ETCS, Regensburg, Germany, 2002.

Hacker, M, Neubauer, M, Untch, H-J, Tessmar, J, Lieb, E, Blunk, T, Goepferich, A, Schulz, MB. 'Solid lipid templating: Macroporous scaffold fabrication from biodegradable polymers'. 5th Annual Meeting of the Tissue Engineering Society, Kobe, Japan, 2002.

2003

Hacker, M, Vogel, T, Neubauer, M, Drotleff, S, Teßmar, J, Blunk, T, Göpferich, A, Schulz, MB. 'Solid lipid templating: Anhydrous scaffold fabrication for tissue engineering'. DPhG Jahrestagung, Würzburg, Germany, 2003.

2004

Neubauer, M, Fischbach, C, Bauer-Kreisel, P, Lieb, E, Hacker, M, Schulz, MB, Goepferich, A, Blunk, T. 'Adipogenesis of mesenchymal stem cells in 3-D cell culture'. Keystone Symposium "Molecular Control of Adipogenesis and Obesity", Banff, Canada, 2004.

Neubauer, M, Hacker, M, Bauer-Kreisel, P, Fischbach, C, Schulz, MB, Göpferich, A, Blunk, T. 'Adipogenesis of mesenchymal stem cells in 3-D cell culture'. International Conference "Strategies in Tissue Engineering", Würzburg, Germany, 2004 [Cytotherapy (2004); **6**: 283].

Fischbach, C, Neubauer, M, Weiser, B, Göpferich, A, Blunk, T. 'Tissue engineering enables 3T3-L1 cells to develop into 3-D fat pads *in vitro* and *in vivo*'. Keystone Symposium "Molecular Control of Adipogenesis and Obesity", Banff, Canada, 2004.

Weiser, B, Neubauer, M, Sommer, F, Göpferich, A, Blunk, T. 'Ascorbic acid enhances adipogenesis of rat marrow stromal cells'. DPhG Joint Meeting, 6-9 October 2004, Regensburg, Germany

Weiser, B, Fischbach, C, Becker, C, Neubauer, M, Hacker, M, Göpferich, A, Blunk, T. '3-dimensional model of adipogenesis: Generation of coherent fat pads *in vitro*'. 2nd International DFG Symposium „Cell Migration in Development and Disease“, Karlsruhe, Germany, 2004.

Weiser, B, Neubauer, M, Fischbach, C, Göpferich, A, Blunk, T. 'Effects of ascorbic acid on adipogenesis of rat BM stromal cells'. International Conference "Strategies in Tissue Engineering", Würzburg, Germany, 2004 [Cytotherapy (2004); **6**: 283].

Danksagung

Zum Schluss möchte ich mich bei allen herzlich bedanken, die zum Gelingen dieser Arbeit beigetragen haben.

Herrn Prof. Göpferich danke ich herzlich für die Überlassung des Themas und für seine vielfältige Unterstützung der Arbeit. Die Anregungen und Diskussionen im Rahmen der „Aventis“-Meetings und der „Polymer-Design“-Meetings waren sehr hilfreich. Insbesondere möchte ich mich dafür bedanken, meine Ergebnisse auf internationalen Konferenzen präsentiert haben zu dürfen und auch für die Ermöglichung des Forschungsaufenthalts in Kyoto.

Mein besonderer Dank gilt Herrn Dr. Torsten Blunk für die äußerst intensive und motivierte Betreuung dieser Arbeit. Von seiner Begeisterung, seiner Gewissenhaftigkeit und seiner Auffassung von Wissenschaft profitierte ich über die gesamten vier Jahre und die Zusammenarbeit mit ihm in freundschaftlicher Atmosphäre bereitete mir große Freude und trug einen sehr großen Teil zum Gelingen dieser Arbeit bei. Von der Versuchsplanung über die Ergebnisdiskussion bis zur Verfassung aller Abstracts, Papers und dieser Arbeit konnte ich jederzeit auf seine Unterstützung zählen.

Weiterhin möchte ich mich bei allen ehemaligen und momentanen Kollegen am Lehrstuhl bedanken. Insbesondere gilt mein Dank:

- Dr. Petra Bauer-Kreisel für die großartige Unterstützung bei den PCR-Versuchen.
- Dr. Michael Hacker für die perfekte und zuverlässige Scaffold-Herstellung.
- Dr. Jörg Teßmar und Sigrid Drotleff für die Synthese der MeO-PEGPLA und ST-NH-PEGPLA-Polymere.
- Dr. Esther Lieb und Dr. Michaela Schulz für das Erlernen der Stammzellisolierung und für die Einführung in die Zellkultur.
- Dr. Claudia Fischbach für die Einführung in die Fettzellkultur.
- Dr. Leoni Kunz-Schughart und Marit Hoffmann für den unermüdlichen Einsatz am FACS und die vielen hilfreichen Ratschläge.
- Dr. Thilo Spruß für die Anleitung zur Durchführung eines Tierversuchs und die Bereitstellung des Gefriermikrotoms.
- Carlos Garcia-Lopez für die Beteiligung an Arbeiten des Kapitels 6.

- Allison Dennis für die exakte und schnelle Durchsicht vieler englischer Texte.
- Herrn Wiesenmayr und Herrn Baumann für die praktische Unterstützung bei den Tierversuchen und für die Kurzzeitpflege der Ratten.
- Frau Thienel und ihrem Team für die Anfertigung der Paraffinschnitte.
- Dr. Dieter Rose, Frau Kühn, Dr. Michael Hacker und Christian Becker für die Unterstützung am Rasterelektronenmikroskop.
- Dr. Günther Bernhard für die Einweisung am FACSCalibur.
- Florian Sommer für die Hilfe beim Kollagenassay.
- Lydia Frommer, Liane Öttl, Stefan Kolb, Albert Weingart und Edith Schindler für allerlei technische und organisatorische Hilfe.
- Andrea Blaimer für die Organisation des Zelllabors.
- Barbara Weiser für zahlreiche Gespräche und Diskussionen rund ums Fettgewebe.
- Allen, die meine Zellen „gesittet“ haben.
- Dem gesamten Bits&Bytes-Team für die Hilfe bei Problemen mit dem PC und insbesondere Bernhard Appel für die Rettung vieler Daten...

Finally, my special thanks go to the Deutsche Akademische Austausch Dienst (DAAD) for the provision of a six-month scholarship at the University of Kyoto. I would like to express my sincere gratitude to all members of the Department of Biomaterials at the Institute for Frontier Medical Sciences, Kyoto University. Special thanks to Prof. Yasuhiko Tabata for the dedicated supervision of my work and the hearty hospitality, and to Makoto Ozeki for the substantial support in performing the radioactive experiments. I wish to thank Dr. Yamamoto for the organization of my stay and the great help in various concerns. I thank Kushibiki San, Tomoshige San, Inazugu San, Kimura San, Inoue San, and all other members of the department for their support, kindness, and friendship. I will never forget the time in Kyoto!